

PROBING PHYSIOLOGICAL MEDIA
COMPOSITION AND POLYMER-PLASTICIZER
INTERACTIONS ON DISSOLUTION OF
pH-RESPONSIVE SYSTEMS



HALA MUHAMMAD FADDA

A THESIS SUBMITTED IN PARTIAL FULFILMENT OF THE
REQUIREMENTS FOR THE DEGREE OF DOCTOR OF PHILOSOPHY

THE SCHOOL OF PHARMACY
UNIVERSITY OF LONDON

SEPTEMBER 2007



This thesis describes research conducted in the School of Pharmacy, University of London between 2003 and 2007 under the supervision of Dr Abdul W. Basit. I certify that the research described is original and that any parts of the work that have been conducted by collaboration are clearly indicated. I also certify that I have written all text herein and have clearly indicated by suitable citation any part of this dissertation that has already appeared in publication.

A solid black rectangular box redacting the signature of the author.

15/10/2007

Signature

Date

BSTRACT

This study explored the *in vitro* dissolution of pH-responsive methacrylic acid methylmethacrylate copolymer coated dosage forms, in particular Eudragit S coated 5-aminosalicylic acid (5-ASA) tablets for ileo-colonic delivery. Ionic parameters that influence the *in vitro* dissolution were identified as ionic strength, pKa of the buffer and its concentration. Physiological bicarbonate buffers (Hanks and Krebs) were explored as potential dissolution media as they are more representative of the ionic and buffer composition of small intestinal fluids. In comparison to compendial phosphate buffers, they were found to provide a better reflection of the *in vivo* disintegration times of these ileo-colonic tablets as reported in the literature. Jejunal fluids were obtained from human volunteers and Hanks buffer provided a very good reflection of buffer capacity and solubility of 5-ASA in these fluids.

The dissolution of acrylic film coatings was found to be influenced by the plasticizer component of the formulation. A small library of plasticizers was screened with the objective of determining parameters that correlate to dissolution of polymer free films. Free film dissolution was measured using two-compartment permeation cells. Dielectric properties of the films were studied by TSDC (thermally stimulated depolarisation currents). Secondary relaxations were deconvoluted and identified. Glass transition temperature (T_g) (indicator of segmental mobility) was measured using TSDC, differential scanning calorimetry (DSC) and dynamic mechanical analysis (DMA).

Plasticizer structure and solubility were identified as determining factors in dissolution of acrylic free films. Low temperature TSDC spectra showed a relationship of the total secondary relaxation area and relaxation area of the carboxylic acid functional group of the polymer with dissolution time. No correlation was found amongst the glass transition temperatures obtained by TSDC, DSC and DMA with dissolution time of the films. Although the T_g trend was similar for the films, T_g values obtained by TSDC were lower than those observed by DMA and DSC.

Immediate release 5-ASA and prednisolone tablets were coated with the different Eudragit S/plasticizer formulations. The formulations with the extreme dissolution profiles gave rise to similar trends for the coated tablets and free films however the formulations with intermediate dissolution onset times displayed different trends in the two states. These differences were reasoned to be due to drug and excipients in the core interacting with the coat. These findings will contribute to a mechanistic approach in formulation development.

*For my best friends and mentors:
Mummy and Daddy*

No knowledge is acquired save through the study of its causes and beginnings; nor completed except by knowledge of its accidents and accompanying essentials."

A. Ibn Sīnā (Avicenna)

(981 – 1037)

ACKNOWLEDGEMENTS

First and foremost, I would like to express my deep gratitude to my supervisor, Dr Abdul Basit, for his constant support and guidance throughout my PhD. I have learnt so much from him, and his motivation and enthusiasm for research have truly inspired me. Thank you!

I would also like to thank Professor Steve Brocchini at The School of Pharmacy and Professor Nery Pérez from the Department of Physics at University Simón Bolívar, Caracas, Venezuela. They have been so generous in sharing their chemistry and physics knowledge. Our collaboration has really enriched me.

Thanks to Dr Roger Jee and Dr Brian Pearce at The School of Pharmacy for their advice on buffer systems. My deep thanks to all of the staff in the pharmaceuticals department, especially Brian Jessenden for all his help with the dissolution apparatus. Now I can confess to all the dissolution vessels I broke in my first year! Thanks to John Frost for the permeation cells and Dave McCarthy for the SEMs. Thanks to Keith Barnes (MBE), Isabel Goncalves and Catherine Baumber for keeping everything in law and order in the pharmaceuticals department!

My heartfelt thanks to all my friends and colleagues at SOP for making my PhD years enjoyable and memorable, especially: Basel, Cyrus, Da, Diane, Emma, Fang, Gabby, Hanan, Hisham, Jonathan, Meena, Mohamed Al-Hanan, Mohamed Mahmoud, Naziha, Rehab, Sally, Tiago, Yacoub and the senior statesmen: Enosh, Richard and Valentine. Special thanks to Matt for his support during the tough times and fabulous sense of humour!

I am grateful to The School of Pharmacy for sponsoring my PhD.

Thanks to my great friends who I am really fortunate to have, particularly: Dana, Deena, Meerna, Awan, Sura and Wafa. I can't thank Khuloud enough for all the help she has given me. She is a truly caring person and I greatly treasure her friendship.

Thanks to all my cousins especially Hazim for his warmth and looking after me during the vacations. He has taught me how to always see the positive side of things.

I don't know how to thank my parents and express my appreciation for all they have done for me. All I can say is that I would never have reached this far without them.

TABLE OF CONTENTS

ABSTRACT.....	ii
ACKNOWLEDGEMENTS.....	v
LIST OF FIGURES.....	xvi
LIST OF TABLES.....	xxii
NOMENCLATURE AND ABBREVIATIONS.....	xxiv
CHAPTER ONE.....	1
INTRODUCTION.....	1
1.1. Overview.....	2
1.2. GASTROINTESTINAL ANATOMY AND PHYSIOLOGY: ITS RELEVANCE TO DRUG DELIVERY.....	3
1.3. GASTROINTESTINAL LUMINAL PHYSIOLOGY: ITS RELEVANCE TO <i>IN VITRO</i> DISSOLUTION TESTING.....	7
1.3.1. Purpose of <i>in vitro</i> dissolution tests.....	7
1.3.2. Gastrointestinal pH	10
1.3.3. Ionic composition and buffer species.....	13
1.3.4. Surfactants.....	16
1.3.5. Gastrointestinal fluid volumes.....	17
1.3.6. Viscosity.....	23
1.3.7. Gastrointestinal transit times.....	24
1.3.7.1. Gastric emptying times.....	25
1.3.7.2. Small intestinal transit times.....	26
1.3.7.3. Colonic transit times.....	27
1.3.8. Motility and hydrodynamics.....	28

1.3.9. Dynamic artificial gut.....	29
1.4. FORMULATION INFLUENCES ON DRUG RELEASE FROM DOSAGE FORMS.....	30
1.5. DRUG TARGETING TO THE ILEO-COLONIC REGION OF THE GASTROINTESTINAL TRACT.....	32
1.5.1. Bacteria-responsive delivery	
1.5.2. pH-responsive delivery.....	34
1.5.3. Mechanism of dissolution of pH-responsive polymers.....	36
1.6. INFLAMMATORY BOWEL DISEASE AND THERAPY.....	38
1.6.1. Presentation of the disease.....	38
1.6.2. Management of ulcerative colitis: maintenance of remission.....	39
1.6.3. Management of ulcerative colitis: induction of remission in active disease....	40
1.6.4. Management of Crohn's disease: maintenance of remission.....	41
1.6.5. Management of Crohn's disease: induction of remission in active disease.....	41
1.7. PREPARATIONS OF 5-AMINOSALICYLIC ACID AVAILABLE IN THE CLINIC.....	42
1.7.1. History of the discovery of 5-aminosalicylic acid.....	42
1.7.2. Serendipitous bacteria-responsive delivery.....	43
1.7.3. The use of pH-responsive and diffusion controlled delivery to achieve 5-aminosalicylic acid delivery to the distal gut.....	45
1.7.4. pH-responsive delivery of corticosteroids to the small and large intestines....	47
1.8. MODEL DRUGS USED IN THE STUDY.....	48
1.9. SCOPE AND PURPOSE OF STUDY.....	49

CHAPTER TWO	51
<i>AN INVESTIGATION INTO THE INFLUENCE OF PHYSIOLOGICAL BICARBONATE BUFFERS ON THE DISSOLUTION OF pH RESPONSIVE DOSAGE FORMS.....</i>	<i>51</i>
2.1. INTRODUCTION.....	52
2.1.1. Osmolality and ionic constituents of gastrointestinal fluids.....	52
2.1.2. Bicarbonate levels in gut luminal fluids.....	53
2.1.3. Physiological bicarbonate buffers as dissolution media.....	54
2.1.4. Ionic factors influencing the dissolution of pH-responsive dosage forms.....	56
2.2. OBJECTIVES.....	57
2.3. MATERIALS AND METHODS.....	58
2.3.1. Materials.....	58
2.3.2. Buffer systems studied.....	59
2.3.3. Buffer capacity determination.....	61
2.3.4. Stabilisation of physiological buffers.....	61
2.3.5. Calculation of ionic strength.....	63
2.3.6. Solubility measurement of 5-aminosalicylic acid in different buffers.....	64
2.3.7. Dissolution studies.....	65
2.3.8. Media uptake by tablets.....	66
2.3.9. Scanning electron microscopy.....	66
2.4. RESULTS AND DISCUSSION.....	67
2.4.1. Comparison of dissolution profiles of pH-responsive systems.....	67

2.4.2. Solubility of 5-aminosalicylic acid in different phosphate and bicarbonate buffers and the implications on drug release from pH-responsive systems.....	68
2.4.3. Dissolution in phosphate media of different buffer capacity and ionic strength.....	70
2.4.4. Dissolution in physiological bicarbonate buffers.....	74
2.4.5. Bronsted catalysis law.....	78
2.4.6. Dissolution in physiological bicarbonate buffers.....	84
2.4.7. Subjecting Eudragit S coated tablets to a pH transition.....	85
2.4.8. Influence of ionic composition on drug release from sustained release ethylcellulose granules.....	86
2.4.9. Comparison of in vitro drug release with published <i>in vivo</i> data and implications on the choice of formulation.....	89
2.5. CONCLUSIONS.....	92

CHAPTER THREE.....94

A COMPARISON OF DRUG SOLUBILITY IN HUMAN JEJUNAL AND ILEOSTOMY FLUIDS WITH PHYSIOLOGICALLY RELEVANT MEDIA: THE RELATIVE IMPORTANCE OF BUFFER COMPOSITION AND INTESTINAL SURFACTANTS.....94

3.1. INTRODUCTION.....	95
3.1.1. Physicochemical properties of 5-aminosalicylic acid and prednisolone	95
3.1.2. Media used for measurement of drug solubility.....	99
3.1.2.1. Phosphate and bicarbonate buffers.....	99
3.1.2.2. Jejunal fluids.....	99

3.1.2.3. Ileostomy fluids.....	100
3.1.3. Intestinal surfactants and media used to simulate them.....	102
3.2. OBJECTIVES.....	106
3.3. MATERIALS AND METHODS.....	107
3.3.1. Materials.....	107
3.3.2. Media used for measurement of drug solubility.....	107
3.3.2.1. Phosphate and bicarbonate buffers.....	107
3.3.2.2. Human fluids.....	108
3.3.3. Preparation of FaSSIF media.....	109
3.3.4. Methodology of solubility studies.....	110
3.3.5. High performance liquid chromatography (HPLC) for assaying drug solubility.....	111
3.3.5.1. Equipment.....	111
3.3.5.2. Drug separation and choice of mobile phase.....	111
3.3.5.3. Chromatographic conditions.....	113
3.3.5.4. Validation of HPLC assay method.....	113
3.3.5.5. Drug calibration curves for HPLC.....	116
3.3.5.6. Specificity/ selectivity/ precision.....	117
3.3.6. pH and buffer capacity measurements.....	120
3.4 RESULTS AND DISCUSSION.....	121
3.4.1. pH and buffer capacity of jejunal and ileostomy fluids.....	121
3.4.2. Solubility of 5-aminosalicylic acid in different media.....	121
3.4.2.1. Comparison of 5-aminosalicylic acid solubility in bicarbonate and phosphate buffers.....	121

3.4.2.2. Comparison of 5-aminosalicylic acid solubility in bicarbonate buffers human fluids.....	122
3.4.2.3. Comparison of 5-aminosalicylic acid solubility with the buffer capacity of human intestinal fluids.....	125
3.4.2.4. The relationship of 5-aminosalicylic acid solubility with surfactant concentration.....	128
3.4.3. Solubility of prednisolone in different media.....	130
3.4.3.1. Solubility of prednisolone in bicarbonate buffers and phosphate buffers with different concentrations of intestinal surfactants.....	130
3.4.3.2. Comparison of prednisolone solubility in human fluids with than in phosphate buffers with intestinal surfactants.....	132
3.4.4. Biopharmaceutical relevance of <i>in vivo</i> solubility results.....	135
3.5. CONCLUSIONS.....	136
 CHAPTER FOUR.....	138
MOLECULAR INTERACTIONS THAT INFLUENCE THE PLASTICIZER DEPENDENT DISSOLUTUION OF ACRYLIC FILMS.....	138
4.1. INTRODUCTION.....	139
4.1.1. Plasticizers in tablet coatings and the changes they induce.....	139
4.1.2. Theories proposed for plasticizer mechanism of action.....	140
4.1.3. Plasticizer influence on moisture permeability and drug release through modified release systems.....	142
4.1.4. Fabrication of Eudragit S polymers with plasticizers.....	143

4.1.5. Thermal characterisation of polymer/plasticizer free films.....	145
4.1.5.1. Differential scanning calorimetry.....	145
4.1.5.2. Dynamic mechanical analysis.....	146
4.1.5.3. Comparison of differential scanning calorimetry and dynamic mechanical analysis.....	147
4.1.5.4. Thermally stimulated depolarisation currents.....	148
4.1.6. Measurement of contact angle.....	150
4.2. OBJECTIVES.....	153
4.3. MATERIALS AND METHODS.....	154
4.3.1. Materials.....	154
4.3.2. Preparation of polymer free films by solvent evaporation.....	157
4.3.3. Preparation of compression molded polymer film.....	158
4.3.4. Film dissolution.....	158
4.3.5. Methodology for dynamic mechanical analysis.....	160
4.3.6. Methodology for immersion dynamic mechanical analysis.....	162
4.3.7. Methodology for differential scanning calorimetry.....	163
4.3.8. Methodology for thermally stimulated depolarisation current technique.....	164
4.3.9. Methodology for contact angle measurement.....	167
4.4. RESULTS AND DISCUSSION.....	169
4.4.1. Dissolution of polymer films.....	169
4.4.2. Wettability of the polymer films.....	171
4.4.3. Glass transition temperature of films as measured by differential scanning calorimetry.....	172

4.4.4. Screening of selected Eudragit S films using TSDC.....	176
4.4.4.1. Secondary relaxations and glass transition temperatures of Eudragit S films prepared with plasticizers from the citrate ester class.....	176
4.4.4.2. Deconvolution of secondary relaxation peaks of plasticized Eudragit S films.....	178
4.4.4.3. The mechanism through which changes in secondary relaxations influences dissolution of Eudragit S films plasticized with citrate esters.....	182
4.4.4.4. Eudragit S functional groups and their contribution to the mono-energetic secondary relaxation peaks.....	183
4.4.4.5. Influence of citrate plasticizers on film dissolution as determined by changes in TSDC glass transitions.....	185
4.4.4.6. How the structure of tributyl citrate accounts for the prolonged dissolution of its corresponding Eudragit S film.....	187
4.4.4.7. Influence of secondary <i>versus</i> segmental polymer relaxations on the dissolution of plasticized Eudragit S films.....	189
4.4.4.8. Dissolution of plasticized Eudragit S films: plasticizer aqueous solubility <i>versus</i> polymer-plasticizer interactions.....	189
4.4.5. Comparison of Tg values as determined by TSDC, DSC and DMA.....	190
4.4.6. Tg of Eudragit S/triacetin films as measured by dynamic mechanical analysis.....	194
4.4.7. Immersion dynamic mechanical analysis.....	196
4.5. CONCLUSIONS.....	198

CHAPTER FIVE.....	200
INTERACTION OF DRUG AND TABLET CORE EXCIPIENTS WITH ACRYLIC FILM COATINGS AND INFLUENCE ON DISSOLUTION	200
5.1. INTRODUCTION.....	201
5.2. OBJECTIVES.....	204
5.3. MATERIALS AND METHODS.....	205
5.3.1. Materials.....	205
5.3.2. Preparation of 5-aminosalicylic acid and prednisolone tablets.....	205
5.3.2.1. Tablet preparation methodology.....	205
5.3.2.2. Uniformity of tablet weight.....	207
5.3.2.3. Content uniformity.....	208
5.3.2.4. Crushing strength.....	208
5.3.3. Film coating.....	208
5.3.3.1. Coating formulation.....	208
5.3.3.2. Film coating process.....	209
5.3.4. Scanning electron microscopy.....	210
5.3.5. <i>In vitro</i> drug release testing.....	211
5.4. RESULTS AND DISCUSSION.....	213
5.4.1. Performance of the tablet cores.....	213
5.4.2. Dissolution of 5-aminosalicylic acid enteric coated tablets.....	213
5.4.2.1. Dissolution trends with different Eudragit S/plasticizer coatings.....	213
5.4.2.2. Reasons for the slower dissolution of cast films in comparison to sprayed films.....	216

5.4.2.3. Interaction of drug and excipients in tablet core with the polymer film coat.....	219
5.4.2.4. Reasons why plasticizers may have different influences on dissolution of tablet film coat in comparison to polymer free films.....	221
5.4.3. Dissolution of enteric coated prednisolone tablets.....	224
5.4.3.1. Dissolution trends with different Eudragit S/plasticizer coatings and their comparison to 5-aminosalicylic coated tablets.....	224
5.4.3.2. Dissolution of Eudragit S coated prednisolone tablets fabricated with the recommended plasticizers and implications on therapeutic efficacy.....	227
5.4.3.3. Dissolution of Eudragit S coated prednisolone tablets fabricated with a homologous series of plasticizers.....	233
5.4.4. Influence of release media composition on dissolution profiles of coated tablets.....	234
5.5. CONCLUSIONS.....	238
CHAPTER SIX.....	239
GENERAL DISCUSSION AND FUTURE WORK.....	239
6.1. GENERAL DISCUSSION AND CONCLUSIONS.....	240
6.2. FUTURE WORK.....	244
REFERENCES.....	246
PUBLICATIONS.....	271

LIST OF FIGURES

CHAPTER ONE

Figure 1.1: Anatomy of the human gastrointestinal tract.....	3
Figure 1.2: pH profiles in different regions of the gastrointestinal tract.....	11
Figure 1.3: Representation of the dissolution of a weakly acidic drug in a buffer solution.....	15
Figure 1.4: Mechanism of dissolution of carboxylic acid polymers.....	37
Figure 1.5. Azo-bond cleavage of sulphasalazine to produce 5-aminosalicylic and sulphapyridine.....	44
Figure 1.6: Structures of 5-aminosalicylic acid (5-ASA) pro-drugs currently available in the clinic.....	45
Figure 1.7: Chemical structure of 5-aminosalicylic acid (5-ASA).....	49
Figure 1.8: Chemical structure of prednisolone.....	49

CHAPTER TWO

Figure 2.1: Structure of poly(methacrylic acid methylmethacrylate) copolymer (Eudragit S).....	57
Figure 2.2: Equilibria for bicarbonate buffer systems	62
Figure 2.3: Comparative dissolution profiles of Asacol, Mesren and Ipocol tablets in 0.05M phosphate buffer pH 7.4.....	68
Figure 2.4: Drug release profiles of Asacol tablets in pH 7.4 phosphate buffers of varying buffer capacity and ionic strength.....	71

Figure 2.5: Drug release profiles of Ipecol tablets in pH 7.4 phosphate buffers of varying buffer capacity and ionic strength.....	72
Figure 2.6: Drug release profiles of Asacol tablets in different pH 7.4 phosphate buffers of varying buffer capacity	73
Figure 2.7: Drug release profiles of Ipecol tablets in different pH 7.4 phosphate buffers of varying buffer capacity.....	74
Figure 2.8: Comparative dissolution profile of Asacol, Mesren and Ipecol in tablets in physiological Hanks buffer.....	75
Figure 2.9: Comparative dissolution profiles of Asacol tablets in Hanks and Krebs buffers (with CO ₂ (g) stabilisation and without CO ₂ (g) stabilisation).....	76
Figure 2.10: Comparative dissolution profiles of Ipecol tablets in Hanks and Krebs buffers (with CO ₂ (g) stabilisation and without CO ₂ (g) stabilisation).....	76
Figure 2.11 a: Mechanism of ionisation of Eudragit S.....	78
Figure 2.11 b: Ionisation of Eudragit S in the presence of a basic salt.....	79
Figure 2.12: Comparative dissolution profiles of Asacol in Krebs buffer (in presence and absence of CO ₂ (g)) and in 0.025 M phosphate buffer with the same ionic strength.....	81
Figure 2.13: Dissolution profile of Asacol in Hanks buffer in the absence and presence of 5 mM HEPES.....	84
Figure 2.14: Comparative dissolution of Asacol tablets in Hanks and equivalent Hanks buffer (not containing KCl, MgSO ₄ and CaCl ₂).....	85
Figure 2.15: Comparative dissolution of Asacol tablets tested directly in pH 7.4 Hanks buffer or following a transition from 0.1 M HCl to pH 6.8 buffer.....	86
Figure 2.16: Comparative dissolution profiles of Pentasa tablets in phosphate and Hanks bicarbonate buffers.....	87

Figure 2.17: Structural formula of substituted cellulose.....87

Figure 2.18: Dissolution of 5-aminosalicylic acid drug powder in phosphate buffer
and Hanks bicarbonate buffer.....88

CHAPTER THREE

Figure 3.1: Ionization of 5-aminosalicylic at different pH values.....97

Figure 3.2: Solubility of 5-aminosalicylic acid at 37 °C in unbuffered water
at different pH values.....98

Figure 3.3a: Chemical structure of taurocholic acid.....102

Figure 3.3b: Chemical structure of glycolate.....103

Figure 3.3c: Chemical structure of phosphatidylcholine.....103

Figure 3.4: Bile salt concentrations along the normal human small intestine
postprandially.....104

Figure 3.5: Chromatogram of blank jejunal fluids.....118

Figure 3.6: Chromatogram of blank ileostomy fluid.....118

Figure 3.7: Chromatogram of 5-ASA dissolved in ileostomy fluid.....119

Figure 3.8: Chromatogram of prednisolone dissolved in ileostomy fluid.....119

Figure 3.9: Solubility of 5-ASA in pH 7.4 bicarbonate (Hanks and Krebs)
and phosphate buffers with different concentrations of buffer species.....122

Figure 3.10: Solubility of 5-ASA in human intestinal fluids in comparison to
Hanks and Krebs bicarbonate buffers.....123

Figure 3.11: 5-ASA solubility and buffer capacity in different batches of
jejunal fluid.....126

Figure 3.12: 5-ASA solubility and buffer capacity (mean \pm SD) in
ileostomy fluids obtained from different patients.....126

Figure 3.13: The relationship between bulk and surface pH for weak acids in
unbuffered media.....128

Figure 3.14: Solubility of prednisolone in pH 6.8 FaSSIF with different concentrations of the surfactant sodium taurocholate (NaTC).....130

Figure 3.15: Solubility of prednisolone (mean \pm SD) in FaSSIF (containing 3 mM NaTC) and in human intestinal fluids.....133

CHAPTER FOUR

Figure 4.1: Illustration of the heating-isothermal mode of step-scan.....145

Figure 4.2: Illustration of a typical DMA plot of a polymer showing the temperature dependence of loss modulus (E''), storage modulus (E') and $\tan \delta$147

Figure 4.3: The fundamental steps underlying the thermally stimulated depolarisation current technique.....150

Figure 4.4: Interfacial forces acting on a drop of liquid that determine its degree of spreading onto a solid surface.....151

Figure 4.5: Schematic diagram of the Wilhelmy plate apparatus.....152

Figure 4.6: Schematic output of a Wilhelmy plate experiment.....153

Figure 4.7: Schematic diagram of the measurement of film dissolution using a two-compartment permeation cell.....159

Figure 4.8: Geometric set up of a Tritec DMA for measuring Tg of films in tension.....161

Figure 4.9: A typical response of the Tg (represented by $\tan \delta$) as a function of frequency.....162

Figure 4.10: A typical DSC thermogram showing how the Tg (half ΔC_p) is obtained.....164

Figure 4.11a: Onset of dissolution of Eudragit S films with or without plasticizers.....170

Figure 4.11b: Onset of dissolution of Eudragit S films formulated with or without very poor aqueous solubility plasticizers (< 0.05 %).....170

Figure 4.12: DSC thermogram of Eu + P-diol film showing the existence of two Tgs.....176

Figure 4.13a: Low temperature TSDC spectra of films composed of Eudragit S with and without plasticizers.....177

Figure 4.13b: High temperature TSDC spectra of films composed of Eudragit S with and without plasticizers.....	178
Figure 4.14: Direct signal analysis results for the secondary relaxations of Eudragit S films.....	179
Figure 4.15: Secondary relaxation areas versus dissolution times for the different plasticized Eudragit S films.....	181
Figure 4.16: Illustration of the decrease in T _g of Eudragit S films with increasing molecular weight of citrate plasticizer.....	187
Figure 4.17: DSC thermograms of Eudragit S with and without citrate plasticizers.....	191
Figure 4.18a: Tan δ of Eudragit S with and without citrate plasticizers, as obtained from DMA.....	191
Figure 4.18b: Loss Modulus of Eudragit S with and without citrate plasticizers, as obtained from DMA.....	192
Figure 4.19: Comparison of the T _g values obtained from the analysis of the TSDC α -peaks, DSC step of specific heat capacity change, and DMA loss modulus of the different film formulations.....	193
Figure 4.20: Correlation of T _g values of the films obtained from the different thermal methods.....	195
Figure 4.21: Loss Modulus of Eudragit S with and without citrate plasticizers, as obtained from immersion DMA.....	197

CHAPTER FIVE

Figure 5.1: Schematic representation of a fluidized bed coater.....	203
Figure 5.2: Summary of the media changes employed in the <i>in vitro</i> dissolution tests.....	212
Figure 5.3: Dissolution profiles of Eudragit S/plasticizer coated 5-aninosalicylic acid tablets in phosphate buffer.....	214
Figure 5.4: Onset of dissolution in pH 7.4 phosphate buffer of Eudragit S isolated cast films fabricated with different plasticizers.....	215
Figure 5.5: Film formation onto solid surfaces by spray coating.....	217
Figure 5.6: Diagram representing enteric polymer dissolution and drug release.....	219

Figure 5.7: Interaction of the binder polyvinyl pyrrolidone (PVP) with poly (acrylic acid) (PAA).....	220
Figure 5.8(a-c): SEM cross-sections of Eudragit S/TEC coated prednisolone tablets after exposure to HCl and buffer for varying lengths of time.....	223
Figure 5.9: Dissolution profiles of Eudragit S/plasticizer coated prednisolone tablets in phosphate buffer.....	225
Figure 5.10: Dissolution of immediate release 5-ASA and prednisolone tablets in pH 7.2 phosphate buffer.....	227
Figure 5.11: Dissolution profiles of Eudragit S/plasticizer coated prednisolone tablets in phosphate buffer.....	228
Figure 5.12(a-d): SEMs of tablets coated with Eudragit S films fabricated with different plasticizers.....	229
Figure 5.13(a-b): SEMs of tablets coated with unplasticized Eudragit S films.....	231
Figure 5.14: Dissolution profiles of Eudragit S/plasticizer coated prednisolone tablets in phosphate buffer.....	234
Figure 5.15: Dissolution profiles of Eudragit S/plasticizer coated 5-aminosalicylic acid tablets in pH 7.4 Krebs bicarbonate.....	235
Figure 5.16: Dissolution profiles of Eudragit S/plasticizer coated 5-aminosalicylic acid tablets in pH 7.4, 0.05 M phosphate buffer.....	236
Figure 5.17: Dissolution profiles of Eudragit S/plasticizer coated prednisolone tablets in pH 7.4 Krebs bicarbonate.....	237
Figure 5.18: Dissolution profiles of Eudragit S/plasticizer coated prednisolone tablets in pH 7.4, 0.05 M phosphate buffer.....	237

LIST OF TABLES

CHAPTER ONE

Table 1.1: Luminal pH measured along the small and large intestine.....	12
Table 1.2: Ionic composition of small intestinal luminal fluids.....	14
Table 1.3: Intraluminal gastrointestinal water content.....	19
Table 1.4: Intraluminal gastrointestinal 'free' water content determined using magnetic resonance imaging.....	21
Table 1.5: Gastrointestinal fluid environment of non-disintegrating capsule determined using magnetic resonance imaging.....	21
Table 1.6: pH-responsive polymers commonly used to coat solid dosage forms for the attainment of delayed drug release.....	35
Table 1.7: 5-aminosalicylic acid preparations for the treatment of inflammatory bowel diseases available in the UK.....	47

CHAPTER TWO

Table 2.1: Comparison of the electrolyte composition and physicochemical properties of small intestinal fluids and pH 7.4 tested buffer media.....	55
Table 2.2: Composition of the buffer systems studied.....	60
Table 2.3: Solubility of 5-aminosalicylic acid in different buffers.....	69

CHAPTER THREE

Table 3.1: Aqueous solubility, lipophilicity and ionisation constants of 5-aminosalicylic acid and prednisolone.....	96
Table 3.2: Comparison of the buffer content, ionic strength and buffer capacity of bicarbonate and phosphate buffers.....	108
Table 3.3: A comparison of 5-ASA peak areas in mobile phase with filtered ileostomy fluids spiked with drug powder.....	115

Table 3.4: A comparison of 5-ASA peak areas in mobile phase with filtered and centrifuged ileostomy fluids spiked with drug powder.....	115
Table 3.5: A comparison of 5-ASA peak areas in mobile phase with filtered and centrifuged ileostomy fluids spiked with drug solution.....	116
Table 3.6: Characterisation of fasted and fed intestinal fluids aspirated from the proximal jejunum of healthy human volunteers.....	124

CHAPTER FOUR

Table 4.1: Structure, molecular weight and water solubility ^a of plasticizers.....	156-7
Table 4.2: Contact angles of different Eudragit S/plasticizer films with phosphate buffer.....	172
Table 4.3: Residual solvent in the Eudragit S polymer films prepared with different plasticizers.....	174
Table 4.4: T _g values as attained by DSC of the Eudragit S polymer films prepared with different plasticizers.....	175
Table 4.5: Direct signal analysis of the secondary relaxations obtained by TSDC.....	180
Table 4.6: Analysis of the glass transition relaxations obtained by TSDC.....	186
Table 4.7: T _g values obtained from the analysis of the DSC step of specific heat capacity change and DMA loss modulus of the different film formulations.....	192

CHAPTER FIVE

Table 5.1: Formula for immediate release 5-aminosalicylic acid and prednisolone 200 mg tablets.....	206
Table 5.2: Lag time and T _{50%} of 5-aminosalicylic acid tablets in pH 7.2 phosphate buffer. Tablets are coated with Eudragit S and one of the different plasticizers.	215
Table 5.3: Lag time and T _{50%} of prednisolone tablets in pH 7.2 phosphate buffer. Tablets are coated with Eudragit S and one of the different plasticizers.	225
Table 5.4: Lag time and T _{50%} of prednisolone tablets in pH 7.2 phosphate buffer. Tablets are coated with Eudragit S and one of the different plasticizers.	228

LIST OF NOMENCLATURE AND ABBREVIATIONS

β	Buffer capacity
FaSSIF	Fasted state simulated intestinal fluid
FeSSIF	Fed state simulated intestinal fluid
GI	Gastrointestinal
HPLC	High performance liquid chromatography
IS	Ionic strength
Log P	Logarithm of octanol water partition coefficient
pKa	Negative logarithm of the ionisation constant
SEM	Scanning electron microscopy
SD	Standard deviation
T _{50%}	Time for 50 % drug release in dissolution test

Thermal analysis nomenclature and abbreviations

TSDC nomenclature and abbreviations

β	Describes the temperature dependence of relaxation time
E _{0i}	Reorientation energy of the i elementary curve of the secondary relaxation
P _{0i}	Contribution to total polarisation
J ₀	Current density amplitude
J _D	Current density

DSC and DMA nomenclature and abbreviations

ΔC_p	Change in specific heat capacity
E'	Storage modulus
E''	Loss modulus
Tan δ	Loss modulus/storage modulus (E''/E')
T _g	Glass transition temperature

DSC	Differential scanning calorimetry
DMA	Dynamic mechanical analysis
TSDC	Thermally stimulated depolarisation currents

Materials

5-ASA	5-aminosalicylic acid (mesalazine)
Eudragit [®] S	poly(methacrylic acid methyl methacrylate) copolymer
NaTC	Sodium taurocholate

Plasticizers

ATEC	acetyl triethyl citrate
DMP	dimethyl phthalate
DBP	dibutyl phthalate
DOP	dioctyl phthalate
PEG 6000	polyethylene glycol 6000
P-glycol	propylene glycol
TA	triacetin
TEC	triethyl citrate
TBC	tributyl citrate
TBP	tributyl phosphate

CHAPTER ONE

Introduction

1.1 Overview

Modified release systems may be utilised to extend or delay drug release to specific regions of the gastrointestinal (GI) tract where optimum drug absorption occurs or for the treatment of local diseases. The focus of this study was pH-responsive dosage forms, with 5-aminosalicylic acid (5-ASA) and prednisolone as model drugs, for targeting to the ileo-colonic region of the GI tract. Drug release from these enteric systems is primarily controlled by the polymer constituting the coating; other excipients in the formulation, however, are also likely to exert an influence. Polymer-plasticizer interactions were investigated in this study and intrinsic properties of this coating system correlated to its dissolution. These findings will help achieve a mechanistic approach to formulation development.

Another influence on formulation behaviour, yet distinctive from this, is the GI luminal environment the dosage form is exposed to and, ultimately, drug releases into. Through identification of the parameters that influence the dissolution of pH-responsive systems a fundamental understanding of the dissolution mechanism is achieved. The relative importance of different media parameters on influencing the solubility of drugs with variable physicochemical properties is identified. The use of appropriate solubility and dissolution media simulating human GI fluids can serve as a prognostic tool for *in vivo* performance.

1.2 Gastrointestinal anatomy and physiology: its relevance to drug delivery

The gastrointestinal (GI) tract functions to uptake nutrients and eliminate unwanted material through the processes of secretion, motility, digestion, absorption and excretion. It can be divided into the oral cavity, oesophagus, stomach, small intestine and large intestine (Figure 1.1). The majority of drugs are administered as immediate release dosage forms that are designed to disintegrate rapidly in the stomach and empty into the small intestine from where the molecules can be absorbed into the systemic circulation.

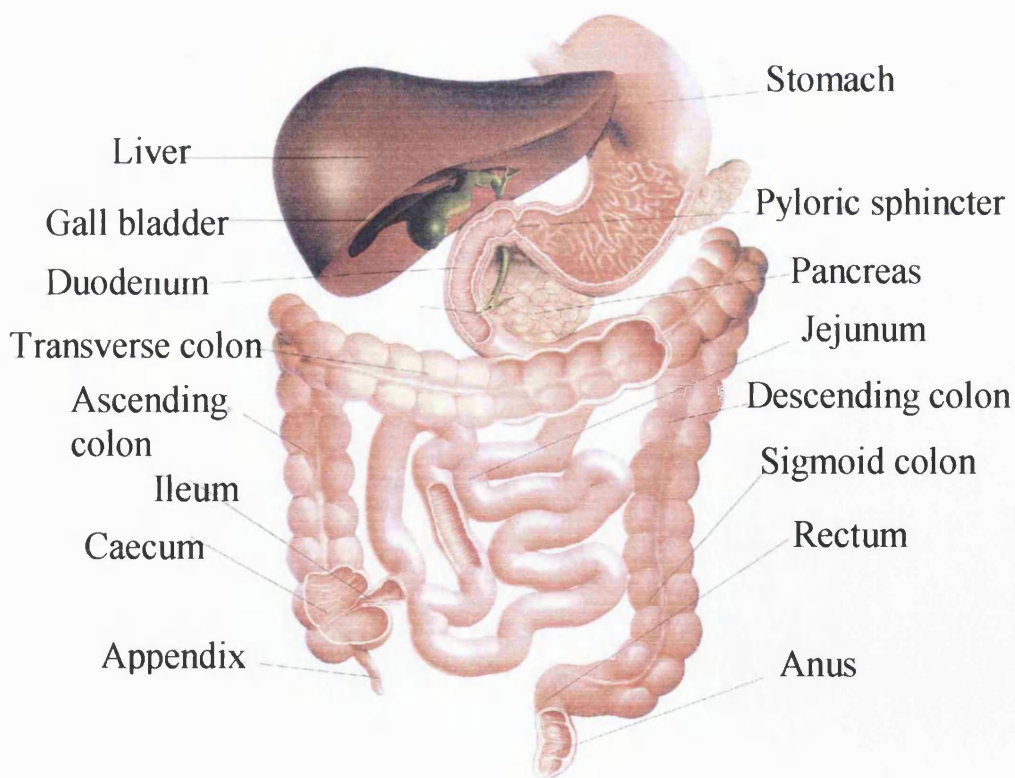


Figure 1.1 Anatomy of the human gastrointestinal tract (courtesy of Biocodex, Inc.)

The **stomach** has three main regions: fundus, body and antrum. It has several functions: acts as a reservoir for food, mechanically and biochemically processes food into chyme, controls the rate of delivery of chyme to the duodenum so that absorption is optimised from the small intestine and produces acid. Acid serves as a bacteriostatic since food consumed is not sterile. The acidic pH also provides optimum activity for the proteolytic enzyme, pepsin (Washington et al., 2001).

The **small intestine** is the longest part of the human GI tract. It is divided into three regions: duodenum, jejunum and ileum. Duodenum is derived from the Latin word *duodeni* which means '12' as the structure is 12 fingerbreadths in length (0.2-0.3 m). The jejunum and ileum are 1 and 2 m in length respectively in a living person, while in a cadaver they are 2.5 and 3.5 m respectively due to loss of smooth muscle tone (Tortora and Grabowski, 1996). The small intestine has several functions: the mixing of chyme with intestinal and pancreatic secretions to complete digestion, absorption of nutrients, movement of unabsorbed material towards the large intestine and prevention of the entry of pathogens. The surface area of the small intestine is greatly enhanced by the presence in the mucosa of plicae circulares, or folds of Kerckring, villi and microvilli. These increase the absorptive surface area to 200 m², whereas the area of the stomach is only about 1m² (Rowland and Tozer, 1995). The absorptive capacity is higher in the duodenum and jejunum, than the ileum due to the more abundant plicae and longer villi (Aiache and Aiache, 1985). This large surface area, coupled with the relatively high fluid volume, makes the small intestine the main site of drug absorption in man.

The submucosa of the duodenum contains Brunner's glands which are involved in the secretion of alkaline mucus that helps neutralise the acidic chyme arriving from the stomach. The Crypts of Lieberkühn, located between adjacent villi are involved in the secretion of mucus, digestive enzymes, entero-endocrine hormones and antibodies. The protection from pathogens is also achieved by the gut-associated lymphoid tissue (GALT) lining the intestine. On top of microvilli exists the glycocalyx, a weakly acidic mucopolysaccharide, presenting a barrier to foreign substances (Tortora and Grabowski, 1996). Above this exists an unstirred layer of aqueous fluid which poses a barrier to lipophilic drugs.

The final region of the small intestine is known as the ileocaecal junction (ICJ). Digestion and absorption of nutrients are effectively complete by the time digesta reach the ICJ; it acts as a physiological sphincter region, regulating the flow of chyme into the colon (Basilico and Phillips, 1993).

The **large intestine** is approximately 1.2 – 1.5 m in length and comprises the caecum, colon, rectum and anal canal. The colon is further subdivided into the ascending (20 cm), transverse (45 cm), descending (30 cm) and sigmoid colon (40 cm). The colonic lumen is wider than that of the small intestine; approximately 6 cm in diameter. The main function of the colon is the reabsorption of water and electrolytes, and the formation and elimination of faecal material. It has been estimated that approximately 1.5 - 2 L of water enters the colon each day which undergoes efficient reuptake throughout its entire length so that only 200 ml is eliminated in faeces. Sodium and chloride are absorbed from the colon in exchange for potassium and bicarbonate (Faigle, 1993).

Surface area of the colon is substantially lower than the small intestine as it lacks well defined villi and microvilli. In the colonic mucosa there is less opportunity for paracellular absorption of drugs due to the 'tighter' junctions between epithelial cells. Moreover, less fluid is available for drug dissolution, particularly beyond the hepatic flexure. Another barrier to colonic drug delivery is the relatively large unstirred water layer at the mucosal surface (Edwards, 1997). All drug molecules must diffuse through this layer to reach mucosa cells and the success of this depends on their physicochemical properties such as molecular weight and polarity. On a biochemical level, the abundant bacterial microflora in the colon can deactivate drugs through reduction or hydrolysis reactions (Farthing et al., 1979; Read et al., 1980).

Residence time in the colon is longer, however, than the small intestine and this longer time may be favourable for the absorption of certain drugs. The colon has been found to be a relatively inert site for the metabolism of drugs by mucosal Cytochrome P450 (CYP) 3A, the major phase I class of drug metabolising enzymes in humans. CYP 3A has clinically compromised the effectiveness of many drugs. Studies have shown CYP 3A activity to be higher in the small intestine compared to the colon (Nakamura et al., 2002), thus drugs which are substrates for this enzyme have a higher absorption from the colon (Berggren et al., 2003). The drug absorption window must therefore be borne in mind when designing enteric and extended release formulations.

The GI tract is a complex organ and numerous hurdles need to be overcome for the desired drug release profile to be achieved by the delivery system. This is of particular concern for extended or delayed release systems which go through diverse

environments on their odyssey through the GI tract. To understand and accurately characterise drug release mechanisms, *in vitro* tests, particularly dissolution tests, need to reflect the complex GI physiology.

1.3 Gastrointestinal luminal physiology: its relevance to *in vitro* dissolution tests

*1.3.1 Purpose of *in vitro* dissolution tests*

In vitro dissolution testing of solid dosage forms is one of the most important biopharmaceutical studies. It serves several purposes (Dressman et al., 1998; Abrahamsson and Ungell, 2004):

- (i) Investigation of drug release mechanisms, especially for modified release formulations.
- (ii) Selection of excipients and candidate formulations that give the desired and most reproducible release profile. Identification of formulations robust to physiological factors; eg. pH, fluid availability and hydrodynamics.
- (iii) *In vitro/in vivo correlations* thus reducing the number of clinical and bioavailability studies needed.
- (iv) Surrogate for bioequivalence tests. Biowaiver can be granted for immediate release formulations with highly soluble and highly permeable drugs on the provision of dissolution results.
- (v) Quality control for ensuring batch-to-batch reproducibility.

USP 24 recognises four types of dissolution apparatus for the testing of oral dosage forms. The European Pharmacopoeia has also adopted these with some modifications to the specifications (Krämer et al., 2005). Apparatus I (rotating basket) and II (paddle

assembly) are the most commonly used because they are simple, robust, and well standardised. USP apparatus I comprises a closed rotating mesh basket attached to a shaft which rotates at a pre-determined speed. The dosage form is contained in the basket which is immersed in transparent vessels heated in a water bath, in common with other apparatus II, III and IV, at a temperature of 37 ± 0.5 °C. Vessels with different capacities, typically in the range of 500 to 2000 ml, can be used. USP II is exactly the same as USP I, however the basket is replaced by a paddle and therefore the dosage form is immersed directly in the vessel.

USP apparatus III is the reciprocating cylinder apparatus which consists of a series of rows containing flat bottomed glass vessels with typical volumes of 200 – 300 ml. Inner cylinders exist within the vessels which vertically reciprocate at a pre-defined speed. The dosage form is contained in the inner cylinders which are closed at the top and bottom with stainless steel mesh. This apparatus is particularly attractive for modified release dosage forms as each row can contain media simulating different regions of the GI tract thus making the process of buffer change much more practical.

USP apparatus IV is the flow-through apparatus and consists of a small volume cell in which the dosage form is contained. Media is continuously circulated through the cell and a filtration device fitted in the cell retains any undissolved material so that it is not analysed. The system may be operated in 'open loop', whereby new medium is continuously introduced, or 'closed loop' so that drug is allowed to accumulate in the medium. 'Open loop' is particularly useful for low solubility drugs.

Several dissolution theories have been proposed, the most prevalent of which is the Noyes-Whitney model developed in 1897 (Equation 1.1) (Martin, 1993b). From this equation, the factors important to drug dissolution can be determined:

$$\frac{dC}{dt} = \frac{A * D}{h} * (C_s - C_t) \quad \text{Equation 1.1}$$

where the dissolution rate, dc/dt , of a substance is a function of the surface area available for dissolution, A , the diffusion coefficient of the compound in the dissolution media, D , the boundary layer thickness, h , and the difference between the concentration of the drug's saturated solubility, C_s , and its concentration in the bulk of the dissolution media at time t , C_t . Hence the essential parameters in determining drug dissolution in the GI tract are composition, volume and hydrodynamics of the luminal fluids.

For *in vitro* dissolution tests to be meaningful they need to reflect physiological conditions in the GI tract. An ideal dissolution test would be a universal one that can be utilised for all solid dosage forms, whether immediate or modified release, and all drugs irrespective of their physicochemical properties. However this would be difficult to achieve in practice especially without compromising the simplicity of the conventional pharmacopoeal tests which make them attractive for all disciplines from regulatory to academia to industry.

This may explain why most research has focused on simulating a certain aspect of the GI environment which may be more critical for certain drugs and formulations than others. The next section is a brief description of the GI milieu and its implications on

in vitro dissolution tests. Particular emphasis was placed on the parameters relevant to pH-responsive systems for targeting drugs to the ileo-colonic region of the GI tract.

1.3.2 Gastrointestinal pH

It is well recognised that there is a sharp increase in pH across the pyloric sphincter from the stomach to the duodenum. Basal stomach pH is low due to secretion of hydrochloric acid by the parietal cells. On meal consumption, the pH in healthy adults increases from a median of 1.7 to a median of 5.0 due to the buffering action of food (Dressman et al., 1990). However in response to the presence of food further gastric acid is secreted and three to four hours after the meal the pH returns to fasting levels. This rise in pH on food consumption and the time it takes to return to basal levels depends on meal composition (Malagelada et al., 1976). pH in the stomach is influenced by additional factors including age, pathophysiological conditions such as achlorhydria (absence of gastric acid secretion) and AIDS, and other medication such as H₂ receptor antagonists and proton pump inhibitors. This has implications on the dissolution and therefore bioavailability of certain drugs such as weakly basic ones as has been shown in the case of ketoconazole in AIDS patients with raised gastric pH (Horter and Dressman, 2001).

The pancreas secretes bicarbonate to neutralise the acidic chyme arriving from the stomach. The pH continues to rise down the small intestine due to further secretion of bicarbonate by mucosal cells of the ileum. Figure 1.2 shows the pH profile of the gut measured in 39 healthy volunteers (Fallingborg et al., 1989). A drop in pH in the caecum is notable and has been attributed to the production of short chain fatty acids (SCFA), predominantly acetate, propionate and butyrate produced from the

fermentation of carbohydrates by colonic bacteria. The pH then rises again along the distal colon due to falling intraluminal concentrations of SCFAs coupled with colonic mucosal bicarbonate secretion (Nugent et al., 2001).

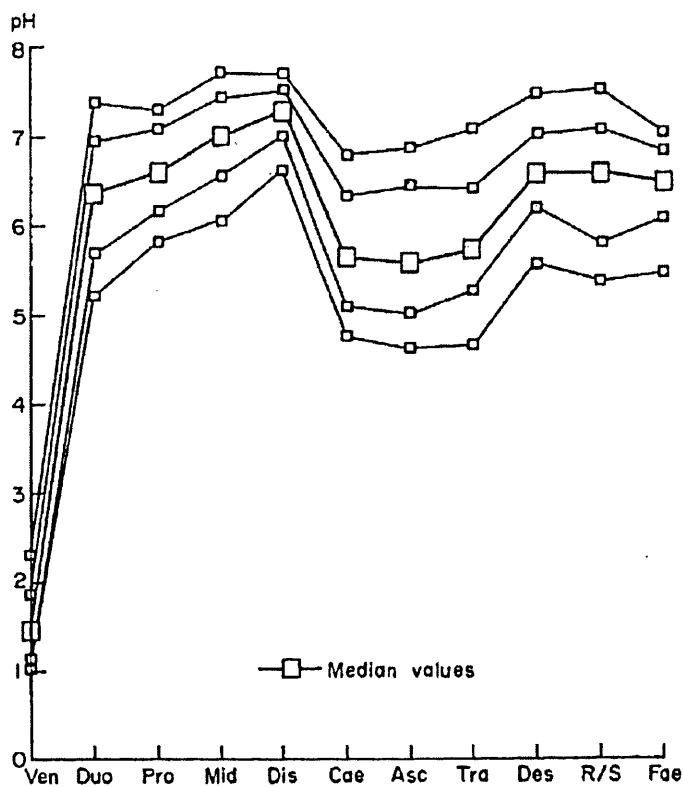


Figure 1.2 Percentiles (90, 75, 59, 25, and 10) of all pH determinations in different regions of the gastrointestinal tract. (Ven = stomach, Duo = duodenum, Pro = proximal small intestine, Mid = mid small intestine, Dis = distal small intestine, Cae = caecum, Asc = ascending colon, Tra = transverse colon, Des = descending colon, R/S = sigmoid colon or rectum, Fae = faeces). Reproduced from Fallingborg et al. (1989).

Table 1.1 summarises gut pH from two studies; Evans et al. (1988) and Fallingborg et al. (1989). Both these studies use radiotelemetry capsules (small encapsulated transmitters) for measuring pH. These two studies were selected as they remain the most comprehensive on pH measurement in different regions of the GI tract. They were both carried out in healthy individuals conducting normal daily activities. Evans' study was performed in 66 healthy adults and Fallingborg study in 39 health adults.

Table 1.1 Luminal pH measured along the small and large intestine.

Intestinal Site	pH (Evans, 1988) Mean pH (\pm SD)	pH (Fallingborg, 1989) Median pH (interquartile range)¹
Proximal small intestine	6.63 (\pm 0.53)	6.6 (6.1 – 7.1)
Mid small intestine	7.41 (\pm 0.36)	7.0 (6.5 – 7.5)
Distal small intestine	7.49 (\pm 0.46)	7.3 (7.0 – 7.6)
Accending colon	6.37 (\pm 0.58)	5.6 (5.0 – 6.4)
Transverse colon	6.61 (\pm 0.83)	5.7 (5.2 – 6.4)
Descending colon	7.04 (\pm 0.67)	6.6 (6.1 – 6.9)

¹ Interquartile range estimated from the figure.

Both studies illustrate a rise in pH from the proximal to mid small intestine. The Fallingborg study further shows a continued rise in pH from the mid to distal small intestine; this rise is not so prominent in the study by Evans. The fall in luminal pH as the small bowel contents empty into the large intestine is distinctive in both studies. However this pH drop is observed to be of larger magnitude in the Fallingborg study and the median does not reach pH 7 again in the descending colon, dissimilarly to the Evans study.

The difficulty in simulating pH is the large intra- and inter-individual variability; particularly in the stomach as this is highly influenced by the food ingested. pH gradients have been used to mimic transit through different regions of the gastrointestinal tract. However these have either not been comprehensive, i.e. the transition not representing all the different regions (Klein et al., 2005) or the pH may

have been simulated however with inadequate unrealistic buffers eg. McIlvaine (Goto et al., 2004). The more recent pharmacopoeial dissolution apparatus III (reciprocating cylinder) and IV (flow-through cell) enable a more efficient and less labour-intensive change of dissolution media. Several media changes can be made within the same run.

1.3.3 Ionic composition and buffer species

From a brief glance at the constituents of small intestinal fluid, it is not difficult to see that the simple compendial media containing sodium and potassium phosphate salts employed in *in vitro* dissolution tests are dissimilar from luminal fluids. Numerous electrolytes exist in the luminal fluids (Na^+ , K^+ , Mg^{2+} , Ca^{2+} , and Cl^-) all of which play a role in orchestrating water and nutrient absorption (Table 1.2). Ionic movement across the cell membranes of gastrointestinal mucosa can occur in several ways to maintain isotonicity of luminal contents with plasma, including diffusion through aqueous channels, active transport and exchange diffusion (Fordtran and Dietschy, 1966).

Table 1.2 Ionic composition of small intestinal luminal fluids.

Electrolyte	Jejunal fluid (Lindahl (1997))	Jejunal fluid (Banwell (1971))	Ileal fluid (Banwell (1971), Phillips and Giller (1973))
Sodium	142	142	140
Potassium	5.4	4.8	4.9
Chloride	126	135	125
Calcium	0.5	-	4.2
Magnesium	-	-	2.8
Ionic strength	0.139	-	-

A consideration of GI physiology reminds us that luminal fluids are buffered by bicarbonate, furthermore phosphate levels are very low. The pancreas secretes bicarbonate into the duodenum to neutralize the acidic chyme arriving from the stomach, bicarbonate is also further secreted by the ileum. Several researchers have independently investigated bicarbonate levels in the human small intestine. Levels reported in the jejunum are 6 to 8.2 ± 5 mM and in the ileum 30 to 40 ± 11 mM (Phillips and Summerskill, 1966; Phillips and Summerskill, 1967; Banwell et al., 1971). *In vitro/in vivo* correlations of drug release from solid dosage forms may be greatly improved by defining the dissolution environment simply in terms of ionic composition.

The dissolution rate of ionisable drugs and excipients has been shown to be influenced by the buffer capacity at a given pH (Mooney et al., 1981; Aunins et al., 1985; Ozturk et al., 1988b; Ramtoola and Corrigan, 1989). Ionisable drugs affect the pH at the boundary layer adjacent to the dissolving surface. The difference in pH between the boundary layer and the bulk medium is affected by the buffer capacity of the medium (Figure 1.3).

While the above studies have considered the influenced of buffer capacity on drug dissolution, to our current knowledge no study has explored the influence of buffer composition on the dissolution of pH-responsive dosage forms; this was therefore one of the study objectives. One of the steps of drug release from these systems is ionisation of the enteric polymer (discussed in detail in section 1.5.2). A further objective was to simulate the ionic composition of GI luminal contents, particularly

the bicarbonate component, which has not been previously explored in the context of dissolution of modified release dosage forms.

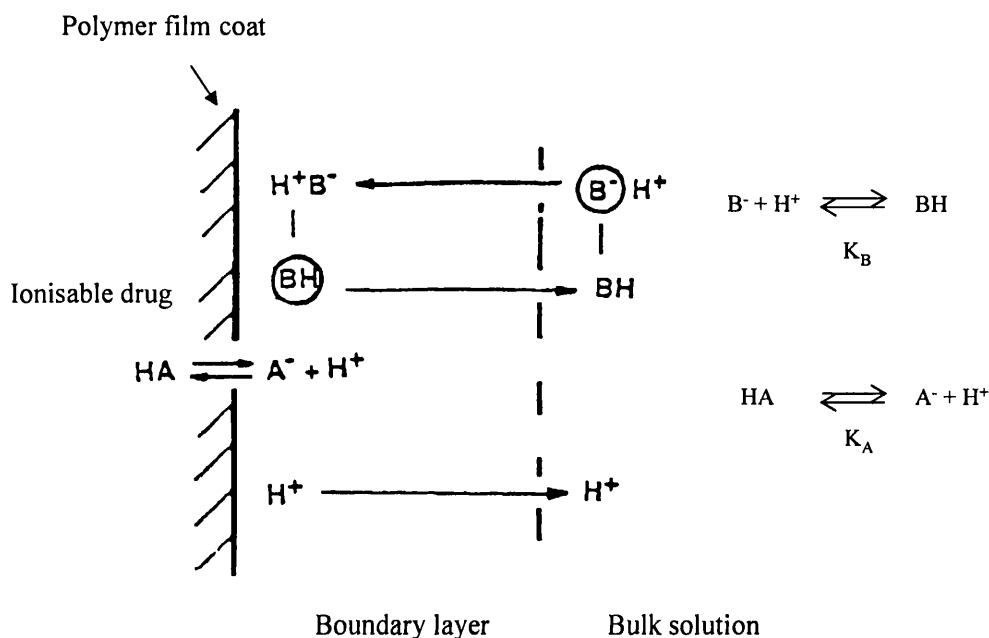


Figure 1.3 Representation of the dissolution of a weakly acidic drug, HA, in a buffer solution, HB. Adapted from Ozturk et al. (1988b).

1.3.4 Surfactants

The surface tension of gastric fluids has been measured by several groups. In recent studies, Efentakis and Dressman (1998) reported values of 35-45 mN/m from the aspirates of eight subjects and Pedersen et al. (2000b) reported values of 28 – 42 mN/m. Surface tension affects wetting of the drug and consequently its dissolution and solubility. Previous attempts to simulate gastric properties have used surfactants that are non-physiologically relevant such as sodium lauryl sulphate or indigenous substances to the stomach such as bile salt surfactants and enzymes (pepsin) however at non-physiologically relevant concentrations. However recent studies have improved the characterisation and simulation of gastric fluids (Vertzoni et al., 2005).

Small intestinal fluids contain phospholipid surfactants in addition to bile salts; together these aid lipid digestion. The effect of these surfactants on solubility and dissolution of very poorly soluble drugs has been extensively explored (Nicolaidis et al., 1999). In this study, solubility of the model drugs, 5-aminosalicylic acid (5-ASA) and prednisolone, was measured in media containing these surfactants (fasted state simulated intestinal fluid, FaSSIF), bicarbonate buffers and conventional phosphate buffers. The results are compared to solubility in jejunal fluids aspirated from healthy subjects and in ileostomy fluids from inflammatory bowel disease patients.

The dissolution of 5-ASA dosage forms coated with pH-responsive polymers was investigated in FaSSIF media and phosphate buffers with no surfactants. Interestingly, there was no difference between the dissolution in the two media (Rudolph et al., 2001). It could be that the surfactants do not improve the wetting of the pH-responsive polymer coat, or if improved wetting does occur it does not influence the dissolution of this coat/ pellet formulation.

1.3.5 Gastrointestinal fluid volumes

Fluid availability in the GI lumen is critical to the dissolution of the formulation and/or drug and is therefore pertinent to the therapeutic efficacy of the medication whether it is intended for local or systemic action. In the fasting state, the human GI tract contains a very small fraction of total body water, in contrast to other animal species (Gotch et al., 1957). The water present in the fasting stomach is either derived from salivary secretions, or presented as HCl from the parietal cells or as mucus from the mucoid cells of the gastric glands.

Post-prandially, water levels in the stomach increase through an input from three different sources: food consumed, digestive secretions and in certain cases down osmotic pressure gradients from plasma to the lumen. Digestive secretions accompanying food ingestion in the small intestine include those from salivary glands, stomach and small intestinal mucus glands, pancreas and gallbladder. It is estimated that the small intestine receives eight to nine litres of fluid per day; of these seven litres is from digestive fluid and 1.5 litres from oral consumption (Fordtran and Ingelfinger, 1968). Most of the intestinal secretions are stimulated and the basal volumes are much less.

The radius of the water-filled pores through which water diffusion occurs in the cell membranes of jejunal and ileal mucosa has been estimated. It has been reported to be 7.5 Å in the jejunum and decreasing to less than a half of that to 3.4 Å in the ileum. Interestingly however, the rate of water diffusion was measured to be approximately the same in these two regions. It was therefore reasoned that pore number and pore length must be greater in the ileum compared to the jejunum (Fordtran and Ingelfinger, 1968). The diffusion rate of water was measured in various areas of the human intestine using deuterium. The isotopically labelled water was administered to the desired region of the intestine via a tube which was swallowed and their rate of the deuterium appearance into the bloodstream was measured. The mean diffusion rate constants were calculated to be 2% from the stomach, 10% from the duodenum and proximal jejunum and 6% from the colon (Scholer and Code, 1954; Reitmeier et al., 1957).

In the 1950s a group of physicians sought to characterise the exchange characteristics of intraluminal gastrointestinal water with the objective of understanding ion transfer (Edelman and Sweet, 1956; Gotch et al., 1957). They determined the water content of different regions of the GI tract using a simple yet efficacious method. The GI tract was removed and its contents studied in 13 human subjects at autopsy within 22 hours of their death. The subjects had different pathological conditions however none of them suffered from gastrointestinal disease and had minimal impairment of fluid and electrolyte balance. The procedures were performed first by placing double ligatures at the cardio-oesophageal junction, pylorus of the stomach, ileocaecal sphincter and just distal to the hepatic flexure of the transverse colon. This position of the transverse colon was chosen as it was the transition point between semi-solid and solid stool pellets. The transition zone was rather sharp and a distinctive change in the consistency of the contents was observed over a short length. The tract was then cut at the ligatures and the sections removed from the peritoneal cavity. Each intact segment was carefully washed and weighed. Each segment was then cut longitudinally and the mucosal surface stripped off by hand. The contents were weighed before and after drying at 105°C for 72 hours.

Table 1.3 shows the calculated water content in the different regions of the GI tract. As would be anticipated, the large intestine displays the least water content due to the water absorption that occurs throughout the intestine. Thus digesta are progressively more viscous as they are transported aborally.

Table 1.3 Intraluminal gastrointestinal water content (Gotch et al., 1957).

	Stomach	Small intestine	Caecum, ascending colon and midway of transverse colon
Mean water content (ml)	118	206	83
Range (ml)	11 – 233	60 – 352	7 – 430

In a similar, more recent study by Cummings et al. (1990) the water composition of the entire large bowel (caecum, ascending, transverse, descending colon, sigmoid and rectum) was measured in 46 adults and the mean was found to be 187 g. Although this is substantially higher than that reported by Gotch et al. (1957), it still falls within the range of 7 – 430 ml. Furthermore, Cummings measured the water content over the entire length of the large intestine, not just up to the mid-transverse colon. Note that grams and mls can be considered interchangeable in these two studies as the density of water is 1 g/ml.

Cummings et al. (1990) found the total content in the large intestine to be 222 ± 21 g (wet) and the % dry matter 14 ± 0.8 % in colon and 23 ± 1.6 % in the sigmoid/rectum. Thus the contents of become drier as we progress down the large intestine. This would be anticipated due to the efficient water reabsorption that occurs.

When considering the above results, however, it is important to bear in mind that this is the total water content; i.e. water bound to digesta as well as free water. In a recent

study by Schiller et al. (2005) they have innovatively used water-sensitive magnetic resonance imaging for estimating the volumes and distribution of free fluid in the GI tract as well as their position in relation to non-disintegrating capsules.

In both the fasted and fed states, 850 ml of water was consumed in the period from two to seven hours before the start of imaging. Despite this, limited free water content seems to exist in the GI lumen (Table 1.4). Moreover, the free water volume in the small intestine decreases in the fed state in comparison to the fasted state which is rather unexpected since an increase would be anticipated due to intestinal secretions. Now the question presents itself as to which fluid volumes, the total or free, are more relevant to simulate when it comes to *in vitro* dissolution tests. Water bound to digesta is still likely to promote dissolution of the drug delivery system and drug, however not to the same extent as 'free' water.

Table 1.4 Intraluminal gastrointestinal 'free' water content determined using magnetic resonance imaging (Schiller et al., 2005).

Gastrointestinal region	Fasted state free fluid volume (ml)	Fed state free fluid volume (ml)
Stomach	45 (\pm 18)	686 (\pm 93)
Small intestine	105 (\pm 72)	54 (\pm 41)
Large intestine	13 (\pm 12)	11 (\pm 26)

The results of the study illustrate that dosage forms in the stomach are in contact with 'free fluid' in the fasted and fed states. However, in the small and large intestine, fluid was found to be distributed into pockets which are not homogeneously spread and large inter-individual variations were observed. Hence the dosage forms transit through fluid pockets and 'dry' segments (Table 1.5).

Table 1.5 Gastrointestinal fluid environment of non-disintegrating capsule determined using magnetic resonance imaging (Schiller et al., 2005).

Contact with liquid	Fasted volunteers		Fed volunteers	
	Small intestine (%) (n=28)	Large intestine (%) (n=3)	Small intestine (%) (n=5)	Large intestine (%) (n=16)
Surrounded	50	0	20	6
Partly surrounded	21	0	20	13
Not in contact	29	100	60	81

After food consumption; small intestinal fluid volumes significantly decreased. This decrease was accompanied by an increase in the number of fluid pockets, from a median of 4 to 6 throughout the length of the small intestine, and a decrease in the fluid volume per pocket from a median of 12 ml to 4 ml. In the colon, fluid volumes were variable before and after the meal. The number of fluid pockets significantly increased from a median of 4 to a median of 5.5, while the liquid volumes per pocket did not significantly change; 2 ml *versus* 1 ml before and after respectively (Schiller et al., 2005).

USP Apparatus 3 (the reciprocating cylinder) may be adapted to mimic these patterns of exposure to wet and dry regions by altering the magnitude of the dip length. The inner tube containing the dosage form may be raised so that it is not in contact with the dissolution medium. The frequency of this 'dry' exposure can be controlled by adjusting the dip rate. Moreover, smaller volumes can be used which are more comparable to the limited volumes available in the GI tract. The 900 ml volumes typically used in the paddle apparatus are far from realistic, particularly when it comes to the large bowel. Large volumes, however, can help maintain sink conditions (less than 20% of saturation concentration). Again, this traditional requirement of sink conditions for all drugs can be argued against as it may not be achieved in-vivo depending on the properties of the drug. For high permeability drugs, i.e. those that penetrate the GI mucosa well and are uptaken by the systemic circulation, sink conditions are likely to be achieved. This however may not be the case for low permeability drugs. 5-ASA acts locally on the mucosa hence its rate of uptake by the mucosal cells and consequent acetylation will influence the concentration in luminal fluids.

1.3.6 Viscosity

Viscosity increases as we progress aborally down the GI tract due to water reabsorption and the presence of indigestible residues. The average human diet is likely to comprise slowly digestible starch, resistant starch (RS) and non-starch polysaccharides (NSP) (Silvester et al., 1995). The latter two pass to the large intestine intact as they are resistant to digestion by pancreatic enzymes however are fermented by the rich anaerobic bacterial environment in the colon to produce short chain fatty acids (Cummings, 1995).

RS and NSP display non-Newtonian behaviour and therefore it is difficult to simulate their rheology *in vitro* as this will be influenced by intestinal motility and flow patterns which vary in different regions of the GI tract and at different times (Ellis et al., 1996). Moreover, dietary fibre modifies the motor function and contraction patterns of the small intestine. These effects change with the type of fibre. A study in dogs showed that normal postprandial patterns of duodenojejunal contractions comprise bursts of 4-10 contractions occurring at a frequency of approximately 5 min. Bran and cellulose increase the number of contractions per burst however decreases the intervals between the bursts. Guar gum was found to decrease the amplitude of contractions. All three types of fibre caused an increase in the transit time, however to different extents (Bueno et al., 1981). What further complicates rheology modelling of polymeric material is particulate matter in digesta. The behaviour of polymers becomes more shear rate dependent with increasing particulate concentrations, known as the power-law behaviour (Ellis et al., 2001).

GI luminal viscosity is therefore difficult to characterise and very complex being influenced by a multitude of factors including diet and health status of the individual. This may explain why no *in vitro* attempt to simulate GI rheology has been made.

1.3.7 Gastrointestinal transit times

Extensive research has been conducted in physiology laboratories on motility patterns of the GI tract. Szurszewski (1969), was the first to describe a regular motility comprising intense action potential activity 'activity front' migrating from the duodenum to the ileum in the fasted dog. These regular cycles of motility and

quiescence are now known as the migrating myoelectric complex (MMC). The MMC has been found to be comprised of four distinctive phases (Code and Marlett, 1975): phase I, quiescence with little or no contractile activity; phase II, intermittent contractions which gradually increase in duration and intensity as the phase progresses; phase III, characterised by intense, large and continuous contractions which sweep the stomach of all indigestible residues; phase IV, a short transition period back to quiescence. Kellow et al. (1986) found the distal oesophagus, gastric antrum, duodenum, proximal and terminal ileum to participate in the MMC. MMCs were most often recorded in the proximal jejunum and found to 'die out' in the ileum; less than 20% passed into the mid-ileum. Cycle length was found to vary within and between subjects with an average cycle length ranging from 66 to 174 min at the proximal jejunum in individual subjects. Phase I and II were found on average to contribute to 21% and 67% of cycle duration respectively and phase III was relatively brief occupying only 12% of the cycle.

1.3.7.1 Gastric emptying times

Gastric emptying (GE) of non-disintegrating dosage forms usually occurs during the high amplitude contractile waves prevalent during phase III or the end of phase II of the MMC. How long the tablet takes to empty from the fasted stomach depends on the phase of the cycle tablet administration coincides with.

Bueno et al. (1975) witnessed the influence of food on motor patterns of the stomach and the resultant interruption of the MMC. In the fed state random/fortuitous emptying arises (Khosla et al., 1989) depending on whether the tablet is located in the

pylorus whereby it can be swept out of the stomach or if it is embedded in the stomach folds demanding the stronger phase III contractions of the fasted state.

The postprandial motor activity of the stomach comprises steady, low amplitude contractions (4-5 per min) prevalent in the antrum with little activity in the gastric body (Bueno and Fioramonti, 1993). Intragastric instillation of milk in dog resulted in all the pacesetter potentials in the stomach wall displaying action potentials, in contrast to phase II of the interdigestive phase where only 10 % of pacesetter potentials were associated with action potentials (Code and Marlett, 1975). Low amplitude contractions may explain why tablets take longer to empty from the stomach in the fed compared to the fasted state.

Multiple-unit dosage forms exhibit more reproducible gastric emptying than single-unit dosage forms. They do not however empty simultaneously with co-administered food and fluid. The study by Coupe et al. (1993) showed 0.8-1.1 mm pellets to have a highly individual pattern of gastric emptying relative to food. In some subjects the pellets emptied from the stomach with food however in others they emptied postprandially in phases II and III of the MMC.

1.3.7.2 Small intestinal transit times

Davis et al. (1986) pooled small intestinal transit data of liquids, pellets and tablets from studies conducted in a total of 201 healthy subjects. No significant difference was found between the transit times of liquids, pellets and tablets. A mean transit value (\pm SD) of 3 ± 1 hours was reported. Two decades later and this is still the value quoted for small intestinal transit time and is the concept underlying time-dependent

formulations. The downside, however, of mean values is that they mask individual transit times. For instance transit times as fast as 1 hour and as slow as 9.5 hours were masked in this mean value. These inter-individual variations can have implications on drug bioavailability particularly if the absorption window of the drug is restricted to the small intestine.

A delay in dosage form transit through the ileo-caecal region is observed in most individuals. This is advantageous for pH-responsive tablets for targeting the colon as this is the region of highest pH in the GI lumen and a long residence time will give an opportunity for the enteric coat to dissolve. If, however, the dosage form is in the terminal ileum on feeding, it may be rapidly propelled through the ICJ and pass within minutes into the colon (Spiller et al., 1987); this is known as the 'gastrocolonic response'. This is likely to have implications in terms of clinical efficacy as rapid propulsion may not allow sufficient time for dissolution of the coat. The opportunity for dissolution is less likely in the colon due to the relatively low pH in the proximal region which is below the pH threshold of the polymer, coupled with the limited fluid availability. Optimal drug release site for pH-responsive dosage forms targeting the colon would therefore be the ileo-colonic region.

1.3.7.3 Colonic transit times

The transit time in the colon of healthy subjects is approximately 35 hours (Metcalf et al., 1987). The ascending and proximal transverse segments of the colon are more attractive for drug delivery in comparison to the rest of the large intestine as they have a higher relative fluid volume. Transit times in this region are between 7 and 14 hours (Metcalf et al., 1987; Parker et al., 1988). Small, multiple-unit preparations tend to

disperse widely and pass through the colon at a slower rate than larger single unit systems. This faster movement of larger objects in the colon is known as 'streaming'.

Motor patterns in the proximal colon are mainly mixing and retropulsive (Edwards, 1997). Patients with inflammatory bowel diseases experience diarrhoea which arises from the failure of colonic water absorption (Snape et al., 1980; Rao et al., 1987). This partly arises from accelerated left colonic transit caused by deficient postprandial colonic contractility. Surprisingly, however, patients with active colitis suffer from proximal colonic stasis (Rao et al., 1987). Diet also influences colonic transit time. A low fibre diet is associated with slow transit (Spiller et al., 1980). There are several extrinsic stimulants to colonic motility. The strongest reported is the awakening from sleep or rest (Bassotti et al., 1993).

These transit times can be simulated in *in vitro* dissolution tests by exposing dosage forms to media mimicking different regions of the GI tract for the corresponding times. Again, the difficulty in this is that wide variability not only inter-individual variability however other factors such as time of day and time relative to meal intake. Nevertheless, a pragmatic approach would be to start by comparing extreme residence times that reflect likely scenarios, then if necessary, intermediate times can be explored. For example, a study in eight healthy volunteers showed that following a standard meal, dosage form GE times vary from 20 min to 270 min (Ibekwe et al., 2007). This time range can be used as a starting point although it is a rather simplistic approach as GE times will depend on the meal composition.

1.3.8 Motility and hydrodynamics

It is considered that the basket and paddle dissolution apparatus provide a good model for an 'upset stomach'. The agitation within the vessels does not reflect the segmental and peristaltic contractions of the intestine and it is important to simulate these as they influence the boundary layer thickness. Efforts have been made to quantify the destructive forces single unit dosage forms are subjected to by designing different 'destructive force-dependent release systems' which release the drug only when they are subjected to a force greater than their pre-determined crushing strength (Kamba et al., 2001). This information can help in using the appropriate rotation speeds in the basket and paddle apparatus which have similar destructive forces to that *in vivo*. However this approach still will not achieve the mixing and turbulent flow experienced in the gastrointestinal lumen.

Abrahamsson et al. (2002) used computer simulations of tablets moving within the stomach derived from magnetic resonance imaging. Tablets were found to experience a wide range of shear forces which varied with the position in the stomach. Low shear stress was experienced in the fundus, moderate shear stress when the tablets moved in the antrum between contraction waves and high shear stress when tablets encountered antral contraction waves.

1.3.9 Dynamic artificial gut

As discussed above there are a considerable number of factors that influence dissolution of dosage forms and drugs. This led to the development a dynamic, multicompartamental *in vitro* system simulating the GI tract by TNO Nutrition and

Food Research (Zeist, The Netherlands). The TNO gastro-intestinal model (TIM) consists of a series of compartments simulating the stomach, duodenum, jejunum and ileum (TIM-1) (Blanquet et al., 2004). TIM-2 exists with additional compartments that simulate the large intestine. Each compartment consists of a glass jacket with a flexible wall inside; water is pumped around the flexible wall and changes in water pressure cause alternate relaxation and compression of the walls thus creating a mixing motion. Media in the stomach can be anything from water to a homogenised meal thus giving an insight into food-drug interactions and the physicochemical influences of food. Simulated gastric, biliary and pancreatic secretions are introduced into the corresponding compartments. Chyme transit from the stomach to the duodenum is controlled by pressure sensors. Water and small molecules eg. products of digestion and dissolved drugs, are removed from the lumen of compartments by pumping fluid through hollow tubes with dialysis membranes. This step is intended to mimic the absorption phase (Blanquet et al., 2004).

To date, this is the closest system that simulates the gut as it takes into account several factors in GI physiology. Work with theophylline matrix tablets shows that it achieves good one to one *in vitro/in vivo correlations* (IVIVC) (Souliman et al., 2007). Other than with theophylline and paracetamol, it has not been extensively investigated and so its IVIVC value cannot yet be established. The downfalls of the system are several; again we do not know how closely the peristaltic activity of the flexible walls simulates that of the GI tract with its additional shear forces, and no information is given as to how the fluid volumes in the different compartments is decided upon. The diffusion through the peristaltic membrane is passive and thus its absorption value is limited for drugs that are absorbed by active transport (mucosal cells are not involved

in the in-vitro system). The technical shortcomings are that it is difficult and time-consuming to set-up and clean. Almost two days of instrument cleaning time are needed per run. It has a low throughput, only one tablet per run and there is no automatic sampling. Moreover, it is very expensive and therefore prohibitive for academic research.

1.4 Formulation influences on drug release from solid dosage forms

The GI physiological parameters that can influence drug release from solid dosage forms have been discussed. However it is not only the dissolution environment and the physicochemical properties of the drug that are critical to its release from a particular delivery system; the formulation is also of great importance.

Several studies have been conducted on the influence of excipients on drug release from diffusion controlled systems in the form of polymer matrices or polymer coats.

Cameron and McGinity (1987) showed that the filler influences release of theophylline from controlled release matrix tablets; this was related to the porosity of the tablet core. Drug release from pellets coated with ethylcellulose was shown to be influenced by the solubility of the drug and filler (Sousa et al., 2002). Generally, drug and filler followed the 'solubility rule' whereby drug release was fastest when the solubility of these two components was greatest; exceptions to the rule however existed and were explained by pellet porosity and specific surface area. The binders selected for granule formation influence the water uptake by disintegrants and therefore their action (Wan and Prasad, 1989).

Siepmann et al (1999) showed that the choice of plasticizer in ethylcellulose film coats influences drug diffusion through the channels. Plasticizers reduce the attractive forces between polymer chains thus creating a higher free volume within the polymer network and greater opportunity for the drug molecule to 'jump' from one cavity to the other; this is known as the 'free volume theory of diffusion' (Siepmann et al., 1999). However there was no evidence for this theory and no proposal as to why different plasticizers influence drug diffusion to different extents.

Little attention has been given to excipient influence, particularly plasticizers, on dissolution of pH-responsive polymers. No study has attempted to correlate intrinsic behaviour of the film coating, such as its molecular motions, to dissolution. To gain a fundamental understanding of the polymer-plasticizer molecular interactions that influence the dissolution of polymethacrylic methylmethacrylate copolymer was one of the objectives of the current study. This information can aid in formulation design so that the optimal drug release profile is achieved. In terms of treating inflammatory bowel diseases, the coating can be tailored so that drug release is achieved at the sites of the gastrointestinal tract affected by disease.

1.5 Drug targeting to the ileo-colonic region of the gastrointestinal tract

Modified release systems may be utilised to extend or delay drug release to specific regions of the GI tract where optimum drug absorption occurs or for the treatment of local diseases. The colon serves as an important site for drug delivery, principally for the therapy of local pathologies which can range in severity from irritable bowel syndrome to the more debilitating inflammatory bowel diseases (ulcerative colitis and

Crohn's disease) through to infections and carcinomas. The colon also has great potential as a route for drug delivery to the systemic circulation which is of value for therapeutic moieties that are poorly absorbed or unstable in the upper regions of the GI tract. One such group of molecules are peptides and proteins that are degraded by hydrochloric acid in the stomach and digested by pepsin and intestinal peptidase. Compared with the stomach and small intestine, the colon is believed to contain lower levels of luminal and mucosal digestive enzymes (Gibson et al., 1989). The inherent lag time in mouth to colon transit can also be exploited to achieve delayed release for the treatment of diseases that are sensitive to circadian rhythms (chronotherapy) such as angina and asthma. A variety of delivery strategies have been proposed for colonic targeting; the trigger mechanisms include: time, pressure, bacteria and pH. However only bacterial and pH triggered systems have reached the clinic.

1.5.1 Bacteria-responsive delivery

There are over 400 different species of bacteria and their population is over 10 million times that of the proximal small intestine. The species are predominantly anaerobic and metabolise endogenous and exogenous substrates that escape digestion in the upper GI tract (Cummings et al., 1989).

5-ASA is the active moiety of sulphasalazine and is liberated by cleavage of the azo bond linking it to sulphapyridine. 5-ASA is rapidly absorbed from the small intestine however when administered as a pro-drug it is too large to be absorbed and therefore reaches the colon where the azo bond is cleaved by colonic bacteria. This concept was used to develop olsalazine and balsalazide both of which constitute 5-ASA azo-

bonded to another 5-ASA, as in the case of olsalazine, or azo-bonded to an inert carrier, as in the case of balsalazide (Chan et al., 1983; Wadworth and Fitton, 1991).

Recently there has been more focus on development of universal systems utilising polysaccharides as coatings or matrices in solid dosage forms. However the polymers of interest are hydrophilic in nature and so swell in gastrointestinal fluids resulting in premature drug release. Chemical modifications to the polymers are thus necessary or combination with hydrophobic, water insoluble polymers which control the swelling in the upper gastrointestinal tract. Polysaccharides that have been explored include: pectin, guar gum, xanthan gum, chitin and chitosan. Although some have provided good results on the bench; most of the formulations developed are not very practical and have not shown promising results *in vivo* (Basit, 2005).

One polysaccharide that has been extensively investigated as a colonic carrier is amylose. Amylose is one of the two major components of starch, and in its glassy, amorphous state is resistant to breakdown by pancreatic enzymes in the small intestine, however undergoes fermentation by amylase producing bacteria in the colon. More than 50% of the bacterial population shows a tendency to digest amylose (Macfarlane and Englyst, 1986). In combination with ethylcellulose, amylose has been applied as a coating to solid dosage forms using conventional coating methods to achieve colon-specific delivery. A number of gamma scintigraphy and pharmacokinetic studies have provided evidence for the colon-targeting potential of this system (Cummings et al., 1996; Thompson et al., 2002; Basit et al., 2004). The amylose system, COLAL™, is the only polysaccharide preparation to progress to clinical trials. Furthermore, the corticosteroid prednisolone metasulphobenzoate

sodium, a more polar and less well absorbed analogue of prednisolone (Lee et al., 1980), was incorporated to provide a new oral treatment for ulcerative colitis (COLAL-PRED™). This product is currently undergoing phase III clinical trials.

1.5.2 pH-responsive delivery

This relies on the pH gradient along the GI tract and the choice of polymer depends on its pKa (Table 1.6) and drug properties such as acidity/basicity and permeability through the enteric polymer film. For conventional enteric coating, whereby it is just necessary to prevent drug release in the stomach and attain rapid release in the proximal small intestine, a polymer with a dissolution pH threshold in the range of 5 to 6 is considered appropriate. Since this pH is unlikely to be reached in the stomach, not even in the fed state, however will definitely be attained in the alkaline intraluminal environment of the duodenum (Kendall and Basit, 2006). However for colonic drug delivery, polymers with a higher pH threshold in the range of 6 to 7 are chosen so that premature release in the proximal small intestine is avoided.

The first colon-targeted pH-responsive delivery system was developed by Dew et al. (1982) and comprised a capsule coated with the polymethacrylic acid methylmethacrylate ester copolymer, Eudragit S (Degussa, Darmstadt, Germany), which has a dissolution pH threshold of 7. This dosage form was found to disintegrate in the distal gut and so it formed the basis for the development of Eudragit S coated 5-ASA tablets marketed as Asacol® MR for treating ulcerative colitis.

Table 1.6 pH-responsive polymers commonly used to coat solid dosage forms for the attainment of delayed drug release

Polymer	Dissolution threshold pH
CELLULOSE DERIVATIVES	
Hydroxypropyl methylcellulose phthalate 50	5.0
Hydroxypropyl methylcellulose phthalate 55	5.5
Hydroxypropyl methylcellulose acetate succinate L	5.5
Cellulose acetate trimellitate	5.5
Hydroxypropyl methylcellulose acetate succinate M	6.0
Cellulose acetate phthalate	6.2
Hydroxypropyl methylcellulose acetate succinate H	6.8
ACRYLIC DERIVATIVES	
Poly(methacrylic acid, ethyl acrylate) 1:1 (Eudragit L55)	5.5
Poly(methacrylic acid, methyl methacrylate) 1:1 (Eudragit L)	6.0
Poly(methacrylic acid, methyl methacrylate, methyl acrylate) 2.5:6.5:1 (Eudragit FS)	6.8
Poly(methacrylic acid, methyl methacrylate) 1:2 (Eudragit S)	7.0
POLYVINYL DERIVATIVES	
Polyvinyl acetate phthalate	5.0

The pH threshold of Eudragit S polymer will be achieved in the mid to distal small intestine however is not met in the ascending colon. When Asacol was originally developed, it was based on the concept that pH continues to rise aborally along the GI tract. It was developed before the confounding evidence of fall in pH in the caecum emerged; this is likely to have serious implications on dissolution of the polymer. Formulating the film coat with the appropriate plasticizers, however, may vary the site of initial polymer dissolution and help achieve the desired release profile.

1.5.3 Mechanism of dissolution of pH-responsive polymers

pH-responsive polymers have acidic or acidic ester groups and thus dissolve and ionise on exposure to alkaline pH. It has been proposed by Nguyen and Fogler (2005) that dissolution of carboxylic acid polymers involves the following processes (Figure 1.4):

- (1) Diffusion of water and buffer ions into the polymer matrix to form a gel.
- (2) The functional carboxylic acid groups of the polymer chains in the gel layer undergo ionisation.
- (3) Polymer chains disentangle out of the gel layer and diffuse to the polymer-solution interface.
- (4) Further ionisation of the carboxylic acid groups on polymer chains at the polymer-solution interface.
- (5) Disentangled polymer chains diffuse away from the interface and towards the bulk solution.

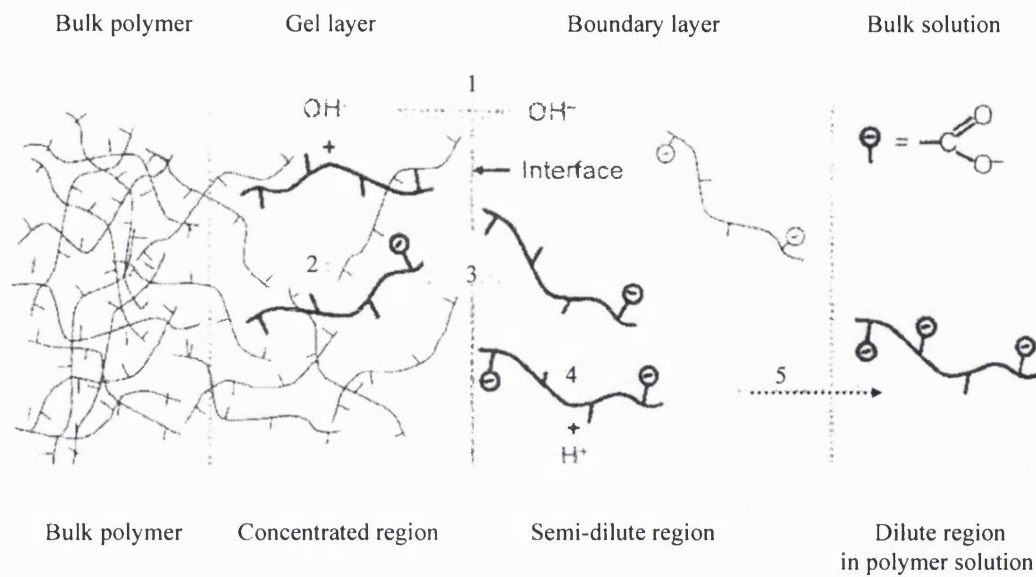


Figure 1.4 Mechanism of dissolution of carboxylic acid polymers. Numbers correspond to the step. Adapted from Nguyen and Fogler (2005).

Diffusion of the ions and water (step 1) and ionisation of the polymer functional groups (steps 2 and 4) are usually relatively fast. Hence enteric polymer dissolution is either disentanglement-limited (step 3) if polymer diffusion away from the interface is faster than the disentanglement rate, or diffusion-limited (step 5) if polymer behaviour is vice versa.

As hydrogen ion concentrations in the gel layer decrease, ionization of the polymer increases and therefore greater repulsion exists between the anionic functional groups. This can cause greater swelling of the gel thus allowing faster polymer disentanglement. This dependence of polymer disentanglement rate on the ionic composition of the release medium draws attention to the importance of accurately

simulating the luminal GI composition when investigating the dissolution of pH-responsive polymers. This was the focus of part of the current study.

1.6 Inflammatory bowel disease and therapy

1.6.1 Presentation of the disease

Inflammatory bowel disease (IBD) has traditionally been categorised into two forms; ulcerative colitis (UC) and Crohn's disease (CD). It is a chronic, non-infectious inflammation of the gut mucosa and patients usually require life-long treatment. The aetiology is not exactly known however it has been associated with environmental triggers, such as infections and drugs, in genetically predisposed individuals (Ardizzone and Porro, 2002). The genetic influence is stronger in CD than UC. Smoking raises the risk of CD however surprisingly lowers the risk of UC through unknown mechanisms. The prevalence of UC is 100 – 200 per 100,000. There are significant differences between ethnic groups, with certain populations, such as Ashkenazi Jews, having a particularly high incidence. The incidence of UC remains stable. CD has a prevalence of 50 – 100 per 100,000; however its incidence may be increasing. Both UC and CD are mainly diseases of young people, with peak incidence between the ages of 10 – 40 years (Rubin et al., 2000; Loftus, 2004).

UC is diffuse mucosal inflammation of the colon. It involves the rectum in about 95 % of patients and may extend proximally in an uninterrupted pattern to affect other parts of the large intestine (Kornbluth and Sachar, 2004). 'Distal disease' may be restricted to the rectum (proctitis) or the rectum and sigmoid colon (proctosigmoiditis). More extensive disease involves 'left sided colitis' up to the

splenic flexure, 'extensive colitis' up to the hepatic flexure and pancolitis affecting the whole colon (Carter et al., 2004). CD is a patchy, transmural disease which can affect any part of the GI tract. In a collective of 414 patients it was shown to most commonly affect the colon (41.7 %), followed by Crohn's ileocolitis (34.1 %) and isolated Crohn's ileitis (20.7 %), rarely does it involve the upper GI tract (Tromm and May, 2005).

The hallmark symptom of UC is bloody diarrhoea, often with colicky abdominal pain, rectal urgency or tenesmus. It is characterised by exacerbations and remissions which may occur spontaneously or as a result of treatment changes or intercurrent illnesses (Meyers and Janowitz, 1989). Symptoms of CD include abdominal pain, diarrhoea and weight loss. Obstruction may occur as a result of strictures or fistulae. CD tends to cause greater disability in patients than UC. Both UC and CD are associated with a greater risk of colon cancer (Carter et al., 2004).

1.6.2 Management of ulcerative colitis: maintenance of remission

The goals of treatment of UC are the induction and maintenance of remission of symptoms and mucosal inflammation to obtain an improved quality of life (Kornbluth and Sachar, 2004). The British Society of Gastroenterology (BSG) guidelines recommend 5-ASA for the maintenance of remission in all patients with ulcerative colitis, especially those with left-sided or extensive disease. 1-2 g is the recommended oral maintenance dose. However recent evidence suggests that higher doses are more effective at maintaining remission. A study in 169 patients found the one year relapse rate to be 33 % for those taking 3 g/day in comparison to 46 % in those taking 1.5 g/day ($P = 0.057$). Although this improvement in remission was not within the 0.05

significance, the high dose was well tolerated and not associated with an increase in adverse effects (Fockens et al., 1995). 5-ASA is available as oral tablets, pellet sachets, suspension, liquid or foam enemas, or suppositories. Suppositories do not have a topical effect above the rectosigmoid junction and 100 ml enemas do not spread above the splenic flexure (Marteau et al., 2005). Oral treatment is therefore required in extensive UC extending beyond the splenic flexure. Distal presentations of the disease can be effectively treated topically, orally, or with a combination of both. Randomised controlled trials have shown that local treatments achieve better remission rates than oral treatment (Cohen et al., 2000). A combination of local and oral treatments can achieve high mucosal concentrations and therefore superior in extensive colitis or left-sided colitis provided they are well tolerated (Marteau et al., 2005; Regueiro et al., 2006). Furthermore, proximal extension of the disease can be reduced on administration of oral treatment to left-sided colitis patients (Regueiro et al., 2006).

1.6.3 Management of ulcerative colitis: induction of remission in active disease

The British Society of Gastroenterology (BSG) guidelines recommend 5-ASA as first-line therapy for active mild-moderate, left-sided or extensive ulcerative colitis (UC) (Carter et al., 2004). There is increasing evidence that raising the dose to > 4 g/day, leads to improved response rates and earlier symptom relief in UC patients; this was investigated in the recent double-blind, randomised and multi-site ASCEND (Assessing the Safety and Clinical Efficacy of a New Dose) studies (Travis, 2006). ASCEND II showed that at six weeks, patients on the 2.4 g/day dose experienced 59 % improvement in comparison to 72 % in patients at the 4.8 g/day dose. There was also no significant increase in the incidence of adverse effects (Hanauer et al., 2005).

Oral corticosteroids are effective at inducing remission in UC, however have no place for maintenance therapy. Commonly prescribed oral corticosteroids include prednisolone, prednisone and budesonide. They are potent anti-inflammatory agents and the therapeutic strategy is to achieve topical effects and reduce systemic side effects. A common starting dose of prednisolone is 40 mg once daily with dose tapering occurring at 5 mg/ week (Carter et al., 2004).

1.6.4 Management of Crohn's disease: maintenance of remission

CD is more resistant to therapy and more difficult to manage. Corticosteroids and aminosalicylates are ineffective in maintaining remission in CD. For remission other agents need to be considered depending on the patient group; these are the immunomodulators and include: azathiopurine, methotrexate and the new anti-TNF biological infliximab. These agents can also be used to induce remission in severe, extensive, active CD (Travis et al., 2006).

1.6.5 Management of Crohn's disease: induction of remission in active disease

Initial published trials concluded that oral 5-ASA is effective in the treatment of mild to moderate ileal, ileocolonic or colonic CD (Singleton et al., 1993; Tremaine et al., 1994). 5-ASA therefore became popular among physicians for mild CD, but in 2004 the conceptions changed. A meta-analysis of three placebo-controlled trials of Pentasa 4 g daily in active CD for a period of 16 weeks in 615 patients showed only a modest superiority of Pentasa over placebo in therapeutic outcome (Hanauer and Strömberg, 2004). The clinical significance of the difference is viewed as debatable. Subgroup

analysis does not provide clear answers as to whether treatment is beneficial in one group of patients more than the other. The consensus by the European Crohn's and Colitis Organisation (ECCO) is that 5-ASA should not be considered more effective than placebo for active ileal or colonic CD (Travis et al., 2006). Budesonide 9 mg daily is the preferred treatment in mild to moderately active localised ileocaecal CD. However there is still a lot of debate in this area as some patients suffer from mild disease that does not warrant steroid therapy and introducing steroids into the treatment regimen of CD patients may present the risk of steroid dependency. Some groups of physician therefore advocate aminosalicylates as first line treatment in mild CD (Lim and Hanauer, 2004).

In mildly active localised ileocaecal CD budesonide 9 mg daily has been shown to be superior to placebo and 5-ASA 4 g/day and achieves remission in 51% to 60% of patients over 8 – 10 weeks (Travis et al., 2006). Budesonide is preferred to prednisolone as less systemic absorption arises and therefore less severe adverse effects, although a Cochrane systemic review showed budesonide to be appreciably less effective (Otley and Steinhart, 2005).

1.7 Preparations of 5-aminosalicylic acid available in the clinic

1.7.1 History of the discovery of 5-aminosalicylic acid

In the late 1930s sulphasalazine was designed by the Swedish physician Dr Nanna Svartz in an attempt to treat rheumatic polyarthritis, which was then thought to be of bacterial origin. The value of salicylates in reducing joint inflammation and pain was well recognised and Dr Svartz believed that rheumatic polyarthritis originated from an

infection, most likely caused by Streptococci. At that time only sulfa antibiotics were active against streptococci (Svartz, 1988). However when aspirin and sulphonamides were administered concomitantly they had no real therapeutic efficacy and it was rationalised that they need to be combined chemically to have an affinity for and concentrate in connective tissue (Watkinson, 1986; Svartz, 1988). Among the compounds produced by Swedish chemists was sulphasalazine, which is an azo bond attachment of the anti-inflammatory active 5-ASA to the antibiotic sulphapyridine. Investigations in rheumatic arthritis patients led the group to conclude that it was therapeutically effective for this indication. When this drug was tried in rheumatoid arthritis patients with UC a great improvement of their colitis symptoms was observed (Watkinson, 1986). In the 1960s, controlled clinical trials definitively established its value over placebo in the treatment of ulcerative colitis (Watkinson, 1986).

1.7.2 Serendipitous bacteria-responsive delivery

In the 1970s it was demonstrated that the azo bond of sulphasalazine (Salazopyrin[®]) is metabolised by colonic bacteria to release sulphapyridine and 5-aminosalicylic acid (Das et al., 1973b; Azadkhan et al., 1977) (Figure 1.5). In 1977 it was proved by Azad Khan's group that 5-ASA is the active therapeutic moiety in the treatment of ulcerative colitis and sulphapyridine behaves as an inert carrier molecule facilitating drug delivery to the colon (Azadkhan et al., 1977). Another finding was that the sulphapyridine moiety of sulphasalazine is responsible for its toxicity profile (Das et al., 1973a; Azadkhan et al., 1980). Adverse effects include: allergies, gastrointestinal, haematological and fertility (Singleton et al., 1979; Birnie et al., 1981; Malchow et al., 1984). These findings have led to the development of new 5-ASA formulations.

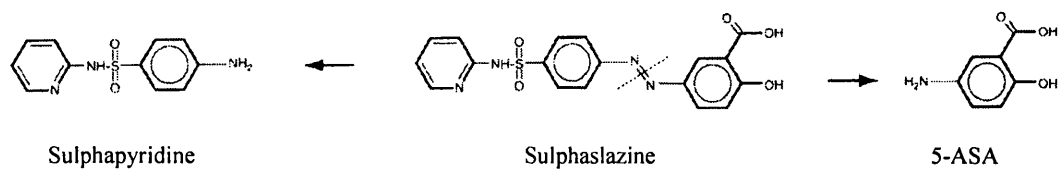


Figure 1.5 Azo-bond cleavage of sulphasalazine to produce 5-aminosalicylic acid (5-ASA) and sulphapyridine. Reproduced from Klotz and Schwab (2005).

The mechanism of action of 5-ASA is still not exactly known however *in vitro* studies have shown it has modulatory action on lipid mediators, metabolites of arachidonic acid (prostaglandins and leukotrienes), cytokines and reactive oxygen species which are involved in the tissue inflammation and damage characterising UC and CD (Larsen and Henson, 1983; Clemett and Markham, 2000). It achieves its therapeutic efficacy mainly by acting on the inflamed mucosa of the GI tract making it necessary for the active substance to be selectively released in the diseased areas.

5-ASA is unstable in gastric acid and is better absorbed from the upper than the lower intestinal tract (Myers et al., 1987). Its permeability is five-fold higher in jejunum in comparison to the ileum (Zhou et al., 1999). To achieve 5-ASA delivery to the colon; carrier molecules conjugated to 5-ASA by an azo bond susceptible to cleavage by colonic bacteria are still exploited. The sulphapyridine has been replaced by another 5-ASA to produce olsalazine (Dipentum[®]) or 4-aminobenzoyl-β-alanine to produce balsalazide (Colazide[®]) (Klotz and Schwab, 2005) (Figure 1.6).

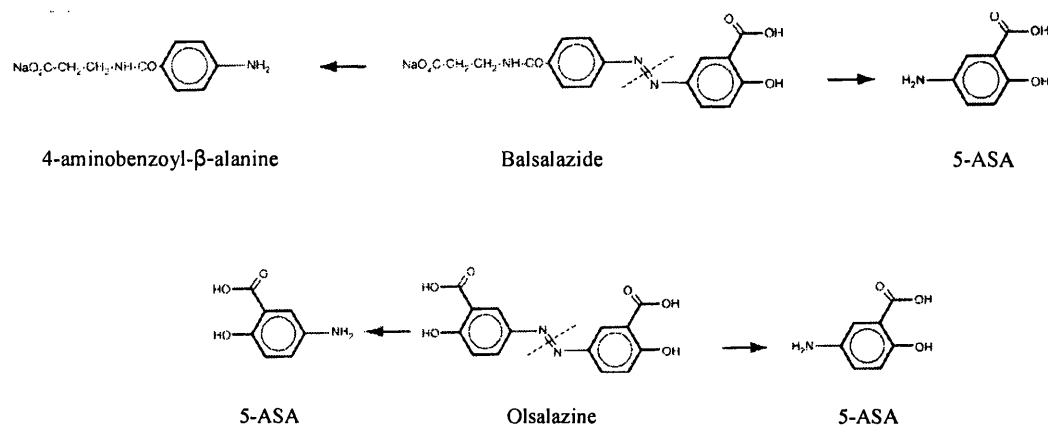


Figure 1.6 Structures of 5-aminosalicylic acid (5-ASA) pro-drugs currently available in the clinic. Reproduced from Klotz and Schwab (2005).

1.7.3 The use of pH-responsive and diffusion controlled delivery to achieve 5-aminosalicylic acid delivery to the distal gut

A number of formulation approaches have been adopted and several preparations are available on the UK market utilising pH or diffusion dependent delivery, or more recently, both (Table 1.7). The enteric polymers used are all acrylic with a pH threshold of 6 or 7. In-vitro dissolution studies in our laboratory have shown that the different formulations give rise to distinctive release profiles under pH values used to simulate different regions of the GI tract. These different release patterns have implications on the luminal concentrations of 5-ASA and its metabolite, acetyl 5-ASA, in different areas of the GI tract (Myers et al., 1987; Devos et al., 1992; Christensen, 2000). Pharmacokinetic studies comparing Asacol and Pentasa showed that 5-ASA release starts in different regions of GI tract and consequentially different fractions of absorption into the systemic circulation arise (Chuong et al., 2006).

The current UK guidelines states that modified release mesalazine preparations are not interchangeable and should therefore be prescribed by their proprietary (brand) name (British Medical Association, 2007). The IBD patient population is heterogeneous in the severity of the disease and the site of the GI tract burdened by disease. The physician should therefore select the most appropriate formulation for each individual patient. Pentasa and Salofalk granules release more proximally; henceforth they are most likely to be effective if the main site of inflammation is found in the ileum.

In a review by Forbes et al. (2003) they conclude that confirming systemic bioequivalence for mesalazine modified release products is not sufficient evidence for their similarity, as is the case with systemically acting modified release products. Additional criteria need to be fulfilled, including: attainment of information from in-vitro dissolution tests and one adequately powered, controlled comparative clinical trial to determine therapeutic equivalence and assessing safety. A clinical study is necessary as luminal concentration of 5-ASA and its metabolite may not necessarily be a surrogate to the therapeutic efficacy of the drug. It would be ideal to assess the concentration of 5-ASA in the intestinal mucosa however this is not currently demanded by regulatory authorities as there is no agreed procedure in terms of the region of gut biopsy and preparation. Moreover, the inter-laboratory reproducibility of such procedures has not been validated (Forbes et al., 2003).

Table 1.7. 5-aminosalicylic acid preparations for the treatment of inflammatory bowel diseases available in the UK.

Product	Dosage form	Polymer type	Site of release	Indication
Asacol [®] MR	Coated tablet	MA-MM (1:2) Eudragit S (release at pH > 7)	Distal small intestine and colon	UC acute/maintenance CD ileocolitis maintenance
Mesren MR [®]	Coated tablet	MA-MM (1:2) Eudragit S (release at pH > 7)	Distal small intestine and colon	UC acute/maintenance
Ipocol [®]	Coated tablet	MA-MM (1:2) Eudragit S (release at pH > 7)	Distal small intestine and colon	UC acute/maintenance
Salofalk [®]	Coated tablet	MA-MM (1:1) Eudragit L (release at pH > 6)	Mid to distal small intestine and colon	UC acute/maintenance
Salofalk [®] Granules	Coated microgranules filled into a sachet	Core MM neutral ester (Eudragit NE). Coat MA-MM (1:1) (Eudragit L). Coat dissolves at pH 6 and then drug release occurs by diffusion through the core.	Mid to distal small intestine and colon	UC acute/maintenance Licensed for use in children above 6 years. Only 5-ASA product licensed for use in children.
Pentasa [®] Granules	Coated microgranules filled into a sachet	Ethylcellulose coat through which drug diffuses out.	Stomach to colon	UC acute/maintenance
Pentasa [®] Tablets	Coated microgranules compressed into tablets	Tablets immediately disintegrates into granules. Drug diffuses out of the ethylcellulose membrane coating the tablets	Stomach to colon	UC acute/maintenance

MM, methyl methacrylate; MA, methacrylic acid

1.7.4 pH-responsive delivery of corticosteroids to the small and large intestines

Two enteric coated controlled release preparations of budesonide licensed for CD commercially available are Entocort[®] and Budenofalk[®]. Entocort constitutes a capsule containing Eudragit L100-55 coated ethylcellulose granules. Drug release starts in the

duodenum (pH threshold of polymer is 5.5) and is slowly continued through the small intestine and colon (Edsbacker et al., 2003). Budenofalk is a capsule that contains Eudragit L/S coated ethylcellulose granules (pH threshold of the enteric coat is 6.4). The release profiles and clinical efficacy of these two formulations have never been compared. These ‘controlled ileal release’ formulations are popular as they are believed to have improved anti-inflammatory action by delivering drug to the site of inflammation (D’Haens, 2006). However it must be borne in mind that glucocorticosteroids exert a ‘global’ anti-inflammatory action, thus different to aminosalicylates. Clinical trials comparing ‘ileal controlled release’ formulations of budesonide with enteric coated prednisolone, showed the former to be less effective (Otley and Steinhart, 2005). Interestingly, the prednisolone preparations used are tablets which comprise just an enteric coat and no controlled release profile. A commonly prescribed enteric brand in the UK is Deltacortril Enteric[®] which is an immediate release tablet with polyvinyl acetate phthalate as the enteric polymer (pH threshold 5). Hence it would be expected that most of the drug is released in the small intestine with minimal amounts reaching the colon for local action. Despite this release profile, clinical efficacy has been confirmed; thus warranting investigation into whether a local effect is really exerted by glucocorticosteroids.

1.8 Model drugs used in the study

Aminosalicylates and glucocorticosteroids were the model class of compounds selected for this study as their efficacy in the treatment of inflammatory bowel diseases has been confirmed and they are formulated for local delivery to the distal small intestine and colon. 5-ASA (Figure 1.7) was chosen as all aminosalicylates are

derived from it. Prednisolone (Figure 1.8) was chosen in preference to budesonide as it is more readily available for research.

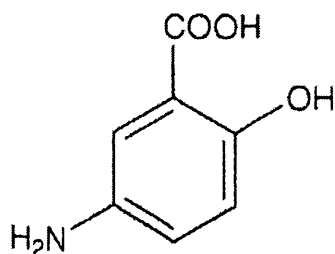


Figure 1.7 Chemical structure of 5-aminosalicylic acid (5-ASA). 5-ASA is light pink crystals with a MW of 153.14. According to the British Pharmacopoeia (2003) it is slightly soluble in water.

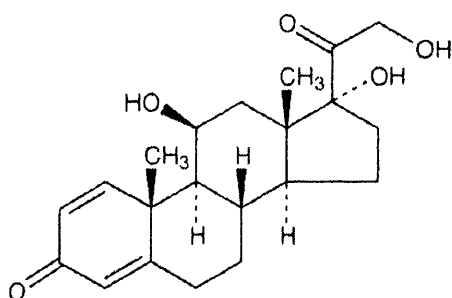


Figure 1.8 Chemical structure of prednisolone. Prednisolone is white crystals with a MW of 360.4. According to the British Pharmacopoeia (2003) it is very slightly soluble in water.

1.9 Scope and purpose of study

Polymer-excipient interactions and gastrointestinal luminal fluids are two distinctive aspects of the biopharmaceutics of modified release dosage forms; yet a thorough

investigation of both of them is necessary for the efficient development of pharmaceutical products.

The aims of this work are:

- To identify ionic luminal fluid components that influence dissolution of tablets with pH-responsive acrylic coatings and to understand the dissolution mechanism of these systems. To develop dissolution media that better simulate gastrointestinal luminal components and thus contribute to achieving improved *in vitro in vivo correlations*.
- To explore drug solubility in human gastrointestinal luminal fluids, conventional phosphate buffers and physiologically relevant media. To identify the relative importance of different media parameters on influencing the solubility of drugs with varying physicochemical properties.
- To identify plasticizer influence on the dissolution of pH-responsive acrylic free films and achieve a fundamental understanding of how this arises. To conduct an in depth study of the molecular mobility of these systems through the use of thermal, mechanical and dielectric techniques. To correlate intrinsic properties with dissolution onset of the systems.
- To evaluate if drug and excipients in the tablet core influence the dissolution of acrylic film coatings. This will be conducted by comparing the dissolution trends of acrylic free films fabricated with different plasticizers with the dissolution trends of coated tablets.

CHAPTER TWO

An investigation into the influence of physiological bicarbonate buffers on the dissolution of pH-responsive dosage forms

2.1 INTRODUCTION

The *in vitro* assessment of drug release from pH-responsive dosage forms is usually conducted by sequential dissolution testing in compendial acid and near neutral pH phosphate buffer systems. While these simple dissolution media are routinely used to represent the pH conditions in the stomach and small intestine respectively, they do not reflect the ionic nature, particularly buffer components, of luminal gastrointestinal (GI) fluids.

2.1.1 Osmolality and ionic constituents of gastrointestinal fluids

The osmolality of stomach contents after hypotonic or hypertonic meals does not tend to equilibrate with plasma with the passage of time. This stable osmolality of gastric contents may be explained by the impermeability of gastric mucosa to water movement in response to osmotic gradients, dilution of the meal by hypoosmotic saliva and gastric secretions, and reaction of secreted HCl with dietary protein (Fordtran and Ingelfinger, 1968). In contrast to the stomach, the proximal small intestine rapidly adjusts the osmolality of both hypotonic and hypertonic meals to values extremely close to that of normal plasma (280 to 300 mOsm/kg) and this is maintained throughout the small intestine. The ability of the proximal small intestine to equilibrate the osmolality of fluids it receives from the stomach is mainly attributable to its large effective pore radius (Fordtran et al., 1965). Moreover, the different ions present in small intestinal luminal fluids are also maintained at rather stable concentrations. In this part of the study, we endeavoured to make *in vitro* dissolution media more physiological by simulating the ionic components of small

intestinal luminal fluids. Particular attention was given to simulating the buffer component, bicarbonate.

2.1.2 Bicarbonate levels in gut luminal fluids

Bicarbonate is secreted in the duodenum and the ileum and absorbed or neutralised by hydrogen protons secreted in the jejunum (Selub, 1994). The mechanism for bicarbonate (HCO_3^-) secretion in the ileum has not been fully elucidated and multiple potential mechanisms have been proposed. One mechanism is the sodium-independent $\text{Cl}^-/\text{HCO}_3^-$ exchange, whereby one molecule of luminal chloride undergoes an electroneutral exchange for one molecule of cellular bicarbonate (Selub, 1994). Another proposed mechanism is $\text{Na}^+/\text{HCO}_3^-$ symport where varying ratios of ions may take part in either basolateral entry or apical exit mechanisms (Stellin, 1997). It has been proposed that another major reason for the high bicarbonate concentration of ileal luminal fluids is the higher permeability of jejunal mucosa to passive bicarbonate diffusion partly due to the aqueous filled pores in the human jejunum having a radius twice as large as the ileal pores (Fordtran et al., 1965). Bicarbonate ions therefore diffuse from the jejunal luminal fluid into the mucoal cells. A further rise in bicarbonate concentration is expressed by water absorption in the ileum giving rise to a volume decrease (Fordtran and Locklear, 1966).

There are different methods for measuring electrolyte composition of the intestinal luminal contents. Banwell et al. (1971) used intestinal intubation whereby samples of luminal fluid were collected and analysed. The bicarbonate content of jejunal and ileal fluids in healthy subjects was measured to be 8.2 ± 5 and 30 ± 11 mM (mean \pm SD) respectively.

Phillips and Summerskill (1966, 1967) studied bicarbonate movement by a segmental perfusion technique whereby a known concentration of the test substance was infused at the desired intestinal region and at a constant rate. The intestinal content was then sampled to determine to what extent the test substance had been removed from or added to the intestinal content per unit time (Fordtran and Ingelfinger, 1968). When high concentrations of the electrolyte are infused, absorption occurs. Whereas when low concentrations are infused, net movements from the plasma to luminal fluids arise. The jejunal concentration of bicarbonate tended to equilibrate at 6 mM, whereas in the ileum equilibration occurred at 40 mM.

2.1.3 Physiological bicarbonate buffers as dissolution media

In this work physiological bicarbonate salt solutions were used as dissolution media; these solutions are traditionally used for the incubation of cultured cells and living tissue in vitro for biochemical and pharmacological studies (Atkins and Peacock, 1997). They comprise various ions which are all present in luminal fluids and are buffered predominantly by bicarbonate (Table 1.1). Furthermore, ionic strength of these buffers resembles that of the GI fluids. Physiological buffers of varying composition exist; dissolution in Hanks buffer was studied as it resembles the proximal small intestine most closely with respect to electrolyte composition, and Krebs buffer resembles the distal small intestine.

Table 2.1 Comparison of the electrolyte composition and physicochemical properties of small intestinal fluids and pH 7.4 tested buffer media. Electrolyte content of lumenal fluid compiled from Banwell et al. (1971), Lindahl et al. (1997), Phillips and Giller (1973).

Electrolyte	Human jejunal fluid	Human ileal fluid	Hanks buffer	Krebs buffer	0.05 M Phosphate buffer
Bicarbonate	7.1	35	4.2	25	Not present
Phosphate	-	-	0.8	1.1	50
Potassium	5.1	4.9	5.8	5.9	50
Sodium	142	140	142	143	39
Chloride	131	125	143	128	Not present
Calcium	0.5	4.2	1.3	2.5	Not present
Magnesium	-	2.8	0.8	1.2	Not present
Ionic strength	0.139	-	0.155	0.161	0.129
Buffer capacity (mmol/L/pH unit)	2.97 ^a	-	1.0	3.7	23

^a measured from lumenal aspirates (see chapter three).
 - indicates not measured

2.1.4 Ionic factors influencing the dissolution of pH-responsive dosage forms

Aside from pH, a number of aspects of dissolution media have been shown to affect drug release from enteric coated dosage forms. Ashford et al. (1993b) compared phosphate buffers of varying composition and buffer capacity. The study conclusively showed that increasing phosphate concentration in the buffer increases dissolution rate, however it does not enable us to determine whether this is attributable to an increase in buffer capacity or ionic strength of the dissolution medium. Karali and co-workers (1995) reported an increase in dissolution rate to the same extent when either NaCl or phosphate are used to increase the ionic strength of the medium, whereas Rudolph et al. (2001) found no modification of the drug release profile of Eudragit S coated formulations with increasing ionic strength. Chan et al. (2001) used a physiological salt solution (Hanks buffer) comprising various electrolytes including bicarbonate. Dissolution in this physiological buffer was found to be significantly slower compared to the conventional phosphate buffers. Ibekwe et al. (2006a) reported a finding similar to this for Eudragit S coated tablets of the non-ionic drug prednisolone. McNamara and co-workers (2003) used a 0.9 % saline solution and continuously sparged it with different partial pressures of CO₂(g) to achieve different concentrations of bicarbonate (HCO₃⁻). They used this media to study the dissolution of low solubility ionisable drugs.

Dissolution of modified release marketed 5-aminosalicylic acid (5-ASA) products, with particular attention to Eudragit S (methacrylic acid methylmethacrylate copolymer) (Figure 2.1) coated tablets, was studied in conventional phosphate and physiological buffer systems. The release profiles were compared to *in vivo* studies in the literature on the disintegration performance of these tablets. The objective of this

was to determine whether bicarbonate buffers improve predictions of the *in vivo* behaviour of modified release systems designed for ileo-colonic drug delivery.

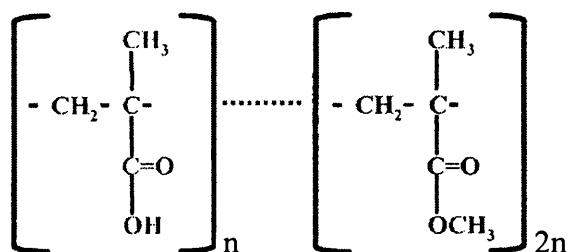


Figure 2.1 Structure of poly(methacrylic acid methylmethacrylate) copolymer (Eudragit S). Ratio of carboxylic acid to ester groups is 1:2.

2.2 OBJECTIVES

- To identify the ionic factors that influence the dissolution of pH-responsive acrylic polymer coated dosage forms. Factors considered are ionic strength, buffer species, buffer capacity and presence of other electrolytes.
- To simulate the ionic composition, with particular attention to buffer species, of GI luminal fluids. To evaluate if dissolution testing of pH-responsive dosage forms in these physiological media improves the prediction of their performance *in vivo*.

2.3 MATERIALS AND METHODS

2.3.1 Materials

5-aminosalicylic acid (5-ASA) used to form the calibration curves was of 99 % purity and obtained from Sigma-Aldrich Chemicals, Dorset, England. All the salts used to prepare the buffers and 5 M HCl were of analytical grade and obtained from VWR Chemical Ltd., Poole, UK. HEPES (N-2-hydroxyethylpiperazine-N'-2-ethanesulfonic acid) and MES (morpholinoethansulfonic acid) buffer salts were obtained from Sigma-Aldrich Chemicals, Dorset, England. The tablets studied were purchased from their manufacturers. Asacol[®] MR was purchased from Procter and Gamble Pharm., Mesren MR[®] from IVAX, Ipocol[®] from Sandoz and Pentasa[®] tablets from Ferring. Asacol, Mesren and Ipocol all contain 400 mg 5-ASA and are pH responsive systems, while Pentasa contains 500 mg of the drug and has a pH-independent mechanism of release. The formulations of these products are as follows:

Asacol[®] MR: lactose, sodium starch glycolate, magnesium stearate, talcum, polyvinylpyrrolidone, methacrylic acid copolymer, dibutylphthalate, polyethylene glycol, yellow iron oxide, red iron oxide.

Mesren MR[®]: The same qualitative formulation as Asacol.

Ipocol[®]: Microcrystalline cellulose, sodium carboxymethyl starch, corn starch, magnesium stearate, polyvinyl pyrrolidone, mannitol, precipitated silica, dimethyl phthalate, methacrylic acid copolymer, dimethicone, talc, titanium dioxide, red ferric oxide.

Pentasa[®]: Povidone, ethylcellulose, magnesium stearate, talc, microcrystalline cellulose.

2.3.2 Buffer systems studied

To study the influence of buffer capacity on dissolution, phosphate buffers of varying strengths (0.05M and 0.2M phosphate) and Sorensen's buffer (0.0687M phosphate) were investigated (Table 2). 0.05M phosphate buffer with a pre-calculated quantity of NaCl to attain the same ionic strength as that of the 0.2M phosphate buffer was prepared.

Physiological salt solutions were also used as dissolution media. Substitutes to physiological Hanks and Krebs buffers were prepared whereby they comprised only the buffer salts (bicarbonate and phosphate) as well as NaCl to maintain the ionic strength. These equivalent buffers were prepared to investigate whether the additional electrolytes K^+ , Mg^{2+} , SO_4^{2-} and Ca^{2+} have an influence on the dissolution of enteric coatings.

Table 2.2 Composition of the buffer systems studied

Buffer component (mM)	0.05 M PBS (phosphate buffer solution) ^a	0.2M PBS	0.05M PBS with NaCl	Sorensen's Buffer ^b	Krebs buffer ^c	Equivalent Krebs buffer	Hanks buffer ^d	Equivalent Hanks buffers	0.00217M PBS
KH ₂ PO ₄	50	200	50	13.2	1.18	1.18	0.441	0.441	2.17
NaOH	39.5	158	39.5						1.72
Na ₂ HPO ₄				53.5					
Na ₂ HPO ₄ .2H ₂ O							0.337	0.337	
NaHCO ₃					24.97	24.97	4.17	4.17	
NaCl			397.2		118.07	135.04	136.99	149.39	149.4
KCl					4.69		5.37		
CaCl ₂					2.52		1.26		
MgSO ₄ .7H ₂ O					1.18		0.812		
Ionic strength	0.129	0.526	0.526	0.174	0.161	0.161	0.155	0.155	0.155
Buffer capacity (mmoles/L/pH unit)	23.0	58.8	23.0	22.1	3.7	3.7	1.0	1.0	1.0

^aBritish Pharmacopoeia (2003)^bLentner (1984)^cLund (1994)^dAtkins and Peacock (1997)

2.3.3 Buffer capacity determination

Buffer capacity is the ability of the buffer to resist changes to its pH. This was measured by adding aliquots of 0.1M HCl to 100 ml of the buffer system. Buffer capacity (β) was then calculated using equation 1 (Martin, 1993a).

$$\beta = \frac{\Delta AB}{\Delta \text{pH}} \quad \text{Equation 2.1}$$

where AB is the small increment in mol/L of the amount of acid or base added to produce a pH change of ΔpH in the buffer. β in all media was measured at a pH change of 0.5 units on addition of acid. This pH direction was chosen as it is the one relevant to our system. At near-neutral pH media 5-ASA and Eudragit S ionise to their anionic forms and protons are generated.

The buffer capacity of 0.05M phosphate buffer (23 mmol/L/pH unit) was compared to that of the physiological buffers. A phosphate buffer was then formulated with the same buffer capacity as Hanks (0.00217M phosphate), in attempt to isolate the influence of buffer capacity from that of buffer species identity. For ionic strength however to be the same as Hanks, a calculated quantity of NaCl was added to the 0.00217M phosphate buffer.

2.3.4 Stabilisation of physiological buffers

A difficulty in using bicarbonate buffers is the progressive rise in pH due to loss of CO_2 from the solution (Perrin and Dempsey, 1974). In aqueous solutions both bicarbonate (HCO_3^-) and carbonic acid (H_2CO_3) exist (Figure 2.2). H_2CO_3 has a pKa of 6.4 and dissociates to yield H_2O and CO_2 (aq). CO_2 evaporates from solution and

therefore the ionisation reaction towards the left (protonation of HCO_3^- to yield H_2CO_3) is promoted to restore the equilibrium. When physiological buffers are used in *in-vitro* cell cultures, they are maintained in a closed system equilibrated with 5% CO_2 in the gas phase to maintain the pH. We adapted this method to stabilise Krebs buffer. Krebs buffer was continuously sparged with 5% CO_2 and 95% O_2 throughout the duration of the dissolution run. This maintenance of CO_2 at steady concentrations prevents the decomposition of H_2CO_3 (to yield H_2O and CO_2) which in turn prevents the protonation of HCO_3^- . Dissolution of the dosage forms in Krebs buffer in the absence and presence of CO_2 were compared.

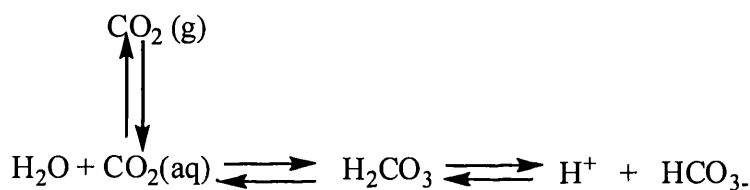


Figure 2.2 Equilibria for bicarbonate buffer systems.

There was difficulty however in stabilising Hanks buffer due to its limited bicarbonate content. Attempts at reducing the 5 % CO_2 gas flow rate to the lowest possible were still too high for the system and the levels of $\text{CO}_2(\text{aq})$ would rise increasing the formation of H_2CO_3 and causing a decrease in pH. A different approach was therefore adopted whereby another buffering agent, HEPES (N-2-hydroxyethylpiperazine-N'-2-ethanesulfonic acid), was added to the system. Numerous other buffers exist however HEPES is commonly used in pharmacology as it is relatively innocuous to living tissue and its pKa is 7.55. Furthermore, the buffering ability of a weakly acidic or

basic group is approximately limited to the range, $\text{pH} = \text{pK}_a \pm 1$, the best buffering ability being at the pH equal to the pK_a.

2.3.5 Calculation of ionic strength

Ionic strength (μ) is used for solutions of weak electrolytes and salts such as those existing in buffer systems. It relates interionic interactions whereby each ion is considered to be surrounded by an 'atmosphere' in which ions of opposite charge are predominant (Florence and Attwood, 1998). It depends on the number of ionic charges and not on the properties of the salts existing in solution (Equation 2.2).

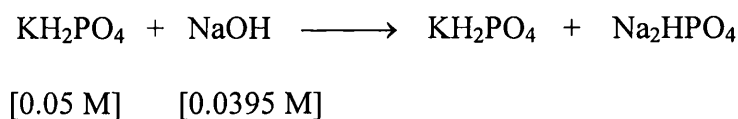
$$\mu = \frac{1}{2} \sum c_i z_i^2 \quad \text{Equation 2.2}$$

where c_i is the concentration in moles per litre of any of the ions and z_i is its valence. Ionic strength is half the sum of the product of concentration and valence for all the ions present in solution.

An example is presented here for the calculation of the ionic strength of pH 7.4, 0.05 M phosphate buffer.

pH 7.4, 0.05 M phosphate buffer is formed from 0.05 M KH_2PO_4 and 0.0395 M NaOH (British Pharmacopoeia, 2003).

On addition of NaOH to KH_2PO_4 the following reaction takes place:



The following species are therefore formed:



$$[\text{K}^+] = 0.05 \text{ M}$$

$$[\text{Na}^+] = 0.0395 \text{ M}$$

$$[\text{HPO}_4^{2-}] = 0.0395 \text{ M}$$

$$[\text{H}_2\text{PO}_4^-] = 0.05 \text{ M} - 0.0395 \text{ M} = 0.0105 \text{ M}$$

$$\mu = \frac{1}{2} \sum c_i z_i^2$$

$$\mu = \frac{1}{2} \sum (0.05 \times 1^2) + (0.0395 \times 1^2) + (0.0395 \times 2^2) + (0.0105 \times 1^2)$$

$$\mu = 0.129$$

The ionic strength of the other buffers was calculated using the same formula. The ionic strength of pH 7.4 0.2 M phosphate buffer was found to be 0.5262. The difference in ionic strength between the 0.2 M and 0.05 M phosphate buffer is 0.3972. Hence amount of NaCl equivalent to a μ of 0.3972 was added to 0.05 M phosphate buffer to give it the same ionic activity as 0.2 M phosphate buffer.

$$\mu \text{ of NaCl} = \frac{1}{2} \sum (c_i z_i^2)$$

$$0.3972 = \frac{1}{2} [(c_i \times 1^2) + (c_i \times 1^2)]$$

$$= \frac{1}{2} [(2c_i)]$$

$$0.3972 \text{ M} = c_i$$

0.3972 moles/L of NaCl (23.21g/L) was added to 0.05 M phosphate buffer for its ionic strength to equal that of 0.2 M phosphate buffer.

2.3.6 Solubility measurement of 5-aminosalicylic acid in the different buffers

Solubility measurements of 5-aminosalicylic acid were performed in phosphate and bicarbonate buffers by adding excess drug to 1 ml of buffer in microcentrifuge tubes (Eppendorf AG, Hamburg, Germany) and placing in a shaking water bath at 37 °C and speed of 400 shakes per min. In the initial preliminary experiments, several

samples were prepared and removed after 2, 5 and 24 hours. Equilibration was achieved within five hours. Based on this data, five hours was considered adequate time to achieve saturation solubility in the different media. Excess drug was then filtered and solubility measured using HPLC-UV; details of which are given in section 3.2.

2.3.7 Dissolution studies

5-ASA release from the dosage forms was assessed by dissolution testing using BP Method II paddle apparatus (model PTWS, Pharma Test, Hainburg, Germany). Tablets from within the same batch and from different batches of the same brand were tested. The volume of the dissolution media was 1000 ml maintained at $37 \pm 0.5^\circ\text{C}$ and a paddle speed of 50 rpm was employed. The amount of 5-ASA released from the dosage form was determined by an in-line UV spectrophotometer (Cecil 2020) model, UK) with 1 mm flow cells at 330 nm in pH 7.4 buffer. As UV readings were automatically taken, no loss of medium occurred through the duration of the dissolution run. These same conditions were used to test the dissolution of 5-ASA powder. 400 mg of the drug was added to 1000 ml of dissolution medium.

In addition to testing the tablets directly in buffer, dosage forms were subjected to pH transitions to simulate the gastrointestinal tract. Tablets were tested in 0.1M HCl for two hours, to simulate the normal maximal limit of gastric residence in a fasting individual, and then transferred to the pH 7.4 buffers. To mimic intestinal conditions even more closely, tablets were subjected to a transition from an acidic pH, to a pH of 6.8 for one hour to mimic the jejunal region of the small intestine (Evans et al., 1988) followed by transfer to the pH 7.4 buffers. The pH of Hanks buffer was adjusted to

6.8 by the addition of MES (morpholinoethansulfonic acid) as it has a suitable pKa of 6.15. During the transition phases the tablets were subjected to the same dissolution conditions (paddle rotation speed of 50 rpm and temperature of 37 ± 0.5 °C).

2.3.8 Media uptake by tablets

To establish if acid is uptaken by the dosage forms during the transition stage, the tablets were subjected to dissolution conditions for 2 hours in 0.1 M HCl. After 2 hours the tablets were removed and excess medium drained and blotted with filter paper from around the tablet. The tablets were then weighed and the uptake calculated.

2.3.9 Scanning electron microscopy

The film thickness of the tablets was examined by scanning electron microscopy (SEM) using a Phillips XL 20 scanning electron microscope (Philips, Cambridge, UK). The tablets were cut in half to enable measurement of the film thickness. Specimens were coated with gold using a sputter coater (model K550, Emitech, Kent) and mounted onto a sample holder and examined using at an accelerating voltage of 5 -15 kV depending on the magnification required. A random sample of 8 tablets from within the same batch and from different batches of the same brand were measured. The average thickness and standard deviations were calculated.

2.4 RESULTS AND DISCUSSION

2.4.1 Comparison of dissolution profiles of the pH-responsive systems

A consideration of the excipients in the pH-responsive preparations shows that Asacol and Mesren have the same qualitative formula. Ipecol however, has a different formulation with different plasticizers. SEMs of the marketed products show intra-batch and inter-batch variation in film coating thickness. Ipecol has the lowest enteric coating thickness of $50 \mu\text{m} \pm 8 \mu\text{m}$. Asacol has a coating thickness of $82 \mu\text{m} \pm 11 \mu\text{m}$ and Mesren has a coating thickness of $75 \mu\text{m} \pm 7.5 \mu\text{m}$. Asacol and Mesren were found to have similar dissolution profiles in all the phosphate buffers studied (0.05 M, 0.2 M phosphate and Sorensen's buffers), attributable to their similar enteric coating thickness (Figure 2.3). The dissolution of Ipecol, however, was much faster compared to the other two products; arising from its thinner coat and/or the coating components (Figure 2.3).

As Ipecol has a faster drug release profile compared to the other two brands, it would be expected to exhibit individual drug availability at different sites of the GI tract. Since the ulcerative colitis patient population is heterogeneous, this would offer physicians the opportunity of matching the different drug release characteristics of the available 5-ASA brands to the site of disease, thus choosing the optimum formulation for their patients (Forbes et al., 2003).

It is noteworthy that the standard deviation error bars of drug release are so wide both within and between batches of the different preparations. These variations may be attributable to the intra-brand differences in coating thickness. Intra-brand dissolution

variations in phosphate buffers have been documented by several sources (Lund, 1994; Ivax Pharmaceuticals, 2003; Sandoz, 2003).

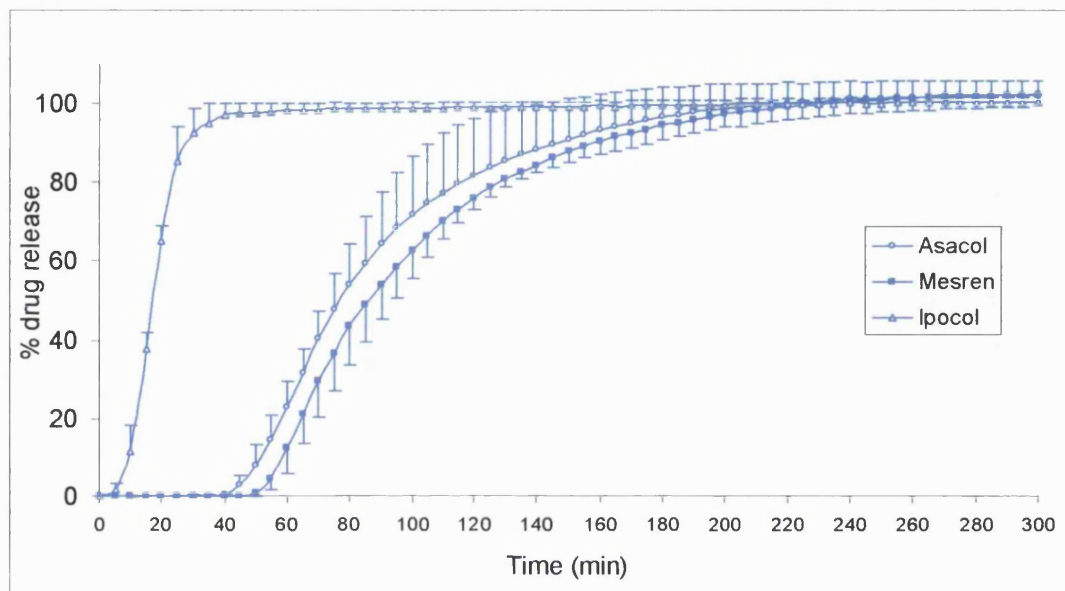


Figure 2.3 Comparative dissolution profiles of Asacol, Mesren and Ipocol tablets in 0.05M phosphate buffer pH 7.4, expressed as mean +SD.

2.4.2 Solubility of 5-aminosalicylic acid in different phosphate and bicarbonate buffers and the implications on drug release from pH-responsive systems

Table 2.3 shows how 5-ASA solubility varies with buffer type and molarity. According to the Noyes-Whitney equation (Equation 1.1), drug solubility in the medium influences its dissolution rate. Since the dissolution rate is proportional to the difference between the concentration of solute, C_s , required to saturate the solution and the solute concentration, C , at any time point ($C_s - C$). Dissolution rate therefore slows down with time as the drug concentration approaches the saturation solubility. However the higher this saturation solubility the greater the difference will be

between it and the drug concentration in the release media at any time and therefore the faster the dissolution.

Table 2.3 Solubility of 5-aminosalicylic acid (mean \pm SD) in different buffers.

Buffer medium	5-aminosalicylic acid solubility (mg/ml)
0.002 M phosphate buffer	1.99 (\pm 0.048)
0.05 M phosphate buffer	6.34 (\pm 0.053)
0.2 M phosphate buffer	13.69 (\pm 0.079)
Hanks bicarbonate buffer	1.83 (\pm 0.043)
Krebs bicarbonate buffer	4.51 (\pm 0.067)

If 'sink conditions' exist, however, whereby the maximum concentration of drug in the dissolution medium does not exceed 20 % of its saturation solubility, then $C_s - C$, may be approximated to C_s . Assuming that $C < 0.2 C_s$, for a dosage form containing 400 mg of 5-ASA, sink conditions are attained in all buffer media used in this study, except Hanks buffer. In Hanks buffer, 20 % of C_s is 0.39 mg/ml, however the maximum concentration reached by a 400 mg 5-ASA tablet is 0.4 mg/ml (1000 ml is the dissolution volume used). Hence it is very close to sink conditions.

The next sections discuss how buffer composition of the dissolution medium alters dissolution rate of the pH-responsive system through influences on ionisation of the acrylic polymer. However ionisation of the polymer cannot be considered in isolation from the behaviour of the drug; any differences that arise are attributable to the system as a whole: drug and polymer.

The influence of drug solubility on the dissolution profile of the enteric coated dosage form is likely to come into play once the polymer has dissolved and drug release arises; i.e. post lag-time. Hence at the initial stages of the system's dissolution, polymer behaviour is more important. Further evidence for this polymer influence is given in chapter five, where the dissolution of Eudragit S coated prednisolone tablets is compared in phosphate and bicarbonate media. A large difference is observed between the dissolution profiles in the two media despite the same solubility of prednisolone in both media due to its non-ionisable character.

2.4.3 Dissolution in phosphate media of different buffer capacity and ionic strength

As depicted in figure 2.4, dissolution of Asacol tablets is faster in 0.2 M phosphate buffer compared to 0.05 M phosphate buffer. Adding NaCl to 0.05 M phosphate buffer (ionic strength: 0.129, β : 23 mM/L/ Δ pH unit) to bring its ionic strength up to the same level as 0.2 M buffer (ionic strength: 0.526, β : 58.8) mM/L/ Δ pH unit) increases the dissolution rate comparative to the 0.05M phosphate buffer, however dissolution is still slower than in the 0.2 M buffer. This indicates that both buffering capacity and ionic strength independently contribute to increasing the dissolution rate of Eudragit S coated formulations. Similar results were observed with Mesren, hence data not shown. This finding is in disagreement with that of Karali et al. (1995) which states that dissolution rate is increased to the same extent whether NaCl or phosphate are used to increase the ionic strength of the dissolution medium.

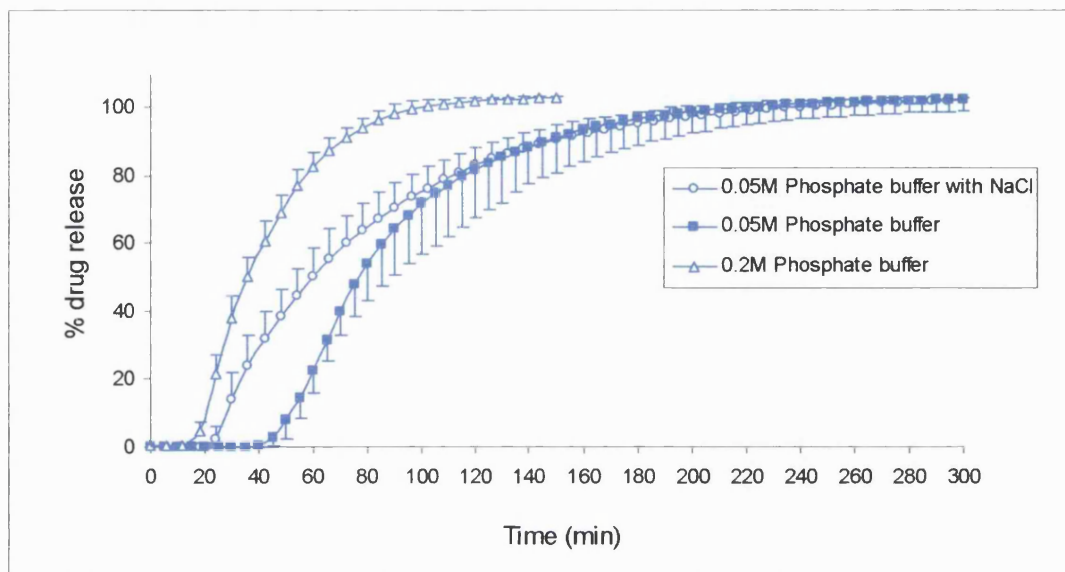


Figure 2.4 Drug release profiles of Asacol tablets in pH 7.4 phosphate buffers of varying buffer capacity and ionic strength, expressed as mean \pm SD

As for Ipecol (Figure 2.5), a difference also arises in its dissolution profile in 0.2 M phosphate buffer compared to 0.05 M buffer, however the difference is less drastic compared to Asacol; attributable to Ipecol's thinner enteric coating. Dissolution in 0.05 M phosphate buffer with NaCl closely resembles that in 0.05 M phosphate buffer alone. This may be that as the dissolution in 0.05 M phosphate buffer is rapid, adding NaCl may not noticeably alter the dissolution profile; despite that increasing buffer capacity does seem to result in an increase in dissolution rate. This may suggest that buffer capacity may have a more prominent influence compared to ionic strength on dissolution of this system.

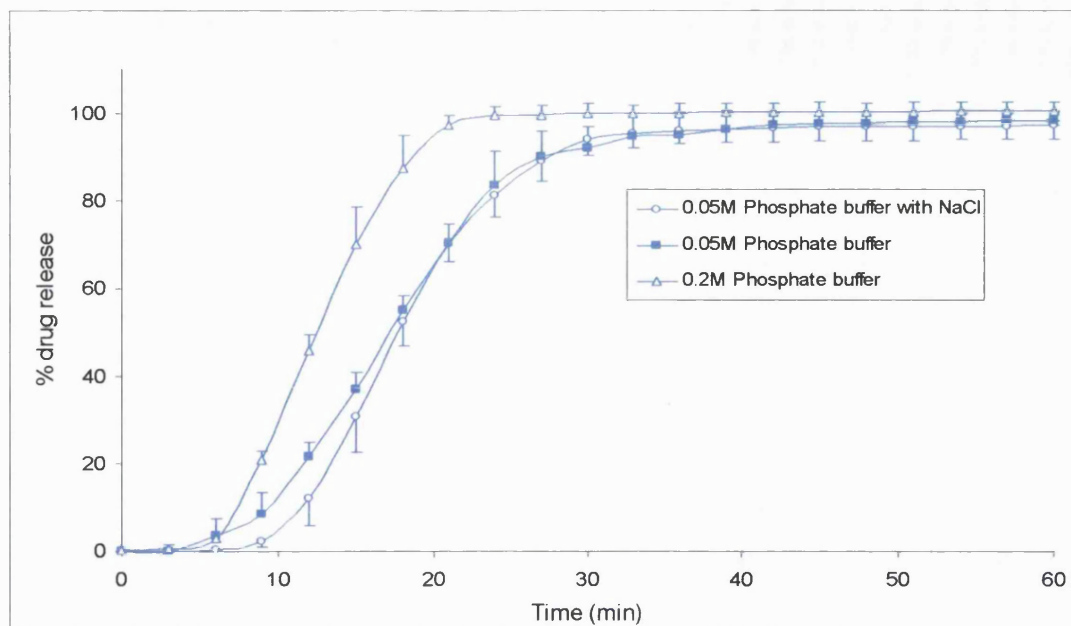


Figure 2.5 Drug release profiles of Ipol tablets in pH 7.4 phosphate buffers of varying buffer capacity and ionic strength, expressed as mean \pm SD.

As previously described one of the steps involved in enteric polymer dissolution is diffusion of ionised disentangled polymer chains away from the polymer interface and into the bulk solution (Nguyen and Fogler, 2005). Two diffusion processes are generally reported for ionic polymers: slow diffusion process whereby the polymers diffuse as clusters and fast diffusion process which corresponds to the coupled diffusion of counterions (eg. hydrogen ions, sodium and potassium ions). The slow diffusive mode is dependent on polymer concentration, while both processes change with ionic strength. Charges on the ionised polymers can be screened by the presence of counterions thus reducing polymer repulsion. Attractive forces can give rise to multichain polymer domains. Furthermore, solution structure and dynamics are influenced by polyion-counterion interactions (Sedlak and Amis, 1992).

Raising the salt concentration may reduce the repulsion forces between the carboxylic groups of the monomer units thus softening the polymer film; this softening and erosion of the film will increase diffusion of drug through the polymer coat (Kararli et al., 1995). A further mechanism through which an increase in ionic strength may accelerate dissolution is through alteration of buffer pKa; change in the pKa influences reaction rate with the polymer.

Another example of the influence of buffer capacity on dissolution of enteric coated products is the work conducted using Sorensen's buffer as the dissolution medium (Figures 2.6 and 2.7). Sorensen's buffer has a phosphate content of 0.066 M and an ionic strength of 0.1737. The individual tablet dissolution profiles were found to be intermediate between that of 0.05 M and 0.2 M phosphate buffer.

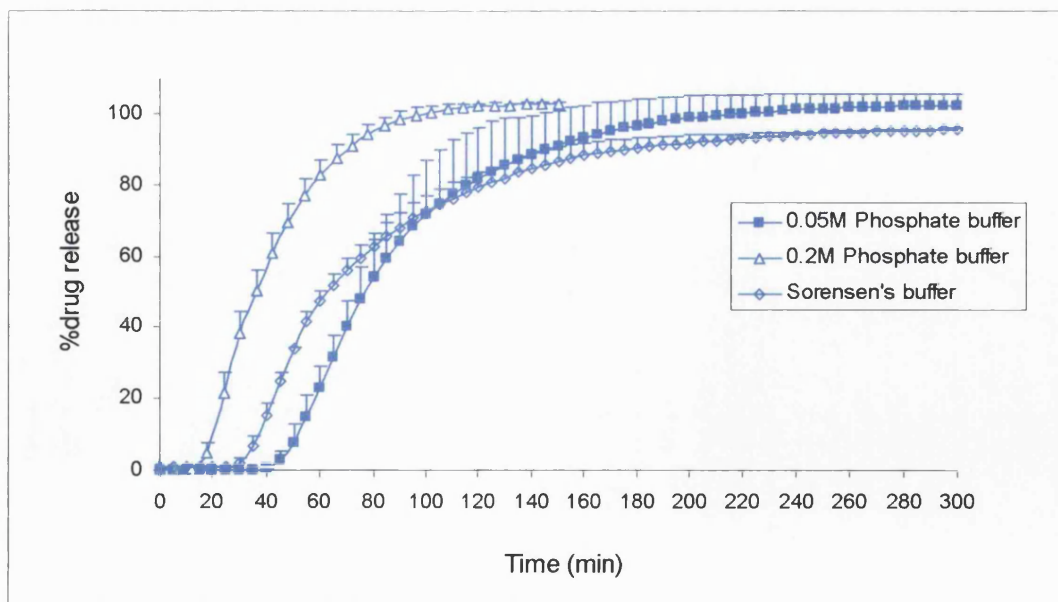


Figure 2.6 Drug release profiles of Asacol tablets in different pH 7.4 phosphate buffers of varying buffer capacity, expressed as mean \pm SD.

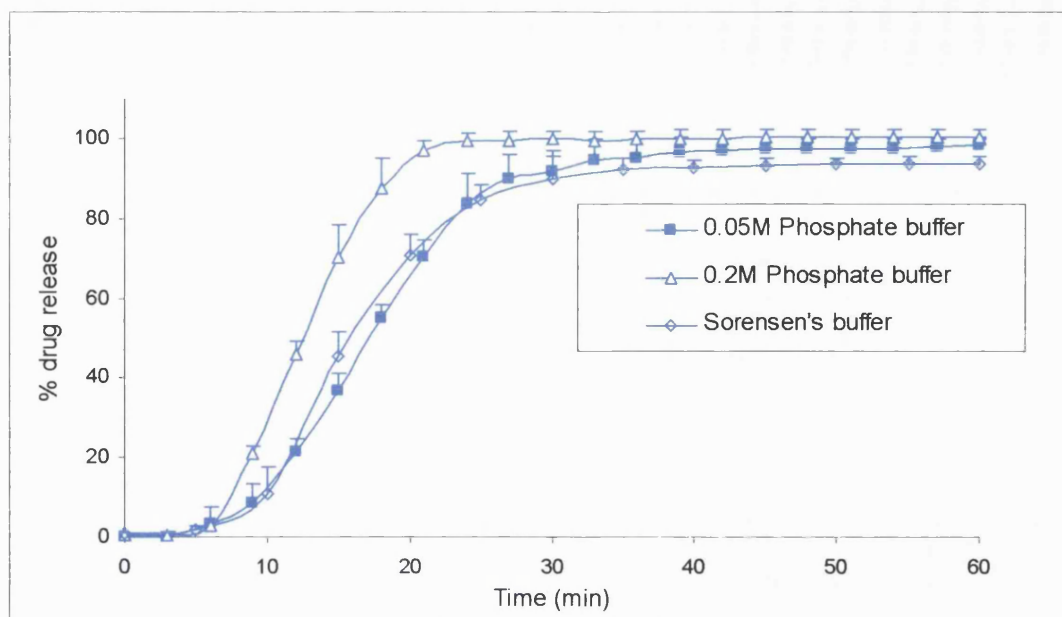


Figure 2.7 Drug release profiles of Ipecol tablets in different pH 7.4 phosphate buffers of varying buffer capacity, expressed as mean \pm SD.

2.4.4 Dissolution in physiological bicarbonate buffers

It is evident from figure 2.8 that the dissolution profiles of the Eudragit S coated tablets is substantially slower in Hanks physiological buffer compared to phosphate buffers. Lag-times in Hanks buffer are 3.5 hours and 50 min for Asacol and Ipecol respectively. The lag-times in 0.05 M phosphate buffer, however, are 45 min and 5 min for Asacol and Ipecol respectively. The dissolution profiles of Asacol and Mesren tablets are also similar in physiological buffers. This is in agreement with the finding by Chan et al. (2001) who reported a slower dissolution of Eudragit S coated dosage forms in Hanks buffer compared to compendial phosphate buffer. Interestingly, Dressman's biorelevant medium to simulate the small intestinal fluid in terms of surfactant composition (Dressman et al., 1998) was not found to influence the dissolution profile of Eudragit S coated 5-ASA dosage forms (Rudolph et al.,

2001); the release observed was the same as that in compendial phosphate buffer. Hence, simulating intestinal surfactant composition alone with no attention to buffer components does not improve prediction of the *in vivo* behaviour of pH responsive formulations.

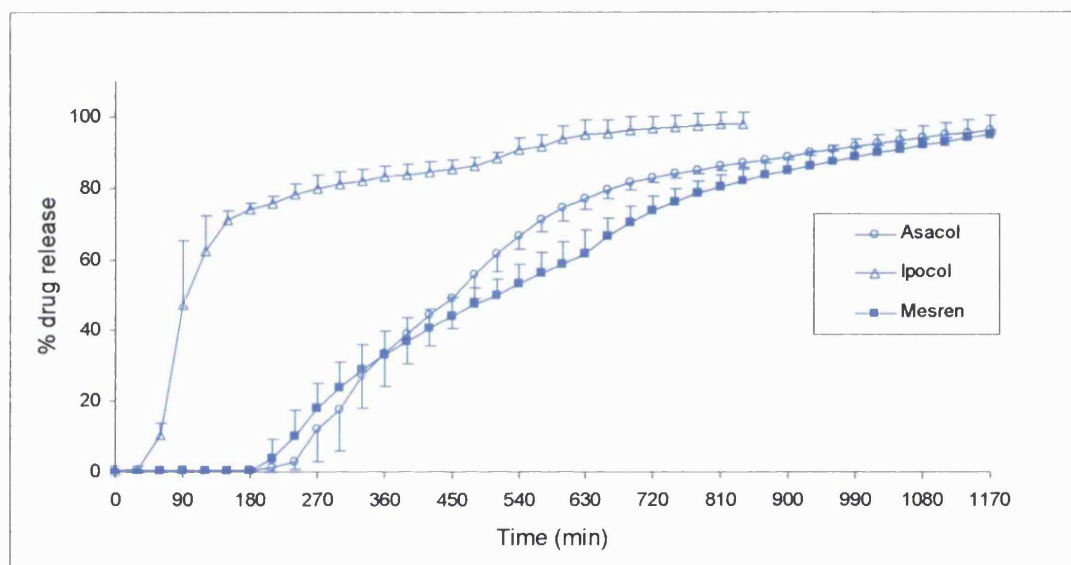


Figure 2.8 Comparative dissolution profile of Asacol, Mesren and Ipocol in tablets in physiological Hanks buffer, expressed as mean \pm SD.

Drug release in the physiological buffers, Krebs and Hanks, was compared to find if using different physiological buffers as dissolution media gives varying release profiles. From figures 2.9 and 2.10, it is evident that the dissolution profiles are faster in Krebs buffer compared to Hanks. Two profiles are shown for Krebs buffer; Krebs stabilised with CO₂ (g) and Krebs without CO₂ (g) stabilisation. Reasons for these different dissolution profiles that arise with and without CO₂ are discussed in section 2.4.4.

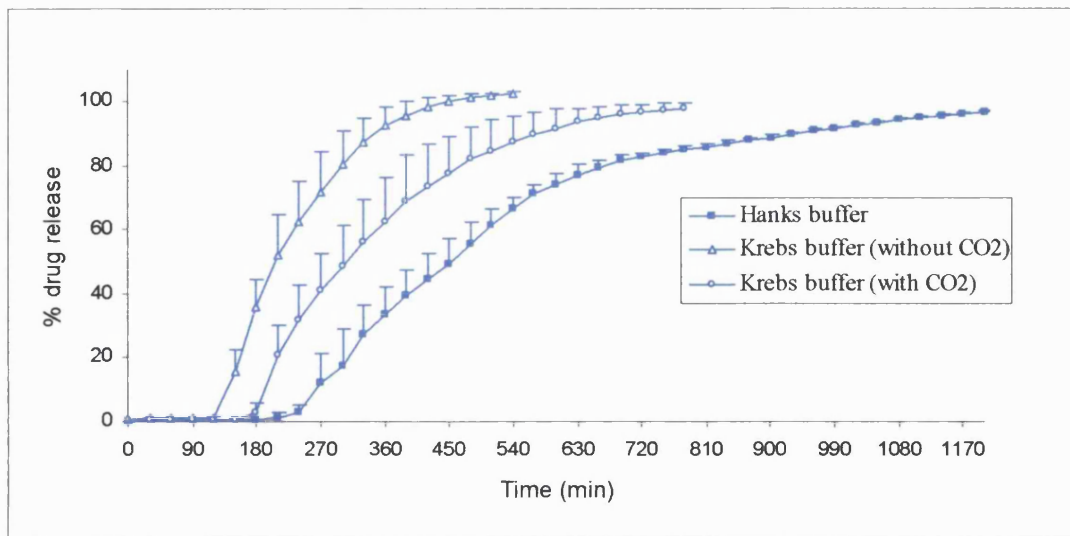


Figure 2.9 Comparative dissolution profiles of Asacol tablets in Hanks and Krebs buffers (with CO₂(g) stabilisation and without CO₂(g) stabilisation), expressed as mean ± SD.

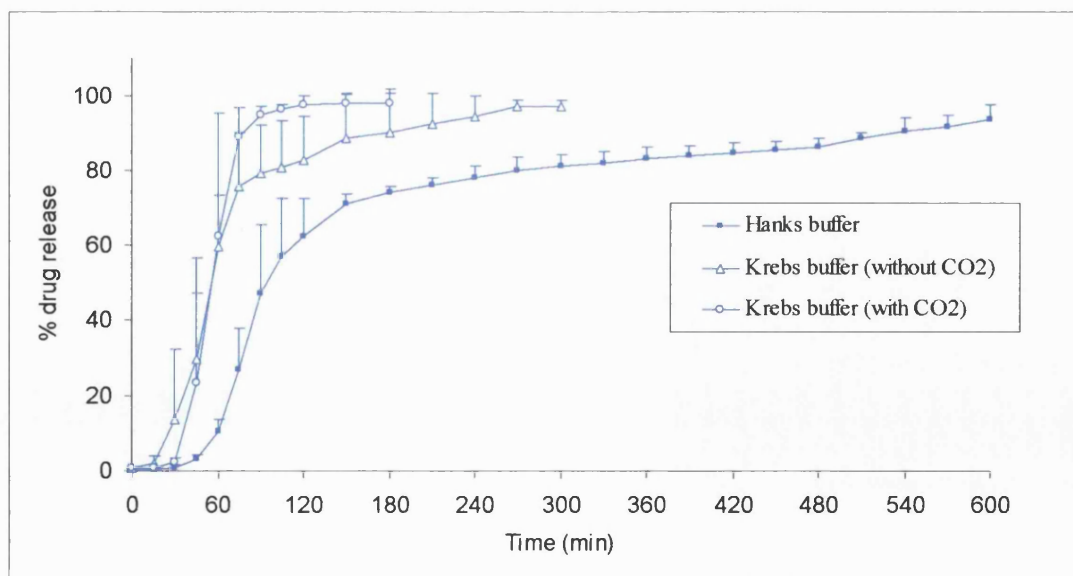


Figure 2.10 Comparative dissolution profiles of Ipolcol tablets in Hanks and Krebs buffers (with CO₂(g) stabilisation and without CO₂(g) stabilisation), expressed as mean ± SD.

The two physiological buffers have similar ionic strengths however different bicarbonate content of 25 mmol/L and 4.17 mmol/L for Krebs and Hanks respectively. Consequently the buffer capacity of Krebs is greater than that of Hanks at 3.7 mmoles/L/pH unit and 1 mmol/L/pH unit respectively. These buffer capacity values are in general agreement with those achieved by Levis et al. (2003) who investigated the effect of buffer media composition on solubility and permeability of ibuprofen. The pH of the boundary layer (that is the pH adjacent to the surface of the dissolving solid) is crucial in determining the dissolution rate, however it can be quite different from the bulk pH depending on the buffer capacity of the dissolution media (Ozturk et al., 1988b; Horter and Dressman, 2001). 5-ASA is an amphoteric molecule, the COOH (carboxyl) group of 5-ASA has a pKa value of 2.30 and the (NH₃⁺)- (amino) group has a pKa of 5.69 (Allgayer et al., 1985). The ionization and solubility characteristics are dependent on the pKa of the drug and the pH of the solution. At higher pH values, 5-ASA reacts with the buffer species, B⁻, and its anionic form is generated. Hence it dissolves and dissociates generating hydrogen ions which lower the pH of the boundary layer (French and Mauger, 1993). A dissolution medium with a low buffer capacity will retard drug dissolution as the low pH environment deters formation of the anionic species. Furthermore, a reduction in pH will also reduce ionization of the methacrylic acid monomer units thus retarding dissolution of the enteric coat. This buffer capacity influence, however, is likely to come into play once drug dissolution starts to occur (i.e. following the lag-time).

2.4.5 Bronsted catalysis law

The explanation for the shorter dissolution lag time observed in Krebs compared to Hanks buffer is the Bronsted catalysis law theory proposed by Spitael and Kinget (1977a). Eudragit S dissolves through the dissociation of its acid monomer units (R-COOH) by proton transfer to the base H₂O, forming conjugate base of the polymer and hydronium ions (Figure 2.11a). Figure 2.11a is a summarised mechanism; more intermediate steps and proton transfers are involved.

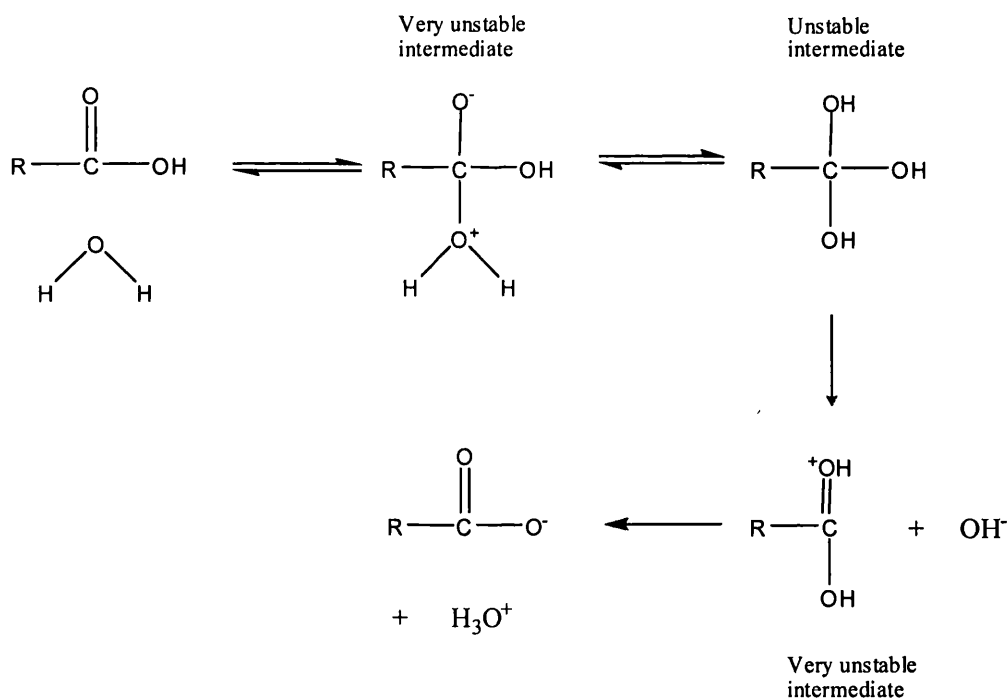


Figure 2.11a Mechanism of ionisation of Eudragit S. Adapted from Bender and Brubacher (1973).

The second structure formed in figure 2.11a is a very unstable intermediate and the charge accumulation that arises is energetically unfavourable. However in the

presence of a basic salt (B^-), such as phosphate (PO_4^{2-}) or bicarbonate (HCO_3^-), the base accepts a proton from the water molecule thereby diffusing the build up of charge and reducing the free energy of activation, thus accelerating the reaction (Figure 2.11b). Hence the oxygen atom of the water molecule now has a greater share of the electrons that formed part of the bond of the leaving proton. It is now more negatively charged and its potential to donate an electron pair to form a new bond with the carbonyl carbon atom is augmented (Bender and Brubacher, 1973). In effect the base accelerates the proton transfer and a general base catalysis mechanism operating.

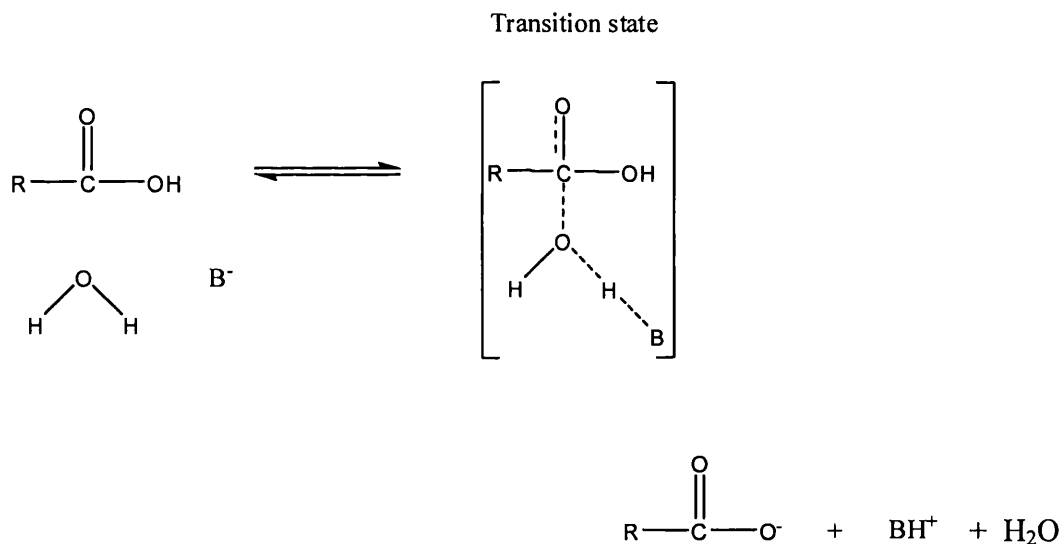


Figure 2.11b Ionisation of Eudragit S in the presence of a basic salt (B^-). (Intermediate steps of proton transfer have not been shown.)

The above mechanisms explain why dissolution rate increases with increasing pK_a of the basic salts (note that pK_a increases with increasing strength of the conjugate base). pK_a values of $H_2PO_4^-$ and HCO_3^- buffers are 7.2 and 6.4 respectively. The total rate of the reaction can be given by equation 2.3 (Bender and Brubacher, 1973).

$$\text{Rate} = (k_0 + k_{\text{cat}} [\text{catalyst}]^n)[\text{S}]$$

Equation 2.3

k_0 = 1st order rate constant

k_{cat} = catalytic rate constant

n = the number of catalyst molecules that participate in the rate determining step

[catalyst] = catalyst concentration

[S] = substrate concentration

From this equation it can be deduced that the relative efficiency of the catalyst is reflected in k_{cat} which increases with increasing strength of the conjugate base. Furthermore, the rate of the reaction is proportional to the concentration of the base; thus explaining the faster dissolution obtained in Krebs compared to Hanks buffer.

This theory is in agreement with the general principle proposed recently by Nguyen and Fogler (2005) whereby the buffer species is described as a ‘diffusion promoter’ as it facilitates the transfer of protons (produced by ionisation of the carboxylic acid groups) from the polymer interface towards the bulk solution. Therefore enhancing polymer ionisation and diffusion.

Further evidence for the Bronsted catalysis law is the dissolution profile observed in 0.00217 M phosphate buffer, which has a buffer capacity equivalent to that of Hanks. On conducting a dissolution test of Asacol tablets in this buffer it was observed after 24 hours that the enteric film coat was still intact and retained its original dimensions. Although 5-ASA release did occur during this period (data not shown), it is likely to have been through hydration of the enteric coat and diffusion of the drug through it (Ebel et al., 1993). This justifies that dissolution is not merely dependent on ionic

strength and buffer capacity, however the identity of the basic salt and its concentration are also determining factors.

The importance of identity of the buffer species is corroborated by the faster dissolution rate of Asacol tablets in 0.025 M phosphate buffer in comparison to 0.025 M bicarbonate buffer (Krebs) (Figure 2.12). According to the Bronsted catalysis law phosphate buffer has a higher K_{cat} than bicarbonate buffer due to its higher pKa, 7.2 *versus* 6.4 respectively, and would therefore be expected to give rise to a faster dissolution rate. Moreover the pKa of phosphate buffer is closer to the pH of the solution (pH 7.4). These two arguments explain the higher efficiency of phosphate buffer at facilitating proton transfer from the polymer interface to the bulk solution. It would be of interest to explore a range of buffers with different pKa values to determine which is more important the absolute buffer pKa value or the magnitude of its difference from the solution pH.

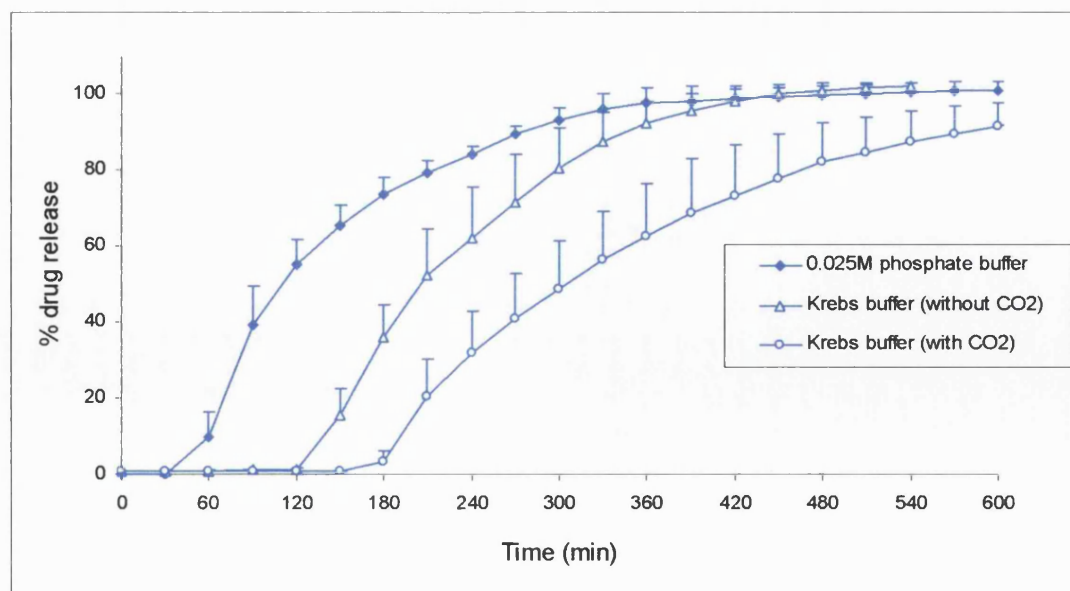


Figure 2.12 Comparative dissolution profiles of Asacol in Krebs buffer (in presence and absence of CO₂(g)) and in 0.025 M phosphate buffer with the same ionic strength, expressed as mean \pm SD.

2.4.5 Stabilisation of the physiological bicarbonate buffers

Physiological bicarbonate buffers are inherently unstable, and so overtime there is an increase in the pH reaching approximately 7.6 after five hours. There is a need to stop this upward drift in pH; gassing the buffers with CO₂ was the approach adopted for Krebs buffer. Dissolution of Asacol tablets in Krebs buffer is faster without sparging with CO₂ (Figure 2.8). Sparging with CO₂ maintains the gas's concentration at constant levels throughout the dissolution test and therefore H₂CO₃ dissociation to CO₂ and H₂O is unfavourable in accordance with the equilibrium illustrated in Figure 2.2. Since H₂CO₃ levels are maintained, HCO₃⁻ levels are also maintained as its protonation to yield H₂CO₃ is no longer promoted (Figure 2.2). However in the absence of CO₂ sparging, the gas evaporates from solution and therefore the decomposition of H₂CO₃ proceeds to restore the CO₂(aq) levels. In turn, the protonation of HCO₃⁻ is promoted. This change in the equilibrium of the system results in a rise in pH which renders faster dissolution.

Sparging Krebs buffer with 5% CO₂ gives rise to different results in Asacol and Ipcol tablets (Figures 2.9 and 2.10). For Ipcol, the release profiles in Krebs buffer with and without CO₂ gas overlap and no difference exists. The reason for Asacol tablets dissolving differently in Krebs buffer in the presence and absence of CO₂ gas, in contrast to Ipcol, may be due to the long lag-time of Asacol (130 minutes) during which the pH of Krebs buffer rises leading to a faster onset of dissolution compared to the presence of CO₂ where the pH is maintained constant. In comparison to Asacol, Ipcol has a much shorter lag time.

Ideally one would compare Krebs and Hanks in the presence of CO₂ gas, however there was difficulty achieving this due the low bicarbonate content of the latter. Nevertheless, one would not expect the presence of CO₂ gas to have a drastic influence in Hanks buffer since the bicarbonate concentration in Hanks buffer is very low (4.17 mM) leading to a slow rate of protonation to carbonic acid and consequent hydration to CO₂ and H₂O. This has been illustrated with the buffer capacity of Hanks remaining constant for 6 hours from the time of preparation and only decreasing slowly thereafter. A stable buffer capacity indicates stable levels of the buffer species, i.e. HCO₃⁻.

Stability of Hanks buffer was achieved for at least 24 hours by the addition of 5 mM of HEPES. However the disadvantage of this approach is that an artificial buffering reagent is added thus compromising the physiological nature of the system. Furthermore, the dissolution rate of Asacol in the presence of HEPES is much faster with a shorter lag time and T_{50%} (Figure 2.13). It will therefore be difficult to attain a good *in vitro/in vivo correlations* using this approach.

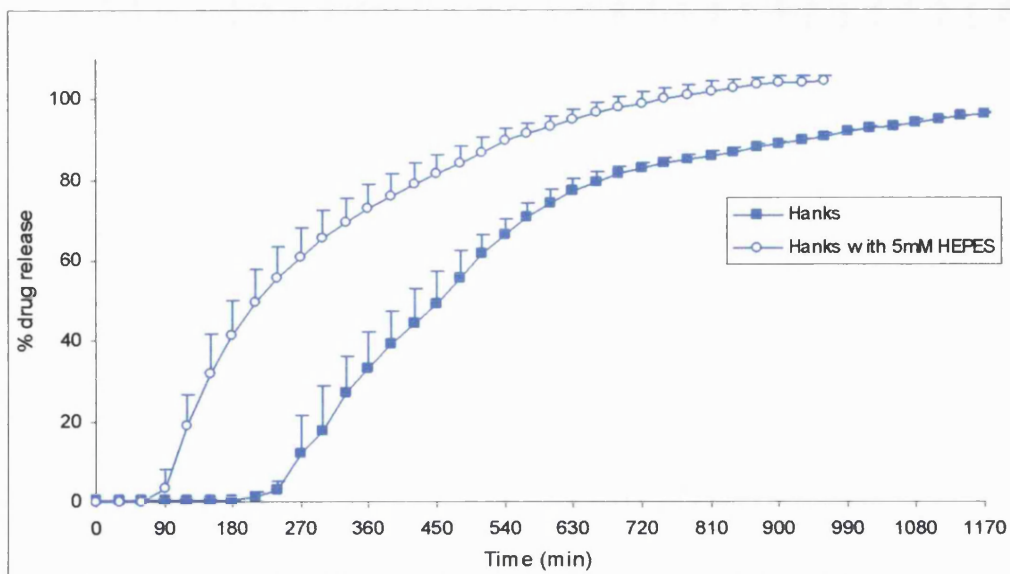


Figure 2.13 Dissolution profile of Asacol in Hanks buffer in the absence and presence of 5 mM HEPES, expressed as mean \pm SD.

2.4.6 Equivalent physiological bicarbonate buffers

Having established the importance of ionic strength, buffer capacity, buffer species and their concentration on dissolution behaviour of Eudragit S coated tablets, it was desirable to determine whether the other electrolytes in GI luminal fluid influence release profiles. The dissolution of Asacol, Mesren and Ipecol tablets in the physiological buffers and their equivalent forms (lacking K^+ , Mg^{2+} , SO_4^{2-} and Ca^{2+}) were found to be superimposable (refer to figure 2.14 for an example). Hence it can be concluded that buffer salts (phosphate and bicarbonate) govern the dissolution of enteric coated tablets; the remaining salts that constitute the physiological buffers (KCl , $MgSO_4$ and $CaCl_2$) do not influence dissolution of the coat.

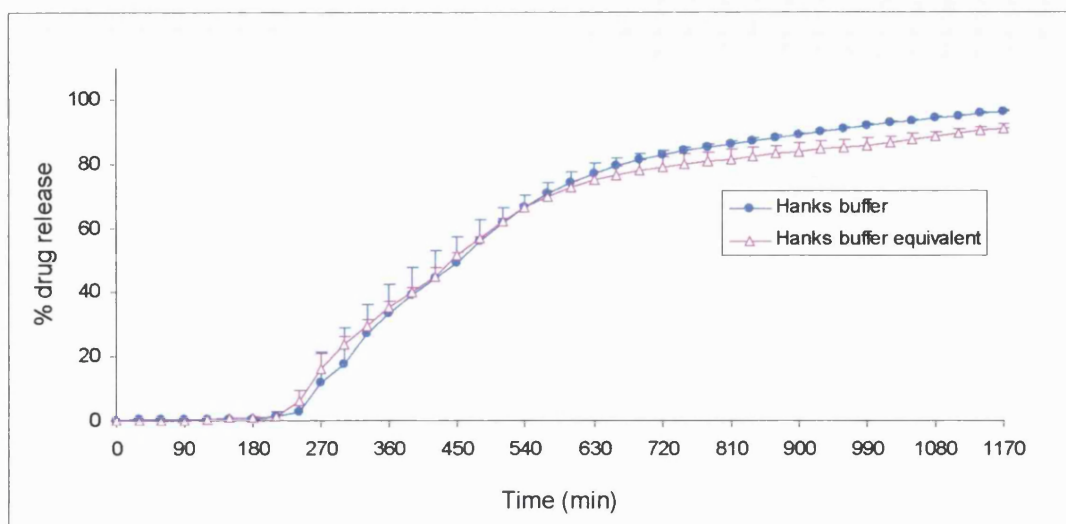


Figure 2.14 Comparative dissolution of Asacol tablets in Hanks and equivalent Hanks buffer (not containing KCl, MgSO₄ and CaCl₂). Results expressed as mean ± SD.

2.4.7 Subjecting Eudragit S coated tablets to a pH transition

The Eudragit S coated tablets were also subjected to a pH transition from acid to pH 6.8 buffer to pH 7.4 buffer. For Asacol and Mesren, this pH gradient gave rise to similar dissolution profiles as direct testing in pH 7.4 buffer. This finding applies to both physiological and phosphate buffers (refer to figure 2.15 for an example). No media uptake was found to occur by the tablets, thus offering a possible explanation as to why dissolution was unaffected. Ibekwe et al. (2006a) however found that drug release of enteric coated tablets in buffer media was influenced by the duration of tablet exposure to acid. These different findings may be attributable to the different tablet formulations of the two studies. As for Ipocol, dissolution of the coating appeared to start at the edges of some of the tablets in 0.1 M HCl. In pH 6.8 buffer, dissolution was noticeable throughout the coat of all tablets.

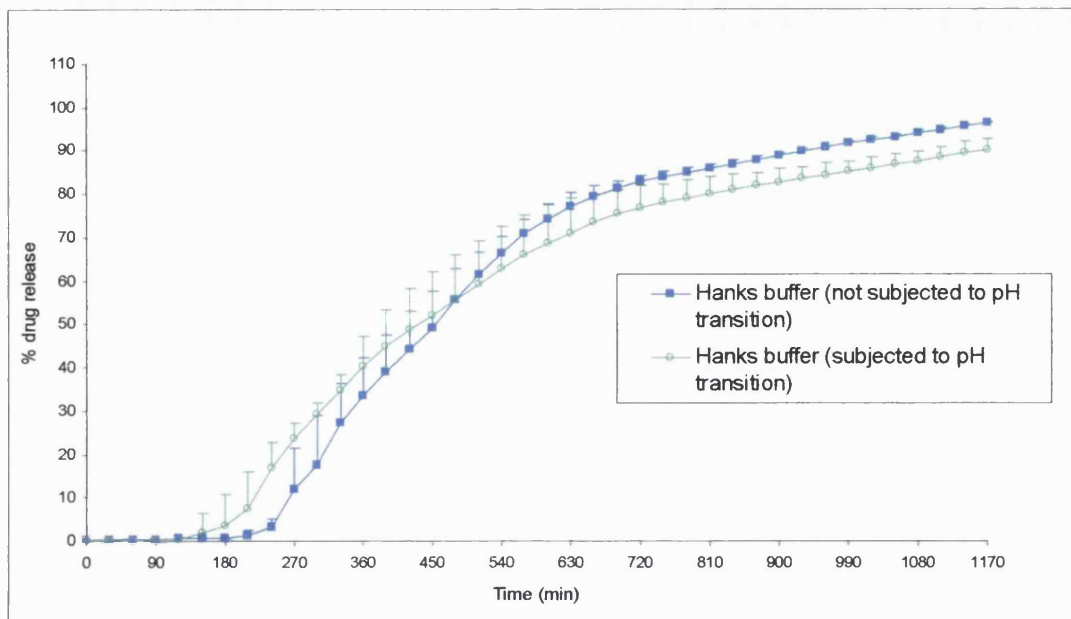


Figure 2.15 Comparative dissolution of Asacol tablets tested directly in pH 7.4 Hanks buffer or following a transition from 0.1 M HCl to pH 6.8 buffer (transition media not shown), expressed as mean \pm SD.

2.4.8 Influence of ionic composition on drug release from sustained release ethylcellulose granules

The previous sections have focused on drug release from pH-responsive systems; now we consider the same drug however from a system which has a different release mechanism. On contact with fluid, Pentasa tablets rapidly disintegrate into discrete granules which have an ethylcellulose coating. 5-ASA release is controlled by diffusion of the drug through the ethylcellulose film. Ethylcellulose is a non-ionic, water-insoluble polymer. Interestingly, a large difference exists between the dissolution profile of Pentasa in phosphate compared to Hanks buffer (Figure 2.16).

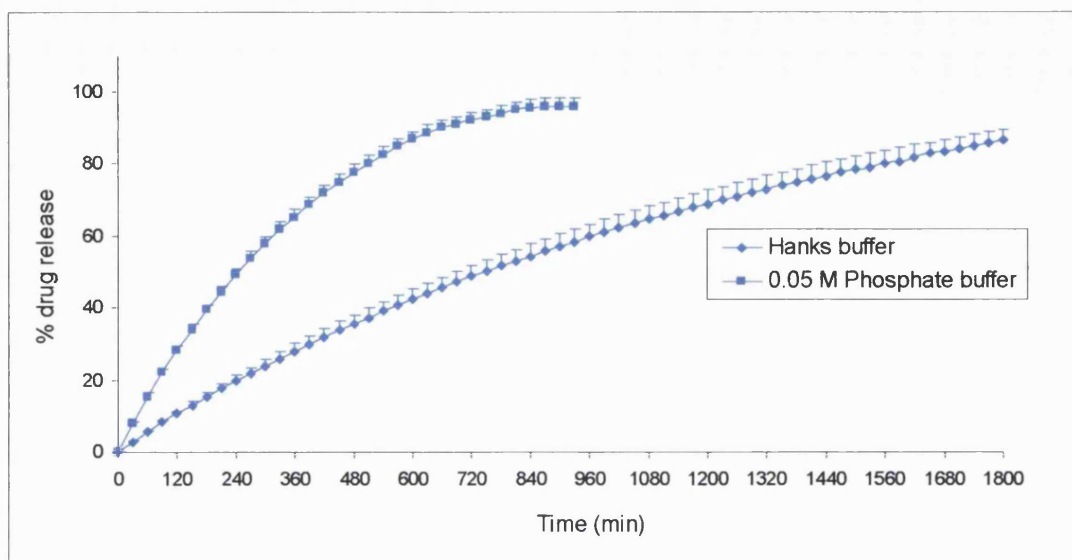


Figure 2.16 Comparative dissolution profiles of Pentasa tablets in phosphate and Hanks bicarbonate buffers, expressed as mean \pm SD.

While hydroxypropylmethylcellulose (HPMC) is another cellulose ether polymer (Figure 2.17) utilised in modified release coatings it has a different mechanism of controlling drug release to that of ethylcellulose. HPMC undergoes hydration and swelling and is sensitive to ions. Ions have a greater affinity for water in comparison to HPMC and therefore exert a 'salting out' effect and dehydrate the polymer retarding its swelling (Lapidus and Lordi, 1968). Ethylcellulose, however, does not undergo this hydration and swelling and so is less likely to be sensitive to the ionic composition of the release medium.

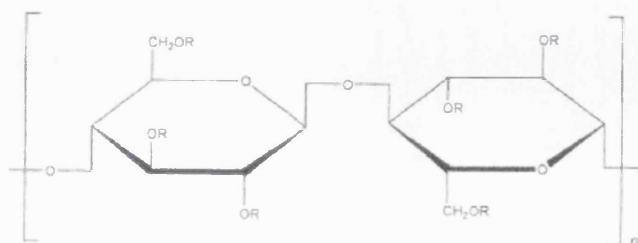


Figure 2.17 Structural formula of substituted cellulose.

For Hydroxypropyl methylcellulose (HPMC) the substituent groups are: H, CH₃, or CH₃CH(OH)CH₂. For Ethylcellulose the substituent groups are H, CH₂ CH₃

As previously discussed, 5-ASA is an ionic drug and its solubility and dissolution are influenced by the buffer composition of the dissolution media. Figure 2.18 shows the dissolution of 5-ASA powder in 0.05 M phosphate and Hanks buffers. The dissolution is very fast initially in both media however after 50 % drug release it becomes substantially slower in Hanks buffer. The buffer media composition seems to have a greater affect on Pentasa than on 5-ASA powder. It can be speculated that the much slower release in Hanks buffer arises due to the pH at the polymer/ solution interface being lower than the bulk solution pH thus retarding diffusion of the acidic drug out of the granule core. Additionally, the grade of ethylcellulose used in Pentasa may have a bearing on its sensitivity to ions. The greater the degree of substitution of the ethylcellulose polymer the more water will be retained by the binding to its hydroxyl groups (Hjartstam and Hjertberg, 1999).

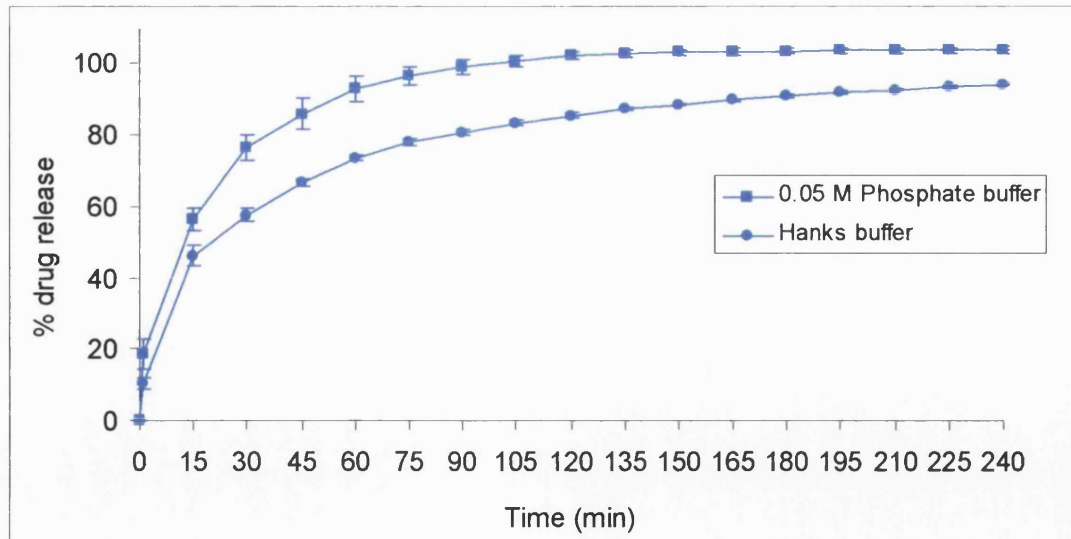


Figure 2.18 Dissolution of 5-aminosalicylic acid drug powder in phosphate buffer and Hanks bicarbonate buffer, expressed as mean \pm SD.

2.4.9 Comparison of in vitro drug release with published in vivo data and implications on the choice of formulation

Several studies have been conducted using gamma scintigraphy in humans to visualise the intestinal transit of enteric coated tablets for ileo-colonic delivery (Sciarretta et al., 1993; Ashford et al., 1993; Wilding, 2000; Sinha et al., 2003; Ibekwe et al., 2006b). Results show a large intra- and inter-individual variability in tablet initial disintegration times. A study of Asacol showed the average time of initial disintegration to be 7 hours post-dose with a standard deviation of 2.3 hours and range of 4-10 hours; initial release occurred in the terminal ileum or beyond in all subjects (Sinha et al., 2003). The appearance of intact tablets in patients' faeces has even been reported (Schroeder et al., 1987). Ashford et al's (1993) *in vivo* study using rapidly disintegrating tablets coated with Eudragit S also showed variable positions and times of release. *In vivo* variations in tablet disintegration are likely to be attributable to variations in small bowel transit time and pH level.

The use of physiological bicarbonate buffers as dissolution media provides a better reflection of the prolonged initial disintegration times of enteric coated tablets compared to that found in phosphate buffers. This can be explained by the similar ionic strength and ionic composition, particularly of the buffer salts, between the bicarbonate buffers and small intestinal luminal fluids. The buffer capacity of the physiological salts is relatively low compared to phosphate buffers, further resembling GI luminal fluids. The limited buffering capacity of the gut is illustrated in a study conducted by Dressman and Amidon (1984), whereby enteric coated tablets containing buffered cores at pH 3, 4 and 5 were administered to dogs. Tablet

disintegration resulted in a pH drop in the upper small intestine due to release of buffer.

The dissolution profile of Pentasa in Hanks buffer is also more representative of the drug release pattern observed *in vivo*. Pharmacokinetic studies in man have measured plasma and small intestine luminal concentrations of 5-ASA and its metabolite acetyl 5-ASA. Post-prandial oral administration of 500 mg Pentasa tablets showed that approximately 80% of the dose was delivered to the colon (Layer et al., 1995); the rest being released in the jejunoileal region. The small intestinal transit time of Pentasa microgranules has been found to be 3 – 4 hours by gamma scintigraphy studies (Wilding et al., 2000). From figure 2.16 it can be seen that ~ 50% of the drug dose is released in phosphate buffer after four hours, however less than half this dose (20%) is released in Hanks buffer. Therefore bicarbonate buffers provide a more realistic insight into Pentasa intestinal delivery patterns.

Pentasa microgranules have been shown to spread over the whole length of the large bowel (Wilding et al., 2000). 5-ASA release therefore occurs over the entire region. Asacol however shows variations in site of disintegration; in some individuals complete disintegration has been observed in the small intestine while in others it only started in the transverse colon. It therefore holds the risk of failing to deliver drug to the inflamed regions of the intestine. Moreover, drug release from Asacol is more susceptible to physiological parameters such as pH, transit time and water availability for dissolution of its coating. If these conditions are sub-optimal drug release from Asacol is likely to be severely compromised. For instance, in one quarter of healthy individuals a pH of 7 is not reached in the small or large intestine (Fallingborg et al.,

1989), and in a similar proportion of ulcerative colitis patients, a luminal pH > 7 was only maintained for less than 30 min (Raimundo et al., 1992). A fall in colonic pH to less than 5.5 was found in two out of six patients with active ulcerative colitis (Nugent et al., 2000). Proximal colonic pH values as low as 2.3 have been detected by Fallingborg et al. (1993).

It has also been shown by our group that the length of exposure of Eudragit S coated tablets to the correct pH may also be a limiting factor; i.e. transit times in the terminal ileum and stagnation at the ileocaecal junction (Ibekwe et al., 2007). The limited fluid availability in the distal gut, particularly its inhomogeneity will present a greater problem for large single unit dosage forms in comparison to multiple unit systems due to its smaller surface area.

2.5 CONCLUSIONS

This work has highlighted the importance of defining the ionic composition of dissolution media when determining the drug release profile of pH responsive dosage forms. Outlining the pH value alone is not sufficient and can give rise to misleading results. Ionic strength, identity of the buffer species and their concentration are all critical factors. Simply by using media that better simulate the buffer components of small intestinal luminal fluids a better reflection of *in vivo* dissolution times can be achieved. The above findings can be extrapolated to other systems with pH-responsive polymers as they all have the same underlying step for dissolution; ionisation of acidic functional groups.

As discussed in chapter one, there remains to be numerous other GI parameters that need to be simulated *in vitro* to achieve better predictions of the *in vivo* behaviour of pH-responsive dosage forms. Only one study has investigated the influence of intestinal surfactants on dissolution of these systems and therefore this warrants further work under different conditions. It would be interesting, for example, to prepare a dissolution medium that combines bicarbonate buffers and intestinal surfactants. It is also of importance to prepare bicarbonate buffers at different pH values without resorting to the addition of external buffer salts. Thus transition of dosage forms through pH gradients of purely physiological buffers can be performed.

The ionic and buffer composition of colonic luminal fluids remain to be characterised, including the surface tension. The distal GI tract is certain to have an elevated

viscosity due the efficient water reabsorption that occurs and the presence of resistant starches and non-starch polysaccharides.

While in this chapter we have looked at the behaviour of the pH-responsive system as a whole, in the next chapter we focus on the drug itself and its solubility in different media. We measure drug solubility in human intestinal fluids and correlate the results to our physiological media.

CHAPTER THREE

A comparison of drug solubility in human jejunal and ileostomy fluids with physiologically relevant media: the relative importance of buffer composition and intestinal surfactants

3.1 INTRODUCTION

We have shown in the previous chapter how dissolution media composition influences the ionisation of pH-responsive polymers; in the context of drug release from enteric coated dosage forms. In this part of the study we focus on the drug and its physicochemical characteristics in relation to its solubility in different physiological media. The solubility of a drug is a major determinant of its dissolution rate and of the proceeding diffusion from the dosage system.

Drug solubility is one of the two factors, the other being permeability across GI mucosa, that are used by the biopharmaceutics classification system (BCS) to characterise drugs into one of four different groups for prediction of bioavailability (Amidon et al., 1995). Suffice to say that solubility is a vital measurement for any chemical entity.

3.1.1 Physicochemical properties of 5-aminosalicylic acid and prednisolone

Solubility is dependent on the drug's physicochemical properties and the composition of the dissolution medium. Here we investigate the value of physiological media in predicting drug solubility in GI fluids. Two drugs are studied, 5-aminosalicylic acid (5-ASA) and prednisolone. A summary of their physicochemical properties is given in table 3.1. Here their solubility is compared in a range of phosphate and bicarbonate buffers and in media containing intestinal lipids and surfactants, i.e. fasted state simulated intestinal fluid (FaSSIF) (Galia et al., 1998) to solubility in human jejunal

fluids aspirated from healthy volunteers and ileosotmy fluids from inflammatory bowel disease patients.

Table 3.1 Aqueous solubility, lipophilicity and ionisation constants of 5-aminosalicylic acid and prednisolone.

	5-aminosalicylic acid (5-ASA)	Prednisolone
Intrinsic solubility ^a (mg/ml)	1.32	0.223
pKa	2.3 and 5.69 ^b	N/A
Log P	0.98 ^c	1.59 ^d

^aSolubility in water at 37 °C (measured in our laboratory)

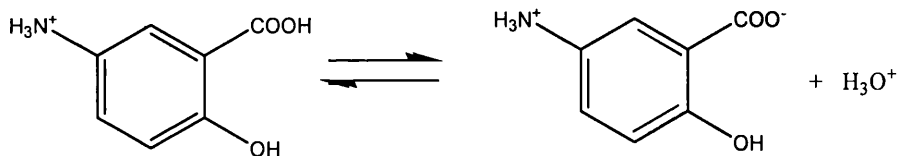
^bFrench and Mauger (1993)

^cNational library of medicine (2007)

^dMachatha and Yalkowsky (2005)

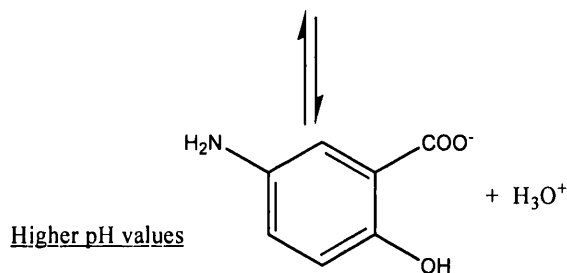
5-ASA and prednisolone are classified as slightly soluble and very slightly soluble respectively by the British Pharmacopoeia. However this classification is in aqueous media and will therefore be different in gut luminal conditions. Furthermore, the luminal environment is complex and the pH, buffer capacity, surfactant concentration, fluid volume and viscosity can vary greatly in different regions of the gastrointestinal tract (Dressman et al., 1998). 5-ASA is an amphoteric drug; carboxyl group has a pKa value of 2.30 and the amino group has a pKa of 5.69 (French and Mauger, 1993). At low pH values, the COO⁻ group of the zwitterionic compound (+A-) reacts with the buffer species, BH, generating the cationic form of the drug (+Ao) and B⁻ (Figure 3.1). At higher pH values, the NH₃⁺ group of the drug reacts with the buffer species, B⁻, generating the anionic form of the drug (oA-) and BH.

Lower pH values



(+A_o) Cationic species predominate at pH values < pI.

(+A⁻) Dipolar species predominate at pH values near the pI.



Higher pH values

(oA⁻) Anionic species predominate at pH values > pI.

Figure 3.1 Ionization of 5-aminosalicylic at different pH values. Adapted from French and Mauger (1993).

Solubility of 5-ASA was measured in unbuffered water at different pH values attained by adjustment with HCl or NaOH. The experimental solubility versus pH was found to have a U-shape whereby solubility increases at acidic values (pH <2.0) and more basic values (pH >5.5), corresponding to the ionization of the functional groups (Figure 3.2). At pH values between 2.0 and 5.5, solubility was found to be minimal due to the presence of only the dipolar species (French and Mauger, 1993).

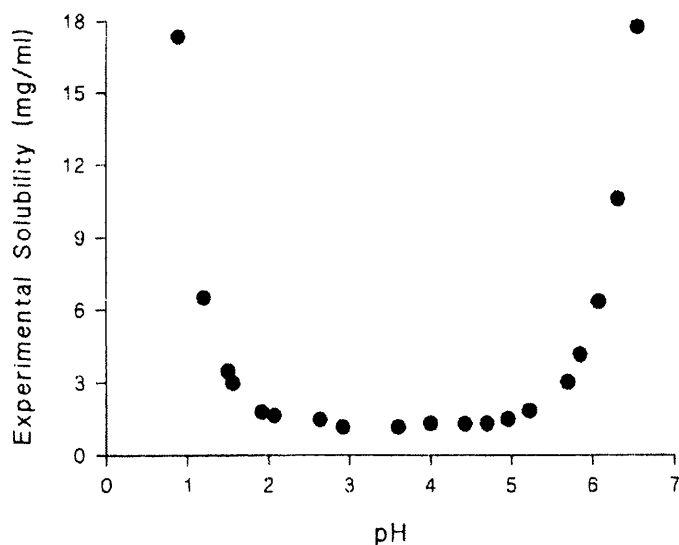


Figure 3.2 Solubility of 5-aminosalicylic acid at 37 °C in unbuffered water at different pH values. Reproduced from French and Mauger (1993).

Prednisolone is a non-ionic drug and is not known to exhibit pH-dependent solubility. However due to its hydrophobic nature its solubility may be influenced by the small intestinal surfactants. Bile salts and phospholipids may improve the solubility of drugs through wetting whereby they decrease the interfacial energy between drug and dissolution medium, thus increasing the effective surface area available for dissolution (Mithani et al., 1996). However the predominant mechanism of solubility enhancement at bile salt concentrations exceeding the critical micelle concentration (CMC) is through solubilisation (incorporation into micelles) (Mithani et al., 1996).

For modified release formulations it is necessary to determine drug solubility under the different environments of pH, buffer capacity and intestinal surfactants that prevail in different regions of the gastrointestinal tract. 5-ASA and prednisolone were chosen as the model drugs not only because they are the cornerstone of inflammatory bowel disease treatment however they also display rather different physicochemical

properties and thus it is interesting to identify which parameters of the dissolution media constitute the most important influence on their solubility.

3.1.2 Media used for measurement of drug solubility

3.1.2.1 Phosphate and bicarbonate buffers

Drug solubility was measured in conventional media (phosphate buffers) and physiologically relevant media; bicarbonate buffers (Hanks and Krebs) and FaSSIF. Bicarbonate buffers are physiologically relevant with respect to their buffer composition and FaSSIF is relevant in terms of its surfactant content. Drug solubility in these media was compared to that in jejunal and ileostomy fluids.

3.1.2.2 Jejunal fluids

Jejunal fluids used in this study were received as a gift from Astra Zeneca (Mölnådal, Sweden). They were aspirated from patients via an oral intubation tube (Loc-I-Gut[®], Synectics Medical, Sweden). The tube is a 175 cm long with an external diameter of 5.3 mm. It is a multichannel polyvinyl tube with two inflatable balloons 10 cm apart and a tungsten weight at the tip (Persson et al., 2005). The position of the tube was checked fluoroscopically (Knutson et al., 1989), and once the desired location was reached only the lower balloon was inflated with 25 to 30 ml of air to prevent fluid from passing down the gastrointestinal tract, thus achieving complete sampling of jejunal fluids. Fluids were collected from the jejunum by continuous vacuum drainage. A separate tube was positioned in the stomach to drain gastric fluid to

prevent nausea. The jejunal fluid aspirated was collected on ice, pooled and stored at -70°C.

It is more difficult however to obtain luminal fluids from more distal regions of the gut and this method has not been adapted to aspirate ileal fluids. Therefore ileostomy fluids from inflammatory bowel disease (IBD) patients were studied as an alternative.

3.1.2.3 Ileostomy fluids

Ileostomy fluids were also a gift from Astra Zeneca. They were obtained from IBD patients which had undergone bowel surgery. End ileostomy is usually constructed as a permanent stoma for patients with ulcerative colitis or Crohn's disease. The terminal ileum is brought through the abdominal wall in the right iliac fossa area. It is usually the outcome of proctocolectomy (Keighley and Williams, 1999). Indications for surgery in IBD patients include failure of medical treatment or because of acute or chronic complications of the disease; including haemorrhage, obstruction and risk of carcinoma (Dozois and Kelly, 2000). In addition, patients with an ileostomy made because of Crohn's disease will have had an ileal resection too, the extent of which depends on the extent of the disease (McNeil et al., 1982). Patients may also have recurrent or residual small bowel disease (Lockhart-Mummery and Morson, 1960).

A major difference between ileal and ileostomy fluid is that about 1.5 litres of fluid passes through the ileo-caecal valve each day, yet average ileostomy contents are less than a third of this (Kanaghinis et al., 1963; Ladas et al., 1986). Ileostomy fluids would therefore be expected to be more concentrated. Furthermore, transit through the final part of the ileum is slower in ileostomates compared to normal subjects. This

slower flow gives rise to greater bacterial flora which would generate metabolites such as short chain fatty acids giving rise to a higher osmolality in ileostomy effluent compared to ileal fluid (Ladas et al., 1986).

The colon serves as a site of electrolyte and water conservation in man due to its large absorptive capacity. With a standard diet in healthy individuals, 1500 ml of water, 200 mM of sodium, 100 mM of chloride and 10 mM of potassium enter through the colon each day. Faecal excretion of these is small as the colon absorbs more than 95% of the sodium, chloride and water and 50% of the potassium traversing the ileocaecal region (Phillips and Giller, 1973). Patients with ileostomies are therefore prone to salt and water depletion (Clarke et al., 1967) arising from the failure to re-absorb fluid and electrolytes passing from the ileum.

McNeil et al. (1982) found a statistically significant correlation of increased ileostomy output with an increased length of ileum resected. The authors use this to explain why Crohn's colitis patients have greater ileostomy outputs in comparison to ulcerative colitis patients. From this study and other evidence they conclude that the terminal ileum is an important site of electrolyte and water conservation in man. Furthermore, malabsorption of fat, vitamin B12 and bile salts occurs proportional to the length of the ileum affected by disease.

It would also have been interesting to compare drug solubility in ileostomy with colostomy fluids. In colostomy, the colon is brought through the abdominal wall and the part of the colon chosen depends on the part obstructed or resected (Keighley and Williams, 1999). Unfortunately however, we were unable to obtain these fluids.

3.1.3 Intestinal surfactants and media used to simulate them

Bile plays a critical role in intestinal lipid digestion and absorption. Average composition of human bile is ~ 84% water, 11.5% bile salts, 3% lecithin (phosphatidylcholine, PC), 0.5% cholesterol, and 1% other components, such as bile pigments, inorganic ions, and proteins (Charman et al., 1997). Bile acid is synthesised by hepatocytes and effective hepatic secretion requires an intact enterohepatic circulation because most bile acids secreted into the small intestine undergo hepatic-enterohepatic recycling through active absorption from the ileum (Dawson et al., 2006) After their synthesis, bile acids are conjugated with taurine or glycine via an amide bond between the carboxyl group of the bile acids and the amino group of glycine or taurine. In humans, most of the bile acids are conjugated to glycine. See Figures 3.3a-b for bile salt structure and figure 3.3c for phosphatidylcholine structure.

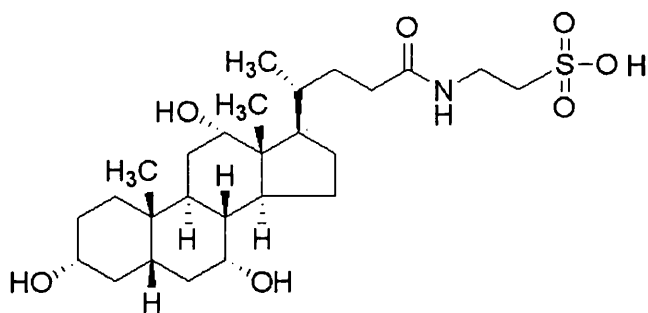


Figure 3.3a Chemical structure of taurocholic acid

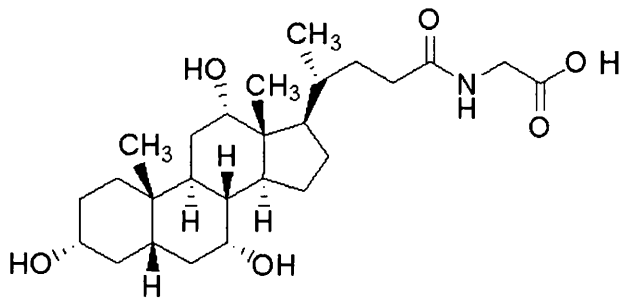


Figure 3.3b Chemical structure of glycolate

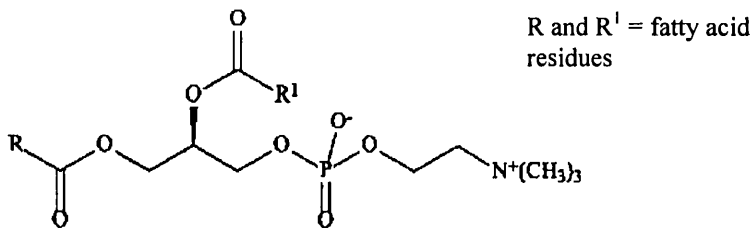


Figure 3.3c Chemical structure of phosphatidylcholine

Amino acid conjugation to bile salts increases hydrophilicity of the latter and the acidic strength of its side chain by converting a weak acid, pKa ~ 5.0, to a strong acid, pKa ~ 3.9 for the glycine conjugate and pKa < 2.0 for the taurine conjugate. Hence the conjugated bile acids are almost completely ionised at the near neutral pH of the small intestine. This limits the passive diffusion of the bile acids across the small intestinal mucosa and absorption only occurs in the presence of the specific membrane carriers in the terminal ileum. Postprandial concentrations of free and

conjugated bile acids along the small intestine were found to be highest in the upper ileum (10 mM) and lowest (2 mM) in the lower ileum (Figure 3.4) (Northfield and Mccoll, 1973).

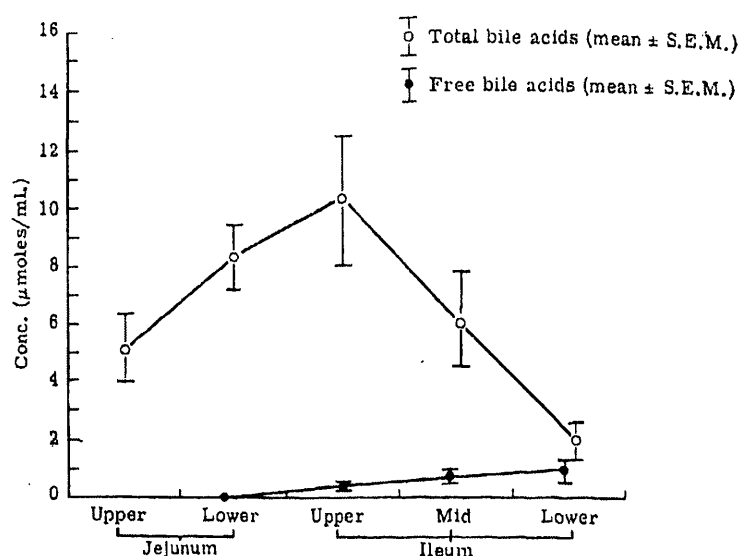


Figure 3.4 Bile salt concentrations along the normal human small intestine postprandially. Reproduced from Northfield and McColl (1973).

Standard FaSSIF with 3 mM NaTC and 0.75 mM lecithin is the biorelevant media commonly used to represent fasted jejunal fluids (Galia et al., 1998). These values are relatively close to those obtained in a recent characterisation study of intestinal fluids in human volunteers. The study found the total bile salt concentration to be 2 ± 0.2 mMol and the phospholipid concentration to be 0.2 ± 0.07 mM (Persson et al., 2005). In this chapter, the solubility of 5-ASA and prednisolone in human jejunal fluids was compared to the solubility in this biorelevant media.

Recently, equivalent biorelevant media have been designed for proximal ileal fluids based on the assumption that no intestinal surfactants exist in the proximal ileum in the fasted state (Klein et al., 2005). This assumption, however, is not based on biological assays of ileal aspirates. From figure 4.4, it can be inferred that this assumption is invalid since bile salt concentrations are highest in the upper ileum. Furthermore, bile acid absorption occurs from the terminal ileum and therefore its concentration will still be high in the proximal region.

It is difficult to define the surfactant concentration in ileostomy fluids as it is dependent on several variables. Profound bile acid malabsorption occurs after ileal resection however we do not know the extent of dysfunction or resection of the ileum, if any, in the patients from whom the ileostomy fluids were obtained. Hence two concentrations of intestinal surfactants were explored in this study: high concentration (7.5 mM NaTC, 1.875 mM lecithin) and a low concentration (1.2 mM NaTC, 0.3 mM lecithin); 2.5 fold more concentrated and diluted than standard FaSSIF respectively. These two concentrations were chosen as an approximate prediction of the possible surfactant concentration in ileostomy fluids. The high concentration was used on the assumption that very little enterohepatic recycling of bile occurs and therefore the concentration in ileostomy fluids is equivalent to the concentration in fed jejunal fluids (ileostomy fluids were obtained from patients in the fed state). The conventional bile salt concentration used in the fed state (fed state simulated intestinal fluid, FeSSIF) is 15 mM NaTC, however this concentration has been found to be twice as high as that of jejunal fluids in the fed state (Persson et al., 2005). The low concentration was used as an estimate of that in the terminal ileum in the fed state in the event of efficient enterohepatic recycling.

A further justification of the use of high bile salt concentrations in ileostomy fluids is the study by Ladas et al. 1986 which showed that a long chain triglyceride (LCT) rich meal and medium chain triglyceride (MCT) rich meal increased bile acid outflow in ileostomy effluent whereas only LCT rich meal increased bile acid outflow from ileum to colon in normal healthy subjects (Ladas et al., 1986). A study in normal subjects showed that MCT rich meals do not stimulate bile acid outflow from the gallbladder into the jejunum whereas LCT rich meals do (Ladas et al., 1984). This study hypothesises that if it is assumed that the gallbladder of ileostomates functions in the same way as normal subjects then the mechanism behind increased bile acid outflow in ileostomy effluent in response to MCT rich meals could be that a greater proportion of the bile acid pool resides in the ileal lumen in ileostomates in comparison to normal subjects.

3.2 OBJECTIVES

- To accurately determine solubility of the model drugs, 5-ASA and prednisolone, in jejunal fluids aspirated from healthy subjects and in ileostomy fluids from IBD patients.
- To compare solubility in these fluids to that in conventional phosphate buffers and in physiologically relevant media, including bicarbonate buffers and FaSSIF.
- To evaluate these physiologically relevant media for predicting drug solubility in human fluids.

- To identify which parameters of the dissolution media constitute the most important influence on solubility of drugs with different physicochemical properties.

3.3 MATERIALS AND METHODS

3.3.1 Materials

Mesalazine (mesalamine, 5-ASA) > 99% purity was obtained from Sigma Aldrich Chemicals (Poole, UK). Micronized prednisolone was obtained from Sanofi-Aventis (Romainville, France). All salts to prepare the buffers were of analytical grade and purchased from VWR Chemicals Ltd., Poole, UK. Sodium taurocholate, 95% pure, batch # 115K1109, was purchased from Sigma-Aldrich Chemicals (Poole, UK). Egg phosphatidylcholine (Lipoid E PC, >99% pure), batch # 105038-2/908, was a gift from Lipoid GmbH (Ludwigshafen, Germany). Methylene chloride (dichloromethane), analytical grade was purchased from Fisher Scientific, Loughborough, UK. Solvents used in HPLC were: distilled water, methanol, acetonitrile and peroxide-free tetrahydrofuran. All were of HPLC grade and purchased from Fisher Scientific, Loughborough, UK.

3.3.2 Media used for measurement of drug solubility

3.3.2.1 Phosphate and bicarbonate buffers

Drug solubility was measured in conventional pH 7.4 phosphate buffers including 0.05 M and 0.2 M phosphate buffers (Table 3.2). The bicarbonate media used were pH 7.4 Hanks and Krebs buffers. Blank FaSSIF (FaSSIF with no surfactants) and

FaSSIF with different concentrations of intestinal surfactants at pH 6.8 was also used for drug solubility measurements.

Table 3.2 Comparison of the buffer content, ionic strength and buffer capacity of bicarbonate and phosphate buffers.

Buffer component (mM)	0.05 M PBS pH 7.4	0.2M PBS pH 7.4	Blank FaSSIF pH 6.8 (no surfactants)	Krebs buffer pH 7.4	Hanks buffer pH 7.4
KH ₂ PO ₄	50	200		1.18	0.441
NaOH	39.5	158	11.70		
NaH ₂ PO ₄ ·2H ₂ O			28.69		
Na ₂ HPO ₄ ·2H ₂ O					0.337
NaHCO ₃				24.97	4.17
NaCl			106.01	118.07	136.99
KCl				4.69	5.37
CaCl ₂				2.52	1.26
MgSO ₄ ·7H ₂ O				1.18	0.812
Ionic strength	0.129	0.526	0.153	0.161	0.155
Buffer capacity (mmoles/L/pH unit)	23.0	58.8	14.8	3.7	1.0

3.3.2.2 Human fluids

Jejunal fluids were supplied by Astra Zeneca (Mölndal, Sweden) from healthy fasted volunteers. Three different batches were studied and each batch was pooled from five people, hence samples were obtained from 15 different people.

Ileostomy fluids were supplied by Astra Zeneca (Mölndal, Sweden) from three different patient volunteers with IBD. The samples were not pooled and therefore each sample corresponds to one patient. Patients were not fasting and their diet was not controlled and therefore they were all eating differently. We do not have information on the patients' medical condition and the extent of IBD and the sites affected.

3.3.3 Preparation of FaSSIF media

Concentrated FaSSIF was first prepared and then diluted with blank FaSSIF to achieve the desired concentration of intestinal surfactants.

1.32 g sodium taurocholate (NaTC) was dissolved in 100 ml of blank FaSSIF in a round bottomed flask. This solution was weighed and the weight noted ('weight 1'). 4.72 ml methylene chloride (dichloromethane) solution containing 100mg/ml lecithin (E PC) (= 0.472 g lecithin, 'weight 2') was added to the sodium taurocholate solution; a milky white emulsion is formed. The methylene chloride was then driven off under vacuum using a rotary evaporator (Rotavapor, R-114, B'U'CHI, Switzerland) at room temperature. This was continued for around 15 min until a clear, micellar solution formed with no perceptible odour of methylene chloride. The weight of the solution was checked and the loss of water that occurred due to evaporation was substituted to obtain an overall weight corresponding to the sum of 'weight 1' and 'weight 2'. Finally, the volume was brought to 200 ml in a volumetric flask with pH 6.8 blank FaSSIF. The resulting FaSSIF concentrate contains 12 mM NaTC and 3 mM lecithin; this is then diluted with blank FaSSIF.

3.3.4 Methodology of solubility studies

An excess of drug (15 mg of 5-ASA and 2 mg of prednisolone) was added to microcentrifuge tubes (Eppendorf AG, Hamburg, Germany) containing 1 ml of the different media and placed in a shaking water bath at 37 °C and speed of 400 shakes per min. In the initial preliminary experiments, several samples were prepared and removed after 2, 5 and 24 hours. Equilibration was found to be achieved within five hours for 5-ASA and prednisolone. Based on this data, five hours was considered adequate time to achieve saturation solubility in the different media.

After five hours the samples were centrifuged at 13,000 rpm for 10 min. Supernatant was transferred to microcentrifuge filter tubes (polysulphone 0.2 µm filters) (VectaSpin Micro, Whatman, England) and centrifuged at 10,000 rpm for 10 min (Centrifuge 5415D, Eppendorf AG, Hamburg, Germany). This was an additional step to remove any particles from the biological fluid or undissolved drug that may still be present. Aliquots of the resultant filtrate were removed and diluted with mobile phase and vortexed for one min. A 40-fold dilution was performed for 5-ASA (50 µl of the solution diluted with 1950 µl of HPLC mobile phase with Gilson pipette) and a 20-fold dilution for prednisolone (50 µl of the solution diluted with 950 µl of mobile phase). Solubility was determined using HPLC-UV. Dilutions were performed so that absorbance readings are within the limit of accurate detection by HPLC. Three aliquots were removed from the same sample and diluted; this was performed to

determine precision of the assay. The filtration step using the microcentrifuge tubes was validated by comparing it to the solubility of solutions not subject to this filtration. Spiking the different media with known concentrations of drug showed a recovery between 95 to 100 %; thus solubility results were not affected by degradation in intestinal fluids or binding to laboratory apparatus such as microcentrifuge tubes, filters or pipette tips. All solubility experiments were performed at least in triplicate.

3.3.5 High performance liquid chromatography (HPLC) for assaying drug solubility

3.3.5.1 Equipment

The equipment consisted of an integrated HP 1050 Series HPLC system comprising an HP1050 autosampler, an HP 1050 pump and an HP 1050 multiple wavelength detector system, a UV-Vis spectrophotometric detector. The detector was interfaced with a pc with PC/Chrom+ Software (H & A Scientific Inc., Greenville, NC, USA).

3.3.5.2 Drug separation and choice of mobile phase

The basis of compound separation by reversed-phase chromatography (RPC) is partitioning between the mobile phase and column. The column, typically a silica support modified with a C₈ or C₁₈ bonded phase, is less polar than the water-organic mobile phase. Sample molecules partition between the polar mobile phase and the non-polar C₈ or C₁₈ stationary phase (Snyder et al., 1997). Retention is less and therefore elution faster for stronger, less polar mobile phases. A more polar mobile

phase has a lower % of organic solvent and more water, and choice of a more polar organic solvent is made.

Short retention times are convenient and allow a large number of samples to be run in a relatively short time. However it was necessary to increase the retention of 5-ASA so that it is distant from the numerous impurities in biological fluids which are eluted at the start. To increase retention as much as possible, a polar mobile phase was used comprising 95 % water and 5 % methanol (polar organic solvent). A less polar column also increases retention time of the compound; therefore a C₁₈ column was used (LiChrospher®100, Merck, Darmstadt, Germany).

5-ASA is a zwitterionic drug and therefore the pH of the mobile phase needs to be controlled (Snyder et al., 1997). Trifluoroacetic acid (TFA) was a suitable choice of buffer as it has a buffering pH range of 1.5 to 2.5. Inclusion of 0.05 % TFA in the mobile phase gives rise to a pH of 2.5. 5-ASA has two pK_a values: the carboxyl group has a pK_a of 2.3 and the amino group a pK_a of 5.69 (French and Mauger, 1993). Therefore at a pH of 2.5, the amino group is protonated and 5-ASA exists in the cationic state.

For the separation of prednisolone; the mobile phase recommended by the United States Pharmacopoeia (USP) (2006) for prednisone was used. This comprises:

68.8% water

25% peroxide-free tetrahydrofuran

6.2% methanol

Column used: Water Symmetry C₈ (5 µm) (Waters, Massachusetts, USA)

Solvent type and solvent strength not only affect compound retention but also influence peak spacing and peak resolution.

3.3.5.3 Chromatographic conditions

5-ASA assay

Injection volume: 20 μ l; Flow rate: 1.0 ml/min; Maximum run time: 10 min; Assay wavelength: 228 nm; Pressure: 1800 psi, and column temperature: 40 $^{\circ}$ C.

Prednisolone assay

Injection volume: 20 μ l; Flow rate: 1.0 ml/min; Maximum run time: 13 min; Assay wavelength: 254 nm; Pressure: 1800 psi, and column temperature: 40 $^{\circ}$ C.

3.3.5.4 Validation of HPLC assay method

Calibration curves for the HPLC assay were not prepared from biological fluids as there were insufficient quantities available and it would be more useful to use them for characterisation and drug solubility measurements. Furthermore, the saturation solubility concentrations achieved were very high and diluted by several fold with mobile phase to be within the linear range of the standard curves for HPLC. Spiking the different solubility media with known concentrations of 5-ASA or prednisolone and then diluting with mobile phase by the same factor used in the solubility measurements gave rise to very similar AUC readings in the different media. The details of this are explained below.

The different media were spiked with drug powder, details of spiking ileostomy fluid are referred to here. In the case of 5-ASA, 0.001225 g was added to 1 ml of ileostomy fluid in an eppendorf to form an 8 mM solution. Complete dissolution of the drug was ensured by leaving in a shaking water bath at 37 °C for five hours and then vortexing for 30 min. Dilutions with mobile phase were performed to achieve 0.8, 0.6 and 0.2 mM drug solutions. Ileostomy fluid was also spiked with a 5 mM 5-ASA solution in mobile phase and further diluted with mobile phase to achieve the desired drug concentrations.

Ileostomy fluids studied have a large number of particulate matter and fibres as they are obtained from patients in the fed state. Hence they were subjected to filtration with a sefar nitex mesh filter of aperture size 350 µm (made from a polyamide basic fabric of PA 6 and PA 6.6 monofilaments) to remove the large particulate matter. A sample of this filtered ileostomy fluid was also subjected to centrifugation at 13000 rpm for 15 min. Peak area readings of 5-ASA in filtered ileostomy fluid were compared to those in ileostomy fluid subjected to filtration and centrifugation.

A 5 mM solution of 5-ASA in mobile phase was prepared and diluted further with the mobile phase to achieve the desired concentrations. These peak area readings were compared to those obtained by dissolving 5-ASA in ileostomy.

A comparison of the 5-ASA peak areas for known drug concentrations in ileostomy fluids (filtered or filtered and centrifuged) with that in mobile phase are shown in tables 3.3 - 3.5. The relative standard deviations (RSD) ranged from 0.033 – 2.60 %. These results show that similar peak areas are obtained for 5-ASA in mobile phase or

by spiking ileostomy fluids with drug and then diluting with mobile phase. Hence calibration curves prepared from mobile phase are reliable for calculating drug solubility in the different media.

Table 3.3 A comparison of 5-ASA peak areas in mobile phase with filtered ileostomy fluids spiked with drug powder. Areas presented as mean \pm SD.

5-ASA concentration (mM)	5-ASA peak area of filtered ileostomy fluid spiked with drug powder	5-ASA peak area in mobile phase	Mean peak area	Std. dev.	Relative Std.dev. (%)
0.8	2148 \pm 40	2149 \pm 16	2148.5	0.71	0.33
0.6	1673 \pm 34	1626 \pm 23	1649.5	33.2	2.01
0.2	517 \pm 37	515 \pm 11	516.0	1.4	0.27

Table 3.4 A comparison of 5-ASA peak areas in mobile phase with filtered and centrifuged ileostomy fluids spiked with drug powder. Areas presented as mean \pm SD.

5-ASA concentration (mM)	5-ASA peak area of centrifuged ileostomy fluid spiked with drug powder	5-ASA peak area in mobile phase	Mean peak area	Std. dev.	Relative Std.dev. (%)
0.8	2161	2149	2155.0	8.48	0.39
0.6	1652	1626	1639.0	18.38	1.12
0.2	523	515	519.0	5.66	1.09

Table 3.5 A comparison of 5-ASA peak areas in mobile phase with filtered and centrifuged ileostomy fluids spiked with drug solution. Areas presented as mean \pm SD

5-ASA concentration (mM)	5-ASA peak area of centrifuged ileostomy fluid spiked with drug solution	5-ASA peak area in mobile phase	Mean peak area	Std. dev.	Relative Std.dev. (%)
0.8	2192	2149	2170.5	30.41	1.40
0.6	1687	1626	1656.5	43.14	2.60
0.2	532	515	523.5	12.02	2.30

To find out if particulate matter in biological fluids influences drug solubility; drug solubility was compared in filtered and centrifuged ileostomy fluids in one batch of ileostomy fluids. The results gave rise to the same solubility and therefore all future experiments were conducted on centrifuged biological fluids as they are easier to handle.

3.3.5.5 Drug calibration curves for HPLC

5-ASA standard solutions (0.2 to 1.5 mM) were prepared in the appropriate mobile phase. The stock standard was prepared by dissolving 0.0766 g of 5-ASA in 100 ml mobile phase in a volumetric flask to achieve a 5 mM 5-ASA solution. Seven standard solutions containing 1.5, 1.2, 1.0, 0.8, 0.6, 0.4 and 0.2 mM 5-ASA were prepared from the stock solution by taking appropriate aliquots of the stock solution and diluting with mobile phase. The calibration curve was linear over the range of 0.2

to 1.5 mM. The equation of the curve relating the peak area (P) to the 5-ASA concentration (C in mM) in this range was: $P = 2694.9C - 30.343, r^2 > 0.999$.

Prednisolone standard solutions (0.0139 to 0.139 M) were prepared in mobile phase. The stock standard was prepared by dissolving 0.02 g of prednisolone in 100 ml mobile phase in a volumetric flask to achieve a 0.555 mM 5-ASA solution. Six standard solutions containing 0.139, 0.083, 0.056, 0.042, 0.028 and 0.014 mM prednisolone were prepared from the stock solution by taking appropriate aliquots of the stock solution and diluting with mobile phase. The calibration curve was linear over the range of 0.0139 to 0.139 mM. The equation of the curve relating the peak area (P) to the prednisolone concentration (C in mM) in this range was: $P = 6788.7C + 9.3239, r^2 > 0.995$.

3.3.5.6 Specificity/ selectivity /precision

This is illustrated by comparing the chromatograms of the blank media with media spiked with drug. No interfering peaks can be seen and the assay produced a stable baseline. The retention time for 5-ASA was 5 min and that for prednisolone was 10 min. (Figures 3.5 – 3.8). All chromatograms are of fluids diluted with mobile phase by a factor of 40 fold for 5-ASA and 20-fold for prednisolone. The coefficient of variation for mesalazine and prednisolone was in the range of 1.76 % and 3.96 % respectively.

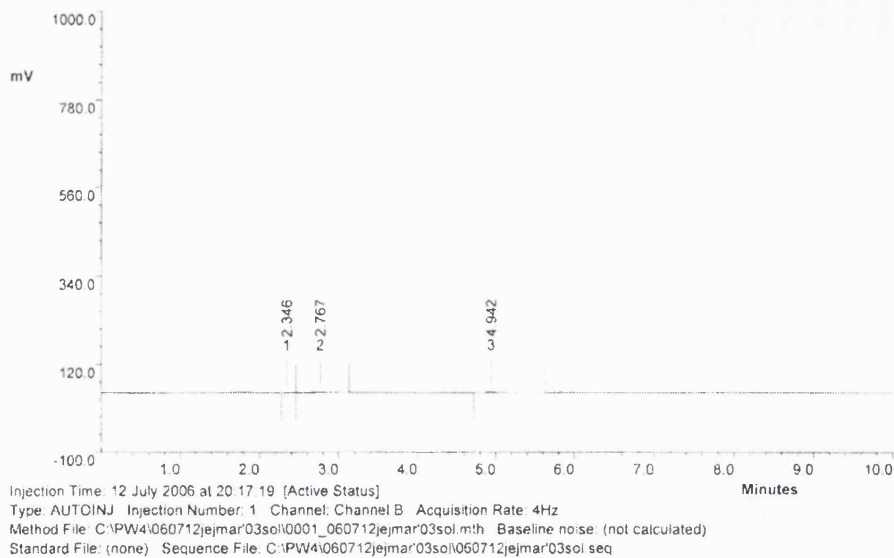


Figure 3.5 Chromatogram of blank jejunal fluids

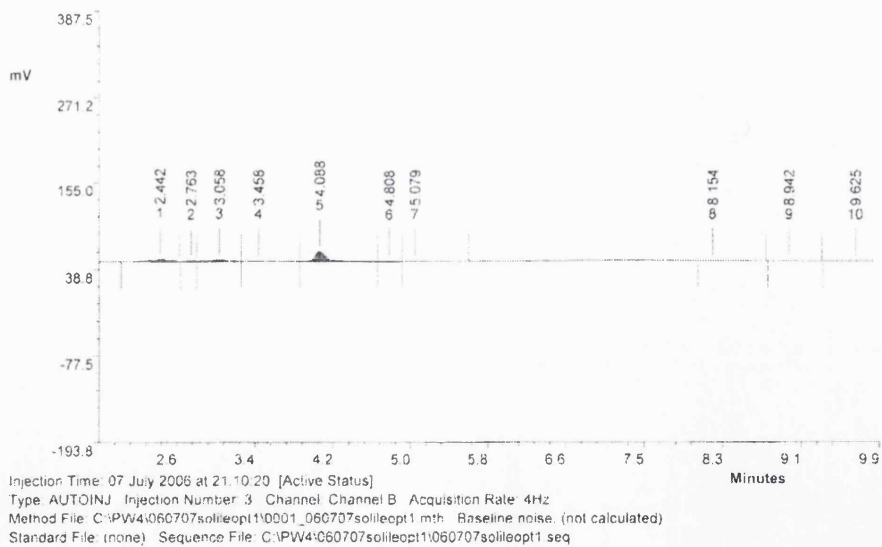


Figure 3.6 Chromatogram of blank ileostomy fluid

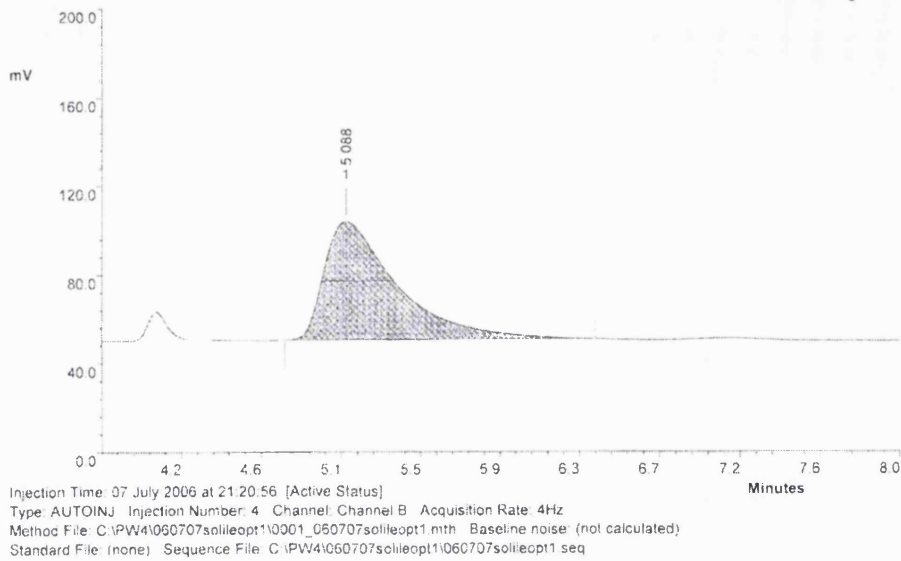


Figure 3.7 Chromatogram of 5-ASA dissolved in ileostomy fluid

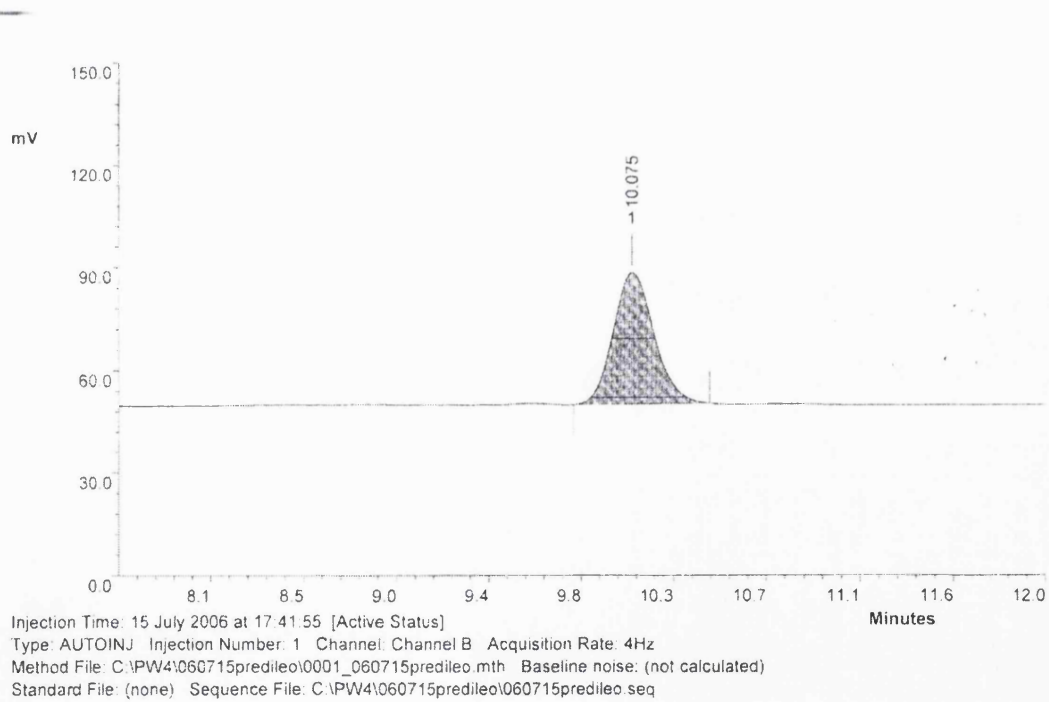


Figure 3.8 Chromatogram of prednisolone dissolved in ileostomy fluid.

3.3.6 pH and buffer capacity measurements

pH and buffer capacity measurements of the human intestinal fluids were performed on centrifuged samples for accuracy of volume measurements which is essential for calculating the buffer capacity.

Explanation of buffer capacity measurements has been described in the previous chapter. Due to the volume restrictions of the biological samples, buffer capacity was measured in just one pH direction, by addition of HCl. This pH direction was chosen based on previous work in the literature which states that for near-neural media, titrating with HCl is more appropriate than titrating with NaOH (Kalantzi et al., 2006a). Furthermore, the anionic species of 5-ASA predominates at high pH values and therefore it is more relevant to measure buffer capacity by titrating with acid.

Buffer capacity in all media was measured at a pH change of 0.5 units. This was obtained by adding 2 μ l of 0.1 M HCl to 100 μ l of jejunal fluid in a 0.5 ml microcentrifuge tube, vortexing and removing one drop of this mixture using a pipette pasteur and placing it on the pH sensor of a pocket sized pH meter (MiniLab IQ125, IQ scientific, California, USA). The same procedure was performed for ileostomy fluids however 10 μ l of 0.1 M to 100 μ l of this fluid. Buffer capacity measurements were performed at least in triplicates for each sample.

3.4 RESULTS AND DISCUSSION

3.4.1 pH and buffer capacity of jejunal and ileostomy fluids

The mean pH and buffer capacity (\pm SD) of jejunal fluids were measured to be 6.9 ± 0.57 and 2.97 ± 1.40 mM/L/ Δ pH unit respectively. These are in good agreement with the values reported in the literature whereby a pH of 7.1 ± 0.6 (Lindahl et al., 1997) and a buffer capacity of 2.4 mM/L/ Δ pH (Persson et al., 2005) was reported for jejunal fluids aspirated from fasted healthy individuals. The mean pH and buffer capacity (\pm SD) of ileostomy fluids was measured to be 6.8 ± 0.93 and 14.07 ± 2.81 mM/L/ Δ pH unit respectively. A value of 7.2 ± 0.3 has been reported by Ladas et al. (1986). No value for the buffer capacity of ileostomy fluids was found in the literature.

3.4.2 Solubility of 5-aminosalicylic acid in different media

3.4.2.1 Comparison of 5-aminosalicylic acid solubility in bicarbonate and phosphate buffers

Figure 3.9 shows that 5-ASA solubility is different in bicarbonate and phosphate buffers at pH 7.4. Moreover, the solubility also varies between bicarbonate and phosphate media of different buffer molarity. This illustrates that defining the pH alone is not sufficient when reporting the solubility and dissolution rates of weak electrolytes; however it is extremely important to define the composition and concentration of the buffer species. This is in agreement with the work of Mooney et al. (1981).

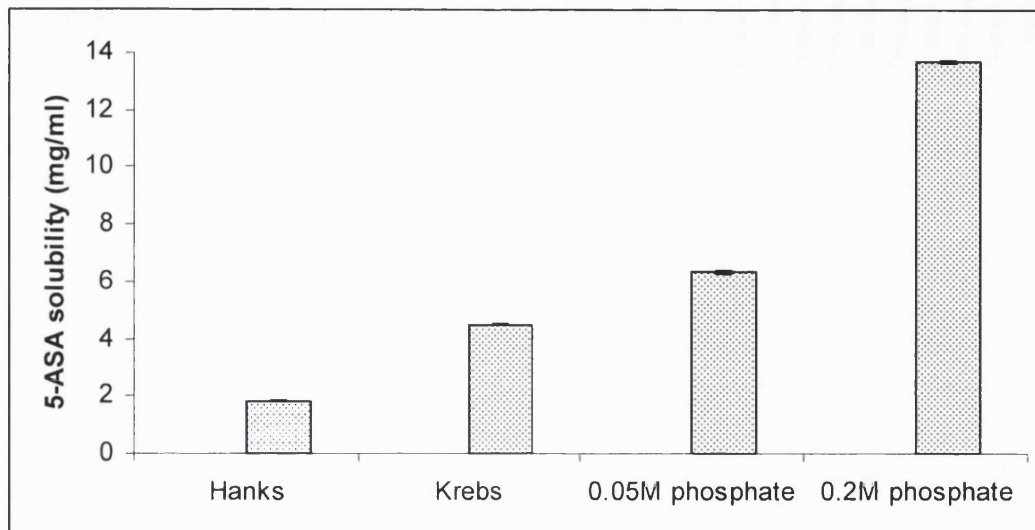


Figure 3.9 Solubility (mean \pm SD) of 5-ASA in pH 7.4 bicarbonate (Hanks and Krebs) and phosphate buffers with different concentrations of buffer species.

3.4.2.2 Comparison of 5-aminosalicylic acid solubility in bicarbonate buffers and human fluids

While the buffer capacity in jejunal fluids is higher than that of physiological Hanks buffer (Table 3.2), the mean 5-ASA solubility is similar in both media; 1.91 ± 0.27 mM and 1.83 ± 0.043 and respectively. The solubility of 5-ASA in Hanks buffer is closer than that in phosphate buffers to jejunal fluids (Figure 3.10). The buffer capacity of jejunal fluids was found to be higher than that of Hanks buffer despite that they have similar bicarbonate content as found in the literature. The higher buffer capacity of jejunal fluids may be explained by the existence of several organic ionic species in biological fluids which in small amounts do not have a great influence on the dissolution of 5-ASA. Organic ionic species include: (i) bile salts (which have strong acidic properties in jejunal fluids), (ii) lecithin (which comprises fatty acid esters at two positions of glycerol with a phosphate ester at the third position; the head

is highly hydrophilic composed of a dipolar ion of phosphate and a quaternary nitrogen (Figure 3.3)), (iii) fatty acids (produced from hydrolysis of triacylglycerols (TGs) in the small intestinal lumen by pancreatic lipases; their structure comprises a long hydrocarbon chain and a carboxylic acid head group, thus displaying weak acidic properties (Abumurad and Storch, 2006) (iv) amino acids (these are made up of a weakly basic amino group and a weakly acidic carboxyl group). Although these organic species are predominant in the fed state, basal levels are present in the fasted state. Table 3.6 illustrates a comparison of the quantities in the fasted and fed state.

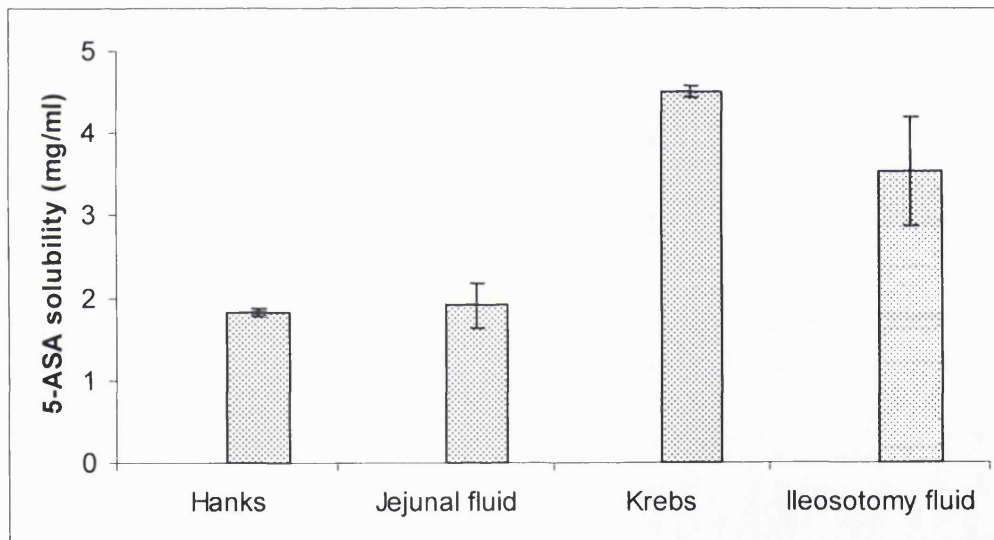


Figure 3.10 Solubility of 5-ASA (mean \pm SD) in human intestinal fluids in comparison to Hanks and Krebs bicarbonate buffers.

Table 3.6 Characterisation of fasted and fed intestinal fluids aspirated from the proximal jejunum of healthy human volunteers (Persson et al., 2005).

	Fasted HIF	Fed HIF
pH	7.5	6.1
Protein conc. (mg/ml)	1± 0.1	5±0.1
Bile salt conc. (mM)	2±0.2	8±0.1
Neutral lipid conc. ^a (mM)	0.1±0.01	22±1
Phospholipid conc. (mM)	0.2±0.07	3±0.3
Surface tension (mN/m)	28±1	27±1
Buffer capacity, acid (mM/L/ΔpH unit)	2.4	14.6

^a Including fatty acids

The buffers species generated by food digestion plays an important role in maintaining the pH value of gut luminal fluids (Vertzoni et al., 2004). Food has been shown to increase the buffer capacity of human intestinal fluids aspirated from the proximal jejunum; buffer capacity increased from an average of 2.4 to mmol/L/ΔpH in the fasted state to 14.6 mmol/L/ΔpH in the fed state (Persson et al., 2005). Although most nutrient absorption occurs in the jejunum, any that has not been absorbed is likely to explain the high buffer capacity observed in ileostomy fluids. However despite this high buffer capacity which is 3.8 fold higher than in Krebs buffer, solubility of 5-ASA is 27 % higher in Krebs. This corroborates the results from the previous chapter whereby it is not only buffer capacity that influences dissolution however the identity and therefore the pKa of the buffer species are highly critical.

It is difficult to define and simulate the GI luminal buffer system in the fed state. Not only because it comprises a complex array of nutrients but it will also be affected by

the type of food consumed. From this study it is difficult to draw definitive conclusions on the value of Krebs buffer in predicting the solubility of ionic drugs in ileal fluids. Ileal fluids cannot be aspirated from human subjects using the Loc-I-Gut® method and so the next best alternative was to study ileostomy fluids although they are different to ileal fluids in several ways. Moreover they are in the fed state and therefore there is an abundance of ionic digestion products and several ionic reactions, other than ionization of 5-ASA, taking place simultaneously. We can only speculate that as Hanks buffer provides good agreement with jejunal fluids, Krebs buffer is likely to reflect solubility in ileal fluids.

3.4.2.3 Correlation of 5-aminosalicylic acid solubility with the buffer capacity of human fluids

5-ASA solubility was measured in each batch of pooled jejunal fluid. A different solubility was found in each batch and these differences are statistically significant (ANOVA, $p < 0.05$) (Figure 5.11). There is also a statistically significant difference in 5-ASA solubility between ileostomy fluids obtained from each patient (ANOVA, $p < 0.05$) (Figure 5.12). 5-ASA solubility appears to correlate to buffer capacity in jejunal and ileostomy fluids, however there is an insufficient number of samples to perform a statistical test to test the significance of this correlation. Interestingly, buffer capacity seems to be more important than pH in determining the solubility of 5-ASA in human fluids.

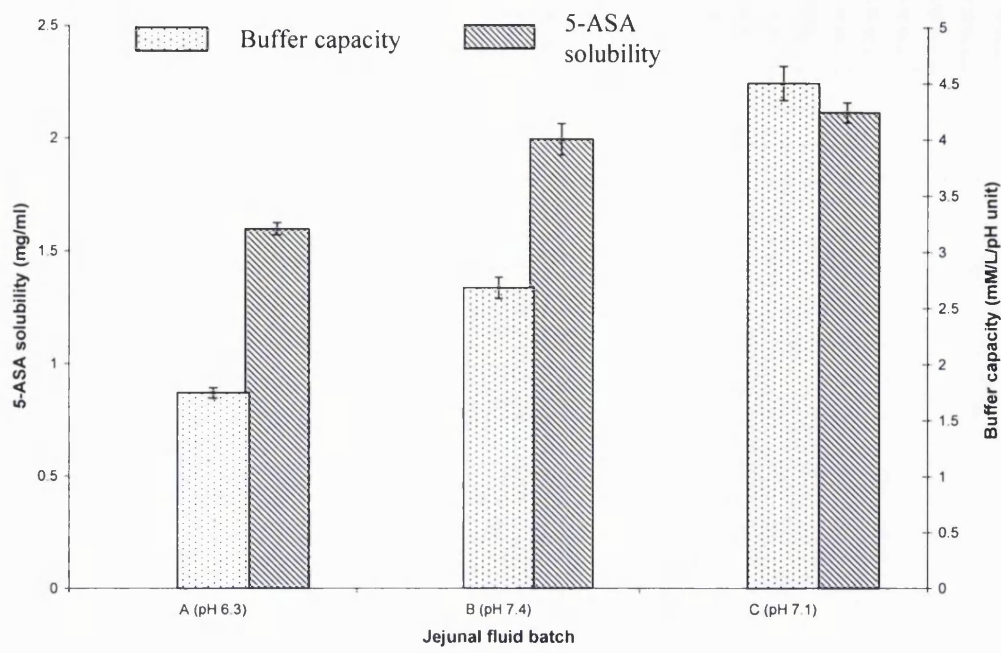


Figure 3.11 5-ASA solubility and buffer capacity (mean \pm SD) in different batches of jejunal fluid.

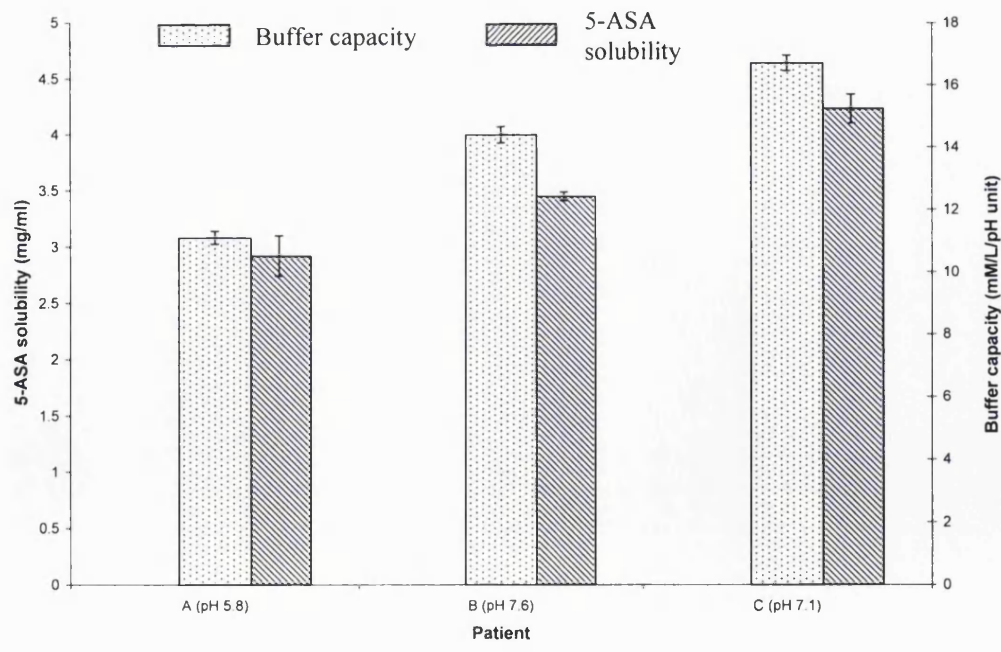


Figure 3.12 5-ASA solubility and buffer capacity (mean \pm SD) in ileostomy fluids obtained from different patients.

For the dissolution of weak electrolytes, the pH of the boundary layer is significant in determining solubility of the drug (Horter and Dressman, 2001). The pH at the solid-liquid interface, pH_0 , is lower than the bulk pH (pH_{bulk}) for weakly acidic drugs. The rate of drug dissolution may asymptotically approach the limit where pH_0 equals pH_{bulk} with increasing total buffer concentration in the bulk solution. Figure 3.13 shows the difference between bulk pH and surface pH of three weak acids, indomethacin, 2-naphthoic acid, and benzoic acid, with pK_a values of 4.17, 4.02 and 4.03 respectively. There is a plateau region at a bulk pH greater than the pK_a of the drug, whereby the surface pH appears to be dictated by the drug rather than the bulk pH. This plateau region represents the ability of the dissolving acidic drug to suppress the surface pH to a value lower than the bulk pH. The extent of this plateau region and the pH over which it occurs depend on the drug's pK_a and its intrinsic solubility. The surface pH is lower and the plateau region more pronounced for drugs with high intrinsic solubilities and low pK_a values, e.g. benzoic acid, than for drugs with lower intrinsic solubilities and higher pK_a values, e.g. indomethacin (Ozturk et al., 1988b). We measured the intrinsic solubility of 5-ASA to be 8.46×10^{-3} M; intermediate between that of benzoic acid and 2-naphthoic acid. Hence it is likely to influence the microenvironmental pH, however the extent of this will depend on the buffer composition of the bulk medium. The use of buffer tends to suppress the pH differences between the surface and the bulk; the deviation becomes smaller as the buffer concentration and pK_a of the basic salt of the buffer increase.

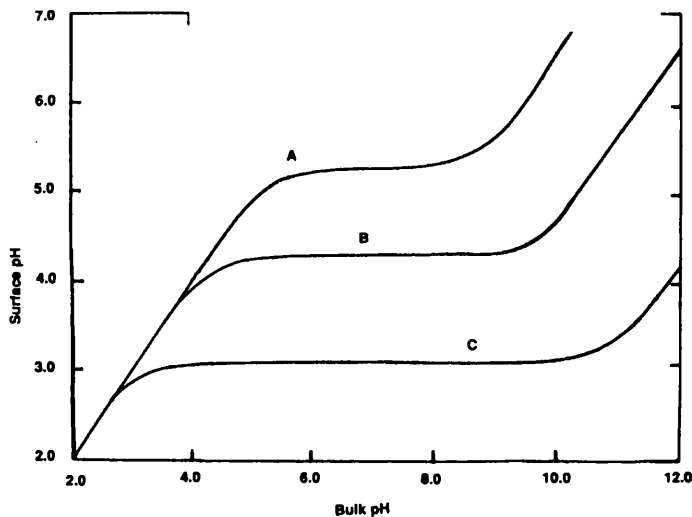


Figure 3.13 The relationship between bulk and surface pH for weak acids in unbuffered media. (A) Indomethacin; (B) 2-naphthoic acid; (C) benzoic acid. Reproduced from Ozturk et al. (1988a).

3.4.2.4 *The relationship of 5-aminosalicylic acid solubility with surfactant concentration*

Lecithin is a major phospholipid component of human bile and its amphiphilic nature renders it instrumental in the formation of mixed micelles. On average, the ratio of lecithin to total bile salt in healthy humans is 1:4 (Naylor et al., 1993). Lecithin decreases the critical micelle concentration (CMC) of bile salts, increases the size of the micelle and its solubilisation capacity (Charman et al., 1997). Addition of lecithin causes an increase in the molecular weight of micelles from 6000 to 150,000 Da (Shankland, 1970). The CMC of sodium taurocholate (NaTC) was found to drop from 4.7 to 0.25 mM in the presence of lecithin at 25% of the bile salt concentration (Naylor et al., 1993). Hence in standard FaSSIF media, the CMC of NaTC is surpassed.

5-ASA solubility in pH 6.8 blank FaSSIF (with no intestinal surfactants) is 2.7 ± 0.02 mg/ml. This does not significantly change in the buffers explored with the three different concentrations of intestinal surfactants. Unlike glycine conjugated bile salts which have a pKa of ~ 3.9 , taurine conjugated bile salts have a pKa < 2 ; therefore they are completely ionised at pH 6.8. Consequently, the mixed micelles formed have a predominantly anionic surface. The carboxylic acid group of 5-ASA has a low pKa of 2.3. Since,

$$\text{pH} = \text{pKa} + \log \frac{[\text{A}^-]}{[\text{HA}]} \quad \text{Equation 3.1,}$$

the following equation can be derived:

$$\text{Percentage ionisation} = 100 / [1 + \text{antilog}(\text{pKa} - \text{pH})] \quad \text{Equation 3.2}$$

(Florence and Attwood, 1998).

The % ionisation of 5-ASA at pH 6.8 is:

$$100 / [1 + \text{antilog}(2.3 - 6.8)] = 99.997 \%$$

The carboxylic acid group of 5-ASA is almost completely ionised to its anionic form at pH 6.8 or pH 7.4 and therefore its partition into the micelles will be hindered by repulsion between its anionic charge and that of the surfactant (Park and Choi, 2006).

This may contribute to explaining why 5-ASA solubility does not significantly change on addition of intestinal surfactants to near-neutral buffers.

3.4.3 Solubility of prednisolone in different media

3.4.3.1 Solubility of prednisolone in bicarbonate buffers and phosphate buffers with different concentrations of intestinal surfactants

Solubility of prednisolone was found to be the same in all bicarbonate and phosphate buffers without surfactants. It was measured to be 0.223 mg/ml. However prednisolone solubility increased with increasing concentrations of intestinal surfactants (Figure 3.14).

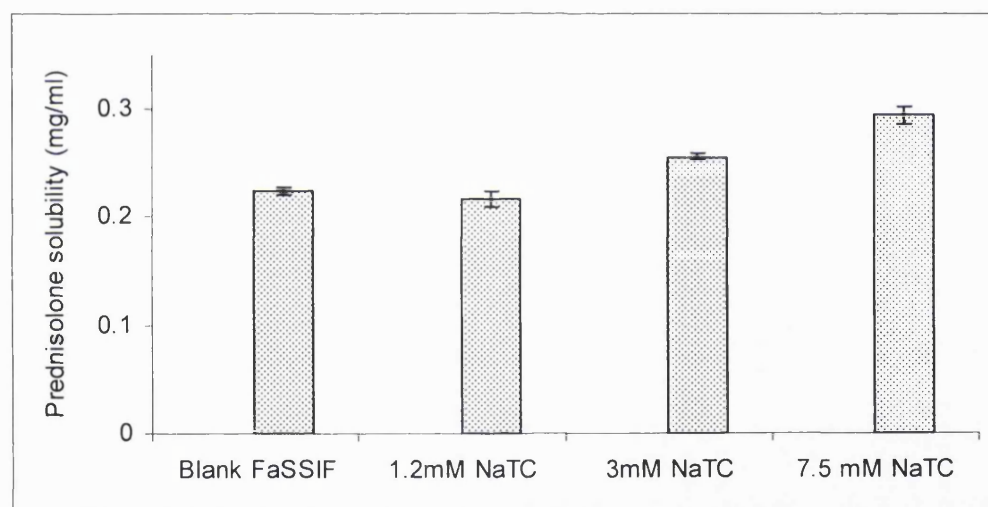


Figure 3.14 Solubility of prednisolone (mean \pm SD) in pH 6.8 FaSSIF with different concentrations of the surfactant sodium taurocholate (NaTC).

At NaTC concentrations of 1.2 mM, the solubility of prednisolone is not significantly different to blank FaSSIF. However at concentrations of 3 mM (FaSSIF) and 7.5 mM, the solubility significantly increased by 14.4% and 31.9% respectively relative to blank FaSSIF (ANOVA, $p < 0.05$).

Mithani et al. (1996) showed that the increase in drug solubility as a function of bile salt concentration can be predicted by the lipophilicity of the compound measured by the logarithm of the octanol/ water partition coefficient (log P) and the aqueous solubility of the compound (Equation 3.3).

$$\text{Log SR} = 2.23 + 0.61 \log P \quad (r^2 = 0.99) \qquad \text{Equation 3.3}$$

Where SR, is the solubilisation ratio and log P is the octanol/ water partition coefficient. An experimental log P value of 1.59 has been reported for prednisolone (Machatha and Yalkowsky, 2005). Based on this equation we calculate the log SR of prednisolone to be 3.2. This log SR, however, is a rough indicator as the calculation is based on micelles composed purely of NaTC without lecithin.

This increase in solubility of prednisolone with increasing intestinal surfactant concentrations is relatively modest in comparison to other drugs that have been screened in the literature. An example is ketoconazole which has a log P of 4.45 and the increase in solubility from the fasted to fed state simulated intestinal fluid was found to be 40-fold. Furthermore, the aqueous solubility of ketoconazole is only 6.9 µg/ml (Kalantzi et al., 2006b) in comparison to prednisolone which has a solubility of 223 µg/ml. Although the solubility increase observed for prednisolone in FaSSIF media is relatively modest, it is not unexpected since bile salts are poor solubilisers.

3.4.3.2 Comparison of prednisolone solubility in human fluids with that in phosphate buffers with intestinal surfactants

The solubility of prednisolone observed in jejunal fluid is over two fold that determined in FaSSIF (3 mM NaTC) (Figure 3.15). Similar deviations in solubility between FaSSIF and human intestinal fluids (HIF) have been observed for other drugs, such as ketoconazole and dipyridamole (Kalantzi et al., 2006b). This poor reflection by FaSSIF may be partially attributable to the bile salt components of simulated intestinal fluid. FaSSIF is only composed of NaTC, however NaTC only comprises 20 % of the bile acids found in fasted HIF (Persson et al., 2005). The predominant bile salt is glycocholic acid constituting 40 % of bile acids. Other major bile salt components in the fasted state include taurochenodeoxycholic acid and glycochenodeoxycholic acid which constitute approximately 20 and 18% respectively. Vertzoni et al. (2004) have substituted crude for pure NaTC in FaSSIF. Crude NaTC has a mixture of bile salts. Some drugs were found to be sensitive to the exact composition of bile salt micelles and had different release profiles depending on the grade of NaTC used. In some cases, crude NaTC even provided a better prediction of the *in vivo* performance. The number of hydroxyl groups in bile salts can be an important parameter in solubilization (Wiedmann and Kamel, 2002) . Human bile is predominantly composed of di- and tri-hydroxy acids (Hofmann, 1993). NaTC is a trihydroxy acid. Furthermore, lysophosphatidylcholine was found to be the dominant phospholipid in the fed and fasted state (> 85%) and not phosphatidylcholine which is what is used to prepare the FaSSIF media.

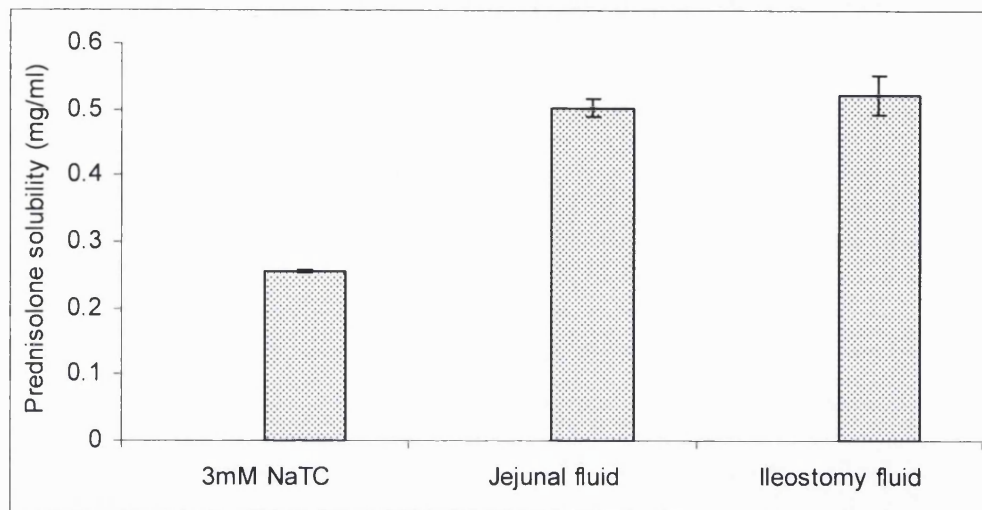


Figure 3.15 Solubility of prednisolone (mean \pm SD) in FaSSIF (containing 3 mM NaTC) and in human intestinal fluids.

Interestingly, the solubility of prednisolone in jejunal fluids is not statistically different to that in ileostomy fluids (Kruskal-Wallis non-parametric analysis, $p < 0.05$) (Figure 3.15). In healthy subjects, bile undergoes enterohepatic recycling through absorption from the terminal ileum. If the ileum is not inflamed or resected, as is usually the case in ulcerative colitis patients, then the concentration of bile salts would be expected to be very low in ileostomy fluids. However if the ileum is dysfunctional or resected, as may be the case in Crohn's disease patients, then bile malabsorption would arise and a substantial amount would be excreted in ileostomy fluids. It appears, however, that prednisolone solubility in HIF is not sensitive to moderate changes in bile salt concentration. Further evidence for this is our finding that there is no statistically significant difference (ANOVA, $p < 0.05$) in the solubility of prednisolone between the different batches of pooled jejunal fluid and between the ileostomy fluids from the different patients. It may be that another parameter may

have a more predominant influence on the solubility of prednisolone in HIF. Alternatively, it may be due to the poor solubilising nature of bile salts. Or it may be necessary for only a certain threshold bile salt concentration to be reached, this could be the CMC, after which further increases in concentration do not alter the solubility. Although prednisolone is classified as very slightly soluble by the British Pharmacopoeia, numerous other commonly used drugs exist, including those on the World Health Organisation (WHO) Essential drug list, of which some have an over 20-fold lower solubility and much higher log P than prednisolone (Kasim et al., 2004).

A study by Pedersen et al. (2000a) on solubility of hydrocortisone solubility in mid-jejunal fluids from 9 different healthy, fasting subjects showed that hydrocortisone solubility does not correlate to bile salt content. Solubility was rather consistent and in the range of 0.5 to 0.6 mg/ml. However bile salt content in the different subjects was variable, ranging from 0.5 to 6 mM. Hydrocortisone solubility, however, did correlate to bile salt levels in simulated intestinal fluids. Solubility was also significantly lower in the simulated fluids with intestinal surfactants in comparison to the HIF.

In this study it would have been interesting to determine the concentration of the different bile salts in each batch of jejunal and ileosotmy fluids and evaluate any differences. This may be conducted using HPLC. Unfortunately, however, time did not permit this to be performed.

3.4.4 Biopharmaceutical relevance of in vitro solubility results

The usual prescribed dose of 5-ASA is 2.4 g daily in three divided doses; hence 800 mg three times a day; although now doses > 2.4 g are increasingly prescribed in active disease as there is accumulating evidence for higher response rates. As has been previously discussed, release of 5-ASA is desirable in the terminal ileum and colon. If we assume drug solubility in Krebs buffer is equivalent to that in the ileum, then the volume (V) of intestinal fluid necessary for complete drug dissolution from the solid dosage forms to occur can be calculated using Equation 3.4:

$$V = \text{Dose} / \text{Solubility (D/S)}; \quad \text{Equation 3.4}$$

$$800 \text{ mg} / 4.51 \text{ mg ml}^{-1} = 177.4 \text{ ml.}$$

The mean free fluid volume in the small intestine is 105 ± 72 ml (Schiller et al., 2005) in the fasted state and decreases postprandially to 54 ± 41 ml. This limited fluid availability will reduce the dissolution of 5-ASA from the dosage form, particularly in regions of the gastrointestinal tract where it displays poor permeability. This problem is likely to be exacerbated in the colon as the fluid volumes are very limited; 13 ± 12 ml vs 18 ± 26 ml in the fasted and fed states respectively (Schiller et al., 2005). The solubility of 5-ASA is also likely to be lower in proximal colonic luminal fluid as the pH is lower in this region compared to the distal small intestine. Hence not only sink conditions are not met however the saturation solubility of the drug is also likely to be exceeded.

The dose of prednisolone in active disease is 40 mg once daily with dose tapering occurring at 5 mg/ week on patient improvement (Carter et al., 2004). $40 \text{ mg} / 0.51 \text{ mg ml}^{-1} = 78.4 \text{ ml}$. Although it has an almost ten fold lower solubility than 5-ASA, the dose is lower therefore requiring less volume for dissolution.

3.5 CONCLUSIONS

The solubility of 5-ASA is dependent on buffer species and buffer capacity of the media. Hanks buffer therefore provided a good reflection of the solubility of this acidic drug in jejunal fluids. This finding can be extrapolated to other ionic drugs as bicarbonate provides a more realistic simulation of the buffer composition of luminal fluids of the human small intestine. Solubility of 5-ASA in ileostomy fluids is substantially lower than in Krebs buffer; yet it is closer to this medium in comparison to phosphate buffer. 5-ASA solubility needs to be measured in ileal fluid aspirates to determine if the prediction provided by Krebs for 5-ASA solubility in ileal fluids is as good as that provided by Hanks for jejunal fluids. Addition of intestinal surfactants to the buffer media was not found to alter the solubility of 5-ASA.

Fasted state simulated intestinal fluids (FaSSIF) with intestinal surfactants (sodium taurocholate and lecithin), did not provide a good prediction of the solubility of the poorly soluble drug, prednisolone, in human intestinal fluids. Although there is abundant evidence in the literature for usefulness of these media for prediction of drug solubility, their value seems to be for drugs which are highly lipophilic and with very poor aqueous solubility. The solubility of prednisolone was unaffected by the buffer composition however it increased with increasing concentrations of intestinal surfactants in simulated media.

Chapters two and three have identified some elements of the dissolution medium that influence drug release from pH-responsive systems. The specific factors pertaining to the physicochemical properties of the drug and the polymer have been evaluated. In the remaining chapters we seek to identify formulation parameters that influence the

performance of pH-responsive systems. Specific reference is made to interactions within the enteric coating.

CHAPTER FOUR

Molecular interactions that influence the plasticizer
dependent dissolution of acrylic films

4.1 INTRODUCTION

We have shown that the composition of the GI luminal environment is critical in determining drug release from pH-responsive systems. The luminal environment influences polymer ionisation and drug solubility. In the next two chapters we seek to evaluate the importance of the enteric film coating formulation in influencing dissolution of the pH-dependent polymer.

Of the different excipients present in film coatings we chose to study the effect of plasticizer component. We anticipated that this component may influence dissolution of the polymer as plasticizers have the potential to interact with the polymer at the molecular level and give rise to micro- and macroscopic changes in properties of film coatings.

4.1.1 Plasticizers in tablet film coatings and the changes they induce

Effective plasticizers are usually high-boiling point, neutral and stable fluids (Dittgen et al., 1997), which have the ability to alter the thermal and physical-mechanical properties of a polymer. Changes in mechanical properties that arise include: increase in strain or film elongation, decrease in elastic modulus and decrease in tensile strength (Aulton et al., 1981; Okhamafe and York, 1983; Gutierrez-Rocca and McGinity, 1994). One of the important thermal changes in the thermal properties of polymers induced by plasticizers is a reduction in the glass transition temperature (T_g).

T_g is the temperature at which an amorphous polymer changes from a hard glassy material to a soft rubbery material. This corresponds to a change from a state of low free volume and high density to a state of higher free volume and less density. The transition can be detected by examining the temperature dependence of such properties as modulus of elasticity, specific heat and dipole orientation and therefore T_g has been widely used to assess plasticizer efficiency. Several authors have demonstrated correlations between plasticizer efficiency and reduction in T_g (Tarvainen et al., 2001). Changes in T_g influence internal stresses in the polymer film coating and therefore crack development (Okhamafe and York, 1985).

Plasticizers are known to alter molecular mobility of the system by configuring between the chains and altering polymer intermolecular interactions thus increasing film flexibility (Banker, 1966). Several theories have been proposed to explain the mechanism of plasticizer action. The most prevalent and most commonly cited in the literature include: lubricity theory, gel theory and free volume theory (Marcilla and Beltrán, 2004).

4.1.2 Theories proposed for plasticizer mechanism of action

The lubricity theory envisages the polymers to exist as planes and the plasticizers orientating between the planes thus reducing the friction between the polymer chains and the force necessary for them to glide past each other. Kirkpatrick (1940) contributed to the lubricity theory and suggested the following factors to be of importance for plasticizer action:

- (i) presence in both the plasticizer and polymer of groups that offer points of mutual attraction
- (ii) appropriate location of these groups relative to each other to allow attractive forces to exist
- (iii) suitable shape of the plasticizer to accommodate between the planes

The gel theory considers polymers to form three-dimensional honeycomb structures sustained by loose attachments between the polymer molecules along their chains. Plasticizers reduce these attachments between the polymer molecules by a dynamic and static mechanism. The dynamic mechanism is through a solvation-desolvation equilibrium whereby the plasticizer diffuses through the polymer network, reducing polymer contacts temporarily, and then moves around to another site, allowing the structure to close behind it in a different position. The static mechanism arises from polymer-plasticizer interactions with mean life times that are long compared with the time-scale of segmental motions (Marcilla and Beltrán, 2004).

The free volume theory emerged from an effort to explain the reduction in glass transition temperature of plasticized polymer systems. It is based on the concept that between atoms and molecules there is nothing but free volume. Sears and Darby (1982) summarised that free volume comes from three main sources; motion of chain ends, motion of side chains and motion of the main chain. These motions, and therefore the free volume, of a polymer system can be inherently increased by:

- (i) Increasing the number of polymer end groups (therefore lower molecular weight polymers).

- (ii) Increasing the number or length of side chains.
- (iii) Increasing the chance of main chain movement by including segments of low steric hindrance and low intermolecular attraction.

The above approaches achieve internal plasticization. If the polymer however is of a large molecular weight and is a long chain with few side groups, then the dipoles of adjacent polymer chains would align thus offering numerous attractions between nearby chains. In contrast, the presence of side groups would 'shield' the dipoles on the opposite polymer chains and therefore separate the polymer chains.

4.1.3 Plasticizer influence on moisture permeability and drug release through modified release polymer films

Efforts have been made to establish a correlation between moisture diffusion and T_g or tensile strength. It was initially proposed that the reduction in molecular order which arises from plasticization enhances diffusion pathways thus facilitating diffusion of water molecules (Okhamafe and York, 1983). However it was later found that plasticization is not always accompanied by increased moisture diffusion (Okhamafe and York, 1988) as plasticizers may extensively hydrogen bond with the polymer or with moisture thus obstructing further moisture permeability (Okhamafe and York, 1987). It has been proposed that plasticizer-induced changes in polymer tortuosity and porosity alter drug diffusion through GI tract insoluble polymer systems, however studies have not substantiated this (Jenquin et al., 1992).

Lecomte and co-workers (2004) have studied polymer coatings comprised of a blend of enteric and GI tract insoluble polymers. Plasticizers were found to more favourably

partition into certain polymers than others. The plasticizer was in some cases found to be associated with the extent of water uptake and consequential drug release. A comparison of a hydrophilic and hydrophobic plasticizer showed that greater leaching of the latter from the film renders decreased mechanical resistance and crack formation which can affect the mechanism of drug release.

4.1.4 Fabrication of Eudragit S polymer films with plasticizers

As a free flowing dry powder, Eudragit S has a high Tg (433 to 444 K). To produce Eudragit S tablet coatings, it is essential to blend this polymer with a plasticizer to reduce coating brittleness and to achieve smooth, crack-free films. The objective of this chapter was to understand the relative influence of plasticizers on enteric polymer free film dissolution. This was investigated through the screening of a small library of plasticizers from different classes and determining the plasticizer and film parameters that correlate to dissolution. Plasticizer aqueous solubility and structure were examined. The wettability and molecular motions of the film coating were studied.

The molecular motions investigated include co-operative segmental mobilities (involving the polymer main chain) as well as side group motions. These relaxations are commonly referred to as α (primary) and β (secondary) relaxations respectively. Segmental relaxations were characterised by measurement of the Tg using differential scanning calorimetry (DSC), dynamic mechanical analysis (DMA) and thermally stimulated depolarisation current (TSDC) techniques. Secondary relaxations were investigated in detail by examining the dielectric properties of the films using TSDC. TSDC work was conducted in collaboration with Professor Steve Brocchini from the Department of Pharmaceutics at The School of Pharmacy and with Professor Nery

Suárez from the Department of Physics at University Simón Bolívar, Caracas, Venezuela.

According to the Gordon Taylor equation (Equation 4.1);

$$T_{g_{mix}} = \frac{w_1 T_{g1} + k w_2 T_{g2}}{w_1 + k w_2} \quad \text{Equation 4.1}$$

where $T_{g_{mix}}$ is the T_g of the mixture, T_{g1} and T_{g2} the glass transition temperatures of component 1 (solid) and component 2 (water or plasticizer), w_1 and w_2 the weight fractions of the solid and water respectively and k a constant calculated from the density (ρ) and the T_g of the components according to:

$$k = \frac{T_{g1} \rho_1}{T_{g2} \rho_2} \quad \text{Equation 4.2}$$

hence the reduction in Tg of the polymer is proportional to the quantity of plasticizer included in the film. The plasticizers used in the current study were all liquids at ambient temperature (apart from one of them) and therefore the Gordon-Taylor equation could not be used to calculate the reduction in Tg of the Eudragit S film.

Tg determination by different methods can result in different values being obtained (Georgoussis et al., 2000). DSC reflects polymer chain movement by measuring the changes in specific heat capacity (C_p) of the sample, DMA reflects the global nature of the sample by measuring mechanical changes, and TSDC detects the Tg through

dipolar rearrangements. DSC and DMA are the two most common methods for determining T_g (Sircar et al., 1999).

4.1.5 Thermal characterisation of polymer/plasticizer free films

4.1.5.1 Differential scanning calorimetry

DSC measures the heat flow into or from a sample as it is subjected to thermal treatment (heated, cooled or maintained at isothermal conditions) in relation to an inert reference that undergoes the same treatment. As the sample undergoes a transition, energy will be absorbed or evolved by the sample. StepScan- DSCTM (SSDC) was employed; this performs relatively fast, repetitive sequences of short heat-hold segments (Figure 4.1). This differs from modulated DSC in that it uses an isothermal step instead of a cooling step.

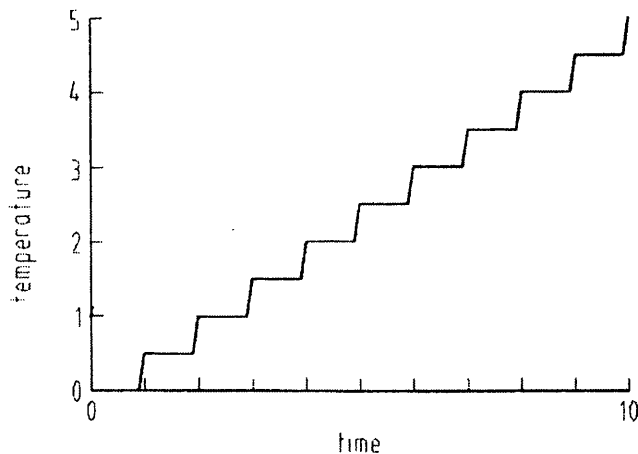


Figure 4.1 Illustration of the heating-isothermal mode of step-scan. Adapted from Hhne et al. (2003).

Similar to modulated DSC, SSDC has the advantage of detecting subtle thermal transitions which in some cases cannot be detected by normal mode DSC and distinguished from baseline noise. It has increased sensitivity without compromising resolution (Verdonck et al., 1999). This was useful for our polymer free films as there was great difficulty in detecting their T_g in normal mode; even at high scan rates. However the disadvantage of SSDC is that it demands long scanning times.

4.1.5.2 *Dynamic mechanical analysis*

In DMA the sample is subjected to an oscillating stress, measured as force per unit area, which results in sample deformation (strain) (Jones, 1999). The data is expressed graphically using two figures: modulus versus temperature, or $\tan \delta$ versus temperature. The modulus is the ratio of applied stress to strain. As most materials are viscoelastic; the modulus has two components: (i) in-phase component with the applied stress (storage modulus, E') which corresponds to the sample's elastic response and (ii) out-phase component with the applied stress (loss modulus, E'') which corresponds to the sample's viscous component. The ratio of the dissipated mechanical energy to stored mechanical energy is represented by the $\tan \delta$ (E''/E') (Lafferty et al., 2002). If an oscillatory stress is applied to a perfectly elastic solid then the deformation (strain) is exactly in line with the stress. However on applying stress to a viscoelastic solid then the deformation lags behind the stress by an angle of δ (Royall et al., 2005).

The T_g of an amorphous material is accompanied by a large change in its mechanical properties. At the T_g , the loss modulus goes through a maximum peak due to the

increase in the dissipated mechanical energy and the storage modulus decreases due to the reduced resistance of the material to deformation (Chartoff, 1997; Jones, 1999). Consequently, the $\tan \delta$ goes through a maximum (Figure 4.2).

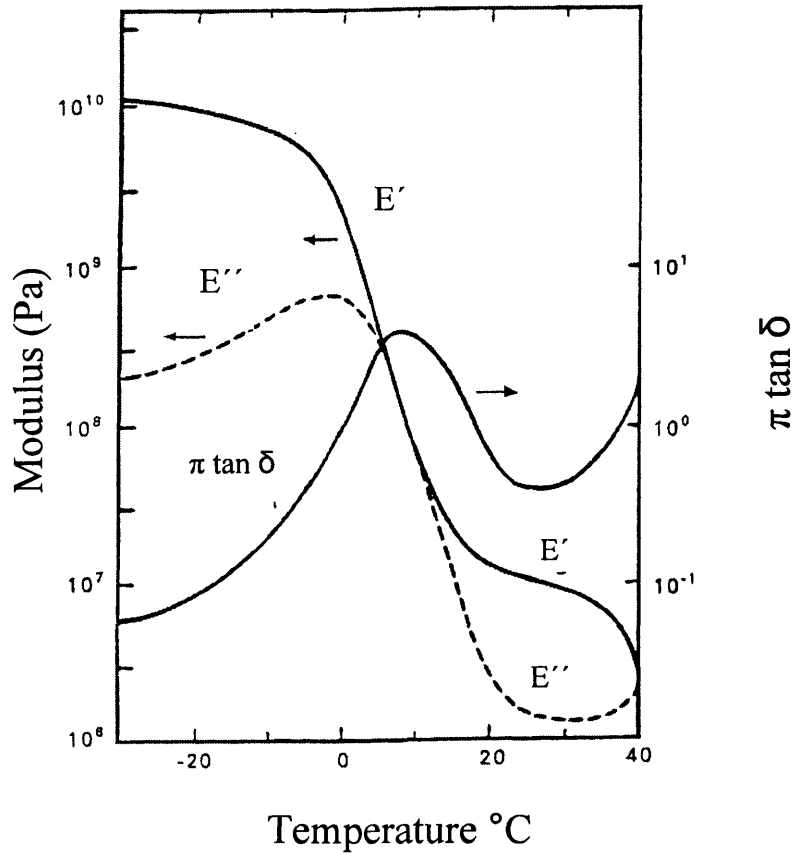


Figure 4.2 Illustration of a typical DMA plot of a polymer showing the temperature dependence of loss modulus (E''), storage modulus (E') and $\tan \delta$. Adapted from Chartoff (1997).

4.1.5.3 Comparison of differential scanning calorimetry and dynamic mechanical analysis

DSC uses relatively small sample masses; down to 2 mg with high speed DSC. However the sensitivity of DSC is not so high and it is sometimes difficult to determine the T_g when it is a minor event (Sircar et al., 1999). It may also be difficult

to determine immiscibility in a mixture whereby one of the components is minor, eg. plasticized/ unplasticized regions in formulations. In contrast, DMA has about 1000 times greater sensitivity for detecting the T_g (Chartoff, 1997), however, a larger sample size is required. In this experiment 6 mm x 2 mm strips were required for clamping in the instrument. Commercial DMA instruments differ in operation and methodology, eg. mode of sample deformation, test frequency, clamping of the sample and its distance from the thermocouples (Chartoff, 1997). This may therefore compromise the reproducibility of measurements attained on different instruments.

4.1.5.4 Thermally stimulated depolarisation currents

TSDC technique is well-established and frequently used in physics however it is relatively novel to the pharmaceutical sciences. It relies on dipolar rearrangements to generate depolarisation currents that can be related to local (secondary relaxations) and cooperative (structural relaxations) molecular mobilities. Its high sensitivity, leads to the detection of very low dipole concentrations (Suarez et al., 1982), and its low equivalent frequency (~ 1 mHz) allows multicomponent peaks to be resolved accurately (Suarez et al., 2001). Hence information can be derived on the interactions and bonding of polymer side groups.

TSDC is composed of the following steps (Figure 4.3) (Suarez et al., 1997; Shmeis et al., 2004):

Step 1 is the polarisation step. The sample is polarised under an electric field for a certain amount of time (t_p) at a given temperature (T_p). Any dipoles within the molecular structure orient themselves along the external electrical field. To study α -relaxations of the specimen, a polarization temperature higher than the T_g is used. Since molecular mobility increases with increasing temperature, the nature and amount of polarization generated by the field is influenced by the polarization temperature.

Step 2 is the cooling step. In the presence of the electric field the sample is quenched rapidly to a very low temperature, usually liquid nitrogen temperature, where molecular motion ceases. The dipolar orientation is thus frozen.

Step 3 is the depolarization step. The polarizing electric field is switched off and the sample temperature is increased at a controlled rate thus decreasing the relaxation time of the molecular motions and allowing return of the sample to the equilibrium state. The disorientation of the dipoles gives rise to a small electric current (depolarization current) which is measured as a function of temperature. Where α and β relaxations arise peaks are observed in the dielectric current spectra.

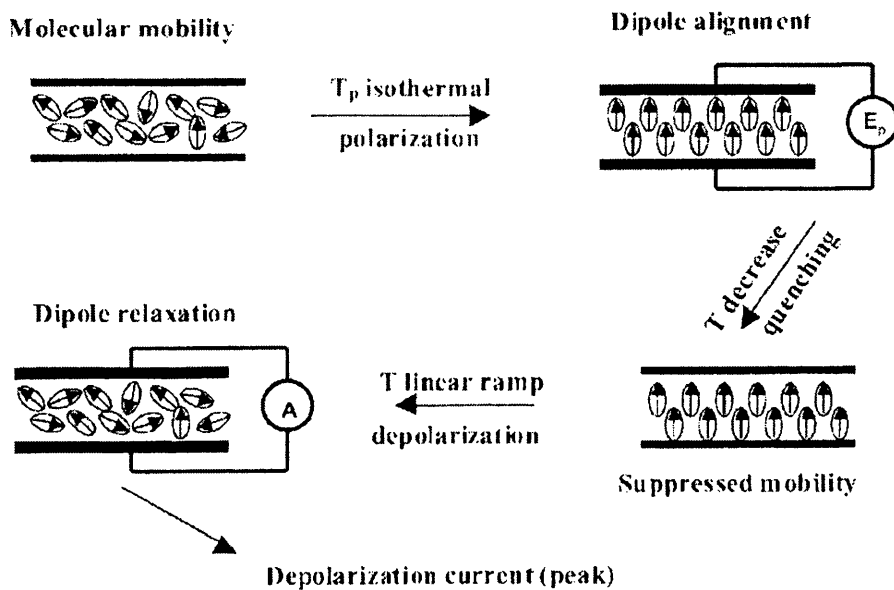


Figure 4.3 The fundamental steps underlying the thermally stimulated depolarisation current technique. Reproduced from Shmeis et al. (2004).

4.1.6 Measurement of contact angle

Interaction at the solid/liquid interface whereby a liquid spreads over a solid surface is known as ‘wetting’. For a solid to dissolve it must first be wetted. The wetting of the different films by buffer medium was assessed by measuring the contact angle (θ) (Figure 4.4). The contact angle gives an indication of the affinity of the two phases for each other. A low contact angle indicates good spreading of the liquid and wettability of the surface; the two phases therefore have affinity for each other (Buckton, 1995).

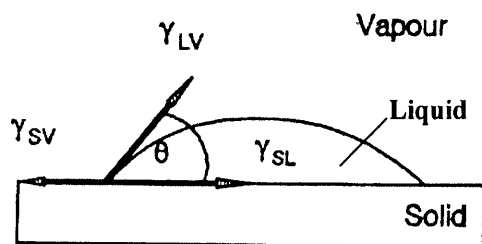


Figure 4.4 Interfacial forces acting on a drop of liquid that determine its degree of spreading onto a solid surface. Contact angle is the balance of three interfacial forces: γ_{SL} (solid-liquid interface), γ_{LV} (liquid-vapour interface) and γ_{SV} (solid-vapour interface). Adapted from Buckton (1995).

One of the methods for measuring the contact angle is the Wilhelmy plate technique (Figure 4.5) (Sheridan et al., 1994). The apparatus is contained within a draught-free cabinet and temperature is controlled at $25 \pm 1^\circ\text{C}$ by water flowing through a jacketed vessel from a circulator (Gallenkamp). The glass plate coated with plasticized polymer film is attached to the microbalance arm via a balanced hook. The liquid is placed onto the motorised platform and raised at a constant speed of $50 \mu\text{ms}^{-1}$ until 10 mm of the plate is immersed under the liquid surface. Force readings are attained at one second intervals as a function of time and stage position. The force detected by the balance (F) at first contact between the plate and the liquid is determined and used to obtain the contact angle using Equation 4.3.

$$F = \rho\gamma_{LV} \cos \theta \quad \text{Equation 4.3}$$

where ρ is the perimeter of the plate, γ_{LV} is the liquid surface tension and θ is the contact angle. Liquids have a zero contact angle on clean glass thus a glass plate can be used to measure the γ_{LV} .

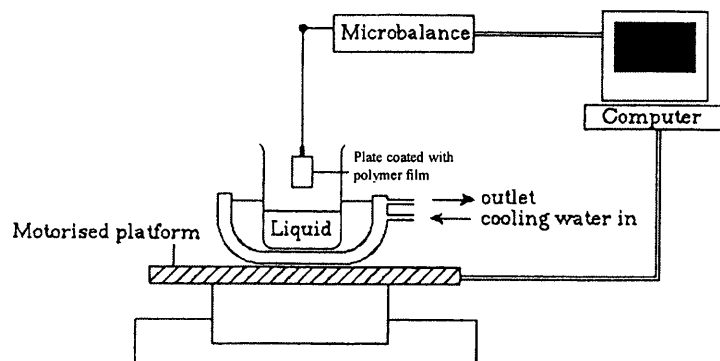


Figure 4.5 Schematic diagram of the Wilhelmy plate apparatus used for measuring surface tension of liquids and contact angle of liquids against a solid surface. Adapted from Buckton, 1995.

Figure 4.6 shows the typical output of a Wilhelmy plate experiment. Contact of the plate with the liquid occurs at point B and the force rapidly rises to point C after which there is a buoyancy slope (C-D) arising from plate immersion in the liquid. Line C-D is extrapolated back to point E which is the true force representing the instantaneous plate/liquid contact. This force is fitted into Equation 4.3 to calculate the advancing contact angle. Receding data (G-J) is obtained by removing the same plate from the liquid; by lowering the platform at the same speed of $50 \mu\text{m s}^{-1}$. Where the slope G-H crosses the perpendicular line drawn from zero contact, the force measurement is used to obtain the receding contact angle (Buckton, 1995).

The line G-J will always be higher than C-D due to hysteresis. One of the reasons hysteresis arises is from the reorientation of the molecules at the solid surface or in the liquid. However for surface tension experiments there should be no difference between C-D and G-H as the contact angle is 0.

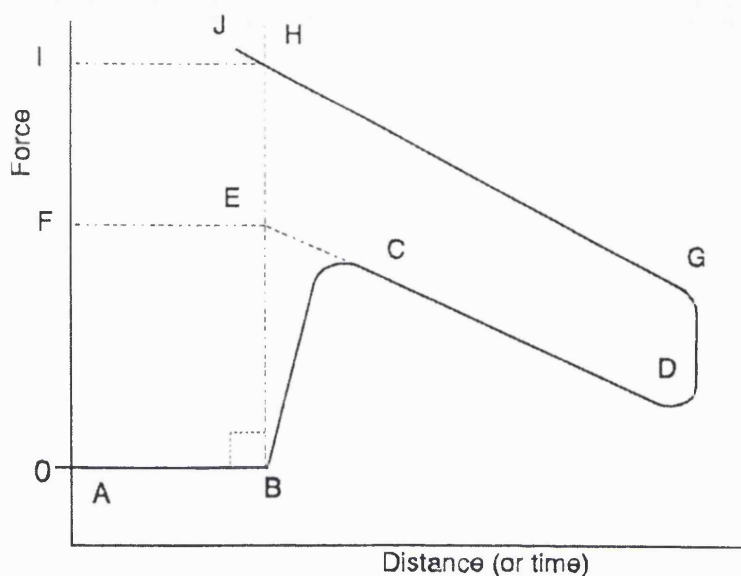


Figure 4.6 Schematic output of a Wilhelmy plate experiment for determining the contact angle of a liquid against a solid surface. Reproduced from Buckton (1995).

4.2 OBJECTIVES

- To investigate plasticizer influence on the dissolution of acrylic pH-responsive polymer free films.
- To investigate plasticizer and film parameters that may correlate to film dissolution. Plasticizer parameters to be explored include aqueous solubility and structure. While polymer film features to be studied include molecular motions and wettability.
- To compare the T_g of polymer films in the wet state (while immersed in dissolution medium) with the dry state using immersion DMA.
- To compare the T_g attained by the different techniques of DSC, DMA and TSDC.

4.3 MATERIALS AND METHODS

4.3.1 Materials

Eudragit S polymer (MW=135,000 g/mol) was donated by Degussa, Darmstadt, Germany. Plasticizers studied from the citrate class are: triacetin (TA), acetyl triethyl citrate (ATEC) (Sigma Aldrich, UK), triethyl citrate (TEC) and tributyl citrate (TBC) (Fluka, Germany). Plasticizers studied from the polyol group: polyethylene glycol (PEG 6000) and propylene glycol (P-diol) purchased from Fluka (Germany) and Fisher Scientific (UK) respectively. Plasticizers studied from the class of phthalate esters: dimethyl phthalate (DMP), dibutyl phthalate (DBP) and dioctyl phthalate (DOP) (Sigma Aldrich, UK). Tributyl phosphate was studied from the class of organic phosphates (Fluka, Germany). Refer to table 4.1 for plasticizer structure and MW. Phosphate buffer was prepared from analytical grade KH_2PO_4 and NaOH purchased from VWR Chemical Ltd., UK.

Table 4.1 Structure, molecular weight and water solubility^a of plasticizers.

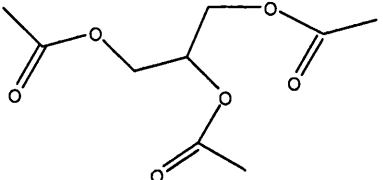
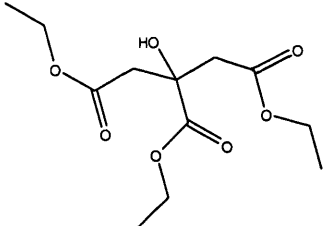
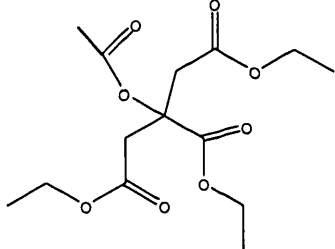
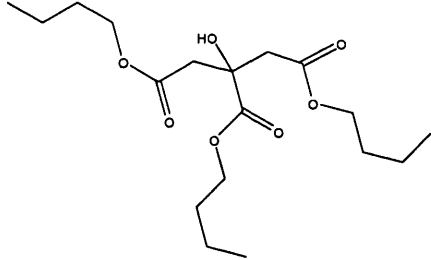
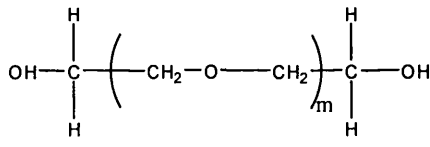
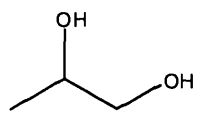
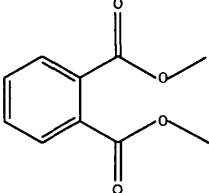
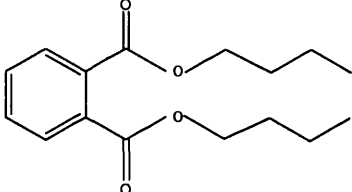
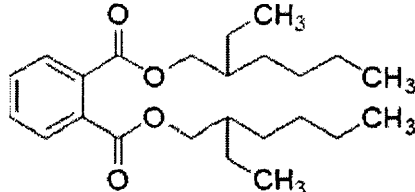
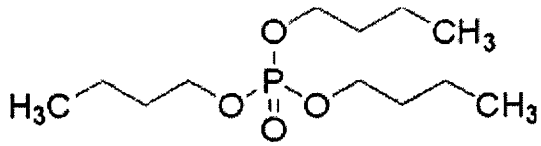
Plasticizer	Structure, g/mol MW	% m/v water solubility
Triacetin (TA)	 <p>MW 218</p>	6.7 – 7.8
Triethyl citrate (TEC)	 <p>MW 276</p>	5.5- 6.9
Acetyl triethyl citrate (ATEC)	 <p>MW 318</p>	0.72
Tributyl citrate (TBC)	 <p>MW 360</p>	< 0.002
Polyethylene glycol 6000 (PEG 6000)	 <p>m ~ 143</p> <p>MW 6000</p>	Very soluble
Propylene glycol (P-diol)	 <p>MW 76</p>	> 10%

Table 4.1 continued.

Plasticizer	Structure, g/mol MW	% m/v water solubility
Dimethyl phthalate (DMP)	 MW 194	0.4%
Dibutyl phthalate (DBP)	 MW 278	0.04%
Diocetyl phthalate (DOP)	 MW 391	0.0002%
Tributyl phosphate (TBP)	 MW 266.	0.042%

^a Aqueous solubility of plasticizers compiled from Rowe et al. (2003) and Yalkowsky and He (2003).

4.3.2 Preparation of polymer free films by solvent evaporation

Eudragit S free films were prepared with plasticizer weight concentrations that are typically recommended for Eudragit S tablet coating applications. Films were fabricated from polymer-plasticizer solutions in ethanol that were cast onto Teflon plates followed by solvent evaporation. The plasticizer, 15 % or 20 %, of polymer weight was first dissolved in 100 g of 95 % ethanol for 30 minutes at room temperature in a beaker. Eudragit S powder (8.5 % w/w of solvent) was gradually added to the ethanolic solution that was rapidly stirred by a Heidolph RZR1 overhead stirrer. The mixing vessel was sealed with Parafilm to prevent solvent evaporation and the solution was stirred overnight for a further 12 hours to ensure complete polymer dissolution. A portion of the solution (9 ml) was poured onto separate Teflon[®] molds (9 cm diameter) and allowed to dry at room temperature, under a funnel, for eight hours. Funnels were employed as they reduce the evaporation rate (by decreasing the exposed surface area) and therefore smoother and more even films arise. The films were then peeled from the Teflon moulds and placed in an oven at 50°C for 48 hours to remove residual ethanol/water. The plasticizers with very low aqueous solubility (DBP, DOP, TBC and TBP) could only be included at a concentration of 15 % of polymer weight before phase separation was observed. Film thickness was measured at different points using a micrometer (Mitutoya, Japan) and was found to be 130 ± 10 μm . The films were subsequently stored under vacuum in a desiccator. To find out the residual solvent of the films thermogravimetric analysis (TGA) was conducted on the films. TGA was performed with a Perkin-Elmer Pyris 6 TGA (Perkin Elmer Instruments, Bucks, UK) using 8-13 mg of film at a scan rate of 10 K/min over a temperature range of 30 to 150°C.

4.3.3 Preparation of compression molded polymer film

Only a control Eudragit S polymer film was prepared using this method as it was performed at another institution (Division of Biomaterials and Tissue Engineering, Eastman Dental Institute, University College London). Eudragit S powder was spread onto an aluminium plate and heat pressed using a Specac Hydraulic Heated Press (Specac, UK) at a temperature of 185 °C, and with a compression force of 5 tons (height 500 µm) for 15 min. The film was peeled off the aluminium plate and stored under vacuum in a desiccator until further testing.

4.3.4 Film dissolution

Film dissolution was measured using a custom made two-compartment permeation cell (Figure 4.7). This is similar to a methodology employed by Spitael and Kinget (1977b). A sample film with an area of 1.8 cm² separated the two compartments with the aid of an O-ring separation. The film was incubated to pH 7.4 in phosphate buffer (0.05 M) under sink conditions. The donor compartment had a volume of 5 ml and was filled with a saturated solution of the drug 5-ASA in pH 7.4 phosphate buffer (6.34 mg/ml). The acceptor compartment also had a volume of 5 ml, however continuous flow was employed in this compartment whereby a volume of 100 ml of pH 7.4 phosphate buffer (0.05 M) maintained at 37 °C was circulated through via a peristaltic pump. The solution in the acceptor compartment was continuously stirred using a magnetic stirrer. Onset of 5-ASA permeation from the donor to the acceptor compartment was determined by UV spectrophotometry at 330 nm and was found to correspond to film dissolution as pores in the film became clearly visible. A very

sharp rise in absorbance arose and this was defined as the breakthrough time of the film. Dissolution results reported correspond to the dissolution onset of the films. UV readings were taken automatically every 15 minutes by an in-line UV spectrophotometer (Cecil 2020, UK). Phosphate buffer continuously circulating the acceptor compartment passed through the UV-spectrophotometer so that UV measurements were taken in real time. All film formulations were tested at least in triplicate.

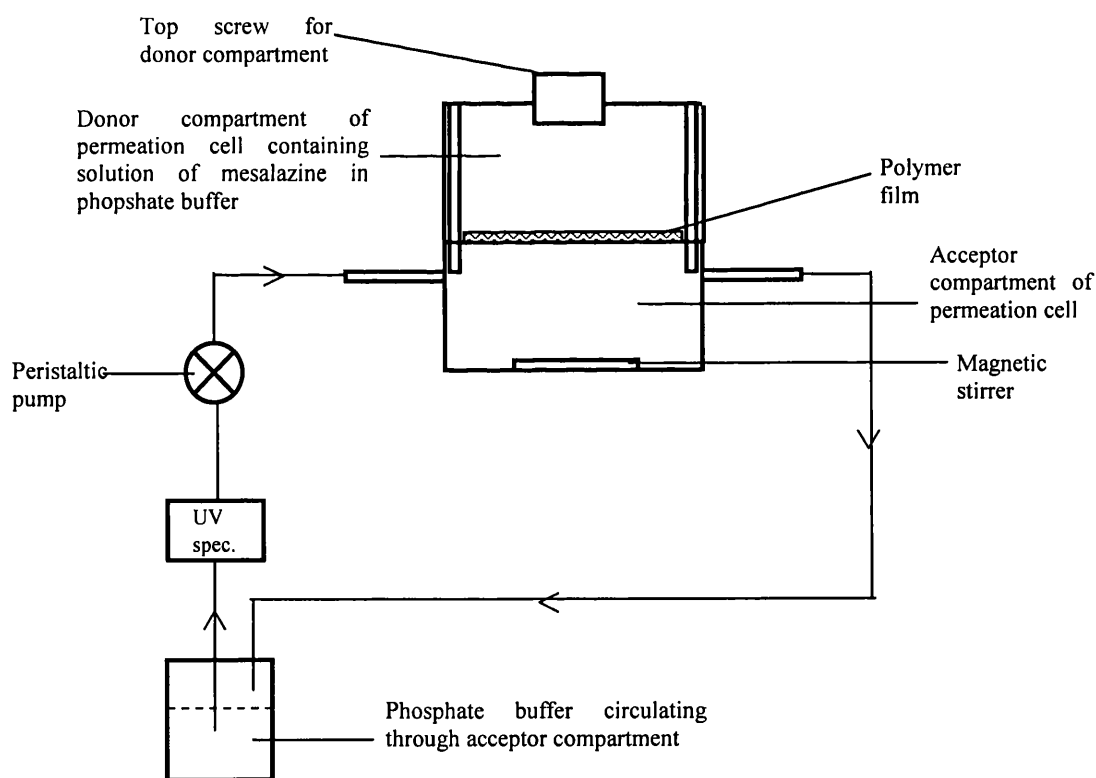


Figure 4.7 Schematic diagram of the measurement of film dissolution using a two-compartment permeation cell.

Phosphate buffer was used as the film dissolution medium since there was no way of maintaining the stability of bicarbonate buffer in the permeation cells. It was not feasible to continuously sparge the compartments with 5 % CO₂. Bicarbonate buffers are more realistic media however in this set of experiments we were not primarily concerned with the absolute dissolution values however we were interested in the trends attained with the different formulations. 0.05 M phosphate buffer was used as opposed to 0.2 M phosphate buffer or Sorensen's buffer since it has the lowest ionic strength and buffer capacity therefore making it more comparable to GI luminal fluids.

4.3.5 Methodology for dynamic mechanical analysis

DMA was conducted using a Tritec 2000 DMA (Triton Technology Ltd., Nottinghamshire, UK). Films were cut into dimensions of 6 mm width and 2 mm length and subjected to a tensile deformation mode at a frequency of 1 Hz, static preload of 0.1 N and dynamic displacement of 10 µm.

The instrument is designed such that there are two pairs of clamps (back and front). The sample is positioned and gripped between these clamps (Figure 4.8). First the sample is tightened in the back (driveshaft) clamp and then a static force of 0.1 N is applied. This brings the driveshaft forward. The sample is then fully tightened in the front clamp (Figure 4.8). As the experiment starts the force is removed thus allowing the sample to stretch. This stretching of the sample avoids buckling during the run. The loaded sample needs to be straight and mounted in the glassy condition, thus loaded when the oven is cooled to the starting temperature.

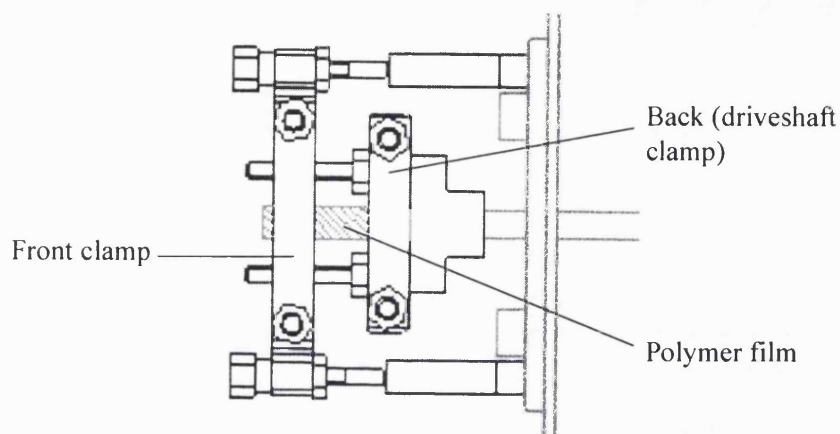


Figure 4.8 Geometric set up of a Tritec DMA for measuring T_g of films in tension. (Adapted from Tritec DMA manual).

A heating rate of 6 K/min was employed from 298 to 473 K. We report the T_g value as the peak loss modulus as opposed to the peak $\tan \delta$. The former is the more appropriate representation as the upper temperature for use of most amorphous polymers is their 'softening point'. Hence by the transition midpoint (peak $\tan \delta$) this softening point would have been exceeded (Chartoff, 1997).

Increase of frequency will show a shift of the moduli and $\tan \delta$ up the temperature scale. Multiple frequencies were employed in our experiments to verify that the transitions we are observing are glass transitions, since glass transition temperature is sensitive to the frequency (the lower the frequency the lower the T_g temperature). Figure 4.9 illustrates this increase in $\tan \delta$ with increasing frequency.

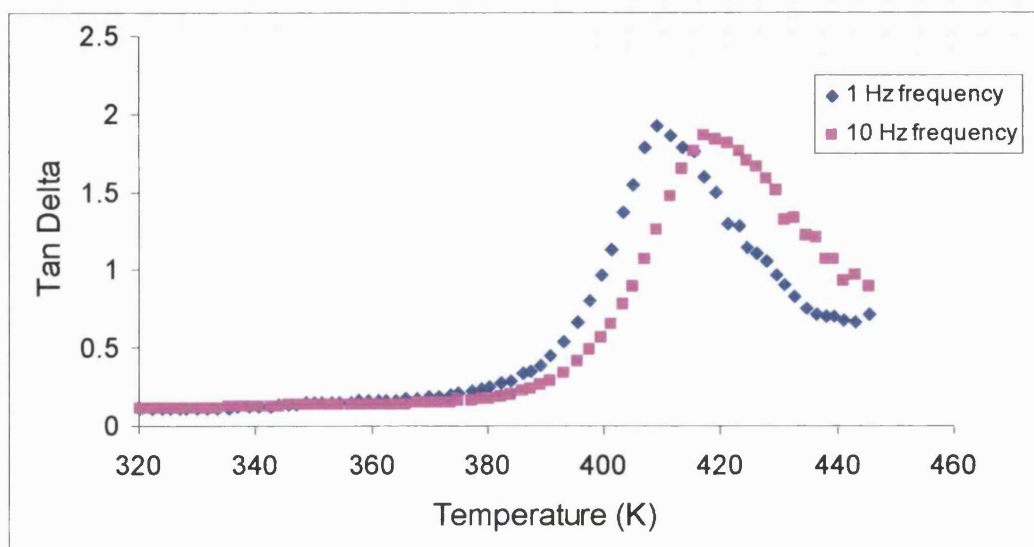


Figure 4.9 A typical response of the Tg (represented by $\tan \delta$) as a function of frequency. This is the result for Eudragit S film with TEC as the plasticizer.

4.3.6 Methodology for immersion dynamic mechanical analysis

DMA instruments which have the capacity to measure the Tg of materials while immersed in a liquid medium have recently been developed. This is useful as it can give an insight into changes in Tg of materials as a result of fluid uptake or plasticizer leaching out into the dissolution media. The same DMA geometry and parameters were used in the immersion mode however the end temperature was only 363 K to prevent the water boiling during the course of the experiment. The liquid medium used was pH 6.8 phosphate buffer to simulate small intestinal pH. pH 7.4 phosphate buffer was not used as in the dissolution experiments because the film starts to dissolve and therefore the thermal properties cannot be reliably measured. Prior to measuring the Tg of films using immersion DMA, the films were subjected to pre-

treatment in pH 6.8 buffer (just by immersion) for three hours. This is to simulate the average small intestinal transit time of dosage forms.

4.3.7 Methodology for differential scanning calorimetry

Films were directly cast into non-hermetically sealed aluminium pans (Perkin-Elmer Instruments, Bucks, UK). Polymer/plasticizer solution was added to the pan using a pipette Pasteur. This was allowed to dry for one hour at room temperature (under a funnel) before another layer was cast on top of it. Three layers were required to attain the required sample mass of 8 – 10 mg necessary to obtain a distinctive glass transition. This procedure was adopted to ensure good thermal contact between the sample and the pan; if however several layers of pre-prepared films were cut and accumulated in the pan then air between the film layers would impose resistance to heat flow. Samples within the pans were dried in an oven at 50 °C for 48 hours and stored in a desiccator over silica gel until analysis. Before analysis the pans were crimped. The pans were accurately weighed while empty and after filling with sample to determine the exact sample mass. The mass of the empty pan and lid were also recorded as this information needs to be known for Step-Scan. An empty pan was also crimped and weighed for use as a reference. A PerkinElmer autobalance AD-4 (Perkin-Elmer Instruments, Bucks, UK) was used.

Film samples were evaluated by Step-Scan DSC using a Pyris 1 instrument (PerkinElmer Instruments, Bucks, UK). The sample was heated at 6 K/min for 2 K increments and then allowed to equilibrate for 0.5 min before being subjected to heating again. The sample was scanned from 298 to 473 K with a nitrogen gas purge at a flow rate of 20 ml/min. The T_g was taken as the half change in specific heat

capacity (ΔC_p) of the sample. Half ΔC_p was calculated from an extrapolation of the baselines for the onset and end of the glass transition step. The transition step was clear and the baselines were stable therefore enabling accurate and reproducible determination of the beginning and end of the transition. Figure 4.10 shows an example of this.

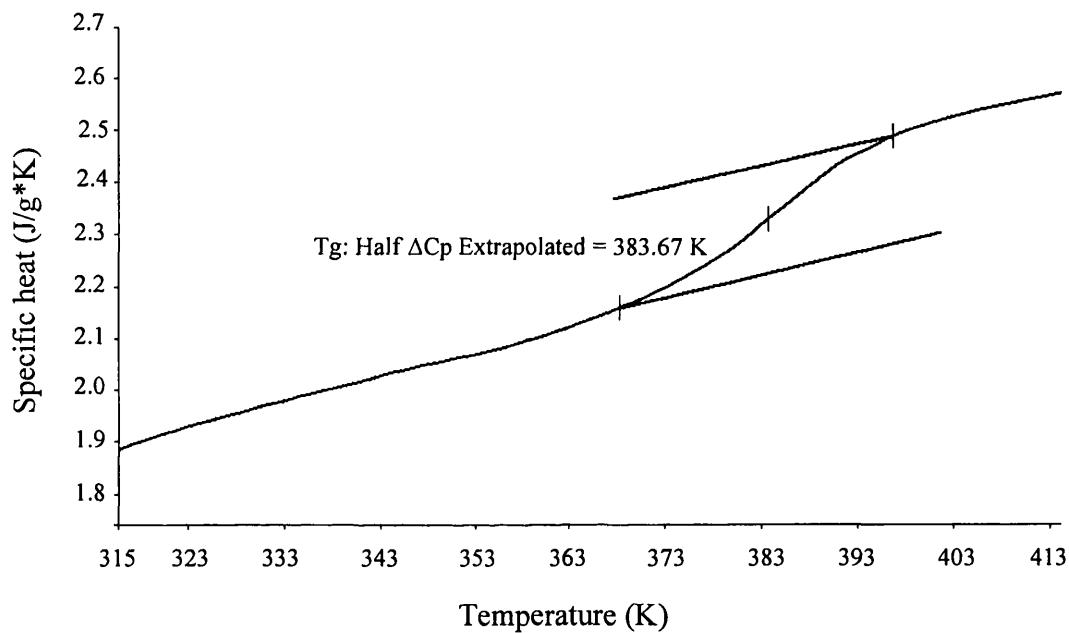


Figure 4.10 A typical DSC thermogram showing how the T_g (half ΔC_p) is obtained. This is the result for Eudragit S film with TEC as the plasticizer.

4.3.8 Methodology for thermally stimulated depolarisation current technique

TSDC was performed at University Simón Bolívar, using an in-house TSDC instrument. The Eudragit film is polarised at a certain temperature (polarisation temperature, T_p) in a electric field (5×10^5 V/m) and the state of polarization is frozen by quenching the sample rapidly (1 Ks^{-1}) to liquid nitrogen temperature. The electric field is then switched off and the sample temperature increased at a controlled rate (0.1 K/s) to record the depolarization current caused by the disorientation of the

dipoles. A Cary Vibrating Reed Electrometer (Model 401) was used to record the depolarization current. The sensitivity of the current measuring system is 10^{-17} A and the signal to noise ratio is greater than 500. The current-temperature data acquisition is fully automatic. To characterize the low temperature region of the dielectric spectra a T_p of 300K was employed. For the high temperature region of the dielectric spectra the samples were polarised at a temperature just above their T_g .

The low temperature TSDC peaks are complex wide bands arising from overlapping peaks; each peak corresponding to the reorientation of a particular functional group. Direct Signal Analysis (DSA) is a curve-fitting procedure that was developed to analyse the complex low temperature TSDC peaks (Aldana et al., 1994). The method consists of finding the elementary curves whose characteristic energies are equally spaced in a given energy window and whose combination best fits the whole experimental TSDC profile. The recorded TSDC current is approximated by Equation 4.4

$$J_D(T_j) = \sum_{i=1}^N \frac{P_{oi}}{\tau_i(T_j)} \exp\left(-\frac{1}{b_h} \int_{T_o}^{T_j} \frac{dT'}{\tau_i(T')}\right), \quad \text{Equation 4.4}$$

with $j = 1, M; \quad N \leq M/2$

where $J_D(T)$ is the current density, b is the rate at which the temperature is raised, $\tau(T)$ is the relaxation time for each elementary process and P_{oi} is its contribution to the total polarization. The temperature dependence of the relaxation time $\tau(T)$ of the low temperature relaxations has been mostly represented by the Arrhenius expression, Equation 4.5.

$$\tau_i(T) = \tau_{oi} \exp(E_{ai} / kT) \quad \text{Equation 4.5}$$

where τ_{0i} is a pre-exponential factor and E_{0i} is the reorientation energy of the i elementary curve. The pre-exponential factor is temperature dependent (proportional to T^{-1}).

The DSA method adjusts $J_D(T)$ (Equation 4.5) to the experimental data using the Marquardt-Levenberg nonlinear least-squares fitting algorithm. The initial parameters are the threshold and width of the energy window which is divided into N equally spaced energy bins, the N τ_{0i} values, one for each energy bin, is read; estimated from the value of the energy and the temperature range where the relaxation takes place.

The initial values for the set of P_{oi} are all equal and normalised, that is $\sum_{i=1}^N P_{oi} = 1$, which is a uniform distribution; i.e. initially every bin contributes equally to the total polarization of the sample. The results of the fitting procedure are summarised into an energy histogram which covers the selected energy window divided into N energy bins and whose height, P_{oi} , is proportional to the area under the curve corresponding to each elementary excitation. The algorithm also fits the τ_{0i} values corresponding to each energy bin. The whole TSDC curve is then simulated by adding all these contributions and plotting them with the experimental points. The whole procedure is then repeated with different starting parameters, until the quality of the fit, is deemed satisfactory.

4.3.9 Methodology for contact angle measurement

Before starting each set of experiments the microbalance of the Wilhelmy plate apparatus was calibrated with a 500 mg weight. Surface tension of water was also measured to confirm the accuracy of the procedures and functioning of the instrument. This was found to be $72.31 \pm 0.12 \text{ mN m}^{-1}$ (mean \pm SD) which is in agreement with the literature (Van Oss and Costanzo, 1992). The surface tension of the phosphate buffer was then measured and entered into the computer and used to solve equation 4.4. Surface tension of buffer was found to be very close to water at $71.7 \pm 0.21 \text{ mN m}^{-1}$.

Polymer films cast on to Teflon plates were cut into square pieces using templates of dimensions 25 mm x 25 mm. However a perfectly smooth and even surface could not be achieved with this method even when the film was not completely dry when it was cut. This led to a not very straight buoyancy slope and unreproducible contact angle measurements. An alternative method was tried which worked successfully. This involved preparation of polymer solutions of Eudragit S with plasticizer as previously described and using them to coat glass microscope coverslips (plates). All microscope coverslips were cleaned thoroughly using blue flame of Bunsen burner to remove any surface contamination. Using forceps, the plates were dipped into the polymer solution for 10 seconds and on removal the plates were inverted several times to achieve uniform distribution of the polymer solution over the plates. The coverslip was then dried on the laboratory bench under normal atmospheric conditions. However the rapid evaporation of ethanol and high interfacial tension resulted in poor film uniformity, especially at the edge of the plates. To resolve this, the polymer solution coated surface was dried in an ethanol environment. This was created by

pouring a solution containing 95 % ethanol and 5 % water into a weighing boat and placing a funnel over it. This ethanol environment was set up one hour prior to exposing the plate to it. The plate was positioned horizontally by attaching it at the edge to an inverted weighing boat. The plates were kept in this environment for 24 hours and then placed in an oven at 50 °C for two days. The plates were thereafter stored in a desiccator over silica gel for at least two days prior to performing the contact angle measurements.

Phosphate buffer used to measure contact angle of the polymer films was prepared from HPLC water. The buffer was then filtered using a 0.45 µm syringe filter. Buffer of 80 ml volume was poured into a 100 ml clean glass beaker and placed on the motorised platform of the Wilhelmy plate apparatus. Small beakers of the buffer were placed around the platform inside the chamber to regulate the vapour. The beaker was filled with fresh buffer every time a new coated plate was used. A minimum of five contact angle measurements were performed for each formulation.

The advancing angle is used to measure the contact angle as this is when the liquid makes contact with a fresh solid surface that has not been previously wetted.

4.4 RESULTS AND DISCUSSION

4.4.1 Dissolution of polymer films

From figures 4.11a and 4.11b it can be seen that plasticizers substantially influence the dissolution onset of Eudragit S films. Figure 4.11b displays the dissolution results for films prepared from plasticizers with very poor aqueous solubility ($< 0.05\%$). All the formulations illustrated in figure 4.11a have a faster dissolution than Eudragit only films. A quick glance at the results and comparison of these two figures may lead us to assume that the higher the aqueous solubility of the plasticizer the faster the dissolution of the enteric polymer film. This assumption can be rationalised by high aqueous solubility plasticizers leaching out of the film thus creating channels/pores through which drug can diffuse out. It may also be anticipated that channels allow aqueous media imbibition into the film thus facilitating film dissolution. However from a more thorough examination of the results we can infer that film dissolution is more complicated than this.

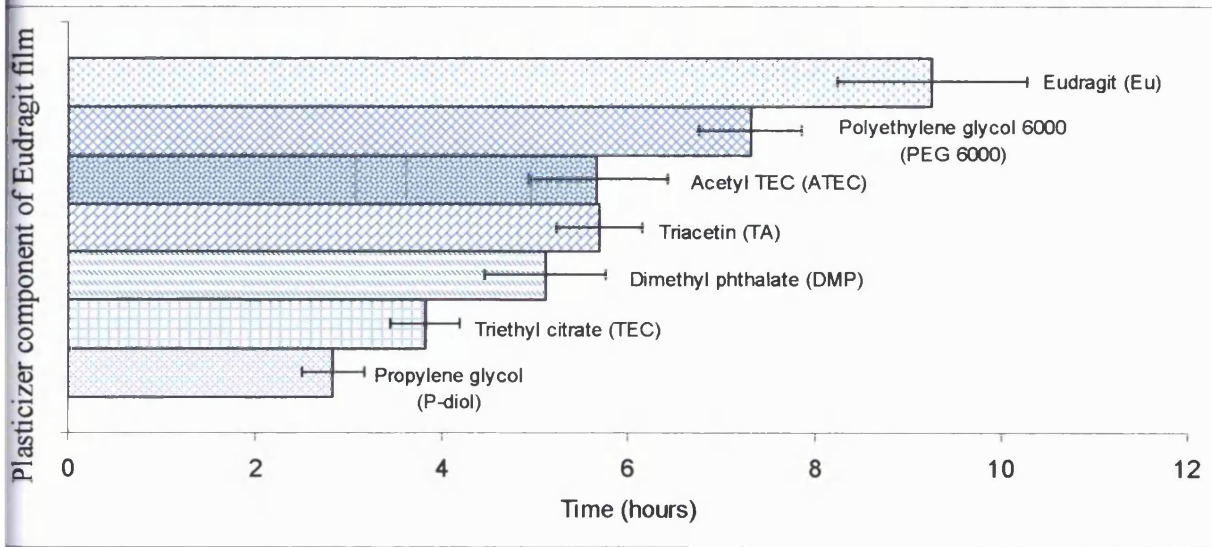


Figure 4.11a Onset of dissolution of Eudragit S films with or without plasticizers. Mean values \pm SD.

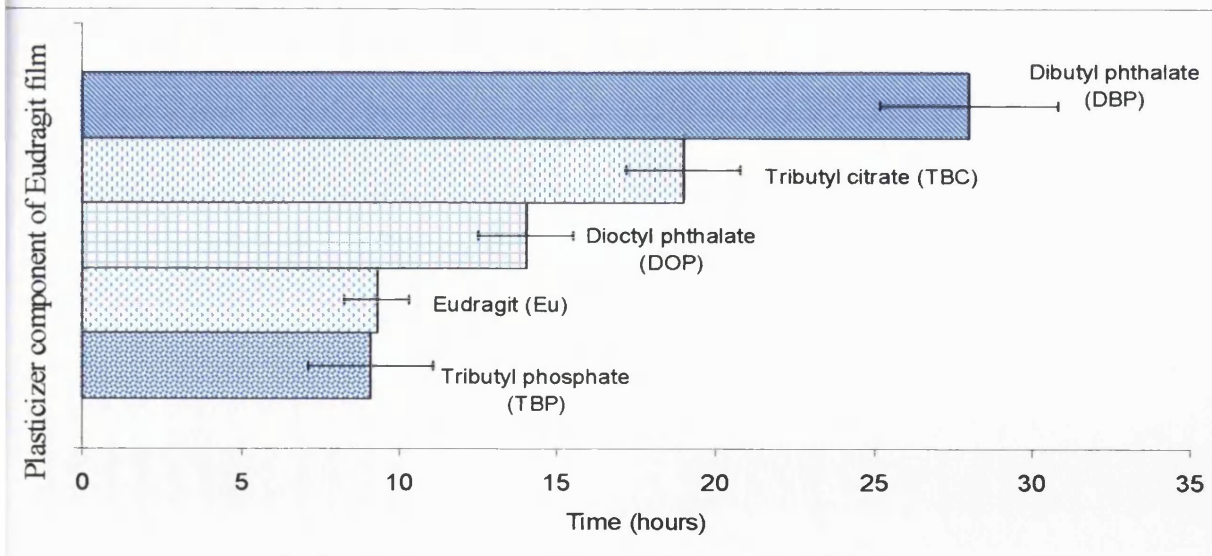


Figure 4.11b Onset of dissolution of Eudragit S films formulated with or without very poor aqueous solubility plasticizers (< 0.05 %). Mean values \pm SD.

The plasticizers TBP and DBP have very similar aqueous solubilities (0.042 % and 0.04 % respectively), yet there is an almost three-fold difference in the dissolution onset of the Eudragit S films fabricated from them. A further example is a comparison of films comprising DMP and triacetin; DMP has an almost 20-fold lower solubility than triacetin yet their corresponding Eudragit S films dissolve at a similar rate. Even a comparison of films constituting plasticizers from the same class illustrates that dissolution is not only dependent on solubility. DOP has a 200-fold lower solubility than DBP, however dissolution onset of the Eu-DOP films is two-fold faster.

4.4.2 Wettability of the polymer films

The next step was to consider wettability of the films as films cannot undergo dissolution before they are wetted. The contact angles of the film formulations with pH 7.4, 0.05 M phosphate buffer are shown in table 4.2. There appears to be no substantial differences between the contact angles of the different films. The contact angle for all films falls in the range of 68.3° to 71.5° and no trends correlating to film dissolution are apparent.

Table 4.2 Contact angles of different Eudragit S/plasticizer films with phosphate buffer.

Formulation	Contact angle (θ°) (\pm SD)
Eu	68.4 (\pm 1.35)
Eu + P- diol	70.0 (\pm 0.83)
Eu + TEC	68.8 (\pm 0.66)
Eu + DMP	68.7 (\pm 0.41)
Eu + TA	69.2 (\pm 0.47)
Eu + ATEC	70.0 (\pm 0.13)
Eu + PEG 6000	69.3 (\pm 0.27)
Eu + TBP	71.5 (\pm 0.33)
Eu + DOP	70.7 (\pm 0.61)
Eu + TBC	69.9 (\pm 0.35)
Eu + DBP	68.3 (\pm 1.55)

4.4.3 Glass transition temperature of films as measured by differential scanning calorimetry

The Tg of the Eudragit S powder was measured in our laboratory to be 436 K. This is in close agreement to the value of 433 K quoted in the literature (Dittgen et al., 1997). However the value we obtained for the Eudragit S control film was substantially lower at ~ 406 K. In attempt to establish the reason for this discrepancy a compression molded film of Eudragit S was prepared; thus avoiding the use of solvent. The Tg of this film was also found to be 436 K. The explanation for the lower than expected Tg

of the Eudragit S film prepared by solvent evaporation is the residual solvent in the film which acts as plasticizer. TGA showed that this control formulation contains 1.09% residual solvent. TGA was conducted on the other film formulations (Table 4.3). The films all had different amounts of residual solvent and no relationship is apparent between this and onset of film dissolution. This difference between the Tg of the polymer powder and solvent cast film is often observed. An example is in the work conducted by Gutierrez-Rocca and McGinity (1994) whereby the physical properties of Eudragit L100-55 (poly(methacrylic acid, ethyl acrylate)) cast films were studied. The Tg of Eudragit L100-55 film cast from isopropyl alcohol was reported by Gutierrez-Rocca and McGinity (1994) to be 358 K, whereas the Tg of the pure powder reported in the literature is 388 K (Dittgen et al., 1997).

Table 4.3 Residual solvent in the Eudragit S polymer films prepared with different plasticizers (expressed as mean % \pm SD).

Film Formulation	% Residual solvent (\pm SD)
Eu	1.09 \pm 0.22
Eu + P-diol	1.43 \pm 0.09
Eu + TEC	0.63 \pm 0.22
Eu + DMP	1.72 \pm 0.19
Eu + TA	1.10 \pm 0.17
Eu + ATEC	1.21 \pm 0.16
Eu + PEG 6000	1.86 \pm 0.25
Eu + TBP	1.68 \pm 0.13
Eu + DOP	1.25 \pm 0.11
Eu + TBC	1.65 \pm 0.08
Eu + DBP	1.82 \pm 0.13

No definitive trends could be seen between film dissolution and Tg measured by DSC (Table 4.4). However films fabricated from plasticizers with very poor aqueous solubility seem to have a higher Tg and slower dissolution onset. Films comprising DBP and TBC display higher Tgs and much slower dissolution compared to their methyl and ethyl counterparts. This slower dissolution is unlikely to be attributable to the large size of the plasticizer molecules since DOP gives rise to a two fold faster dissolution compared to DBP. Therefore the structure of the plasticizer, and

consequently its interaction with the polymer, seem to be implicated in film dissolution.

Table 4.4 Tg values as attained by DSC of the Eudragit S polymer films prepared with different plasticizers (expressed as mean \pm SD).

Film formulation	Tg (K) (half ΔC_p) (\pm SD)
Eu	405.9 \pm 0.14
Eu + P-diol	Two Tgs : 378 \pm 0.71, 405.8 \pm 0.61
Eu + TEC	383.7 \pm 1.03
Eu + DMP	385.7 \pm 1.72
Eu + TA	377.9 \pm 3.62
Eu + ATEC	390.8 \pm 2.27
Eu + PEG 6000	381.5 \pm 0.93
Eu + TBP	397.1 \pm 1.31
Eu + DOP	404.4 \pm 2.89
Eu + TBC	394.0 \pm 0.94
Eu + DBP	399.7 \pm 1.68

Interestingly, Eu + P-diol film has two Tg values which indicates there are two phases in the films; a plasticized and unplasticized phase (Figure 4.12). The unplasticized phase has a Tg of \sim 406 K which corresponds to the Tg of Eu only film.

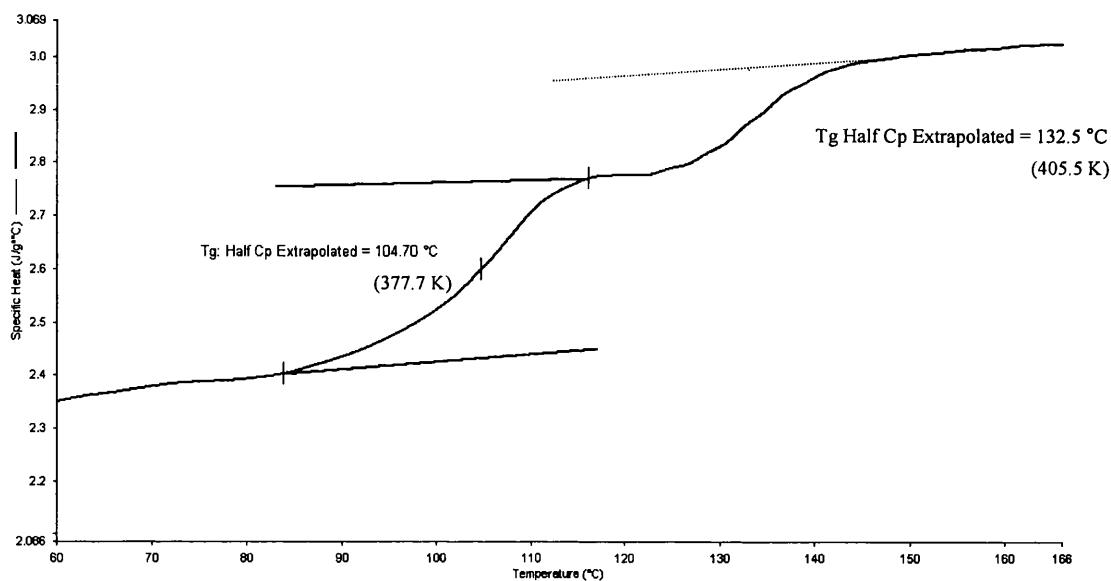


Figure 4.12 DSC thermogram of Eu + P-diol film showing the existence of two Tgs.

4.4.4 Screening of selected Eudragit S films using TSDC

4.4.4.1 Secondary relaxations and glass transitions of Eudragit S films prepared with plasticizers from the citrate ester class

Conclusions on parameters influencing film dissolution could not be drawn from the screening of these plasticizers with such diverse structures. Therefore selected films fabricated with plasticizers from the citrate class were screened in depth using TSDC. Particular attention was paid to examining the secondary relaxations and comparison of the Tg values to those attained using DSC and DMA.

The low temperature TSDC dielectric spectra of the Eudragit only film and films with citrate plasticizers (TA, TEC, ATEC and TBC) are shown in figure 4.13a. The low temperature zones in Figure 4.13a display broad multi-component peaks (secondary relaxations), with the EU-ATEC film displaying the most intense peak. Compared to the Eudragit S film, the maximum for this broad band had shifted to slightly higher temperatures for all the plasticized films. The high temperature dielectric spectra (glass transitions) are shown in Figure 4.13b. The α peaks of the blended films display a lower temperature than that observed for Eudragit S alone. Amongst the blended films, there are different temperature maxima and signal intensities.

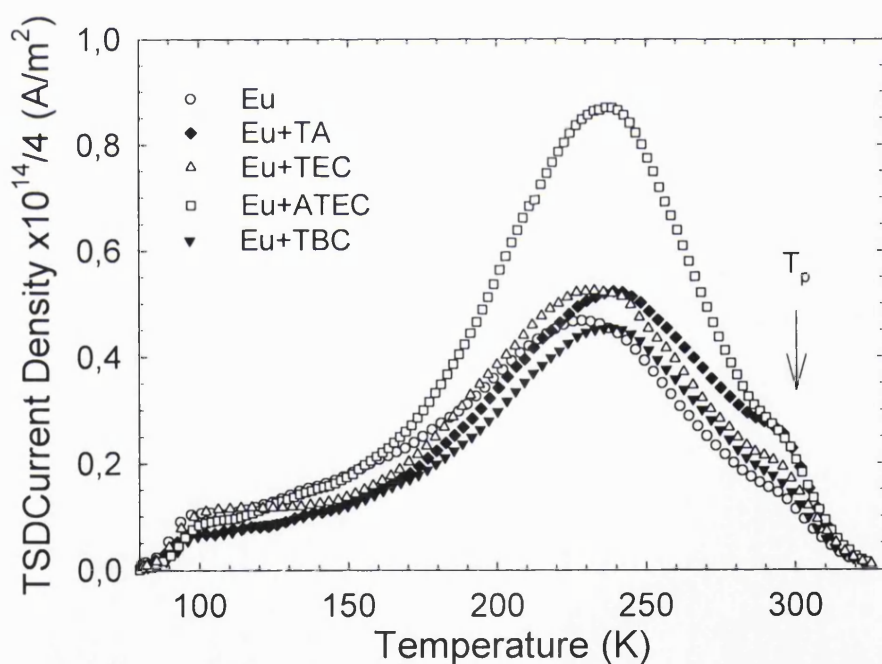


Figure 4.13a Low temperature TSDC spectra of films composed of Eudragit S with and without plasticizers. The continuous lines are the fitted curves. The density current was normalized to an electric field of 1V/m.

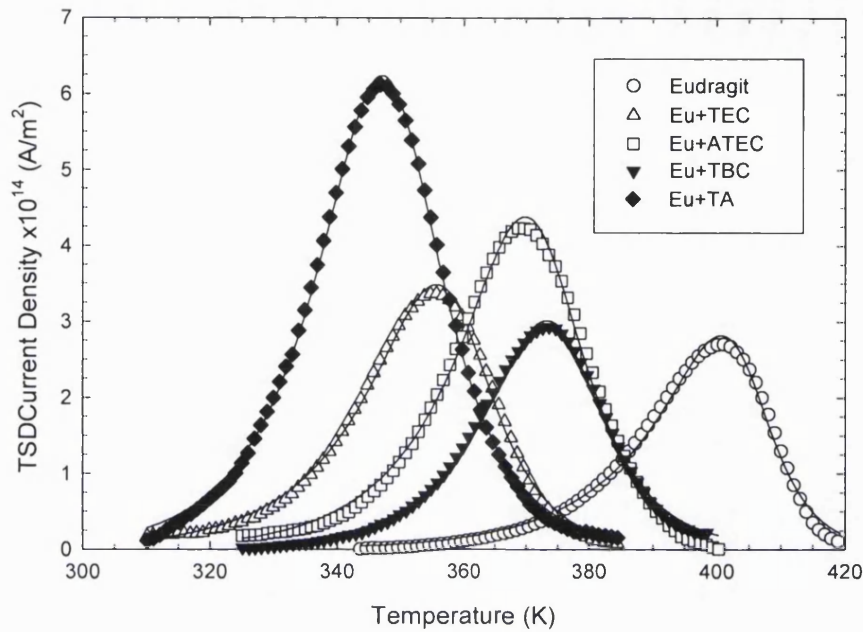


Figure 4.13b High temperature TSDC spectra of films composed of Eudragit S with and without plasticizers. The continuous lines are the fitted curves. The density current was normalized to an electric field of 1V/m.

4.4.4.2 Deconvolution of secondary relaxation peaks of plasticized Eudragit S films

The low spectra have several overlapping and non mono-energetic peaks that cannot be described by assuming an elementary Debye process (Bucci and Fieschi, 1964), since the neighbouring dipoles will be exerting directional forces on each other. Deconvolution is thus required to separate the contributions of individual dipolar species to the overall depolarisation current that is measured. Representative results of the DSA are shown in figure 4.14 for the Eudragit S film. The curve fitting together with the position in temperature and relative contribution of the Debye elementary processes which best fit the data are shown in figure 4.14a. The energy window for the best fit ranged from 0.16 to 0.90 eV and the resulting histogram is shown in figure 4.14b. The variation of the pre-exponential factor τ_{oi} corresponding to each energy beam is plotted in figure 4.14c.

The pre-exponential factors varied between 10^{-5} and 10^{-13} . The energy histogram was fitted to four mean distributed components, assuming a Gaussian profile for each component (Laredo et al., 1981). The four Gaussian curves, labelled in the order of increasing energy (γ_1 , γ_2 , β_1 , β_2), are shown in figure 4.14b. All the films had these four components in their respective energy histograms. The corresponding mean energies for each peak in the films are listed in table 4.5. The mean energy of the γ_1 component remained constant in all films at approximately 0.19 eV. However, for the γ_2 component, the energy is higher in the plasticized samples than that observed for the Eudragit film alone.

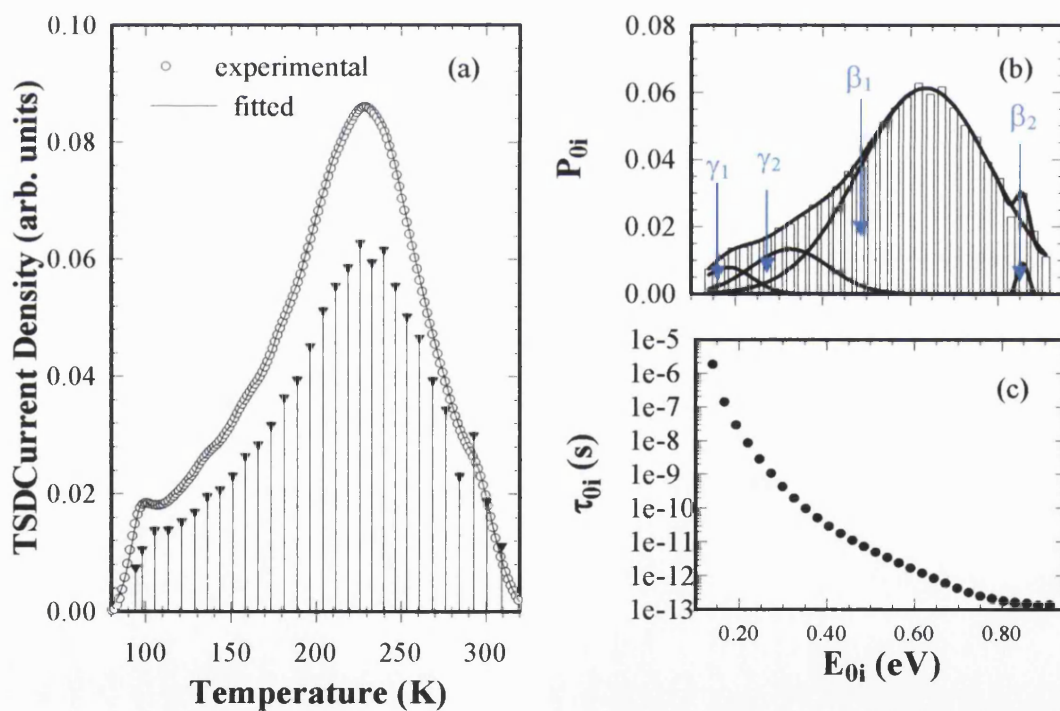


Figure 4.14 Direct signal analysis results for the secondary relaxations of Eudragit S film: (a) experimental (empty circles) and fitted (straight line) spectrum. The position in temperature and relative contribution of the Debye elementary processes which best fit the experimental curve are also represented. (b) Energy histogram of the contribution to the polarization of each Debye component peak. (c) Variation of the Arrhenius preexponential factor with the activation energy.

Table 4.5 Direct signal analysis of the secondary relaxations obtained by TSDC. Mean energies (E_0) and width distributions (σ) for each component.

Sample	$E_{0\gamma_1}(\sigma_{\gamma_1})$ (eV)	$E_{0\gamma_2}(\sigma_{\gamma_2})$ (eV)	$E_{0\beta_1}(\sigma_{\beta_1})$ (eV)	$E_{0\beta_2}(\sigma_{\beta_2})$ (eV)
Eu	0.19 (0.05)	0.33 (0.09)	0.64 (0.15)	0.85 (0.01)
Eu-TBC	0.18 (0.05)	0.37 (0.10)	0.67 (0.13)	0.87 (0.02)
Eu-ATEC	0.19 (0.06)	0.37 (0.10)	0.65 (0.12)	0.85 (0.02)
Eu-TEC	0.18 (0.05)	0.36 (0.10)	0.64 (0.13)	0.85 (0.03)
Eu-TA	0.19 (0.05)	0.37 (0.10)	0.65 (0.15)	0.84 (0.01)

The absolute polarization values of each component and the total polarization of the global low temperature band as a function of the dissolution time are calculated and shown in figure 4.15. The calculation was made using an electric field strength of 1 V/m. The predominant contribution to polarisation is from the β_1 component. The γ_1 and β_2 components display the smallest contribution to polarization. The contribution of the γ_2 component is about 5 times greater than the γ_1 and β_2 components. The total secondary relaxations area can be obtained directly from the TSDC spectrum, measuring the area below the global curve (Figure 4.13b). The partial contributions of the different peaks were obtained from the information contained in figure 4.14 (b). From the relations amongst the areas, the ratio of each contribution with respect to the total polarization was found. By multiplying each ratio by the total area below the global TSDC curve the area of each TSDC component can be calculated.

Figure 4.15 shows that as the β_1 area and the total secondary relaxation area increase, the films display faster dissolution rates. This inverse linear correlation exists between both the β_1 and the global low temperature peak areas with the dissolution time for all

the films except for the EU-ATEC film. The β_1 component is most likely to be derived from carboxylic acid functional groups (vide infra). Facile deprotonation of the carboxylic acid moieties results in ionization which will have a major influence on film dissolution (Spitael and Kinget, 1979; Krause et al., 1997).

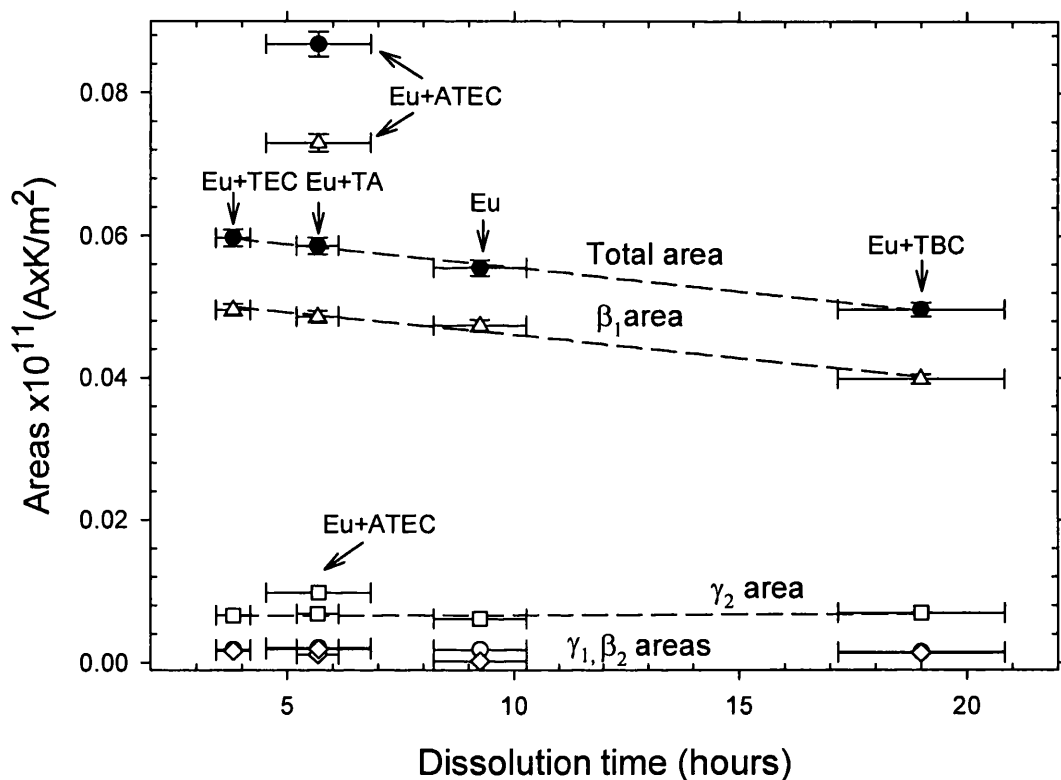


Figure 4.15 Total polarization of the global low temperature band (filled symbol) and the polarization of each of the four main components (open symbols) *versus* dissolution onset times of the different Eudragit S films. The dash lines are the best fit to straight lines.

4.4.4.3 The mechanism through which changes in secondary relaxations influence the dissolution of Eudragit S films plasticized with citrate esters

Variations in the secondary relaxation caused by plasticizer can result in changes in the local free volume, i.e., packing efficiency variations (Shuster et al., 1994), local free volume fluctuations (Xiao et al., 1999), or dynamic interactions and constraints between the polymer and plasticizer (Ngai et al., 1991). Plasticizers can reduce the resistance of polymer molecules to slide past each other by favourably interacting with the polymer by dipolar interactions (Kirkpatrick, 1940; Moorshead, 1962; Marcilla and Beltrán, 2004) or by other non-covalent interactions, especially hydrogen bonds (Wu and McGinity, 2003). Hydrogen bonding with a plasticizer may weaken intermolecular polymer-polymer interactions. This may potentially increase the propensity for water imbibation into the films to facilitate faster dissolution times. The large secondary relaxation area for EU-A TEC may thus contribute to dissolution rates faster than would be anticipated from the relative aqueous solubility of the plasticizer. This disruption of polymer-polymer interactions that sufficiently decreases the polymer packing efficiency facilitates the reorientation of localized dipolar entities.

Structurally TEC and A TEC differ only by the acetylation of the tertiary hydroxyl group in A TEC. This results in A TEC being approximately 10 times less water soluble than TEC. A TEC is a hydrogen bond acceptor only, while TEC is both a hydrogen bond acceptor and donator. Being only a hydrogen bond acceptor, A TEC may interact relatively more efficiently with the carboxylic acid H-bond donors on Eudragit S to reduce polymer-polymer interactions. This relative reduction in

polymer-polymer chain interactions would result in faster dissolution which cannot be anticipated by the water solubility of ATEC alone.

4.4.4.4 Eudragit S functional groups and their contribution to the mono-energetic secondary relaxation peaks

Since the γ_1 component of the secondary relaxation peak has the lowest reorientation energy, it should originate from the most easily reorientable dipoles (Suarez et al., 1997). The γ_1 component dipoles also have the smallest contribution to the overall polarisation, so these dipoles should have a small dipole moment in Eudragit S. In a study of the structurally related homopolymer, poly(methyl methacrylate) (PMMA), a small mechanical loss peak was reported (McCrum et al., 1991). The cause of this loss was assigned to the rotation of the methyl groups that are attached directly to the polymer main chain. The rotation of these methyl groups was also observed by nuclear magnetic resonance line-width measurements. Furthermore; nuclear magnetic resonance analysis on poly(bisphenol-A carbonate) (Matsuoka and Ishida, 1966) and ultrasonic attenuation experiments (Tanabe et al., 1970) revealed an activation energy for the relaxing methyl groups of about 0.2 eV for the methyl protons in the temperature region from 100 to 130 K. Both the temperature range of the γ_1 peak and its reorientation energy (Table 4.5) are very close to these reported values. Consequently, the dielectric γ_1 peak of the Eudragit S samples is assigned to the orientation of the CH_3 dipoles that are covalently bound to the Eudragit S main chain.

The reorientation energy of the γ_2 processes (Table 5) ranges from 0.33 up to 0.37 eV. These values are similar to the activation energy of 0.4 eV, obtained by dielectric and

mechanical methods for the low temperature γ relaxation that was detected for a series of n-alkyl methacrylate polymers that were examined by McCrum et al. (1991). They ascribed the mechanism for the γ relaxation to motions of the pendent ester methyl group. From the McCrum study, the motions of the ester methyl were independent of the substitution along the polymer main chain. The similar activation energies of the γ process reported by McCrum and the γ_2 processes from our study suggest that this reorientation should be assigned to the ester methyl groups in Eudragit S. The increase of the reorientation energy of the γ_2 process in the plasticized film samples compared to the EU control films may be due to plasticizer molecules hindering the motions of the ester methyl groups.

The broad β_1 component (Table 4.5) suggests that it is a combined process involving a weighted sum of elementary processes occurring in different local environments. In other studies at the same temperature range, a similar β relaxation was observed by mechanical and TSDC techniques for poly(2-chlorocyclohexyl methacrylate) (Sanchis et al., 1999). The value of the activation energy associated with the processes responsible for the dipolar relaxation was calculated to 0.7 eV. The origin of the process was attributed to the rotations of the entire side chain. The similarity among the energy and temperature range of these results and those obtained in this work for the β_1 peak supports its assignment to a combined process caused by the rotation of the pendent $-\text{COOCH}_3$ and $-\text{COOH}$ groups about the C-C bonds which link them to the main chain. As the β_1 area increases, the number of available carboxylic acid functional groups participating in this relaxation becomes larger. Hence the exposed sample must have a greater number of carboxylic acid functional groups that are accessible for ionization by water. This would cause faster dissolution.

Both ATEC and TA are exclusively hydrogen bond acceptors and must compete with the carboxylic acid pendent groups in Eudragit S. TA has three ester and ATEC has four ester functionalities, so TA has fewer accepting sites than ATEC. The contribution of non-covalent interactions from the ATEC molecules with Eudragit S should not be disregarded, and it can be accounted for by its large secondary relaxation area. The molecular volume, shape and polarity of the ATEC as well as the accessibility of its carbonyl groups influence its interaction with the polymer (Tarvainen et al., 2001).

The high reorientation energy of the β_2 component (approximately 0.85 eV) is associated with low pre-exponential Arrhenius factors and could be due to overlapping with the low temperature tail of the α transition. It is possible that this relaxation arises from the carbon-carbon bonds along the main chain whose motion would be the initial motions, especially near the chain ends, as the primary glass transition temperature is approached.

4.4.4.5 Influence of citrate plasticizers on film dissolution as determined by changes in TSDC glass transitions

To better understand the influence of plasticizer on the dielectric manifestation of the glass transition, the high temperature TSDC profiles were evaluated. Table 4.6 shows the characteristic fitted parameters of the glass transition relaxation peak, i.e., J_0 , β , and T_g . The first parameter is the current density amplitude (peak amplitude); the second describes the temperature dependence of the relaxation time (inversely

proportional to peak width); the third is the measured T_g of the relaxation (Puma, 1997). Decreased intermolecular polymer-polymer interactions are indicated by the higher β parameters for the plasticized samples compared to the net film (Table 4.6).

Table 4.6 Analysis of the glass transition relaxations obtained by TSDC.

Sample	$J_0 \times 10^{11}$ (A/m ²)	β (K ⁻¹)	T_g (K)
Eu	0.005	0.0781	404.2
Eu-TBC	0.0059	0.0968	375.3
Eu-A TEC	0.0084	0.0864	372.3
Eu-TEC	0.0066	0.0816	358.6
Eu-TA	0.0122	0.0969	348.8

Our data shows that there is a decrease of the fitted T_g values as the molecular weight of the citrate plasticizer diminishes and its solubility increases (Tables 4.1 and 4.6). This may have arisen partly because the plasticizers were blended by weight percent rather than by molar percent. For a lower MW plasticizer there are more molecules for a given composition and therefore more molecules are available to occupy the accessible sites along the polymer structure (Mathew and Dufresne, 2002). The T_g values obtained by DMA and DSC techniques also display a tendency to decrease when the molecular weight and the solubility of the citrate plasticizers decrease and increase respectively (Figure 4.16). This tendency demonstrates that the separation of polymer chains and reduction of the intermolecular forces between the chains is dependent on the aqueous solubility and the MW of the plasticizer. This result contrasts with the DSC results obtained for similar methacrylic acid copolymer films

(Eudragit L100-55) (Gutierrez-Rocca and McGinity, 1994) that were plasticized with the same additives as those used in the present work.

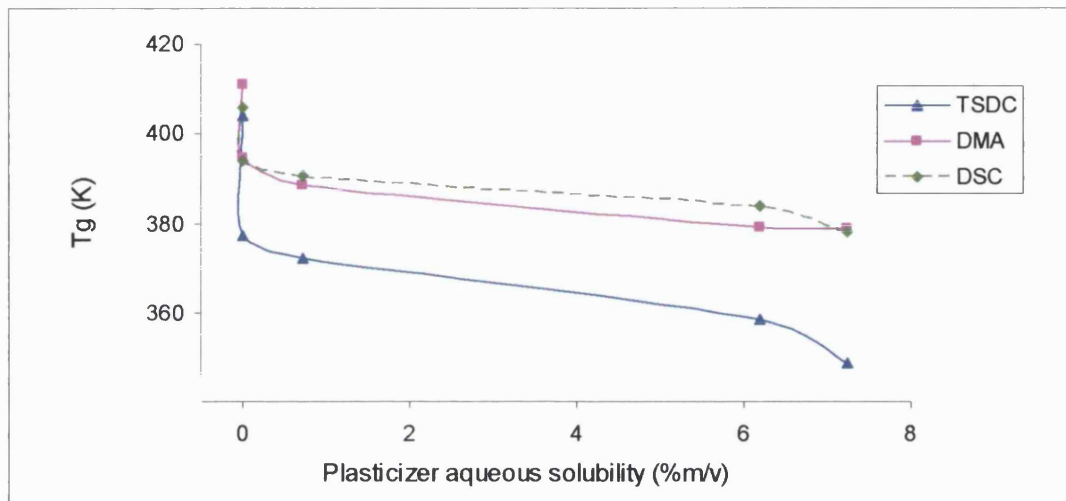


Figure 4.16 Illustration of the decrease in T_g of Eudragit S films with increasing molecular weight of citrate plasticizer.

4.4.4.6 How the structure of tributyl citrate accounts for the prolonged dissolution of its corresponding Eudragit S film

It is interesting to compare the TSDC results obtained with EU-TEC and EU-TBC. These are the fastest and slowest dissolving films respectively. They differ only in the number of carbons in their ester chains (2 and 4 for TEC and TBC respectively). The moieties capable of participating in hydrogen bonds are the same for these two plasticizers with the three ester groups potentially acting as hydrogen bond acceptor sites. The tertiary hydroxyl group has both hydrogen bond donating and accepting character. There is approximately a 19 K difference in the glass transition temperature of the films, and 8 K difference in their global secondary relaxation temperature maximum, with EU-TBC displaying the higher temperature values. It is possible that

the butyl alkyl chains of TBC reside more readily between the Eudragit S polymer chains to orient the ester and hydroxyl functional groups with the polar groups on the polymer. These non-covalent interactions would decrease the local polymer-polymer free volume fluctuations, and consequently cause improved packing, thus facilitating enhanced polymer-additive interactions.

Interactions may occur between hydroxyl groups of TBC and hydrogen bond acceptor moieties (e.g. carbonyl in acid and ester groups) of the polymer in addition to interactions of the carbonyl groups of the plasticizer with the hydrogen bond donating moiety (carboxylic acid proton) on the polymer. This latter interaction could cause the increase of the reorientation energy of the β_1 process on Eu-TBC, which may explain the shift to higher temperatures of the global secondary spectrum. This would result in a decrease in the free volume of the system and may explain the higher relative T_g , the increase of the secondary relaxation reorientation energies, and the lower secondary relaxation area that was obtained for EU-TBC. Interactions of the carbonyl groups of TBC with the carboxylic acid proton of EU would also decrease the amount of free hydroxyl groups which are accessible to water (Mathew and Dufresne, 2002).

The combination of low TBC water solubility and increased polar polymer-plasticizer interactions would be consistent with the prolonged dissolution time observed for EU-TBC. The fast dissolution time for EU-TEC could then be related to the high relative aqueous solubility of TEC and its structure favourably interacting with the Eudragit polymer.

4.4.4.7 Influence of secondary versus segmental polymer relaxations on the dissolution of plasticized Eudragit films

While the T_g of EU-TBC film is lower than that of EU alone (Tables 4.2 and 4.5); the opposite is true when comparing the areas and maxima of the secondary relaxations for the two films. TBC enhances segmental mobility while hindering the mobility of the pendent chain moiety of Eudragit S. These opposing effects of the plasticizer on primary and secondary relaxations of polymer systems has previously been reported by Ngai et al. (1991).

Our results show that the T_g values of the polymer films do not correlate to Eudragit S polymer film dissolution; however the secondary relaxations areas do. From this we can infer that the local environment of the side chains, particularly interactions and free volume fluctuations of the carboxylic acid group, have a predominant effect on polymer film dissolution in comparison to the cooperative mobility of the system.

4.4.4.8 Dissolution of plasticized Eudragit S films: plasticizer aqueous solubility versus polymer-plasticizer interactions

The relative contribution of plasticizer aqueous solubility and its extent of disrupting polymer-polymer interactions on the dissolution of Eudragit S films can be established from a comparison of the dissolution rate of EU-TEC and EU-A TEC films. These two systems displayed relatively small differences in their dissolution times despite an almost 10-fold lower aqueous solubility of A TEC compared to TEC.

This suggests that disruption of polymer-polymer interactions can make a significant contribution towards increasing the rate of Eudragit S film dissolution.

Referring back to the dissolution of Eudragit S films fabricated from polyols (P- diol and PEG 6000) in Figure 4.11a; the dissolution onset of EU/P-diol is almost three-fold faster than the dissolution onset of Eu/PEG 6000 films despite the very high aqueous solubility of both plasticizers. On comparison of the structures, P-glycol has a small MW composed of two hydroxyl groups attached to methyl ethylene. However PEG 6000 is of large MW and has only two hydroxyl groups attached to a long repeating sequence of oxyethylene groups ($m \sim 143$). Thus the former plasticizer has a comparatively greater potential to hydrogen bond with the carbonyl groups of the polymer. As previously discussed, hydrogen bonding between plasticizer and polymer weakens intermolecular polymer-polymer interactions. This may potentially increase the propensity for water imbibation into the films to facilitate faster dissolution.

4.4.5 Comparison of Tg values as determined by TSDC, DSC and DMA

Comparative Tg values were obtained by DSC (Figure 4.17) and by DMA (Figure 4.18a and 4.18b). A comparison is shown in table 4.7 and figure 4.19.

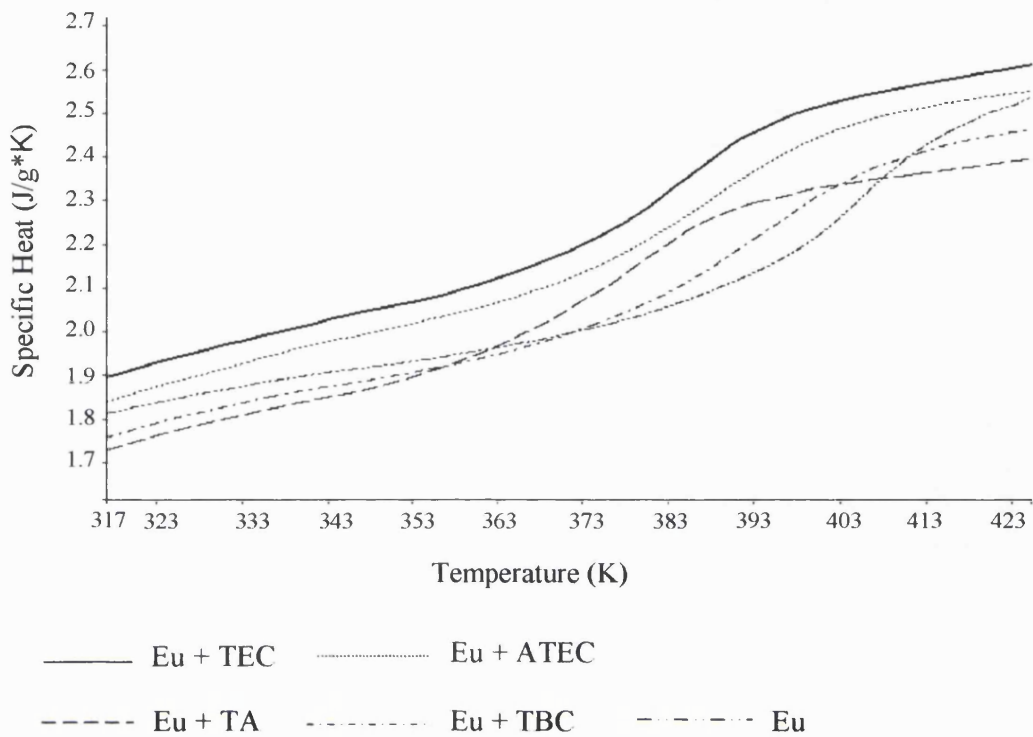


Figure 4.17 DSC thermograms of Eudragit S with and without citrate plasticizers.

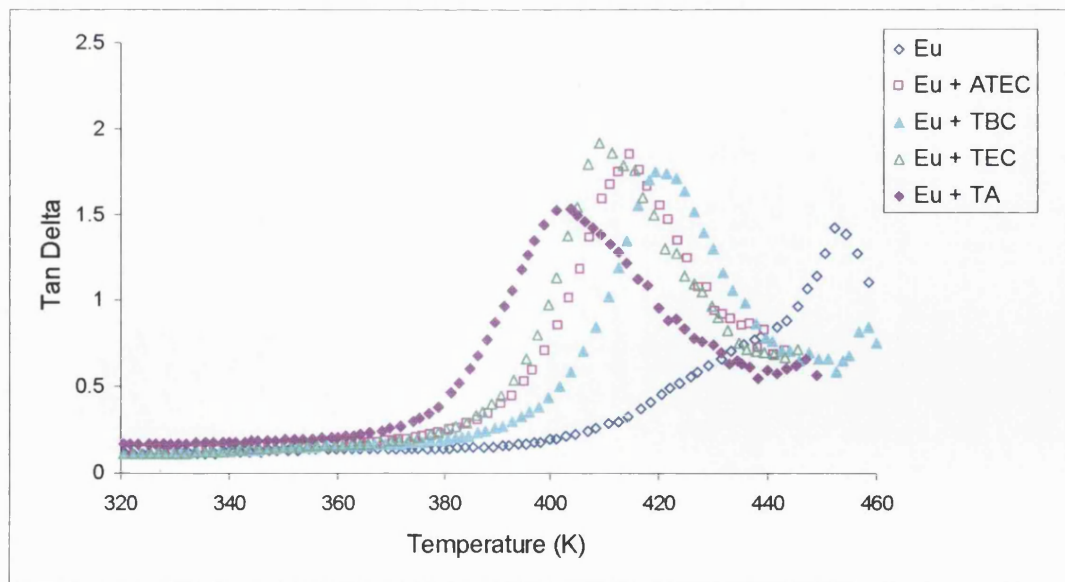


Figure 4.18a $\tan \delta$ of Eudragit S with and without citrate plasticizers, at 1Hz, as obtained from DMA

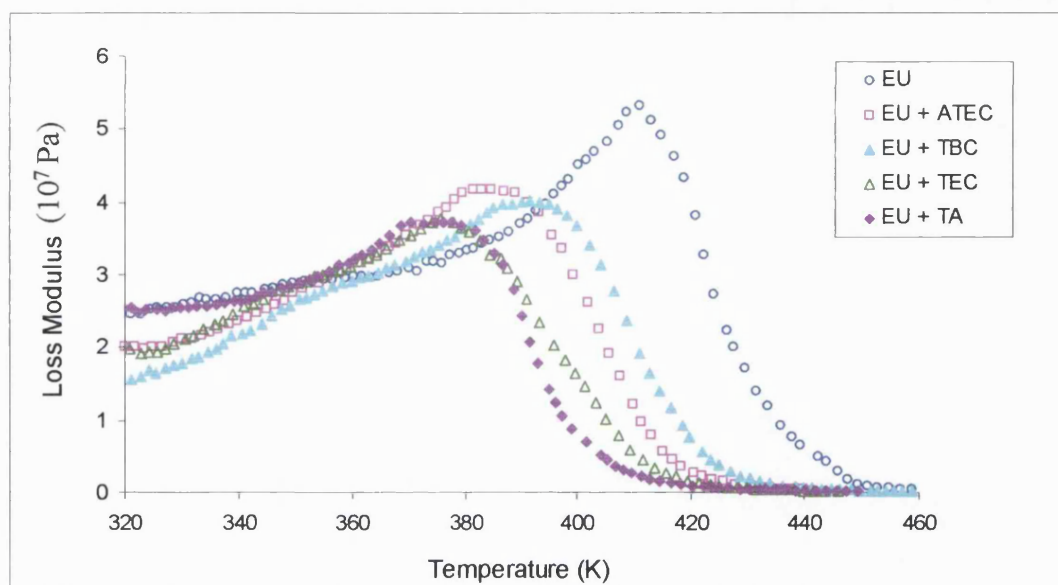


Figure 4.18b Loss Modulus of Eudragit S with and without citrate plasticizers, at 1Hz, as obtained from DMA. The loss modulus values were used to represent the Tg.

Table 4.7 Tg values obtained from the analysis of the DSC step of specific heat capacity change and DMA loss modulus of the different film formulations.

Film	Tg (DSC) (K)	Tg (DMA) (K)
EU	405.9 ± 0.14	410.8 ± 1.0
EU-TBC	394.0 ± 0.94	394.7 ± 2.1
EU-ATEC	390.8 ± 2.27	388.5 ± 1.2
EU-TEC	383.7 ± 1.03	379.0 ± 0.6
EU-TA	377.9 ± 3.62	378.9 ± 1.3

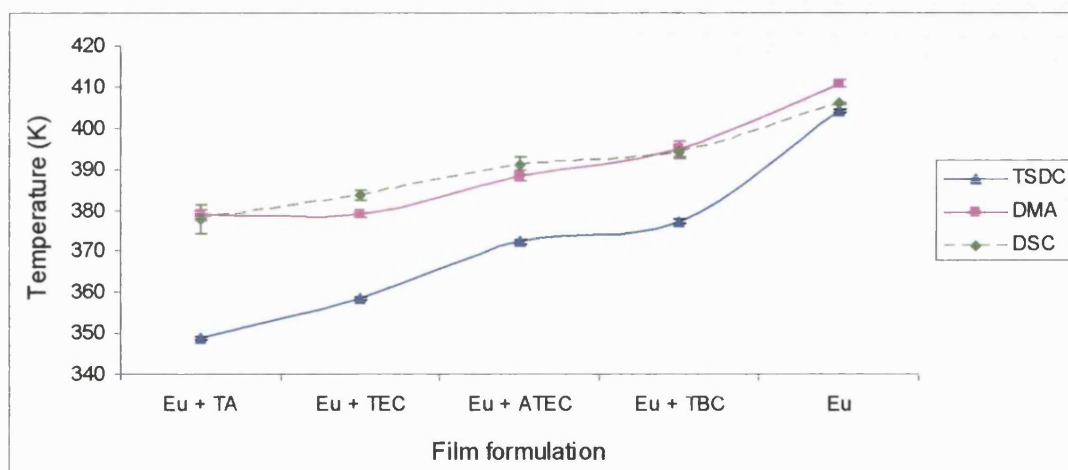


Figure 4.19 Comparison of the Tg's obtained from the analysis of the TSDC α -peaks, DSC step of specific heat capacity change, and DMA loss modulus of the different film formulations. The lines are drawn to guide the eye.

All three techniques gave a similar value for Eudragit S (DSC/DMA: 402 K and TSDC: 405.9 K). While the trend was similar for the plasticized films, the Tg values that were obtained by TSDC were lower than the Tg values determined by DSC and DMA, which were similar. There was a greater difference between the TSDC and DSC/DMA derived Tg values for the lower molecular weight plasticizers (TA and TEC). Also the DMA Tg value for EU-TEC was 4.7 K lower than the DSC derived Tg value. Although this difference is relatively small, the data are reproducible with very little variation. Regarding the difference in the Tg values obtained by TSDC and DSC/DMA, Leroy et al. (2002) reported a similar observation in their study of poly(vinyl methyl ether)/polystyrene blends. The observed Tg differences between the TSDC and DSC values were rationalized on the basis of the Lodge and McLeish model (2000) of the "effective concentration" concept. This model links the effective glass transition temperature to the average segmental mobility of the dielectrically active component in the blend. Leroy et al concluded that the TSDC technique allows

measurement of the effective T_g in a blend. Effective T_g takes into account differences in the local environment. For example in a miscible blend of two polymers A and B, the local environment of a region of polymer A will have a greater abundance of polymer A in comparison to the bulk composition (Chung et al., 1994; Leroy et al., 2002). For a lower MW plasticizer more molecules are available to occupy the accessible sites along the polymer structure, and consequently the polymer segment will sense greater variations in the effective local concentration. According to the Lodge and McLeish model (2000), this would produce greater differences of the effective local glass transition that can be observed by dipolar interactions in comparison to the macroscopic T_g obtained by DSC or DMA. The results in figure 4.19 are also consistent with the predictions of this model. This is why a greater difference is seen between TDSC and DSC/DMA for the low molecular weight plasticizers.

4.4.6 T_g of Eudragit S/triacetin films as measured by dynamic mechanical analysis

The correlation of the T_g values obtained by the different thermal methods are plotted in figure 4.20. There is a linear correlation between the TSDC and DSC results. Additionally, there are also linear relations among the T_g values obtained from TSDC and DSC with respect to that of the DMA, with the exception of the T_g of the sample with the smallest plasticizer (EU-TA), which is lower than expected by the linearity shown by the other samples (i.e. the T_g for EU-TA is below the two lines in Figure 20 for DMA-TSDC and DMA-DSC). TA seems to be the most effective plasticizer in interrupting the polymer-polymer interactions, as EU-TA displays the lowest T_g and the highest β -parameter (Table 6). The relatively higher T_g value for EU-TA that was observed by DMA indicates that there are additional plasticizer

effects that are manifested in the mechanical relaxations, but not through dielectric and thermal relaxations.

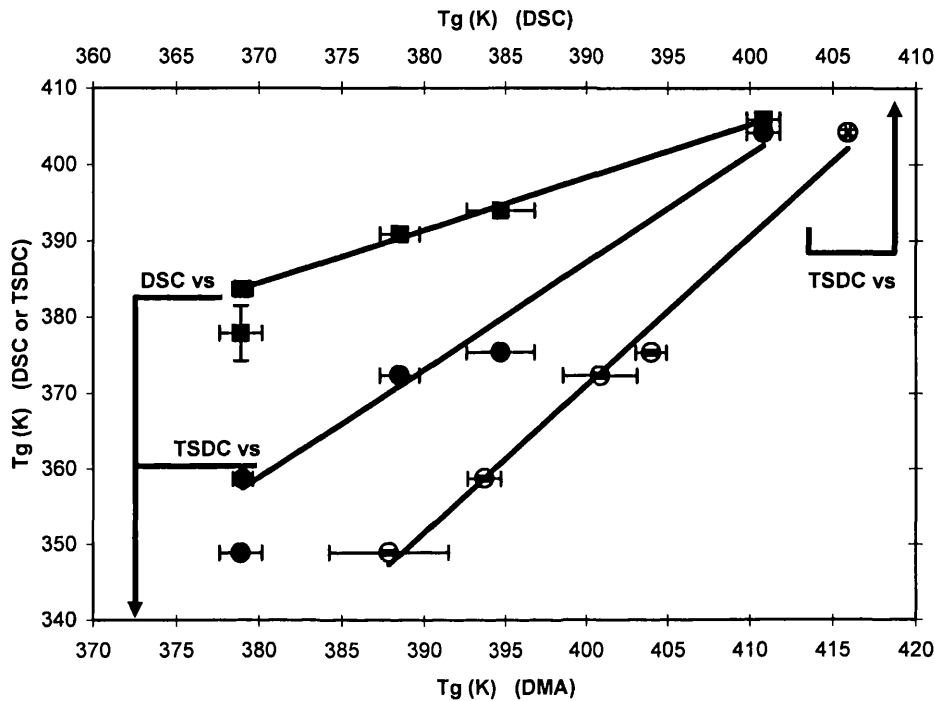


Figure 4.20 Correlation of Tg values of the films obtained from the different thermal methods. TSDC Tg versus DMA Tg (filled circles), TSDC Tg versus DSC Tg (empty circles) and DSC Tg versus DMA Tg (filled squares). The lines are the best fit to straight lines.

Anderson et al. (1995) studied polystyrene/mineral oil blends and reported the existence of polymer chain end effects that restrict their mobility thus resulting in higher moduli and strength than expected. These effects occur when the average diameter of the mineral oil domains was less than or equal to the average size of the free volume voids of the polymer chain ends. In agreement with this result, it could be that as TA is the smallest plasticizer, the chain end effects could affect the mean mechanical relaxation of EU-TA while the dielectric and thermal relaxations could be

mainly influenced by the extent of the disruption of polymer-polymer interactions. In Table 1 it can be seen that TA is the only plasticizer that has a tri-substituted carbon. The other plasticizers all have a quaternary carbon. TA has a smaller volume and more mobility due to its tertiary substitution. These characteristics of TA could explain its ability to pack more efficiently at the chain ends of the polymer. This restriction of the mobility at the chain ends affects mostly the mechanical relaxation and therefore the T_g of Eu-TA obtained from DMA is higher than would be expected from the trend in Figure 20. In contrast, TSDC α peak of EU-TA (Table 6) had the highest intensity, smallest width and the lowest T_g . This indicates that the cooperative movements are extended freely along the polymer chain, resulting in disruption of the polymer-polymer interactions in this sample.

4.4.7 Immersion dynamic mechanical analysis

Eudragit control film and Eudragit film fabricated with TEC, TBC or ATEC plasticizers were tested using immersion DMA. The results show a decrease in the T_g of the films compared to the dry state. This must have arisen from water imbibition into the film since water acts as a plasticizer. Eudragit control film has the highest glass transition in comparison to the Eudragit plasticizer films; this can be explained by the small plasticizer molecules attracting water into the films. The higher T_g of Eudragit control film in the dry and wet state coupled to its slower dissolution in comparison to Eu-TEC and Eu-ATEC films indicates that free film dissolution is unlikely to be triggered by mechanical weaknesses or cracks in the film. Since if this was the mechanism of release, Eudragit only film would have the faster dissolution as its higher T_g renders reduced polymer mobility and therefore reduced film flexibility.

It would be useful to utilise TSDC to study the secondary relaxations of these systems while they are immersed in liquid media.

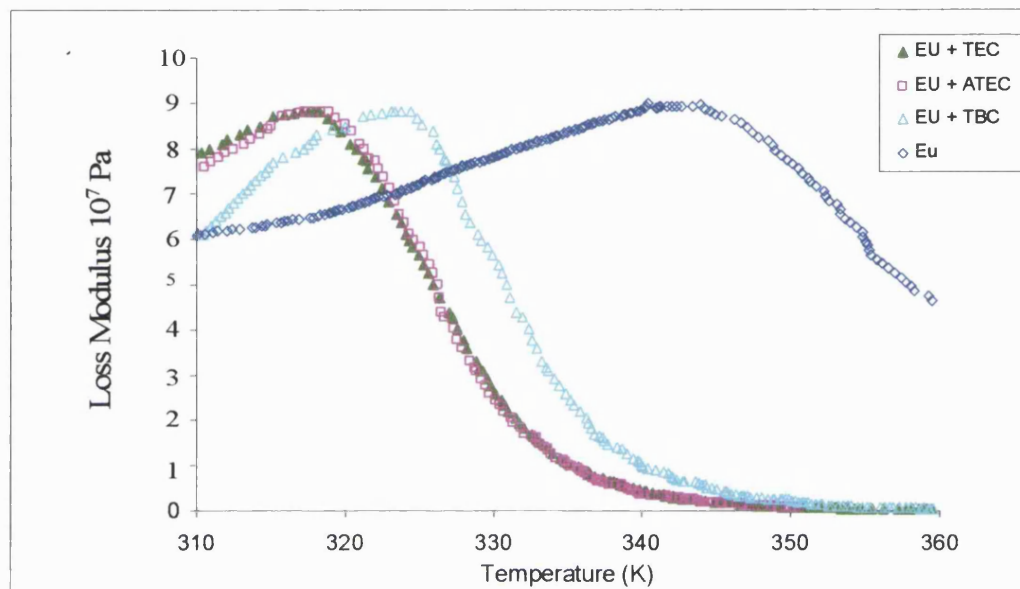


Figure 21 Loss Modulus of Eudragit S with and without citrate plasticizers, at 1Hz, as obtained from immersion DMA. The loss modulus values were used to represent the T_g.

4.5 CONCLUSIONS

Dissolution of methacrylic acid methylmethacrylate copolymer films is influenced by the solubility and structure of the citrate plasticizers that were incorporated in the blend. The TSDC dielectric spectra indicate that subtle variations between plasticizer size and structure can have a distinctive influence on the dissolution behavior of these films. Detailed analysis of the low temperature TSDC spectra of the samples provided the means of identifying several secondary relaxation components. Relaxation of the carboxylic acid functional group was identified. Its peak area and the total secondary relaxation peak area linearly correlated with the dissolution time for all the films except EU-A TEC which was significantly higher. Secondary relaxation areas are related to polymer plasticizer interactions, and the differences between the films, especially EU-A TEC were mainly attributed to hydrogen-bonding, particularly between the plasticizer as a hydrogen bond acceptor and the carboxylic acid group of Eudragit S as a hydrogen bond donator. Hydrogen bonding can cause disruption of polymer-polymer interactions which increases the propensity for water imbibation into the films which contributes to faster dissolution.

The T_g values that were obtained by TSDC linearly correlated with T_g values measured by DSC. The shift in the T_g values indicates that the effective local T_g sensed by the dipoles is lower than the macroscopic T_g of the plasticized samples. No correlation however was found among the T_g values obtained by TSDC, DSC and DMA techniques with the dissolution time of the films. Polymer-plasticizer interactions have different influences on side chain and segmental relaxations. For these Eudragit films, the local environment of the carboxylic acid groups, particularly

their interactions with plasticizer and their free volume fluctuations, have the predominant effect on film dissolution.

The above results indicate that the dielectric secondary relaxations may be a powerful probe to predict the molecular interactions between a plasticizer and a polymer. For this study we evaluated in depth the interactions between Eudragit S and citrate based plasticizers. These findings contribute towards a better understanding of formulation influence on dissolution of pH-responsive dosage forms. This will achieve a mechanistic approach to formulation design.

CHAPTER FIVE

Interaction of drug and tablet core excipients with acrylic
film coatings and influence on dissolution

5.1 INTRODUCTION

In the previous chapter, dissolution onset of enteric polymer films has been shown to be influenced by plasticizers at the molecular level. In this chapter we seek to establish to what extent these intrinsic properties manifest on the dissolution of enteric coated tablets. We seek to establish if the dissolution differences observed in polymer free films with different plasticizers are as substantial in tablets with acrylic polymer film coatings. Tablets are coated with an organic solution of the same polymer, Eudragit S.

Extensive research has been conducted on the inclusion of drugs into film coats; this is known as carrier coating and can be utilised for low dose drugs or for the separation of incompatible ingredients. Aulton et al. (1983) have shown that in carrier coatings drug can migrate from the coat to the table core. This affects the mechanical properties of the film and the drug release profile. Similarly, the migration of drug or excipients from the tablet core into the film coating can potentially occur through comparable mechanisms. This could alter molecular interactions in the coating which in turn influences membrane fluidity and permeability.

Migration of water soluble drugs or excipients from the tablet core into the coat could occur by their dissolution into the adsorbed moisture of film coatings. Moisture can arise from humidity in the storage environment (Okhamafe and York, 1989) or from atmospheric compressed air used in coating. Migration can also occur by drug or excipient dissolution in the solvent during the coating process. Alternatively, for drugs which are very soluble in the coating solvent, an intermediate surface layer of

solubilised and subsequently dried drug material can be formed at the interface between the tablet core and polymer film (Simpkin et al., 1983).

Tablets in this study were coated using a fluidized bed coater (Figure 5.1). This comprises a vertical cylindrical column with a perforated base and a metal mesh lid. Air is supplied to the chamber from the bottom of the column and the exhaust air is removed from the top. A large air flow is required to maintain fluidization of the dosage forms. The dosage forms continuously pass up the column and fall back down again due to the expansion at the top of the chamber which causes a reduction in air velocity. The coating solution can be delivered from below or above the tablet bed and is fed into the path of a pressurised air stream which causes atomisation of the liquid into fine droplets. The instrument used in this study utilises a bottom spray coater. Important parameters that need to be controlled include: air pressure, which determines the size of the droplets, spray rates, air flow and temperature. The rate balance between solution spray rate and evaporation needs to be established to prevent aggregation of the dosage forms or spray drying of the polymer solution (Cole et al., 1995; Bauer et al., 1998).

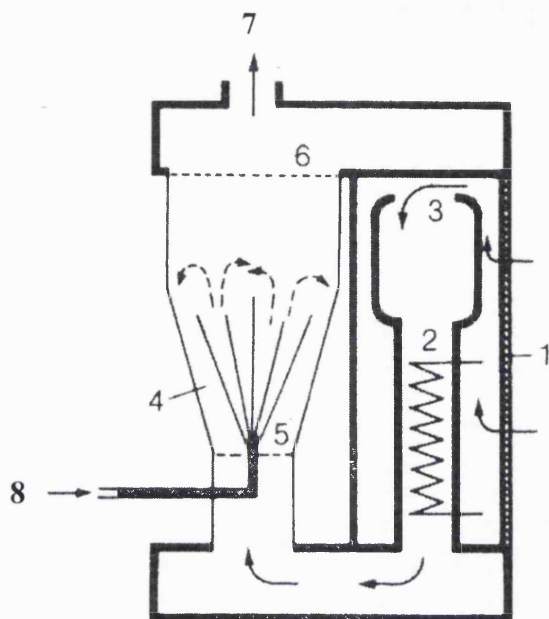


Figure 5.1 Schematic representation of a fluidized bed coater. 1: inlet air filter, 2: air heater, 3:air flap, 4:fluid bed column, 5:spray nozzle, 6:bag filter, 7:explosion flap, 8: spray fluid. Reproduced from Bauer et al. (1998).

Immediate release tablets were prepared with either 5-aminosalicylic acid (5-ASA) or prednisolone as actives in the core. The dissolution profiles of 5-ASA and prednisolone coated tablets were compared to elucidate the influence of drug on dissolution of the enteric coat. In a comprehensive study, Ozturk et al. (1988a) have shown the influence of an acidic drug, aspirin, on reducing the pH of the drug core/polymer boundary layer relative to the bulk thus retarding dissolution of the polymer coating. In this study we are comparing two different actives, ionisable and non-ionisable, in the tablet core; hence a difference in their release profiles would be anticipated. However the pertinent question is if the physicochemical property of the drug alters the dissolution trend observed in polymer film coats fabricated with different plasticizers.

5.2 OBJECTIVES

- To compare the dissolution trends of tablets coated with the acrylic polymer, Eudragit S, fabricated with different plasticizers with polymer free films of the same formulation.
- To evaluate how representative the dissolution trends of the polymer free films are when applied to a pharmaceutical product with an active and other excipients in the core.
- To determine if the physicochemical property of the drug in the tablet core alters the dissolution trend observed in polymer film coats fabricated with different plasticizers.
- Comparison of the dissolution profiles and trends of the different formulations in bicarbonate buffers with phosphate buffers.

5.3 MATERIALS AND METHODS

5.3.1 Materials

5-ASA of > 99% purity was purchased from Sigma Aldrich (Poole, UK). Micronized prednisolone was purchased from Sanofi-Aventis (Romainville, France). Lactose was obtained from Ellis and Everand (Essex, UK). Polyvinyl pyrrolidone (PVP) was purchased from VWR International Ltd (Poole, UK). Ac-Di-Sol (croscarmellose sodium) was a gift from FMC International, Eire. Plasticizers studied: polyethylene glycol (PEG 6000), propylene glycol (P-diol), triacetin (TA), triethyl citrate (TEC), tributyl citrate (TBC), dimethyl phthalate (DMP), dibutyl phthalate (DBP) and dioctyl phthalate (DOP).

5.3.2 Preparation of 5-aminosalicylic acid and prednisolone tablets

5.3.2.1 Tablet preparation methodology

Tablets with 5-ASA or prednisolone as the active ingredients were prepared to 200 mg weight by wet granulation according to the formula in Table 5.1. Batch sizes were 300 g and the uncoated tablets from each batch were tested to ensure batch-to-batch reproducibility.

Table 5.1 Formula for immediate release 5-aminosalicylic acid and prednisolone 200 mg tablets.

Component	% w/w per tablet	Weight (mg) per tablet	Function
5-ASA or prednisolone	5	10	Active
Lactose	88.5	177	Diluent / filler
Ac-Di-Sol (<i>half added intragranularly and half extragranularly</i>)	0.5	1	Disintegrant
Polyvinyl pyrrolidone (PVP)	5	10	Binder
Magnesium stearate ¹	1	2	Lubricant

¹ Added to dry granules and the percentage added accounted for the losses during the granulation process.

(i) All the powders were sifted before use to break up any agglomerates and remove foreign material. Lactose was added by trituration to half of the Ac-Di-Sol. The active ingredient and PVP were added to this mix in the bowl of a planetary mixer (model KM400/410, Kenwood, Hoban, UK) and dry blended at medium speed for 15 min.

(ii) De-ionised water (granulating fluid) was added drop-wise under continuous stirring. Consistency of the water is regularly checked and sufficient amount is added until a moist, coherent mass is achieved.

(iii) The moist blend is passed through a 710 µm sieve plate to form granules.

(iv) Granules were then spread out on a metal tray in an oven at 60 °C. Granules were turned at frequent intervals to ensure even drying. Granules were also weighed at 10

min intervals to determine water loss and drying continued until the loss was no greater than 0.1 % of granule weight.

(v) Dried granules were then milled through a 710 μm sieve to break up any clumps and remove any large granules. Granules $> 710 \mu\text{m}$ in size were discarded. The granules were next milled through a 90 μm sieve to remove any fine granules. Therefore granules in the size range of 90 – 710 μm were selected for compression to attain uniformity of weight, content and hardness.

(vi) The granules were weighed and their mass noted.

(vii) Granules were added by trituration to the remaining half of the Ac-Di-Sol. This was then transferred to an amber glass jar and roller-mixed for 10 min.

(viii) Magnesium stearate equivalent to 1% of the granule weight measured in (vi) was added to the granules. This was roller mixed for 5 min.

(ix) The granules were compressed using a single punch Manesty Type F3 eccentric tablet press (Manesty, Speke, UK) equipped with a biconvex 8 mm punch and die set. The fill volume of the die was adjusted to yield 200 mg tablets with a crushing strength in the yield of 70 – 80 N.

5.3.2.2 Tablet weight uniformity

During tablet compression, the weight of the tablets is determined by the volume of the die; hence similar size and shape of granules is important to attain weight uniformity. This can be evaluated using the British Pharmacopoeia (BP) methodology whereby 20 tablets are selected at random from the batch and individually weighed. The mean weight is calculated.

5.3.2.3 Tablet content uniformity

Ten tablets were selected at random from the batch and assayed individually by crushing and dissolving in 0.1 M HCl. The resulting solution was then passed through a 0.45 μm filter and the amount of 5-ASA or prednisolone measured using UV spectrophotometry at 247 and 301 nm respectively and the amount calculated against a calibration curve.

5.3.2.4 Crushing strength

The compression load needs to be set so that tablets pass the pharmacopoeial disintegration and dissolution tests and are robust enough to withstand the impact stress during the first few minutes of coating without attrition, chipping or capping. The crushing strength was regularly monitored during tablet compression using a tablet crushing strength tester model CT40 (Engineering systems, Nottingham, UK).

5.3.3 Film coating

5.3.3.1 Coating formulation

Eudragit S was dissolved in 95% ethanol under high speed magnetic stirring until a clear solution was obtained. Plasticizers were added (20% and 15% on dry polymer for the water-soluble and water insoluble plasticizers respectively). No other additives were added so that the tablet coating resembles the free cast films prepared in the previous chapter. Moreover, it was desirable to simplify the coating to reduce the possibility of any interactions of the core with excipients and more confidently elucidate the influence of plasticizer on dissolution. The absence of glidants, such as

glyceryl monostearate (GMS) or talc, which serve to overcome the tacky phase during film formation however made the coating process more difficult.

5.3.3.2 Film coating process

The tablets were coated using an Aeromatic Strea-1 laboratory scale fluidised bed spray coater (Aeromatic AG, Bubendorf, Switzerland). The coater is equipped with a bottom spray pneumatic gun and a 1.2 mm nozzle but without a Wurster insert. A Gilson peristaltic pump (Type M312, Gilson, Gambetta, France) with the capability of speed adjustment was used to deliver coating solution to the fluid bed chamber. The coating parameters were optimised for each formulation to achieve maximum efficiency, and minimum chipping with no agglomeration. Optimisation was particularly made to solution spray rate, atomising pressure and air supply. The coating was visually inspected for any discontinuities or imperfections and once satisfied with its uniformity scanning electron microscopy (SEM) was performed on the coated tablets.

Tablets were weighed before coating and at appropriate intervals based on the calculated theoretical coating time. Tablets were however dried in an oven at 30°C for 15 minutes before checking the weight gain after the theoretical coating time. Film thickness measured as the total weight gain by the tablets (% TWG) (Equation 5.1). After achieving the desired coating weight gain, tablets were placed in an oven at 30 °C for one hour to ensure complete solvent evaporation. Dried tablets were placed in airtight containers until further testing.

$$\text{Total weight gain (\%)} = \frac{\text{Wt. of tablets before coating} - \text{Wt. of tablets after coating}}{\text{Weight of tablets before coating}} \times 100$$

Equation 5.1

For enteric coatings to achieve gastro-resistance, the recommended application is 4-6mg polymer per cm² of tablet surface (Rohm Pharma Polymers, 2001). 5 mg per cm² was chosen which corresponds to a TWG of 4.9%; this was calculated using equations 5.2a and 5.2b.

Surface area (*S*) of a standard concave tablet is based on its diameter (*d*) and height (*h*). Height of tablet cores was measured to be 3.85 mm using a micrometer gauge (Mitutoya Corporation, Japan).

$$\begin{aligned} S &= \pi (d \cdot h + 0.5d^2) && \text{Equation 5.2a} \\ &= \pi (8 \cdot 3.85 + 0.5 \cdot 8^2) \\ &= 197 \text{ mm}^2 \end{aligned}$$

$$\begin{aligned} \text{Coating weight (\%)} &= \frac{S \text{ (mm}^2\text{)} \cdot A \text{ (mgcm}^{-2}\text{)}}{w \text{ (mg)}} && \text{Equation 5.2b} \\ &= \frac{197 (5)}{200} = 4.9\% \end{aligned}$$

5.3.4 Scanning electron microscopy

The film thickness of the tablets was examined by scanning electron microscopy (SEM) using a Phillips XL 20 scanning electron microscope (Phillips, Cambridge,

UK). The tablets were cut in half to enable measurement of the film thickness. Specimens were coated with gold using a sputter coater (model K550, Emitech, Kent) and mounted onto a sample holder and examined at an accelerating voltage of 5 -15 kV depending on the magnification required. A random sample of 4 tablets from each formulation was measured. The average thickness and standard deviations were calculated.

5.3.5 In vitro drug release testing

Drug release from the coated tablets was assessed by dissolution testing using a USP XXIV type II paddle dissolution apparatus (model PTWS, Pharma Test, Hainburg, Germany). The tests were conducted in triplicates, at a paddle speed of 50 rpm in 900 ml dissolution medium maintained at $37 \pm 0.5^\circ\text{C}$. Coated tablets were first pre-exposed to 0.1 M HCl for two hours and then subjected to a pH transition in 0.05 M phosphate buffer: pH 6.8 (1 hour) to pH 7.0 (1 hour) to pH 7.2 until dissolution is complete. Phosphate buffer was used as the dissolution medium to maintain consistency with chapter four. pH changes in phosphate buffer were performed using ~ 0.4 ml of 10 M NaOH, the pH was adjusted and checked in each dissolution vessel using a pH meter. 0.1 M HCl was used to simulate gastric fluid, pH 6.8 buffer the proximal small intestine, pH 7.0 the mid small intestine and pH 7.2 the distal small intestine. pH 7.2 buffer was chosen as it is more discriminative of dissolution performance than pH 7.4 phosphate buffer (Ibekwe et al., 2006a) . Film dissolution studies could not be conducted in pH 7.2 phosphate buffer as it was extremely slowly and therefore not practical.

Dissolution was also conducted in pH 7.4 Krebs bicarbonate buffer and pH 7.4 phosphate buffer following two hour tablet pre-exposure to 0.1 M HCl (Figure 5.2). The objective of this was to compare the release profiles of the different formulations in bicarbonate buffers with conventional phosphate buffers. A further objective was to investigate the influence of several pH transitions in near neutral buffers on the dissolution performance of enteric coated tablets. Ideally, a comparison between phosphate and bicarbonate buffers would be made however the pH of bicarbonate buffer could only be altered by the inclusion of an additional buffering agent, which would compromise the physiological property of the system.

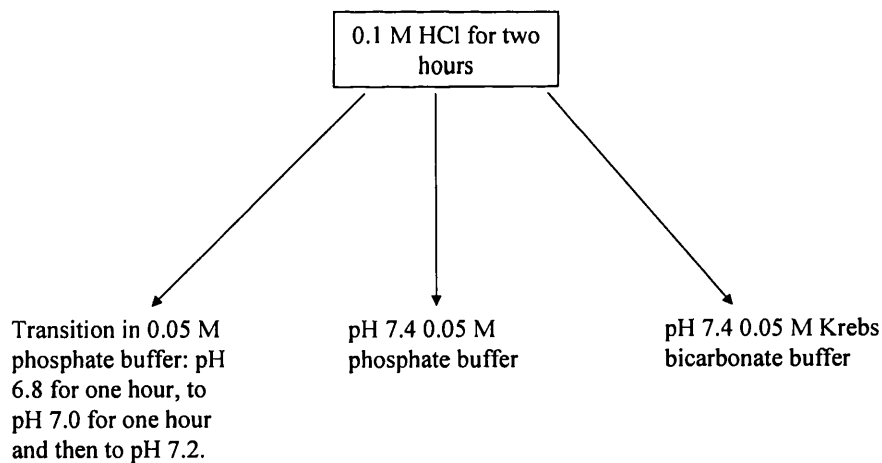


Figure 5.2 Summary of the media changes employed in the *in vitro* dissolution tests.

5.4 RESULTS AND DISCUSSION

5.4.1 Performance of the tablet cores

The weight uniformity of 5-ASA and prednisolone tablets was 208.36 ± 4.8 mg and 201.22 ± 3.78 mg respectively. The tablets comply with BP specifications whereby it is not acceptable for more than two tablets to deviate from the mean weight by more than 7.5 %, and also, no single tablet to differ from the mean by more than 15 %.

The content uniformity of 5-ASA and prednisolone was 9.85 ± 0.16 mg/ml and 9.90 ± 0.11 mg/ml respectively. The crushing strength was 73.2 ± 4.49 and 74.0 ± 4.91 N for 5-ASA and prednisolone respectively. The tablets therefore exhibit a good degree of content and weight uniformity. They are also sufficiently robust to withstand fluidization during coating. The onset of drug release is rapid for both drugs from the uncoated tablets (results discussed in a later section) thus drug release can be assumed to be controlled by dissolution of the film coating.

5.4.2 Dissolution of 5-aminosalicylic acid enteric coated tablets

5.4.2.1 Dissolution trends with different Eudragit S/ plasticizer coatings

A selection of plasticizers from different groups were separately used to reduce the brittleness of the Eudragit S film coating to achieve a flexible, coherent, crack-free tablet coating. The plasticizers selected were: propylene glycol (P-diols), polyethylene glycol 6000 (PEG 6000), dimethyl phthalate (DMP) and tributyl citrate (TBC). P-diols

and PEG 6000 are polyols, DMP is an organic phthalate ester and TBC is an organic citrate ester. These particular plasticizers were selected as they gave rise to different dissolution results when incorporated into isolated cast films, furthermore the differences were of large magnitude. Hence this small group of plasticizers will give us an insight into whether the same dissolution trends are observed on coated tablets.

Figure 5.3 shows the drug release profiles of 5-ASA tablets coated with different formulations of Eudragit S/plasticizer to a TWG of 4.9 %. Each formulation gives rise to a different dissolution profile; the lag-times and time to 50 % drug release ($T_{50\%}$) are shown in Table 5.2.

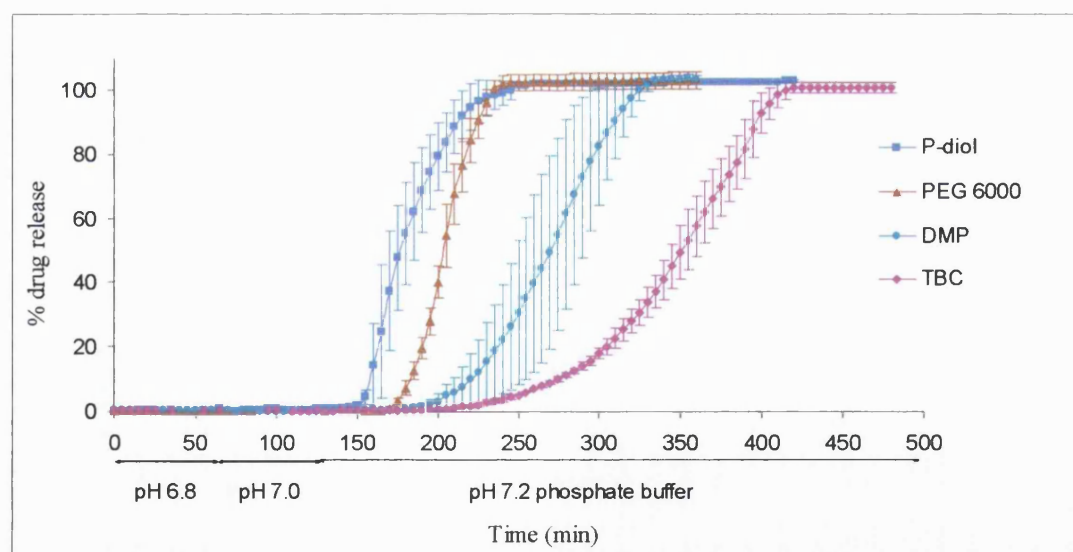


Figure 5.3 Dissolution profiles of Eudragit S/plasticizer (P-diol, PEG 6000, DMP and TBC) coated 5-aminosalicylic acid tablets in phosphate buffer (following a 2 hour exposure to acid-not shown). Mean values \pm SD.

Table 5.2 Lag time and $T_{50\%}$ (min) of 5-aminosalicylic acid tablets in pH 7.2 phosphate buffer (times include 2 hour total pre-exposure to pH 6.8 and pH 7.0 phosphate buffer) following a 2 hour exposure to acid. Tablets are coated with Eudragit S and one of the different plasticizers.

Plasticizer blended with Eudragit S	Lag-time (min)	$T_{50\%}$ (min)
P-diol	140	175
PEG 6000	170	205
DMP	185	270
TBC	205	350

Referring back to the results from the previous chapter, it is noticeable that the dissolution onset of isolated cast films (Figure 5.4) is substantially longer than the lag-time of drug release from coated tablets.

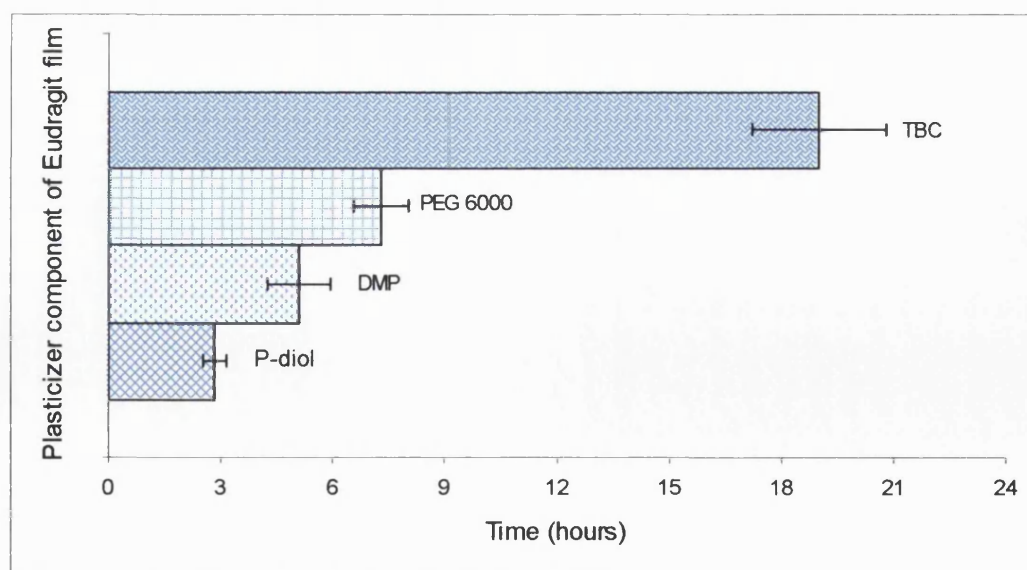


Figure 5.4 Onset of dissolution in pH 7.4 phosphate buffer of Eudragit S isolated cast films fabricated with different plasticizers. Mean values \pm SD.

From a comparison of figures 5.3 and 5.4, it can be inferred that polymer free films are predictive of the dissolution trends for the coated formulations with the extreme profiles, however not necessarily predictive for the coated formulations with intermediate release patterns. P-diol and TBC plasticizers blended with Eudragit S give rise to the fastest and slowest dissolution respectively for both free films and coated tablets. However for the plasticizers which give rise to intermediate polymer dissolution, PEG 6000 and DMP, the trend is different for the free films and coated tablets.

5.4.2.2 Reasons for the slower dissolution of cast films in comparison to sprayed films

From figures 5.3 and 5.4 it can be noticed that free films dissolve much slower than tablet coatings. The magnitude of the difference between the two coatings with the extreme dissolution trends (P-diol and TBC) is almost seven-fold greater for the free films in comparison to the coated tablets. This can partly be explained by the polymer film formation process (cast *versus* sprayed). In solution, the polymer molecules are mobile, and on solvent evaporation the polymers intertwine to form a gel-like state at a relatively high polymer concentration. This gel-like state eventually ends up into a solvent-free polymeric film. The properties of the film depend on the evaporation rate. Cast films are formed under ambient conditions, whereas for tablet coatings solvent evaporation is assisted by air flow and elevated temperatures. Spraying of droplets onto the surface and evaporation of solvent occur simultaneously for tablet coatings (Figure 5.5) (Bando and McGinity, 2006). The rate of solution application and drying contribute to determining how uniformly the droplets are distributed on the tablet surface and the quality of the film. For spray coated films, the solution is added layer by layer and formed by coalescence of droplets, however for cast films, all the

solution is added at the same time. These differences in the process of film formation will influence the intertwining of polymer chains and final film structure.

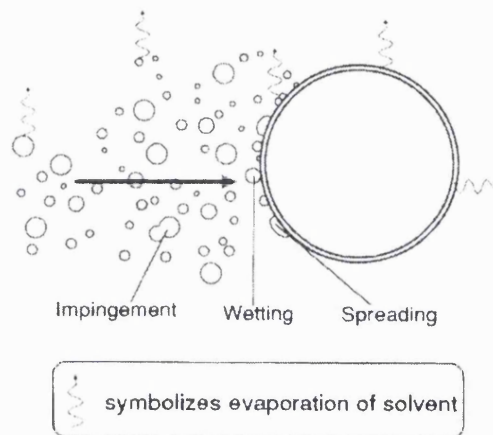


Figure 5.5 Film formation onto solid surfaces by spray coating. Reproduced from Arwidsson and Rudén (1993).

Spitael and Kinget (1977b) have described sprayed films as having a ‘droplet’ structure with a higher degree of porosity. They compared the permeability of caffeine and HCl in sprayed and cast free films of cellulose acetate phthalate (prepared from organic solutions), and found the former to be substantially more permeable. A comparison of spray-coated and solution cast films of ethylcellulose pseudolatex membranes has been conducted (Sun et al., 1999). The authors found sprayed films to be harder and more brittle than cast films, however it is uncertain the extent to which the findings of this study are applicable to organic films. Pickard et al. (1972), found the moisture permeation to be almost three-fold greater for air-sprayed in comparison to cast films of HPMC/ethylcellulose.

A further explanation for these differences in the absolute dissolution times may be explained by the film thickness. Film thickness is greater for isolated cast films in comparison to tablet coatings at 120-130 μm and $60.1 \pm 3.85 \mu\text{m}$ respectively. Furthermore, the coating thickness is even lower at the tablet edge reaching $35.2 \pm 9.67 \mu\text{m}$.

Tablet film coatings have two boundaries: drug/polymer film boundary and polymer film/dissolution medium boundary. The drug is in the solid state blended with other excipients in the core. Whereas in the free film dissolution study the drug is in solution and therefore ionised. 5-ASA is dissolved in the phosphate buffer and is in its anionic form; this results in a lower pH near the polymer film/drug boundary which in turn reduces polymer dissolution rate. As for the tablet, dissolution rate of the film is initially fast at the polymer/dissolution medium interface however then slows down due to the generation of H^+ from the ionisation of 5-ASA (Figure 5.6). This lower pH at the drug/polymer interface retards polymer film dissolution near the tablet surface. Enteric tablet coating have been reported to stay intact up to the point when 90 % of it has dissolved. Tablet core disintegration starts to occur when 95 % of the coating has dissolved (Ozturk et al., 1988a). As the edge of the tablet has the thinnest coating, this region is observed to be the first to completely dissolve.

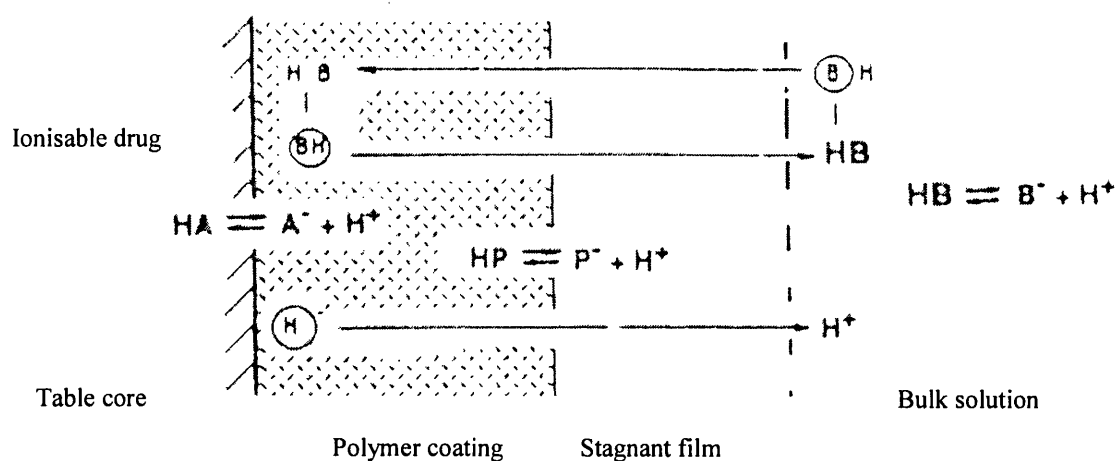


Figure 5.6 Diagram representing enteric polymer dissolution and drug release. HA is weakly acidic drug, HP is enteric polymer and HB is buffer. Adapted from Ozturk et al. (1988a).

5.4.2.3 Interaction of drug and excipients in tablet core with the polymer film coat

The tablet core is likely to impart an affect on polymer film dissolution. As previously mentioned, interaction of the drug and core excipients with the polymer film coating can occur. With specific reference to this tablet formulation, complexes between the binder, polyvinyl pyrrolidone (PVP), and Eudragit S are possible. Interaction can occur at the core/polymer boundary or PVP may even permeate into the coat. Possible mechanisms of interaction are inter-macromolecular hydrogen bonds between the undissociated carboxylic groups of Eudragit S and the carbonyl groups of PVP (Jin et al., 2005) (Figure 5.7a). Alternatively, the partial positive charge on the nitrogen atom of PVP can facilitate its bonding to the carbonyl from Eudragit S (Figure 5.7b). However the formation of the latter structure is less favourable due to steric hindrance arising from the ring and polymer chain thus rendering the nitrogen atom inaccessible. Another possibility is the formation of two hydrogen bonds between one

monomer of PVP and one monomer of Eudragit S (Kaczmarek et al., 2001). An aqueous media is required to initiate this reaction which could become available from humidity in the atomizing and drying air during the spray coating process, or from HCl and buffer permeation into the tablet core during the dissolution process.

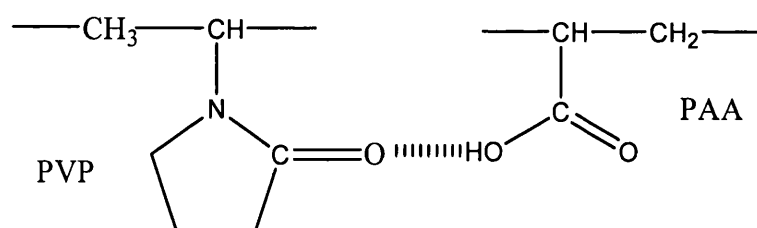


Fig. 7a

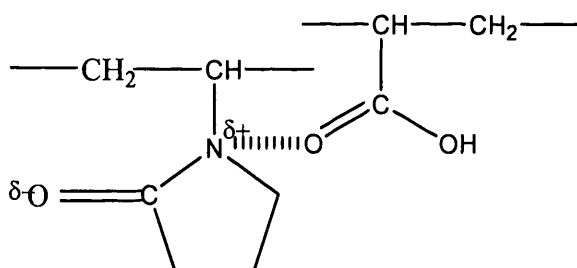


Fig. 7b

Figure 5.7 Interaction of the binder polyvinyl pyrrolidone (PVP) with poly (acrylic acid) (PAA). Reproduced from Kaczmarek et al. (2001).

PVP also has the potential to interact with carbonyls present in plasticizers. Carbonyls in plasticizers may be more accessible than those of the Eudragit polymer as they are not part of a macrochain. The plasticizers studied have different numbers of carbonyl groups in their structure with different accessibilities which will determine their interaction with PVP.

The disintegrant, croscarmellose sodium, is a cross-linked form of carboxymethylcellulose sodium (NaCMC). The carboxyl group on NaCMC has a pKa of 4.3, the sodium carboxylate groups could react with protons to form carboxylic acids (Rohrs et al., 1999). This protonation needs to be mediated by moisture. Protonation may occur during the two hour acid exposure whereby the acid imbibes into the core. The extent of this acid imbibition depends on the porosity and tortuosity of the hydrated polymer coating which in turn depends on its microstructure. Protonation of the disintegrant has been shown to alter the dissolution profile of delavirdine tablets, this may be related to impairment in the wicking and swelling ability of the disintegrant (Rohrs et al., 1999).

Drug migration from the tablet core into the polymer coat may occur. A study by Okhamafe and York, 1989 showed that incorporation of up to 10 % drug into polymer cast films alters their glass transition and crystallinity. Eudragit S is an amorphous polymer, however if the crystalline drug 5-ASA dissolves in it then this may promote the formation of crystalline regions in the polymer film.

5.4.2.4 Reasons why plasticizers may have different influences on dissolution of tablet film coats in comparison to polymer free films

Plasticizers have been shown to alter the permeability of enteric coatings to water vapour and gastric juice (HCl). Whether this permeability is reduced or enhanced and its extent is dependent on a number of mechanisms; one of which is the plasticizer's ability to reduce polymer-polymer interactions thus increasing segmental mobility and consequently reducing the activation energy for diffusion (Porter and Ridgway, 1982). Water vapour permeability hydrates the polymer layer and may further enhance the

permeability due to the plasticizing effect of water. On the other hand, diffusivity may be reduced due to extensive hydrogen bonding between the water and plasticizers or other non-polymeric additives (Okhamafe and Iwebor, 1986). Increased permeability of the film to buffer species is likely to influence dissolution profile of the tablet and as previously discussed, sprayed films have different permeabilities to cast films. Ion transfer between the buffer solution and the film involves two steps: penetration of the electrolytic solution into the film and diffusion of ions within it (Raffin et al., 1995). Permeability to gastric juice, more specifically H^+ ions, during the two hour pre-exposure to HCl will affect the commencing ionization of the polymer on exposure to buffer.

Although drug permeability coefficients are usually inversely proportional to film thickness; this is not always the case. Ion permeability through different formulations of cellulose acetate phthalate films (no plasticizer/ triacetin/ diethylphthalate) showed that the permeability coefficient decreases with increasing film thickness except in the case of diethylphthalate films (Raffin et al., 1996). From this it can be inferred that the rate of Eudragit S film dissolution may not always correlate to film thickness for the different formulations. This may explain why the intermediate dissolution trends were different for free films and films coated onto tablets.

Internal stresses develop within the film coating when the polymeric solution is applied to a solid surface (Rowe, 1978). The stress is proportional to the elastic modulus of the film and if the internal stress exceeds the cohesive strength of the film then the coating will split or crack (Felton and McGinity, 2002). It may be argued that leaching of plasticizer out of the polymer film may have arisen while tablet is

immersed in HCl or buffer media, thus increasing the internal stress of the film and the incidence of crack formation. However all the tablet coatings were examined by SEM at different intervals from the time of immersion in the dissolution media, and they showed no appearance of cracks. Hence we are confident that the onset of drug release was not through a crack or flaw in the coating however due to dissolution of the polymer (Figures 5.8a and 5.8b).

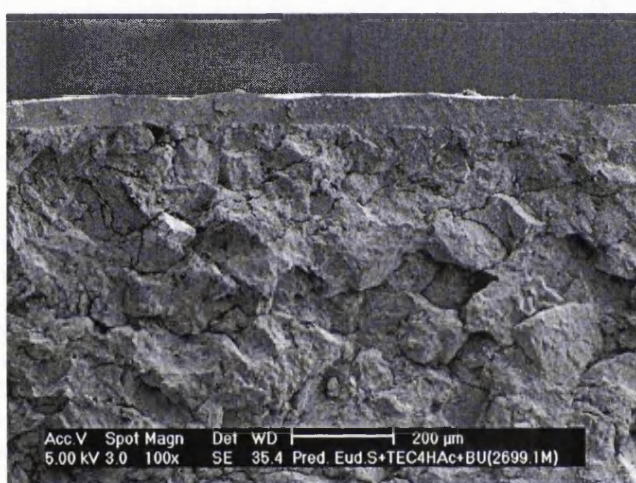


Figure 5.8a

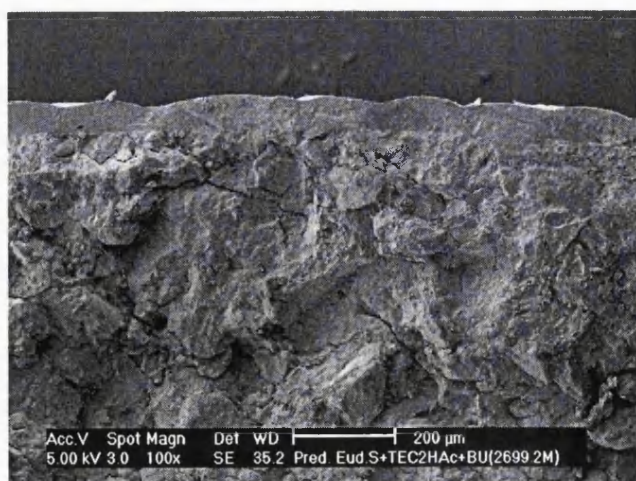


Figure 5.8b

Figure 5.8 SEM cross-sections of Eudragit S/TEC coated prednisolone tablets after exposure to HCl for 2 hrs (a) and after exposure to HCl for 2 hrs followed by buffer for 2 ½ hrs (b) .

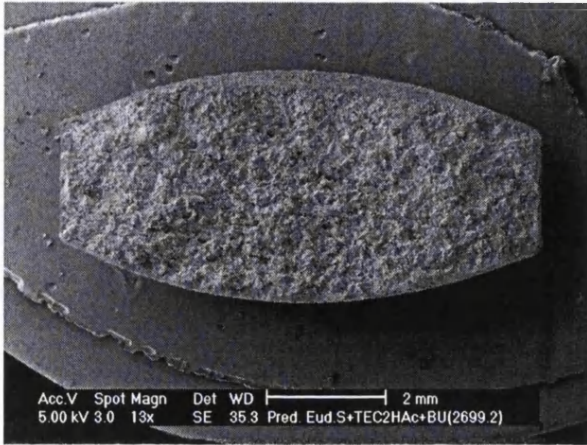


Figure 5.8c

Figure 5.8 SEM cross-sections of Eudragit S/TEC coated prednisolone tablets after exposure to HCl for 2 hrs followed by buffer for 2 ½ hrs (c)

5.4.3 Dissolution of enteric coated prednisolone tablets

5.4.3.1 Dissolution trends with different Eudragit S/plasticizer coatings and their comparison to 5-aminosalicylic acid coated tablets

The Eudragit S/plasticizer formulations used to coat 5-ASA tablets were applied to prednisolone tablets to elucidate any drug influences on dissolution (Figure 5.9 and Table 5.3).

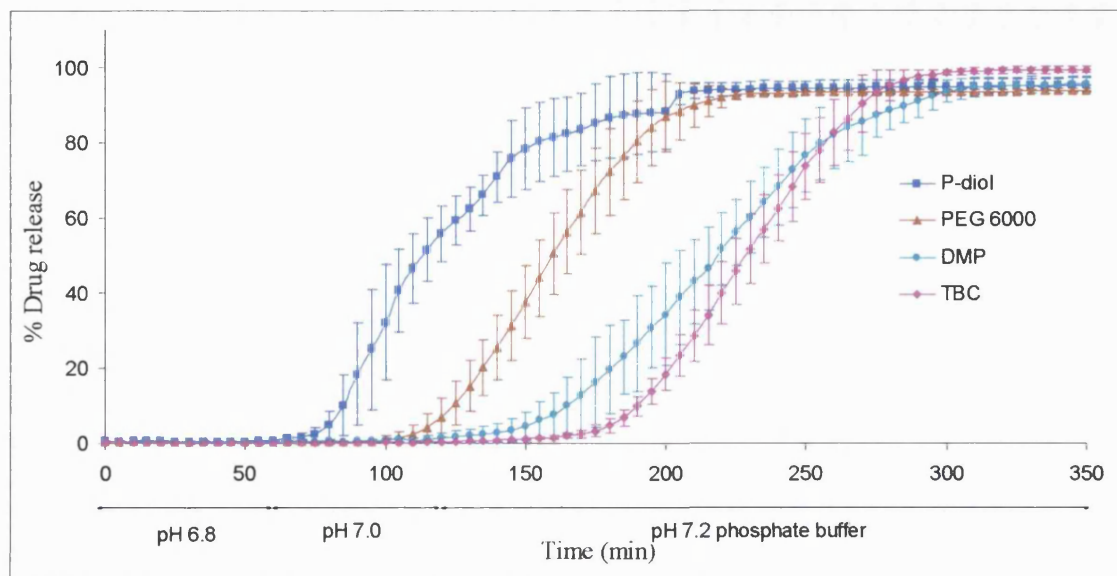


Figure 5.9 Dissolution profiles of Eudragit S/plasticizer (P-diol, PEG 6000, DMP and TBC) coated prednisolone tablets in phosphate buffer (following a 2 hour exposure to acid-not shown). Mean values \pm SD.

Table 5.3 Lag time and $T_{50\%}$ (min) of prednisolone tablets in pH 7.2 phosphate buffer (times include 2 hour total pre-exposure to pH 6.8 and pH 7.0 phosphate buffer) following a 2 hour exposure to acid. Tablets are coated with Eudragit S and one of the different plasticizers.

Plasticizer blended with Eudragit S	Lag-time (min)	$T_{50\%}$ (min)
P-diol	70 (starts to dissolve in pH 7.0 phosphate buffer)	115
PEG 6000	105	185
DMP	130	220
TBC	160	230

Interestingly, the dissolution lag times and $T_{50\%}$ are considerably shorter for prednisolone tablets compared to 5-ASA tablets despite the lower solubility of the former drug in pH 7.2 phosphate buffer and the consequential slower dissolution of the uncoated tablets (Figure 5.10). A possible explanation for this is the ionization of 5-ASA creating an acidic environment around the surface of the tablet core which retards polymer film dissolution. Furthermore, with the different actives a difference in the dissolution trend arises. Eudragit S/TBC and Eudragit S/DMP prednisolone coated tablets have similar dissolution onset times and profiles; however Eudragit S/TBC gives rise to a much slower release for 5-ASA tablets. Moreover, the difference between the dissolution profiles of Eudragit S/P-diol and Eudragit S/PEG 6000 coated prednisolone tablets is of greater magnitude than that observed for 5-ASA coated tablets. These differences between 5-ASA and prednisolone tablets can only be attributable to the active ingredient, as everything else in the tablet core or coating formulation is the same. It appears that the tablet core and the polymer film coating are not two discrete entities, however interact with one another in some way that influences the dissolution of the polymer film and thus the drug release that proceeds. From these results it can be proposed that the molecular interactions of the plasticizer with the polymer have the predominant influence on determining the dissolution of the polymer film; however the components of the tablet core, including the active and excipients can also exert an affect through different mechanisms.

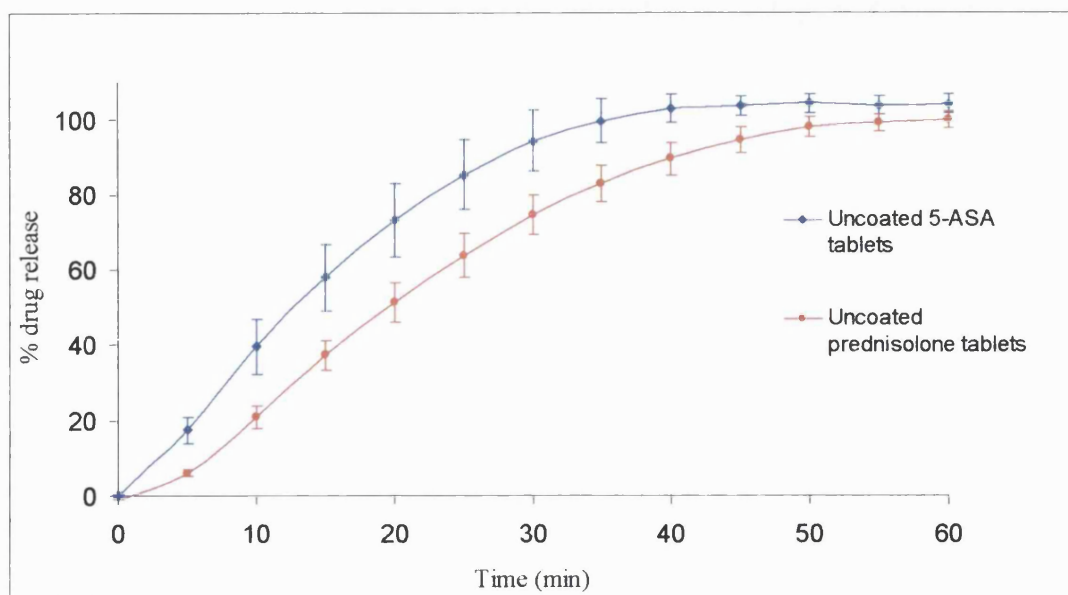


Figure 5.10 Dissolution of immediate release 5-ASA and prednisolone tablets in pH 7.2 phosphate buffer. Mean values \pm SD.

5.4.3.2 Dissolution of Eudragit S coated prednisolone tablets fabricated with the recommended plasticizers and implications on therapeutic efficacy

Degussa (producer of Eudragit S) recommends certain plasticizers for use with the poly(methacrylic acid methylmethacrylate) copolymer on the basis of their compatibility and favourable alteration of the mechanical properties of the film coating. These recommended plasticizers are: triethyl citrate (TEC), triacetin (TA), P-diols and PEG 6000 (Rohm Pharma Polymers, 2001). The drug release profile of prednisolone tablets coated with different formulations of Eudragit S and the recommended plasticizers are shown in Figure 5.11 and Table 5.4.

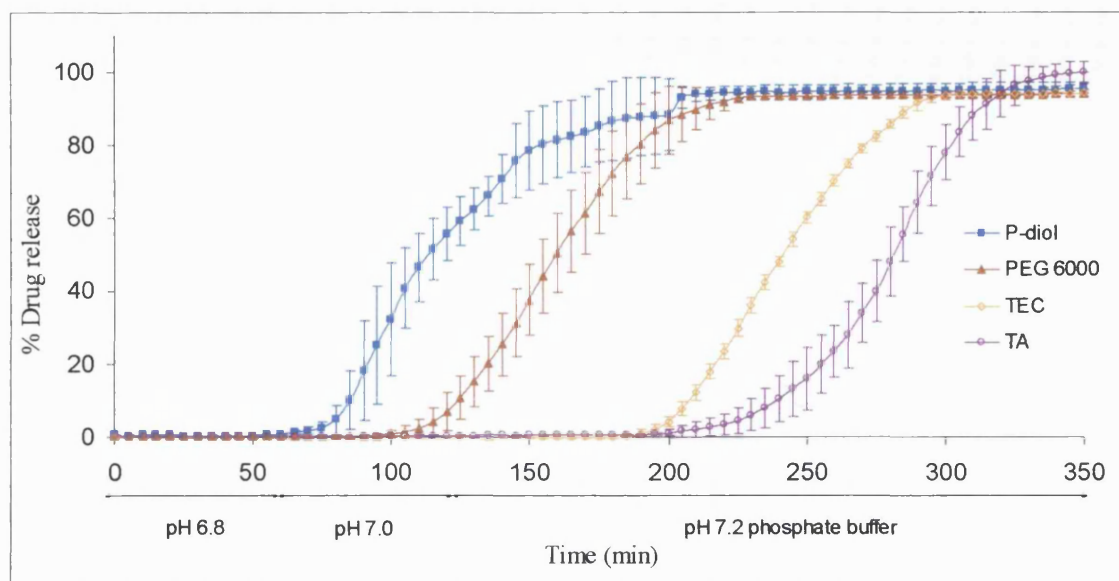


Figure 5.11 Dissolution profiles of Eudragit S/plasticizer (P-diol, PEG 6000, TEC and triacetin) coated prednisolone tablets in phosphate buffer (following a 2 hour exposure to acid). Mean values \pm SD.

Table 5.4 Lag time and $T_{50\%}$ (min) of prednisolone tablets in pH 7.2 phosphate buffer (times include 2 hour total pre-exposure to pH 6.8 and pH 7.0 phosphate buffer) following a 2 hour exposure to acid. Tablets are coated with Eudragit S and one of the different plasticizers.

Plasticizer blended with Eudragit S	Lag-time (min)	$T_{50\%}$ (min)
P-diol	70	115
PEG 6000	155	185
TEC	190	245
TA	320	420

The recommended plasticizers give rise to different drug release profiles. These profiles, as with isolated free films, do not appear to correlate to the glass transition temperature. SEMs of all the Eudragit S/plasticizer tablet coatings show similar coating thicknesses and smooth, crack-free coatings (Figure 5.12a-12c). This is even the case for the Eudragit S/P-diol coating (Figure 5.12d) for which two glass transition temperatures were detected in the previous chapter; these were ascribed to plasticized and non-plasticized regions in the free film.

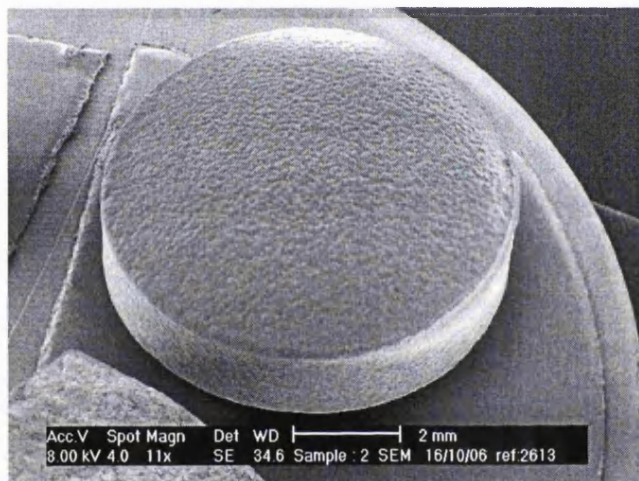


Figure 5.12a SEM of the surface of Eudragit S/TEC coated prednisolone tablet

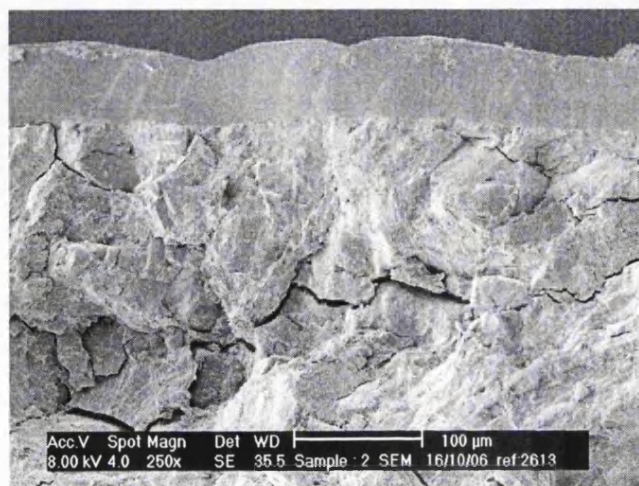


Figure 5.12b SEM cross-section of Eudragit S/TEC coated prednisolone tablet

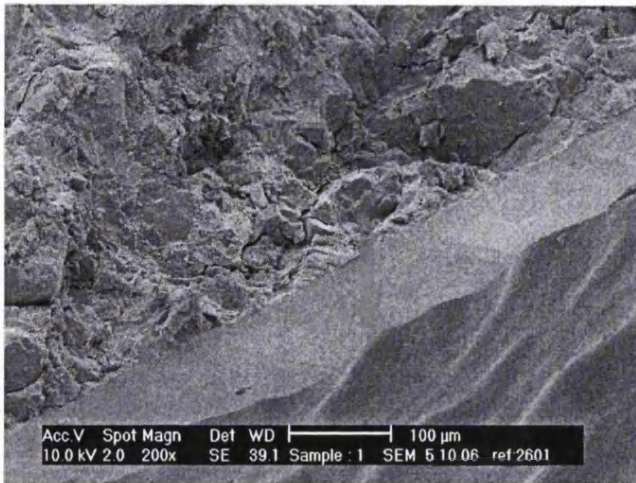


Figure 5.12c SEM cross-section of Eudragit S/PEG 6000 coated prednisolone tablet

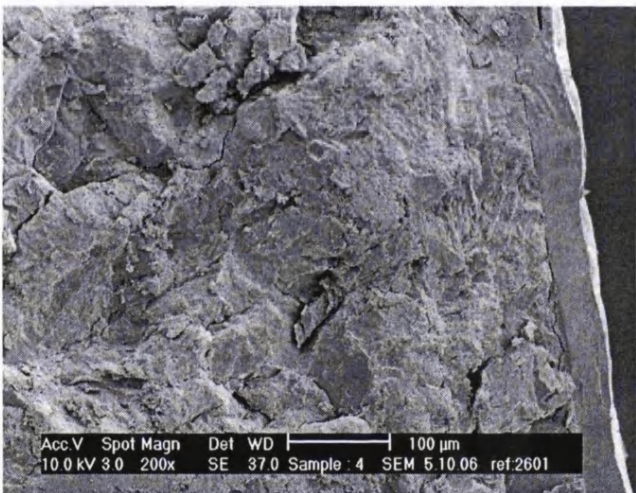


Figure 5.12d SEM cross-section of Eudragit S/P-diol coated prednisolone tablet

For Eudragit S only coatings with no plasticizer, however, there are very apparent cracks on the surface and cross-section of the coating layer (Figure 5.13a,b). Despite this the enteric coating was robust for two hours in acid and release was observed after 30 minutes in pH 6.8 buffer, i.e. below the pH threshold of the polymer. Internal stresses and rigidity within the film, however, probably give rise to core disintegration and drug release prior to 95 % of the coating dissolving. This result was therefore not directly compared to the other coating formulations as we believe the mechanism underlying drug release to be different.



Figure 5.13a Surface SEM of Eudragit S coated prednisolone tablet (no plasticizer).



Figure 5.13b SEM cross-section of Eudragit coated prednisolone tablet (no plasticizer)

These dissolution differences between the formulations have important implications particularly as the Eudragit S polymer is utilised for site-specific delivery. Its current use in pharmaceutical products for the treatment of inflammatory bowel diseases (IBD) is critical that drug is released at the inflamed regions of the intestine. Hence by an alteration of the plasticizer in the film coating therapeutic efficacy of the drug may

be compromised. This influence that excipients impart on drug release from dosage forms is not a new phenomenon in pharmaceuticals. In the 1960s and 70s differences in the bioavailability of the immediate release antidiabetic drug, tolbutamide, and the steroid, prednisolone, were reported between brands due to different excipients in the formulation (Campagna et al., 1963; Levy, 1964). Toxicity was reported with phenytoin when calcium sulphate was replaced with lactose (Tyrer et al., 1970).

Nevertheless, this plasticizer influence on drug release from enteric formulations can be favourably utilised by pharmaceutical scientists and physicians. Formulations can be designed and prescribed to treat different regions of the gut affected by disease. As an example, P-diol can be used as a plasticizer in pH-responsive preparations to treat patients where the inflamed regions have reached proximal regions of the gut. However if a more distal release is desired then the appropriate formulation can be chosen, for example with TBC as a plasticizer, and designed into a multiple unit dosage form. High surface area to volume ratio dosage forms are more desirable; since slow *in vitro* dissolution will be further exaggerated in the large intestine, partly due to its limited fluid availability.

These findings can be utilised for other enteric polymers designed to release drugs in the proximal small intestine. Enteric coatings are not without their problems. A lag time of 1.5 to 2 hours post-gastric emptying has been reported for complete disintegration of an enteric coated capsule (Wilding et al., 1993; Ebel et al., 1993). This is not favourable if the drug has very poor solubility which would therefore demand complete release before reaching the large intestine. Slow dissolution is also not desirable if a rapid therapeutic effect is needed, for example analgesic action by

non-steroidal anti-inflammatory drugs (NSAIDs). Extensive research is being carried out on ways to achieve rapid small intestinal drug release (Pearnchob et al., 2004; Liu et al., 2007) , use of the appropriate plasticizer in conjunction with other formulation strategies may help achieve rapid release.

5.4.3.3 Dissolution of Eudragit S coated prednisolone tablets fabricated with a homologous series of plasticizers

Prednisolone tablets were coated with Eudragit S plasticized with one of phthalate ester: dimethyl phthalate (DMP), dibutyl phthalate (DBP) or dioctyl phthalate (DOP). The longer the alkyl chain length the lower is the aqueous solubility of the plasticizer with DMP, DBP and DOP having solubilities of 0.4 %, 0.15 % and 0.0002 % m/v respectively. Despite the different aqueous solubilities of the plasticizers and the different glass transition temperatures of the free films, the dissolution profiles of the coated tablets are very similar (Figure 5.14). This is a surprising result considering that the free films have very different dissolution times. It may be that the interactions of drug and excipients in the core with the coating, outweighs the differences in molecular interactions arising from the different chain length phthalates with Eudragit S polymer.

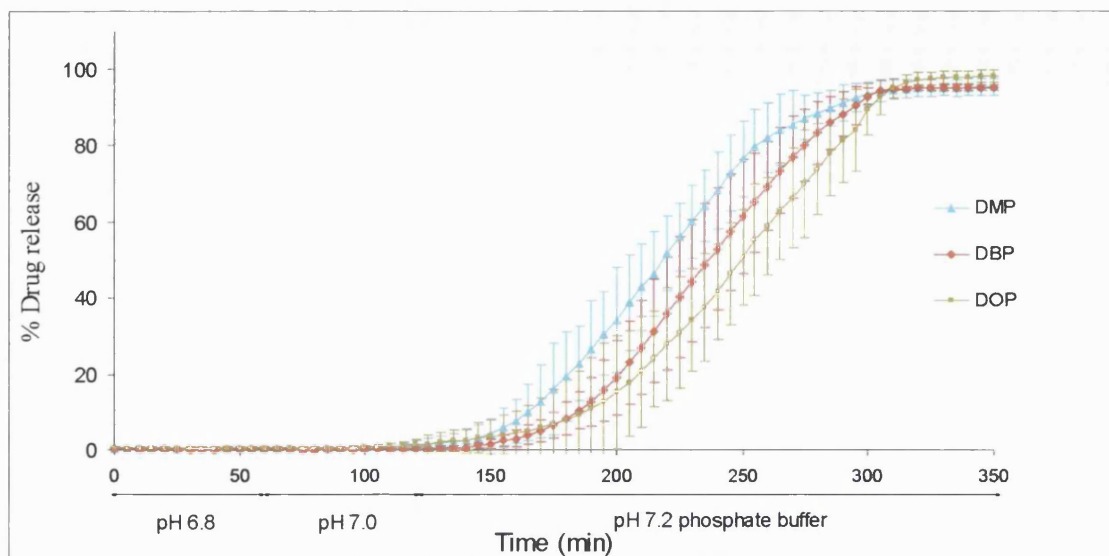


Figure 5.14 Dissolution profiles of Eudragit S/plasticizer (DMP, DBP and DOP) coated prednisolone tablets in phosphate buffer (following a 2 hour exposure to acid-not shown). Mean values \pm SD.

5.4.4 Influence of release media composition on dissolution profiles of coated tablets

As explained in chapter four, dissolution of the films could not be measured in bicarbonate buffers due to the technical difficulties in maintaining buffer stability in permeation cells. In this set of experiments the dissolution profile of a selection of coated 5-ASA and prednisolone tablets is explored in Krebs bicarbonate buffer stabilised using 5 % CO₂. The main objective was to investigate if bicarbonate buffer media give rise to different dissolution trends to those observed in phosphate buffers. Another objective was to evaluate if a pH transition in near neutral buffers affects the dissolution trends. The formulations selected were the same as those in the first part of the study so that the plasticizers represent the different groups.

Tablets were exposed to 0.1 M HCl for two hours and then transferred to pH 7.4 Krebs bicarbonate buffer or 0.05 M phosphate buffer at the same pH for a direct comparison. Figures 5.15 and 5.16 show the dissolution trends of coated 5-ASA tablets in Krebs bicarbonate buffer and phosphate buffer respectively. The dissolution trends of the four formulations are the same in the two different media. In Krebs buffer, however, the lag-time is 60 minutes longer. This corroborates the findings from chapter two whereby the dissolution profile of enteric coated tablets is dependent on the buffer species, its concentration and buffer capacity. Furthermore, the trends observed in these two figures are similar to those in figures 5.3 whereby the tablets undergo a transition through different near neutral pH phosphate buffer media.

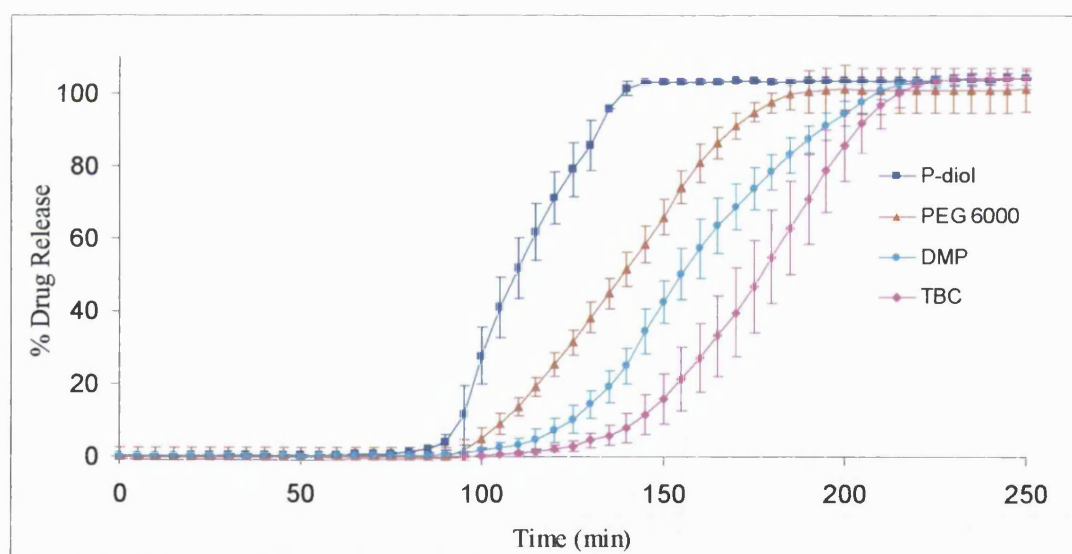


Figure 5.15 Dissolution profiles of Eudragit S/plasticizer (P-diol, PEG 6000, DMP and TBC) coated 5-aminosalicylic acid tablets in pH 7.4 Krebs bicarbonate (following a 2 hour exposure to acid-not shown). Mean values \pm SD.

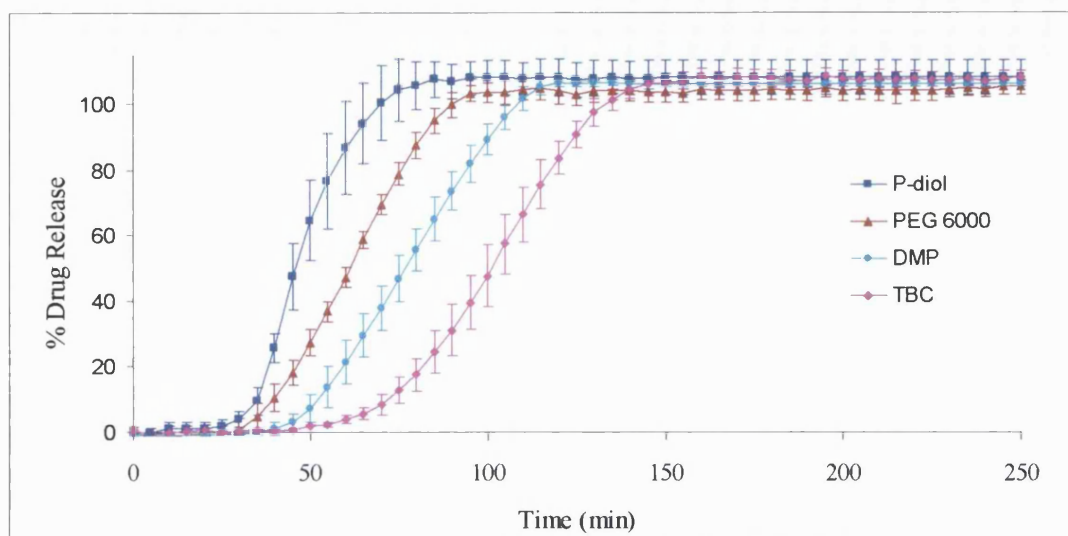


Figure 5.16 Dissolution profiles of Eudragit S/plasticizer (P-diol, PEG 6000, DMP and TBC) coated 5-aminosalicylic acid tablets in pH 7.4, 0.05 M phosphate buffer (following a 2 hour exposure to acid-not shown). Mean values \pm SD.

Figures 5.17 and 5.18 show the dissolution trend of coated prednisolone tablets in Krebs bicarbonate buffer and phosphate buffer respectively. Again, the lag-time is longer in Krebs buffer in comparison to phosphate buffer. Interestingly, the lag-time is prolonged by 60 min, which is of the same magnitude as that for 5-ASA tablets. This confirms the propositions we put forward in chapter two concerning the Bronsted catalysis theory and its role in ionisation of enteric polymers. The buffer medium composition is not only critical for the dissolution of ionic drugs, but also for modified release dosage forms formulated with ionisable polymers. The last two figures illustrate this for the non-ionisable drug prednisolone which has the same solubility in different aqueous media.

Moreover, once drug release starts, the actual dissolution profile of prednisolone tablets is slower in Krebs buffer with a much longer time to 100 % drug release in

comparison to phosphate buffer. This was also observed for 5-ASA tablets however not to the same extent. This may be related to the poorer aqueous solubility of prednisolone whereby the slower dissolution of the coating manifests to a greater extent on its release from the core.

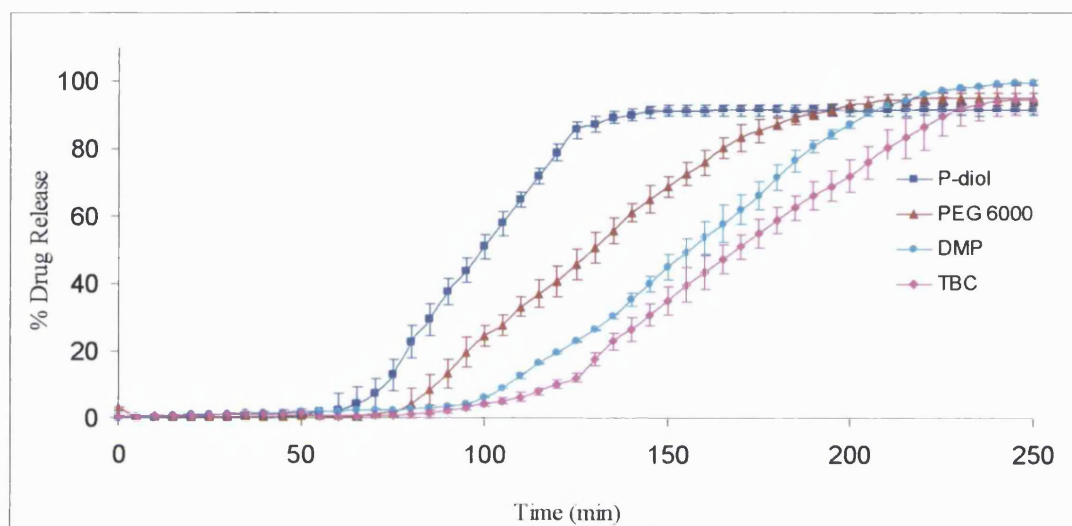


Figure 5.17 Dissolution profiles of Eudragit S/plasticizer (P-diol, PEG 6000, DMP and TBC) coated prednisolone tablets in pH 7.4 Krebs bicarbonate (following a 2 hour exposure to acid). Mean values \pm SD.

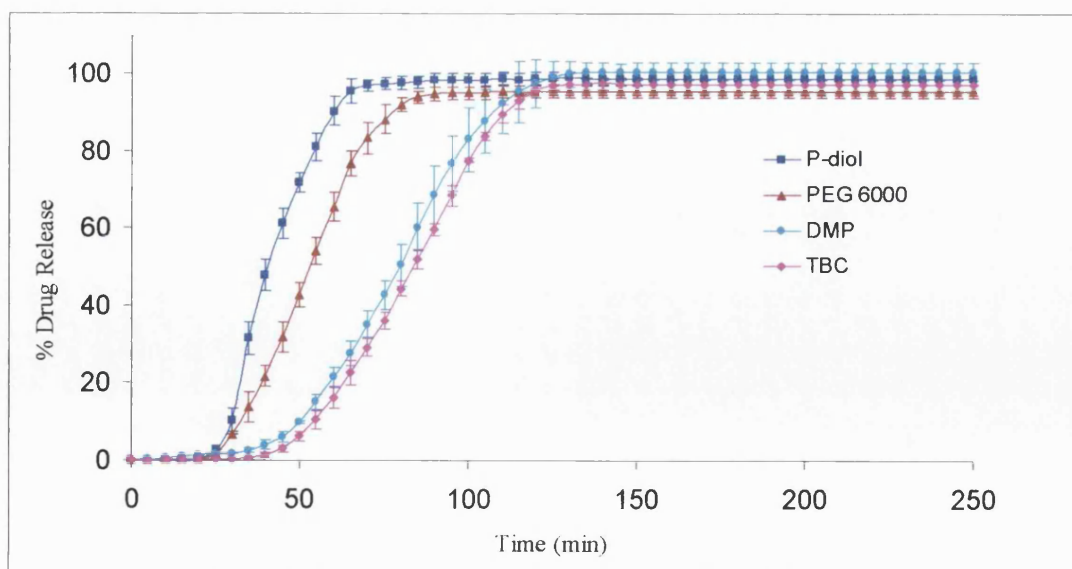


Figure 5.18 Dissolution profiles of Eudragit S/plasticizer (P-diol, PEG 6000, DMP and TBC) coated prednisolone tablets in pH 7.4, 0.05 M phosphate buffer (following a 2 hour exposure to acid- not shown). Mean values \pm SD.

5.5 CONCLUSIONS

This chapter shows that drug release from enteric coated tablets is influenced by the plasticizer component of the film coating. Polymer free film studies are predictive of the dissolution trends for the coated tablets with the extreme profiles, however not necessarily predictive for the formulations with the intermediate release patterns. It is speculated that leaching of drug and core excipients into the film coat and the molecular and physical interactions that arise also influence dissolution of the pH-responsive polymer.

Prednisolone and 5-ASA tablets coated with Eudragit S films fabricated with different plasticizers achieve the same dissolution trends in bicarbonate buffers as with phosphate buffers. However the release profiles for both drugs are markedly slower in the bicarbonate buffer. This emphasises the need to define the buffer composition of the dissolution medium as it is not only critical for the dissolution of ionic drugs, but also for modified release dosage forms formulated with ionisable polymers.

CHAPTER SIX

General discussion and future work

6.1 GENERAL DISCUSSION AND CONCLUSIONS

Modified release systems may be utilised to extend or delay drug release to specific regions of the gastrointestinal (GI) tract where optimum drug absorption occurs or for the treatment of local diseases. The focus of this study was on pH-responsive dosage forms for targeting of the model drugs, 5-aminosalicylic acid (5-ASA) and prednisolone, to the ileo-colonic region of the GI tract for inflammatory bowel disease (IBD) therapy. We endeavoured to understand the behaviour of these systems and the elements that influence drug release from them. We achieved this through the characterisation and simulation of human small intestinal luminal fluids as well as investigation of the interaction of excipients in the formulation, primarily plasticizers, with the pH-responsive polymer. This improved understanding enables selection of appropriate media for use in dissolution tests and brings us closer to attaining *in vitro*/*in vivo* correlations. An understanding of polymer-plasticizer interactions will help reduce the empirical approach to formulation design.

The work started with identification of ionic factors that influence dissolution of the pH-responsive polymer, Eudragit S (methacrylic acid methylmethacrylate copolymer). Polymer ionisation was proved to be regulated by the Bronsted catalysis law and therefore the pKa of the buffer species and its concentration in the dissolution medium. The ionic luminal environment of small intestinal fluids was simulated *in vitro* through the use of physiological bicarbonate buffers at electrolyte concentrations and ionic strength corresponding to those in jejunal and ileal fluids. Bicarbonate media were shown to provide a better reflection of the *in vivo* disintegration times published in the literature of these ileo-colonic delivery systems. On designing dissolution tests

it is important to accurately define the ionic composition of the dissolution medium to attain meaningful results. These findings can be extrapolated to other systems with pH-responsive polymers as they all have the same underlying step for dissolution; ionisation of acidic functional groups.

The next focus was on the drug and its physicochemical characteristics in relation to solubility in different physiological media. Drug solubility was measured in human intestinal fluids (HIF) and compared to that in physiological media. Bicarbonate buffers provided a good reflection of the solubility of 5-ASA in jejunal fluids. The HIF solubility of the non-ionisable drug, prednisolone, was not well reflected by any of the physiological media, including fasted state simulated intestinal fluid (FaSSIF) containing intestinal surfactants. This may arise because the bile salt composition in HIF is not accurately simulated in FaSSIF. Physiological bicarbonate buffers can provide a surrogate to HIF for examining the solubility of ionisable drugs. HIF are not only difficult and expensive to attain however also ethically questionable and therefore not feasible for routine use.

Knowledge of drug solubility and fluid availability in different regions of the GI tract can contribute to the decision making process in dosage form design. Currently, only drugs that are in class I of the biopharmaceutics classification system (BCS) (high solubility, high permeability) are considered for waiving *in vivo* bioequivalence testing for the approval of new immediate release dosage forms. In future years, biowaivers may be approved if the drug expresses high solubility in the region of the GI tract it is designed to target; not just high solubility in water. For example non steroidal anti-inflammatory drugs which are usually enteric coated display low

solubility in the stomach however higher solubility in the near neutral pH of the small intestine (Sheng et al., 2006). This further stresses the importance of realistic *in vitro* dissolution tests as the results derived from them are heavily relied upon for granting biowaiver status to an oral dosage form.

Now that elements of the dissolution medium influencing drug release from pH-responsive systems have been identified, the rest of the study focused on the system's formulation; with particular reference to polymer-plasticizer interactions and their influence on dissolution. Plasticizers are known to alter molecular mobility of the system by configuring between the chains and altering polymer intermolecular interactions thus increasing film flexibility. We therefore thoroughly investigated molecular mobility of the film systems through characterisation of their segmental (glass transition) and local (secondary) relaxations. A range of techniques were employed including differential scanning calorimetry (DSC), dynamic mechanical analysis (DMA) and thermally stimulated depolarisation currents (TSDC). Eudragit S polymer free films formulated with different plasticizers were screened. Onset of film dissolution was measured using two-compartment permeation cells.

Film dissolution was found to be influenced by the solubility and structure of the plasticizer. Plasticizer structure affects its interaction, particularly hydrogen bonding, with the polymer. This is supported by the TSDC results whereby the total secondary relaxation area and relaxation area of the carboxylic acid functional group of Eudragit S were found to correlate with dissolution times of the films. Hydrogen bonding can cause disruption of polymer-polymer interactions thus increasing the propensity for water imbibation into the films and increasing dissolution rate. No correlation

however was found among the glass transition temperatures obtained by TSDC, DSC and DMA techniques with dissolution time of the films. For pH-responsive films, the local environment of the carboxylic acid groups of the polymer predominates over segmental relaxations in influencing film dissolution.

The next step was to establish if the dissolution trends observed with the different film formulations are representative of Eudragit S coated immediate release 5-ASA and prednisolone tablets. The drug release from enteric coated tablets was also found to be influenced by the plasticizer component of the film coating. The polymer free films are predictive of the dissolution trends for the coated tablets with the extreme profiles, however not necessarily predictive for the formulations with the intermediate release patterns. It is speculated that leaching of drug and core excipients into the film coat and the molecular and physical interactions that arise also influence dissolution of the pH-responsive polymer.

These findings will aid in mechanistic formulation development. This will reduce time and resources, and more importantly, achieve improved drug bioavailability. With reference to IBD, formulations can be designed to treat different groups of the heterogeneous patient population. Hence if more proximal regions of the small intestine are affected, a plasticizer which gives rise to a faster onset of tablet dissolution can be selected.

6.2 FUTURE WORK

- ❖ It would be of interest to characterise the ionic composition of fluids from different regions of the large intestine. This information, coupled with the available information in the literature on the gastric environment, will allow simulation of the dosage form as it passes through the entire GI tract.

Now that promising results with bicarbonate buffers have been achieved it would be beneficial to simulate other GI parameters and mimic them collectively in dissolution tests *in vitro*. A parameter that warrants investigation is viscosity of GI luminal fluids, particularly of the distal small intestine and large intestine. While this will be difficult to simulate, our preliminary dissolution experiments using media with elevated viscosity have shown interesting results.

- ❖ Drug solubility was tested in ileostomy fluids from patients with IBD as an alternative to ileal fluids. It would be useful if we attained specimens of ileal fluid from healthy patients and compared drug solubility in these two media. The same can be performed for colonic and colostomy fluids. This will give an insight into drug behaviour in patients and special considerations may need to be made when designing the formulation. Measurements of intrinsic drug solubility would also be beneficial.
- ❖ The solubility findings with 5-ASA and prednisolone can be generalised to other drugs with similar physicochemical properties. Nevertheless, it would be useful to screen a small library of actives; including acidic and basic drugs with different

pKa values as well as poorly soluble drugs with different log P values to establish how the influence of buffer species and intestinal surfactants along with their concentrations changes with these properties.

- ❖ Immersion DMA is one of the few techniques that can study the properties of a system while it is actually immersed in liquid. Only one media was used during the course of our study with this technique; the next step would be to experiment with different media. Of particular interest would be changing the ionic strength of the media or inclusion of intestinal surfactants.

A 'powder pocket' has recently been innovated for use in DMA (Royall et al., 2005). This can contain a sample, such as a powder, and allow its mechanical properties to be measured as a function of temperature. Prior to this novel method only self-supporting materials could be studied by DMA. Although this method has only been developed for use in the dry state, it has implications for the study of dosage forms such as pellets or fragments from a tablet. Useful information can be derived such as drug or core excipients leaching into functional coatings and their affect on the thermal-mechanical properties of the system. It may be possible to adapt this powder pocket so that it also effectively functions in immersion mode.

- ❖ There was only time to investigate the influence of one concentration of plasticizer on the dissolution of pH-responsive films. It would be worthwhile to test a range of concentrations for each plasticizer.

REFERENCES

- British Pharmacopoeia, 2003. TSO, London.
- United States pharmacopoeia and national formulary, 2006. United States Pharmacopoeial Convention, Rockville, Md.
- Abrahamsson, B., Pal, A., Schwizer, W., Hebbard, G., and Brasseur, J.G., 2002. Simulation of shear forces on tablets in the fed stomach. *Eur.J.Pharm.Sci.* 17S.
- Abrahamsson, B., Ungell, A.-L., 2004. Biopharmaceutical support in formulation development. In: Gibson, M. (Ed.), *Pharmaceutical preformulation and formulation: a practical guide from candidate drug selection to commercial dosage*, Interpharm/CRC Press, Boca Raton, 239-291.
- Abumurad, N., Storch, J., 2006. Role of membrane and cytosolic fatty acid binding proteins in lipid processing by the small intestine. In: Johnson, L.R., Barrett, K.E., Ghishan, F.K., Merchant, J.L., Said, H.M., Wood, J.D. (Eds.), *Physiology of the gastrointestinal tract*, Elsevier Academic Press, Burlington, MA, 1693-1709.
- Aiache, J.M., Aiache, S., 1985. The fate of dosage forms in the gastrointestinal-tract. *Pharmacy International*, 6, 18-21.
- Aldana, M., Laredo, E., Bello, A., Suarez, N., 1994. Direct signal analysis applied to the determination of the relaxation parameters from TSDC spectra of polymers. *J. Polym. Sci. , Part B: Polym. Phys.* 32, 2197-2206.
- Allgayer, H., Sonnenbichler, J., Kruis, W., Paumgartner, G., 1985. Determination of the pK values of 5-aminosalicylic acid and N-acetylaminosalicylic acid and comparison of the pH dependent lipid-water partition-coefficients of sulphasalazine and its metabolites. *Arzneimittel-Forschung/Drug Research*, 35-2, 1457-1459.
- Amidon, G.L., Lennernas, H., Shah, V.P., Crison, J.R., 1995. A theoretical basis for a biopharmaceutic drug classification - the correlation of in-vitro drug product dissolution and in-vivo bioavailability. *Pharm. Res.*, 12, 413-420.
- Anderson, S.L., Grulke, E.A., Delassus, P.T., Smith, P.B., Kocher, C.W., Landes, B.G., 1995. A Model for Antiplasticization in Polystyrene. *Macromolecules*, 28, 2944-2954.

Ardizzone, S., Porro, G.B., 2002. Inflammatory bowel disease: new insights into pathogenesis and treatment. *J. Intern. Med.*, 252, 475-496.

Arwidsson, H.G., Rudén, M., 1993. Film coating by the spray process. In: Sandell, E. (Ed.), *Industrial aspects of pharmaceuticals*, Swedish Pharmaceutical Press, Stockholm, 212-226.

Ashford, M., Fell, J.T., Attwood, D., Sharma, H., Woodhead, P.J., 1993. An in-vivo investigation into the suitability of pH dependent polymers for colonic targeting. *Int. J. Pharm.*, 95, 193-199.

Ashford, M., Fell, J.T., Attwood, D., Woodhead, P.J., 1993. An in-vitro investigation into the suitability of pH dependent polymers for colonic targeting. *Int. J. Pharm.*, 91, 241-245.

Atkins, T.W., Peacock, S.J., 1997. In vitro biodegradation of polyhydroxybutyrate-hydroxyvalerate microcapsules exposed to Hank's buffer, newborn calf serum, pancreatin and synthetic gastric juice. *J. Microencapsul.*, 14, 35-49.

Aulton, M.E., Abdulrazzak, M.H., Hogan, J.E., 1981. The mechanical properties of hydroxypropylmethylcellulose films derived from aqueous systems .1. The influence of plasticizers. *Drug Dev. Ind. Pharm.*, 7, 649-668.

Aulton, M.E., Richards, J.H., Abdul-Razzak, M.H., Hogan, J.E., 1983. Migration of active ingredients between film coats and tablet cores. *Proc. Third. Int. Conf. Pharm. Technol.*, III, Paris, 154-162.

Aunins, J.G., Southard, M.Z., Myers, R.A., Himmelstein, K.J., Stella, V.J., 1985. Dissolution of carboxylic acids .3. The effect of polyionizable buffers. *J. Pharm. Sci.*, 74, 1305-1316.

Azadkhan, A.K., Howes, D.T., Piris, J., Truelove, S.C., 1980. Optimum dose of sulphasalazine for maintenance treatment in ulcerative colitis. *Gut*, 21, 232-240.

Azadkhan, A.K., Piris, J., Truelove, S.C., 1977. Experiment to determine active therapeutic moiety of sulfasalazine. *Lancet*, 2, 892-895.

Bando, H., McGinity, J.W., 2006. Physicochemical properties of enteric films prepared from aqueous dispersions and organic solutions. *Int. J. Pharm.*, 313, 43-48.

Banker, G.S., 1966. Film coating theory and practice. *J. Pharm. Sci.*, 55, 81-89.

Banwell, J.G., Gorbach, S.L., Pierce, N.F., Mitra, R., Mondal, A., 1971. Acute undifferentiated human diarrhea in tropics .2. Alterations in intestinal fluid and electrolyte movements. *J. Clin. Invest.*, 50, 890-900.

Basilico, G., Phillips, S. F., 1993. The small bowel and ileocaecal region. In: Kumar, D., Wingate, D. (Eds.), *An illustrated guide to gastrointestinal motility*, Churchill Livingstone, Edingburgh, 410-426.

Basit, A.W., 2005. Advances in colonic drug delivery. *Drugs*, 65, 1991-2007.

Basit, A.W., Podczeck, F., Newton, J.M., Waddington, W.A., Ell, P.J., Lacey, L.F., 2004. The use of formulation technology to assess regional gastrointestinal drug absorption in humans. *Eur. J. Pharm. Sci.*, 21, 179-189.

Bassotti, G., Crowell, M.D., Whitehead, W.E., 1993. Contractile Activity of the Human Colon - Lessons from 24 Hour Studies. *Gut*, 34, 129-133.

Bauer, K.H., Lehmann, K., Osterwald, H. P., Rothgang, G., 1998. Equipment for sugar coating and film coating processes. In: *Coated pharmaceutical dosage forms: fundamentals, manufacturing techniques, biopharmaceutical aspects, test methods and raw materials*, CRC Press, Boca Raton, 153-181.

Bender, M.L., Brubacher, L. J., 1973. Catalysis involving acids and bases. In: Bender, M.L., Brubacher, L.J. (Eds.), *Catalysis and enzyme action*, McGraw-Hill Book Company, New York, 40-65.

Berggren, S., Lennernas, P., Ekelund, M., Westrom, B., Hoogstraate, J., Lennernas, H., 2003. Regional transport and metabolism of roivacaine and its CYP3A4 metabolite PPX in human intestine. *J. Pharm. Pharmacol.*, 55, 963-972.

Birnie, G.G., Mcleod, T.I.F., Watkinson, G., 1981. Incidence of sulfasalazine-induced male-infertility. *Gut*, 22, 452-455.

Blanquet, S., Zeijdner, E., Beyssac, E., Meunier, J.P., Denis, S., Havenaar, R., Alric, M., 2004. A dynamic artificial gastrointestinal system for studying the behavior of orally administered drug dosage forms under various physiological conditions. *Pharm. Res.*, 21, 585-591.

British Medical Association. 2007. *British National Formulary*. 53rd Ed., BMJ and RPS, London.

Bucci, C., Fieschi, R., 1964. Ionic thermoconductivity. Method for the investigation of polarisation in insulators. *Phys. Rev. Lett.*, 12, 16-19.

Buckton, G., 1995. Interfacial phenomena in drug delivery and targeting. Harwood Academic, Chur, Switzerland.

Bueno, L., Fioramonti, J., 1993. Food and gastrointestinal motility. In: Kumar, D., Wingate, D. (Eds.), *An illustrated guide to gastrointestinal motility*, Churchill Livingstone, New York, 130-144.

Bueno, L., Fioramonti, J., Ruckebusch, Y., 1975. Rate of flow of digesta and electrical activity of small-Intestine in dogs and sheep. *J. Physiol. - London*, 249, 69-85.

Bueno, L., Praddaude, F., Fioramonti, J., Ruckebusch, Y., 1981. Effect of dietary fiber on gastrointestinal motility and jejunal transit-time in dogs. *Gastroenterology*, 80, 701-707.

Cameron, C.G., McGinity, J.W., 1987. Controlled-release theophylline tablet formulations containing acrylic resins .3. Influence of filler excipient. *Drug Dev. Ind. Pharm.*, 13, 303-318.

Campagna, F.A., Cureton, G., Mirigian, R.A., Nelson, E., 1963. Inactive prednisolone tablets USP XVI. *J. Pharm. Sci.*, 52, 605-606.

Carter, M.J., Lobo, A.J., Travis, S.P.L., 2004. Guidelines for the management of inflammatory bowel disease in adults. *Gut*, 53.

Chan, R.P., Pope, D.J., Gilbert, A.P., Sacra, P.J., Baron, J.H., Lennardjones, J.E., 1983. Studies of 2 novel sulfasalazine analogs, ipsalazide and balsalazide. *Dig. Dis. Sci.*, 28, 609-615.

Chan, W.A., Boswell, C.D., Zhang, Z., 2001. Comparison of the release profiles of a water soluble drug carried by Eudragit-coated capsules in different in-vitro dissolution liquids. *Powder Technol.*, 119, 26-32.

Charman, W.N., Porter, C.J.H., Mithani, S., Dressman, J.B., 1997. Physicochemical and physiological mechanisms for the effects of food on drug absorption: The role of lipids and pH. *J. Pharm. Sci.*, 86, 269-282.

Chartoff, R.P., 1997. Thermoplastic polymers. In: Turi, E.A. (Ed.), *Thermal characterisation of polymeric materials*. Vol. 1. Academic Press, New York, 483-743.

Christensen, L.A., 2000. 5-aminosalicylic acid containing drugs - Delivery, fate, and possible clinical implications in man. *Dan. Med. Bull.*, 47, 20-41.

Chung, G.C., Kornfield, J.A., Smith, S.D., 1994. Compositional dependence of segmental dynamics in a miscible polymer blend. *Macromolecules*, 27, 5729-5741.

Chuong, M., Christensen, J., and Corvallis, O., 2006. Deconvolution of mesalamine delayed release tablet and extended release capsule to relate absorption time to absorption site. *AAPS J* 8[S2].

Clarke, A.M., Chirnside, A., Hill, G.L., Pope, G., Stewart, M.K., 1967. Chronic dehydration and sodium depletion in patients with established ileostomies. *Lancet*, 2, 740-743.

Clemett, D., Markham, A., 2000. Prolonged-release mesalazine - A review of its therapeutic potential in ulcerative colitis and Crohn's disease. *Drugs*, 59, 929-956.

Code, C.F., Marlett, J.A., 1975. Interdigestive myo-electric complex of stomach and small bowel of dogs. *J. Physiol. - London*, 246, 289-309.

Cohen, R.D., Woseth, D.M., Thisted, R.A., Hanauer, S.B., 2000. A meta-analysis and overview of the literature on treatment options for left-sided ulcerative colitis and ulcerative proctitis. *Am. J. Gastroenterol.*, 95, 1263-1276.

Cole, G., Hogan, J.E., Aulton, M.E., 1995. Pharmaceutical coating technology. Taylor and Francis, London.

Coupe, A.J., Davis, S.S., Evans, D.F., Wilding, I.R., 1993. Do pellet formulations empty from the stomach with food? *Int. J. Pharm.*, 92, 167-175.

Cummings, J.H., 1995. A new look at dietary carbohydrates. *MRC News*, Autumn, 36-40.

Cummings, J.H., Banwell, J.G., Segal, I., Coleman, N., Englyst, H.N., and Macfarlane, G.T., 1990. The amount and composition of large bowel contents in man. *Gastroenterology* 98, A408.

Cummings, J.H., Macfarlane, G. T., Drasar, B. S., 1989. The gut microflora and its significance. In: Whitehead, R. (Ed.), *Gastrointestinal and oesophageal pathology*, Churchill Livingstone, Edinburgh, 201-219.

Cummings, J.H., Milojevic, S., Harding, M., Coward, W.A., Gibson, G.R., Botham, R.L., Ring, S.G., Wraight, E.P., Stockham, M.A., Allwood, M.C., Newton, J.M., 1996. In vivo studies of amylose- and ethylcellulose-coated [C-13]glucose microspheres as a model for drug delivery to the colon. *J. Controlled Release*, 40, 123-131.

D'Haens, G., 2006. The practical use of steroids in inflammatory bowel diseases. In: Blumberg, R.S., Gangl, A., Manns, M.P., Tilg, H., Zeitz, M. (Eds.), *Gut-liver interactions: basic and clinical concepts*, Springer, Dordrecht, Netherlands, 62-66.

Das, K.M., Eastwood, M.A., Mcmanus, J.P.A., Sircus, W., 1973a. Metabolism of salicylazosulphapyridine in ulcerative colitis .1. Relationship between metabolites and response to treatment in in-patients. *Gut*, 14, 631-641.

Das, K.M., Eastwood, M.A., Mcmanus, J.P.A., Sircus, W., 1973b. Metabolism of salicylazosulphapyridine in ulcerative colitis .2. Relationship between metabolites and progress of disease studied in outpatients. *Gut*, 14, 637-641.

Davis, S.S., Hardy, J.G., Fara, J.W., 1986. Transit of pharmaceutical dosage forms through the small-intestine. *Gut*, 27, 886-892.

Dawson, P.A., Shneider, B. L., Hofman, A. F., 2006. Bile formation and the enterohepatic circulation. In: Johnson, L.R., Barrett, K.E., Ghishan, F.K., Merchant, J.L., Said, H.M., Wood, J.D. (Eds.), *Physiology of the gastrointestinal tract*, Elsevier Academic Press, Burlington,MA, 1437-1462.

Devos, M., Verdievil, H., Schoonjans, R., Praet, M., Bogaert, M., Barbier, F., 1992. Concentrations of 5-Asa and Ac-5-Asa in human ileocolonic biopsy homogenates after oral 5-ASA preparations. *Gut*, 33, 1338-1342.

Dew, M.J., Hughes, P.J., Lee, M.G., Evans, B.K., Rhodes, J., 1982. An oral preparation to release drugs in the human colon. *Br. J. Clin. Pharmacol.*, 14, 405-408.

Dittgen, M., Durrani, M., Lehmann, K., 1997. Acrylic polymers - A review of pharmaceutical applications. *STP Pharma Sci.*, 7, 403-437.

Dozois, R.R., Kelly, K., 2000. The surgical management of ulcerative colitis. In: Kirsner, J. (Ed.), *Inflammatory bowel diseases*, W.B.Saunders, Philadelphia, 626-657.

Dressman, J.B., Amidon, G.L., 1984. Radiotelemetric method for evaluating enteric coatings in vivo. *J. Pharm. Sci.*, 73, 935-938.

Dressman, J.B., Amidon, G.L., Reppas, C., Shah, V.P., 1998. Dissolution testing as a prognostic tool for oral drug absorption: immediate release dosage forms. *Pharm. Res.*, 15, 11-22.

Dressman, J.B., Berardi, R.R., Dermentzoglou, L.C., Russell, T.L., Schmaltz, S.P., Barnett, J.L., Jarvenpaa, K.M., 1990. Upper gastrointestinal (GI) pH in young, healthy-men and women. *Pharm. Res.*, 7, 756-761.

Ebel, J.P., Jay, M., Beihn, R.M., 1993. An in-vitro in-vivo correlation for the disintegration and onset of drug release from enteric-coated pellets. *Pharm. Res.*, 10, 233-238.

Edelman, I.S., Sweet, N.J., 1956. Gastrointestinal water and electrolytes. I. The equilibration of radiosodium in gastrointestinal contents and the proportion of exchangeable sodium (Na_e) in the gastrointestinal tract. *J. Clin. Invest.*, 35, 502-511.

Edsbacker, S., Bengtsson, B., Larsson, P., Lundin, P., Nilsson, A., Ulmius, J., Wollmer, P., 2003. A pharmacoscintigraphic evaluation of oral budesonide given as controlled-release (Entocort) capsules. *Aliment. Pharmacol. Ther.*, 17, 525-536.

Edwards, C., 1997. Physiology of the colorectal barrier. *Adv. Drug Deliv. Rev.*, 28, 173-190.

Efentakis, M., Dressman, J.B., 1998. Gastric juice as a dissolution medium: Surface tension and pH. *Eur. J. Drug Metab. Pharmacokinet.*, 23, 97-102.

Ellis, P.R., Rayment, P., Wang, Q., 1996. A physico-chemical perspective of plant polysaccharides in relation to glucose absorption, insulin secretion and the entero-insular axis. *Proc. Nutr. Soc.*, 55, 881-898.

Ellis, P.R., Wang, Q., Rayment, P., Ren, Y., Ross-Murphy, S. B., 2001. Guar gum. Agricultural and botanical aspects, physicochemical and nutrition properties, and its use in the development of functional foods. In: Sungsoo Cho, S., Dreher, M.L. (Eds.), *Handbook of dietary fiber*, Marcel Dekker, New York, 613-657.

Evans, D.F., Pye, G., Bramley, R., Clark, A.G., Dyson, T.J., Hardcastle, J.D., 1988. Measurement of gastrointestinal pH profiles in normal ambulant human subjects. *Gut*, 29, 1035-1041.

Faigle, J.W., 1993. Drug metabolism in the colon wall and lumen. In: Bieck, P.R. (Ed.), *Colonic drug absorption and metabolism*, Marcel Dekker, New York, 29-54.

Fallingborg, J., Christensen, L.A., Ingeman-Nielsen, M., Jacobsen, B.A., Abildgaard, K., Rasmussen, H.H., 1989. pH-profile and regional transit times of the normal gut measured by a radiotelemetry device. *Aliment. Pharmacol. Ther.*, 3, 605-613.

Fallingborg, J., Christensen, L.A., Jacobsen, B.A., Rasmussen, S.N., 1993. Very low intraluminal colonic pH in patients with active ulcerative colitis. *Dig. Dis. Sci.*, 38, 1989-1993.

Farthing, M.J.G., Rutland, M.D., Clark, M.L., 1979. Retrograde spread of hydrocortisone containing foam given intra-rectally in ulcerative-colitis. *Br. Med. J.*, 2, 822-824.

Felton, L.A., McGinity, J.W., 2002. Influence of insoluble excipients on film coating systems. *Drug Dev. Ind. Pharm.*, 28, 225-243.

Florence, A.T., Attwood, D., 1998. Physicochemical properties of drugs in solution. In: *Physicochemical principles of pharmacy*, Macmillan, Basingstoke, 56-100.

Fockens, P., Mulder, C.J.J., Tytgat, G.N.J., Blok, P., Ferwerda, J., Meuwissen, S.G., Tuynman, H.A.R.E., Dekker, W., vanHees, P.A.M., Schrijver, M., vanHogezand, R.A., vanOlffen, G.H., Breed, J.G.S., vanderHeide, H., Cozijin, D., 1995. Comparison of the efficacy and safety of 1.5 compared with 3.0 g oral slow-release mesalazine (Pentasa) in the maintenance treatment of ulcerative colitis. *Eur. J. Gastroenterol. Hepatol.*, 7, 1025-1030.

Forbes, A., Cartwright, A., Marchant, S., McIntyre, P., Newton, M., 2003. Review article: oral, modified-release mesalazine formulations - proprietary versus generic. *Aliment. Pharmacol. Ther.*, 17, 1207-1214.

Fordtran, J.S., Dietschy, J.M., 1966. Water and electrolyte movement in the intestine. *Gastroenterology*, 50, 263-285.

Fordtran, J.S., Ingelfinger, F. J., 1968. Absorption of water, electrolytes, and sugars from the human gut. In: Code, C.F. (Ed.), *Handbook of physiology. Section 6: Alimentary canal. Vol.3 Intestinal Absorption*, American Physiology Society, Washington D.C., 1457-1490.

Fordtran, J.S., Locklear, T.W., 1966. Ionic constituents and osmolarity of gastric and small-intestinal fluids after eating. *Am. J. Dig. Diseases*, 7, 503-521.

Fordtran, J.S., Rector, F.C., Jr., Ewton, M.F., Soter, N., Kinney, J., 1965. Permeability characteristics of the human small intestine. *J. Clin. Invest*, 44, 1935-1944.

French, D.L., Mauger, J.W., 1993. Evaluation of the Physicochemical Properties and Dissolution Characteristics of Mesalamine - Relevance to Controlled Intestinal Drug-Delivery. *Pharmaceutical Research*, 10, 1285-1290.

Galia, E., Nicolaidis, E., Horter, D., Lobenberg, R., Reppas, C., Dressman, J.B., 1998. Evaluation of various dissolution media for predicting in vivo performance of class I and II drugs. *Pharm. Res.*, 15, 698-705.

Georgoussis, G., Kyritsis, A., Bershtein, V.A., Fainleib, A.M., Pissis, P., 2000. Dielectric studies of chain dynamics in homogeneous semi-interpenetrating polymer networks. *J. Polym. Sci. , Part B: Polym. Phys.*, 38, 3070-3087.

Gibson, S.A.W., Mcfarlan, C., Hay, S., Macfarlane, G.T., 1989. Significance of microflora in proteolysis in the colon. *Appl. Environ. Microbiol.*, 55, 679-683.

Gotch, F., Nadell, J., Edelman, I.S., 1957. Gastrointestinal water and electrolytes. IV. The equilibration of deuterium oxide (D₂O) in gastrointestinal contents and the proportion of total body water (T.B.W.) in the gastrointestinal tract. *J. Clin. Invest.*, 36, 289-296.

Goto, T., Tanida, N., Yoshinaga, T., Sato, S., Ball, D.J., Wilding, I.R., Kobayashi, E., Fujimura, A., 2004. Pharmaceutical design of a novel colon-targeted delivery system using two-layer-coated tablets of three different pharmaceutical formulations, supported by clinical evidence in humans. *J. Controlled Release*, 97, 31-42.

Gutierrez-Rocca, J.C., McGinity, J.W., 1994. Influence of water-soluble and insoluble plasticizers on the physical and mechanical properties of acrylic resin copolymers. *Int. J. Pharm.*, 103, 293-301.

Hanauer, S.B., Sandborn, W.J., Kornbluth, A., Katz, S., Safdi, M., Woogen, S., Regalli, G., Yeh, C., Smith-Hall, N., Ajayi, F., 2005. Delayed-release oral mesalamine at 4.8 g/day (800 mg tablet) for the treatment of moderately active ulcerative colitis: The ASCEND II trial. *Am. J. Gastroenterol.*, 100, 2478-2485.

Hanauer, S.B., Strömberg, U., 2004. Oral Pentasa in the treatment of active Crohn's disease: a meta-analysis of double-blind, placebo-controlled trials. *Clin. Gastroenterol. Hepatol.*, 2, 388.

Hjartstam, J., Hjertberg, T., 1999. Effect of hydroxyl group content in ethyl cellulose on permeability in free films and coated membranes. *J. Appl. Polym. Sci.*, 72, 529-535.

- Hofmann, A.F., 1993. The enterohepatic circulation of bile acids in health and disease. In: Sleisenger, M.H., Fordtran, J.S. (Eds.), *Gastrointestinal disease, pathophysiology, diagnosis, management*, W.B.Saunders Co., Philadelphia, 127-150.
- Höhne, G.W.H., Hemminger, W.F., Flammersheim, H.-J..2003. *Differential scanning calorimetry*. Second Ed., Springer, Berlin.
- Horter, D., Dressman, J.B., 2001. Influence of physicochemical properties on dissolution of drugs in the gastrointestinal tract. *Adv. Drug Deliv. Rev.*, 46, 75-87.
- Ibekwe, V.C., Fadda, H.M., Khela, M.K., Evans, D.F., Parsons, G.E., Basit, A.W., 2007. Drug delivery systems for treating inflammatory bowel diseases: The extent to which gastrointestinal pH influences drug release from enteric coated products. *Gut*, 56, A39.
- Ibekwe, V.C., Fadda, H.M., Parsons, G.E., Basit, A.W., 2006a. A comparative in vitro assessment of the drug release performance of pH-responsive polymers for ileo-colonic delivery. *Int. J. Pharm.*, 308, 52-60.
- Ibekwe, V.C., Liu, F., Fadda, H.M., Khela, M.K., Evans, D.F., Parsons, G.E., Basit, A.W., 2006b. An investigation into the in vivo performance variability of pH responsive polymers for ileo-colonic drug delivery using gamma scintigraphy in humans. *J. Pharm. Sci.*, 95, 2760-2766.
- Ivax Pharmaceuticals, 2003. Interchangeability of oral mesalazines. *Pharm. J.*, 271, A8-A9.
- Jenquin, M.R., Sarabia, R.E., Liebowitz, S.M., McGinity, J.W., 1992. Relationship of film properties to drug release from monolithic films containing adjuvants. *J. Pharm. Sci.*, 81, 983-989.
- Jin, S.P., Liu, M.Z., Chen, S.L., Chen, Y., 2005. Complexation between poly(acrylic acid) and poly(vinylpyrrolidone): Influence of the molecular weight of poly(acrylic acid) and small molecule salt on the complexation. *Eur. Polym. J.*, 41, 2406-2415.
- Jones, D.S., 1999. Dynamic mechanical analysis of polymeric systems of pharmaceutical and biomedical significance. *Int. J. Pharm.*, 179, 167-178.
- Kaczmarek, H., Szalla, A., Kaminska, A., 2001. Study of poly(acrylic acid)-poly(vinylpyrrolidone) complexes and their photostability. *Polymer*, 42, 6057-6069.

Kalantzi, L., Goumas, K., Kalioras, V., Abrahamsson, B., Dressman, J.B., Reppas, C., 2006a. Characterization of the human upper gastrointestinal contents under conditions simulating bioavailability/bioequivalence studies. *Pharm. Res.*, 23, 165-176.

Kalantzi, L., Persson, E., Polentarutti, B., Abrahamsson, B., Goumas, K., Dressman, J.B., Reppas, C., 2006b. Canine intestinal contents vs. simulated media for the assessment of solubility of two weak bases in the human small intestinal contents. *Pharm. Res.*, 23, 1373-1381.

Kamba, M., Seta, Y., Kusai, A., Nishimura, K., 2001. Evaluation of the mechanical destructive force in the stomach of dog. *Int. J. Pharm.*, 228, 209-217.

Kanaghinis, T., Lubran, M., Coghill, N.F., 1963. The composition of ileostomy fluid. *Gut*, 4, 322-338.

Kararli, T.T., Kirchoff, C.F., Truelove, J.E., 1995. Ionic strength dependence of dissolution for Eudragit S-100 coated pellets. *Pharm. Res.*, 12, 1813-1816.

Kasim, N.A., Whitehouse, M., Ramachandran, C., Bermejo, M., Lennernas, H., Hussain, A.S., Junginger, H.E., Stavchansky, S.A., Midha, K.K., Shah, V.P., Amidon, G.L., 2004. Molecular properties of WHO essential drugs and provisional biopharmaceutical classification. *Mol. Pharm.*, 1, 85-96.

Keighley, M.R., Williams, N. S., 1999. Ileostomy. In: Keighley, M.R., Williams, N.S. (Eds.), *Surgery of anus, rectum and colon*, W.B.Saunders, London, 190-257.

Kellow, J.E., Borody, T.J., Phillips, S.F., Tucker, R.L., Haddad, A.C., 1986. Human interdigestive motility - variations in patterns from oesophagus to colon. *Gastroenterology*, 91, 386-395.

Kendall, R.A., Basit, A. W., 2006. The role of polymers in solid oral dosage forms. In: Uchegbu, I.F., Schätzlein, A.G. (Eds.), *Polymers in drug delivery*, CRC Press, Boca Raton, 35-48.

Khosla, R., Feely, L.C., Davis, S.S., 1989. Gastrointestinal transit of non-disintegrating tablets in fed subjects. *Int. J. Pharm.*, 53, 107-117.

Kirkpatrick, A., 1940. Some relations between molecular structure and plasticizing effect. *J. Appl. Phys.*, 11, 255-261.

- Klein, S., Stein, J., Dressman, J., 2005. Site-specific delivery of anti-inflammatory drugs in the gastrointestinal tract: an in-vitro release model. *J. Pharm. Pharmacol.*, 57, 709-719.
- Klotz, U., Schwab, M., 2005. Topical delivery of therapeutic agents in the treatment of inflammatory bowel disease. *Adv. Drug. Deliv. Rev.*, 57, 267-279.
- Knutson, L., Odland, B., Hallgren, R., 1989. A new technique for segmental jejunal perfusion in man. *Am. J. Gastroenterol.*, 84, 1278-1284.
- Kornbluth, A., Sachar, D.B., 2004. Ulcerative colitis practice guidelines in adults (update): American College of Gastroenterology, Practice Parameters Committee. *Am. J. Gastroenterol.*, 99, 1371-1385.
- Krämer, J., Grady, L. T., Gajendran, J., 2005. Historical development of dissolution testing. In: Dressman, J.B., Krämer, J. (Eds.), *Pharmaceutical dissolution testing*, Taylor and Francis, Boca Raton, 1-38.
- Krause, S., Mcneil, C.J., Armstrong, R.D., Ho, W.O., 1997. Behaviour of pH sensitive polymers on metal electrodes. *J. Appl. Electrochem.*, 27, 291-298.
- Ladas, S.D., Isaacs, P.E., Murphy, G.M., Sladen, G.E., 1984. Comparison of the effects of medium and long chain triglyceride containing liquid meals on gall bladder and small intestinal function in normal man. *Gut*, 25, 405-411.
- Ladas, S.D., Isaacs, P.E., Murphy, G.M., Sladen, G.E., 1986. Fasting and postprandial ileal function in adapted ileostomates and normal subjects. *Gut*, 27, 906-912.
- Lafferty, S.V., Newton, J.M., Podczek, F., 2002. Dynamic mechanical thermal analysis studies of polymer films prepared from aqueous dispersion. *Int. J. Pharm.*, 235, 107-111.
- Lapidus, H., Lordi, N.G., 1968. Drug release from compressed hydrophilic matrices. *J. Pharm. Sci.*, 57, 1292-1301.
- Laredo, E., Puma, M., Suarez, N., Figueroa, D.R., 1981. Analysis of the ionic thermal current peaks with a distribution in the reorientation energy. *Physical Review B*, 23, 3009-3016.
- Larsen, G.L., Henson, P.M., 1983. Mediators of inflammation. *Annu. Rev. Immunol.*, 1, 335-359.

Layer, P.H., Goebell, H., Keller, J., Dignass, A., Klotz, U., 1995. Delivery and fate of oral mesalamine microgranules within the human small intestine. *Gastroenterology*, 108, 1427-1433.

Lecomte, F., Siepmann, J., Walther, M., Macrae, R.J., Bodmeier, R., 2004. Polymer blends used for the aqueous coating of solid dosage forms: importance of the type of plasticizer. *J. Controlled Release*, 99, 1-13.

Lee, D.A.H., Taylor, M., James, V.H.T., Walker, G., 1980. Rectally administered prednisolone-evidence for a predominantly local action. *Gut*, 21, 215-218.

Lentner, C., 1984. Buffer solutions. In: Geigy scientific tables. Vol.3 Physical Chemistry; Composition of blood; Haematology and Somatometric data, Ciba-Geigy, Basle, 58-60.

Leroy, E., Alegria, A., Colmenero, J., 2002. Quantitative study of chain connectivity inducing effective glass transition temperatures in miscible polymer blends. *Macromolecules*, 35, 5587-5590.

Levis, K.A., Lane, M.E., Corrigan, O.I., 2003. Effect of buffer media composition on the solubility and effective permeability coefficient of ibuprofen. *Int. J. Pharm.*, 253, 49-59.

Levy, G., 1964. Effect of dosage form properties on therapeutic efficacy of tolbutamide tablets. *Can. Med. Assoc. J.*, 90, 978-979.

Lim, W.-C., Hanauer, S.B., 2004. Controversies with aminosalicylates in inflammatory bowel disease. *Rev. Gastroenterol. Disord.*, 4, 104-117.

Lindahl, A., Ungell, A.L., Knutson, L., Lennernas, H., 1997. Characterization of fluids from the stomach and proximal jejunum in men and women. *Pharm. Res.*, 14, 497-502.

Liu, F., Basit, A.W., Lizio, R., Petereit, H.U., Meier, C., and Damm, M., 2007. Solid dosage forms comprising an enteric coating with accelerated drug release. PCT/EP2007/054398.

Lockhart-Mummery, H.E., Morson, M.C., 1960. Crohn's disease (regional enteritis) of the large intestine and its distinction from ulcerative colitis. *Gut*, 1, 87-105.

Lodge, T.P., Mcleish, T.C.B., 2000. Self-concentrations and effective glass transition temperatures in polymer blends. *Macromolecules*, 33, 5278-5284.

- Loftus, E.V., 2004. Clinical epidemiology of inflammatory bowel disease: Incidence, prevalence, and environmental influences. *Gastroenterology*, 126, 1504-1517.
- Lund, W., 1994. The Pharmaceutical Codex: Principles and Practice of Pharmaceutics. 12th Ed., Pharmaceutical Press, London.
- Macfarlane, G.T., Englyst, H.N., 1986. Starch utilization by the human large intestinal microflora. *J. Appl. Bacteriol.*, 60, 195-201.
- Machatha, S.G., Yalkowsky, S.H., 2005. Comparison of the octanol/water partition coefficients calculated by ClogP((R)), ACDlogP and KowWin((R)) to experimentally determined values. *Int. J. Pharm.*, 294, 185-192.
- Malagelada, J.R., Longstreth, G.F., Summerskill, W.H.J., Go, V.L.W., 1976. Measurement of gastric functions during digestion of ordinary solid meals in man. *Gastroenterology*, 70, 203-210.
- Malchow, H., Ewe, K., Brandes, J.W., Goebell, H., Ehms, H., Sommer, H., Jesdinsky, H., 1984. European Cooperative Crohns-Disease Study (ECCDS) - results of drug treatment. *Gastroenterology*, 86, 249-266.
- Marcilla, A., Beltrán, M., 2004. Mechanisms of plasticizer action. In: Wypych, G. (Ed.), Handbook of plasticizers, ChemTec Publishing, Toronto, 106-125.
- Marteau, P., Probert, C.S., Lindgren, S., Gassul, M., Tan, T.G., Dignass, A., Befrits, R., Midhagen, G., Rademaker, J., Foldager, M., 2005. Combined oral and enema treatment with Pentasa (mesalazine) is superior to oral therapy alone in patients with extensive mild/moderate active ulcerative colitis: a randomised, double blind, placebo controlled study. *Gut*, 54, 960-965.
- Martin, A., 1993a. Buffered and Isotonic Solutions. In: Physical Pharmacy, Lippincott Williams and Wilkins, Baltimore, 169-190.
- Martin, A., 1993b. Diffusion and dissolution. In: Physical Pharmacy, Lippincott Williams and Wilkins, Baltimore, 324-361.
- Mathew, A.P., Dufresne, A., 2002. Plasticized waxy maize starch: Effect of polyols and relative humidity on material properties. *Biomacromolecules*, 3, 1101-1108.
- Matsuoka, S., Ishida, Y., 1966. Multiple transitions in polycarbonate. *J. Polym. Sci. , Part C: Polym. Symp.*, 14, 247-259.

- McCrum, N.G., Read, B.E., Williams, G., 1991. Anelastic and dielectric effects in polymeric solids. Dover, New York.
- McNamara, D.P., Whitney, K.M., Goss, S.L., 2003. Use of a physiologic bicarbonate buffer system for dissolution characterization of ionizable drugs. *Pharm. Res.*, 20, 1641-1646.
- McNeil, N.I., Bingham, S., Cole, T.J., Grant, A.M., Cummings, J.H., 1982. Diet and health of people with an ileostomy. 2. Ileostomy function and nutritional state. *Br. J. Nutr.*, 47, 407-415.
- Metcalf, A.M., Phillips, S.F., Zinsmeister, A.R., MacCarty, R.L., Beart, R.W., Wolff, B.G., 1987. Simplified assessment of segmental colonic transit. *Gastroenterology*, 92, 47.
- Meyers, S., Janowitz, H.D., 1989. The natural history of ulcerative colitis - an analysis of the placebo-response. *J. Clin. Gastroenterol.*, 11, 33-37.
- Mithani, S.D., Bakatselou, V., Tenhoor, C.N., Dressman, J.B., 1996. Estimation of the increase in solubility of drugs as a function of bile salt concentration. *Pharm. Res.*, 13, 163-167.
- Mooney, K.G., Mintun, M.A., Himmelstein, K.J., Stella, V.J., 1981. Dissolution kinetics of carboxylic acids .2. Effect of buffers. *J. Pharm. Sci.*, 70, 22-32.
- Moorshead, T.C., 1962. Some thoughts on PVC plasticization. In: Kaufman, M. (Ed.), *Advances in PVC compounding and processing*, Maclaren, London, 20-31.
- Myers, B., Evans, D.N.W., Rhodes, J., Evans, B.K., Hughes, B.R., Lee, M.G., Richens, A., Richards, D., 1987. Metabolism and urinary-excretion of 5-aminosalicylic acid in healthy volunteers when given intravenously or released for absorption at different sites in the gastrointestinal tract. *Gut*, 28, 196-200.
- Nakamura, T., Sakaeda, T., Ohmoto, N., Tamura, T., Aoyama, N., Shirakawa, T., Kamigaki, T., Nakamura, T., Kim, K.I., Kim, S.R., Kuroda, Y., Matsuo, M., Kasuga, M., Okumura, K., 2002. Real-time quantitative polymerase chain reaction for MDR1, MRP1, MRP2, and CYP3A-mRNA levels in Caco-2 cell lines, human duodenal enterocytes, normal colorectal tissues, and colorectal adenocarcinomas. *Drug Metab. Dispos.*, 30, 4-6.

National library of medicine., 2007. ChemIDplus Lite.
<http://chem.sis.nlm.nih.gov/chemidplus> .

Naylor, L.J., Bakatselou, V., Dressman, J.B., 1993. Comparison of the mechanism of dissolution of hydrocortisone in simple and mixed micelle systems. *Pharm. Res.*, 10, 865-870.

Ngai, K.L., Rendell, R.W., Yee, A.F., Plazek, D.J., 1991. Antiplasticization effects on a secondary relaxation in plasticized glassy polycarbonates. *Macromolecules*, 24, 61-67.

Nguyen, D.A., Fogler, H.S., 2005. Facilitated diffusion in the dissolution of carboxylic polymers. *AIChE J.*, 51, 415-425.

Nicolaidis, E., Galia, E., Efthymiopoulos, C., Dressman, J.B., Reppas, C., 1999. Forecasting the in vivo performance of four low solubility drugs from their in vitro dissolution data. *Pharm. Res.*, 16, 1876-1882.

Northfield, T.C., Mccoll, I., 1973. Postprandial Concentrations of Free and Conjugated Bile-Acids Down Length of Normal Human Small-Intestine. *Gut*, 14, 513-518.

Nugent, S.G., Kumar, D., Rampton, D.S., Evans, D.F., 2001. Intestinal luminal pH in inflammatory bowel disease: possible determinants and implications for therapy with aminosalicylates and other drugs. *Gut*, 48, 571-577.

Nugent, S.G., Kumar, D., Rampton, D.S., Yazaki, E., Evans, D.F., 2000. Gut pH and transit time in ulcerative colitis appear sufficient for complete dissolution of pH-dependent 5-ASA-containing capsules. *Gut*, 46, A9.

Okhamafe, A.O., Iwebor, H.U., 1986. Moisture permeability mechanisms of some aqueous-based tablet film coatings containing soluble additives. *Proc. 4th Int. Conf. Pharm. Technol.*, V, Paris, 103-113.

Okhamafe, A.O., York, P., 1983. Analysis of the permeation and mechanical characteristics of some aqueous-based film coating systems. *J. Pharm. Pharmacol.*, 35, 409-415.

Okhamafe, A.O., York, P., 1985. Relationship between stress, interaction and the mechanical properties of some pigmented tablet coating films. *Drug Dev. Ind. Pharm.*, 11, 131-146.

Okhamafe, A.O., York, P., 1987. Interaction phenomena in pharmaceutical film coatings and testing methods. *Int. J. Pharm.*, 39, 1-21.

Okhamafe, A.O., York, P., 1988. Studies of interaction phenomena in aqueous based film coatings containing soluble additives using thermal-analysis techniques. *J. Pharm. Sci.*, 77, 438-443.

Okhamafe, A.O., York, P., 1989. Thermal characterization of drug/polymer and excipient/polymer interactions in some film coating formulation. *J. Pharm. Pharmacol.*, 41, 1-6.

Otley, A., Steinhart, A.H., 2005. Budesonide for induction of remission in Crohn's disease. *Cochrane Database of Systematic Reviews*.

Ozturk, S.S., Palsson, B.O., Donohoe, B., Dressman, J.B., 1988a. Kinetics of release from enteric coated tablets. *Pharm. Res.*, 5, 550-565.

Ozturk, S.S., Palsson, B.O., Dressman, J.B., 1988b. Dissolution of ionizable drugs in buffered and unbuffered solutions. *Pharm. Res.*, 5, 272-282.

Park, S.H., Choi, H.K., 2006. The effects of surfactants on the dissolution profiles of poorly water-soluble acidic drugs. *Int. J. Pharm.*, 321, 35-41.

Parker, G., Wilson, C.G., Hardy, J.G., 1988. The effect of capsule size and density on transit through the proximal colon. *J. Pharm. Pharmacol.*, 40, 376-377.

Pearnchob, N., Dashevsky, A., Bodmeier, R., 2004. Improvement in the disintegration of shellac-coated soft gelatin capsules in simulated intestinal fluid. *J. Controlled Release*, 94, 313-321.

Pedersen, B.L., Brondsted, H., Lennernas, H., Christensen, F.N., Mullertz, A., Kristensen, H.G., 2000a. Dissolution of hydrocortisone in human and simulated intestinal fluids. *Pharm. Res.*, 17, 183-189.

Pedersen, B.L., Mullertz, A., Brondsted, H., Kristensen, H.G., 2000b. A comparison of the solubility of danazol in human and simulated gastrointestinal fluids. *Pharm. Res.*, 17, 891-894.

Perrin, D.D., Dempsey, B., 1974. Practical limitations in the use of buffers. In: Buffers for pH and metal ion control, Chapman and Hall, London, 55-61.

Persson, E.M., Gustafsson, A.S., Carlsson, A.S., Nilsson, R.G., Knutson, L., Forsell, P., Hanisch, G., Lennernas, H., Abrahamsson, B., 2005. The effects of food on the dissolution of poorly soluble drugs in human and in model small intestinal fluids. *Pharm. Res.*, 22, 2141-2151.

Phillips, S.F., Giller, J., 1973. The contribution of the colon to electrolyte and water conservation in man. *J. Lab Clin. Med.*, 81, 733-746.

Phillips, S.F., Summerskill, W.H., 1966. Occlusion of the jejunum for intestinal perfusion in man. *Mayo Clin. Proc.*, 41, 224-231.

Phillips, S.F., Summerskill, W.H., 1967. Water and electrolyte transport during maintenance of isotonicity in human jejunum and ileum. *J. Lab Clin. Med.*, 70, 686-698.

Pickard, J.F., Rees, J.E., Iworthy, P.H., 1972. Water vapour permeability of poured and sprayed polymer films. *J. Pharm. Pharmacol.*, 24, Suppl:139P.

Porter, S.C., Ridgway, K., 1982. The permeability of enteric coatings and the dissolution rates of coated tablets. *J. Pharm. Pharmacol.*, 34, 5-8.

Puma, M., 1997. Phenomenological model to describe the glass transition relaxation peaks for depolarization current experiments. *Polym. adv. technol.*, 8, 39-43.

Raffin, F., Duru, C., Jacob, M., 1996. Permeability to hydrogen ions of an enteric coating polymer and interaction of film formulation factors. *Int. J. Pharm.*, 145, 247-252.

Raffin, F., Duru, C., Jacob, M., Sostat, P., Sandeaux, J., Sandeaux, R., Pourcelly, G., Gavach, C., 1995. Physicochemical characterization of the ionic permeability of an enteric coating polymer. *Int. J. Pharm.*, 120, 205-214.

Raimundo, A.H., Evans, D.F., Rogers, J., and Silk, D.B., 1992. Gastrointestinal pH profiles in ulcerative colitis. *Gastroenterology* 102.

Ramtoola, Z., Corrigan, O.I., 1989. Influence of the buffering capacity of the medium on the dissolution of drug-excipient mixtures. *Drug Dev. Ind. Pharm.*, 15, 2359-2374.

Rao, S.S.C., Read, N.W., Brown, C., Bruce, C., Holdsworth, C.D., 1987. Studies on the mechanism of bowel disturbance in ulcerative colitis. *Gastroenterology*, 93, 934-940.

Read, N.W., Miles, C.A., Fisher, D., Holgate, A.M., Kime, N.D., Mitchell, M.A., Reeve, A.M., Roche, T.B., Walker, M., 1980. Transit of a meal through the stomach, small intestine, and colon in normal subjects and its role in the pathogenesis of diarrhea. *Gastroenterology*, 79, 1276-1282.

Regueiro, M., Loftus, E.V., Steinhart, A.H., Cohen, R.D., 2006. Clinical guidelines for the medical management of left-sided ulcerative colitis and ulcerative proctitis: Summary statement. *Inflamm. Bowel Dis.*, 12, 972-978.

Reitmeier, R.J., Code, C.F., Orvis, A.L., 1957. Comparison of the rate of absorption of labeled sodium and water from upper small intestine of healthy human beings. *J. Appl. Physiol.*, 10, 256-260.

Rohm Pharma Polymers.2001. Practical courses in film coating of pharmaceutical dosage forms with Eudragit®. Degussa, Darmstadt.

Rohrs, B.R., Thamann, T.J., Gao, P., Stelzer, D.J., Bergren, M.S., Chao, R.S., 1999. Tablet dissolution affected by a moisture mediated solid-state interaction between drug and disintegrant. *Pharm. Res.*, 16, 1850-1856.

Rowe, R., Sheskey, P., Weller, P., 2003. Handbook of pharmaceutical excipients. 4th Ed., Pharmaceutical Press, London.

Rowe, R.C., 1978. Measurement of adhesion of film coatings to tablet surfaces - effect of tablet porosity, surface-roughness and film thickness. *J. Pharm. Pharmacol.*, 30, 343-346.

Rowland, M., Tozer, T.N., 1995. Clinical pharmacokinetics: concepts and applications. Williams and Wilkins, Baltimore.

Royall, P.G., Huang, C.Y., Tang, S.W.J., Duncan, J., Van-de-Velde, G., Brown, M.B., 2005. The development of DMA for the detection of amorphous content in pharmaceutical powdered materials. *Int. J. Pharm.*, 301, 181-191.

Rubin, G.P., Hungin, A.P.S., Kelly, P.J., Ling, J., 2000. Inflammatory bowel disease: epidemiology and management in an English general practice population. *Aliment. Pharmacol. Ther.*, 14, 1553-1559.

Rudolph, M.W., Klein, S., Beckert, T.E., Petereit, H., Dressman, J.B., 2001. A new 5-aminosalicylic acid multi-unit dosage form for the therapy of ulcerative colitis. *Eur. J. Pharm. Biopharm.*, 51, 183-190.

Sanchis, M.J., Calleja, R.D., Gargallo, L., Hormazabal, A., Radic, D., 1999. Relaxational study of poly(2-chlorocyclohexyl methacrylate) by thermally stimulated current, dielectric, and dynamic mechanical spectroscopy. *Macromolecules*, 32, 3457-3463.

Sandoz, 2003. Mesalazine as a treatment for ulcerative colitis. *Pharm. J.*, 270, A8-A9.

Schiller, C., Frohlich, C.P., Giessmann, T., Siegmund, W., Monnikes, H., Hosten, N., Weitschies, W., 2005. Intestinal fluid volumes and transit of dosage forms as assessed by magnetic resonance imaging. *Aliment. Pharmacol. Ther.*, 22, 971-979.

Scholer, J.F., Code, C.F., 1954. Rate of absorption of water from stomach and small bowel of human beings. *Gastroenterology*, 27, 565-577.

Schroeder, K.W., Tremaine, W.J., Ilstrup, D.M., 1987. Coated Oral 5-Aminosalicylic Acid Therapy for Mildly to Moderately Active Ulcerative-Colitis - A Randomized Study. *N. Engl. J. Med.*, 317, 1625-1629.

Sciarretta, G., Furno, A., Mazzoni, M., Ferrieri, A., Malaguti, P., 1993. Scintigraphic study of gastrointestinal transit and disintegration sites of mesalazine tablets labeled with Tc-99M. *Scand. J. Gastroenterology*, 28, 783-785.

Sears, J.K., Darby, R.R., 1982. The technology of plasticizers. J. Wiley, New York.

Sedlak, M., Amis, E.J., 1992. Concentration and molecular-weight regime diagram of salt-free polyelectrolyte solutions as studied by light-scattering. *J. Chem. Phys.*, 96, 826-834.

Selub, S.E., 1994. Digestion and absorption. In: Haubrich, W.S., Schaffner, F., Berk, J.E. (Eds.), Part 1: Water, electrolyte and vitamin transport., Bockus Gastroenterology, Saunders, Philadelphia, 941-954.

Shankland, W., 1970. Equilibrium and structure of lecithin-cholesterol mixed micelles. *Chem. Phys. Lipids*, 4, 109-118.

Sheng, J.J., Kasim, N.A., Chandrasekharan, R., Amidon, G.L., 2006. Solubilization and dissolution of insoluble weak acid, ketoprofen: Effects of pH combined with surfactant. *Eur. J. Pharm. Sci.*, 29, 306-314.

Sheridan, P.L., Buckton, G., Storey, D.E., 1994. The extent of errors associated with contact angles .2. Factors affecting data obtained using a Wilhelmy Plate technique for powders. *Int. J. Pharm.*, 109, 155-171.

Shmeis, R.A., Wang, Z.R., Krill, S.L., 2004. A mechanistic investigation of an amorphous pharmaceutical and its solid dispersions, part I: A comparative analysis by thermally stimulated depolarization current and differential scanning calorimetry. *Pharm. Res.*, 21, 2025-2030.

Shuster, M., Narkis, M., Siegmann, A., 1994. Polymeric Antiplasticization of Polycarbonate with Polycaprolactone. *Polym. Eng. Sci.*, 34, 1613-1618.

Siepmann, J., Lecomte, F., Bodmeier, R., 1999. Diffusion-controlled drug delivery systems: calculation of the required composition to achieve desired release profiles. *J. Controlled Release*, 60, 379-389.

Silvester, K.R., Englyst, H.N., Cummings, J.H., 1995. Ileal recovery of starch from whole diets containing resistant starch measured in-vitro and fermentation of ileal effluent. *Am. J. Clin. Nutr.*, 62, 403-411.

Simpkin, G.T., Johnson, M.C.R., Bell, J.H., 1983. The influence of drug solubility on the quality of film-coated tablets. *Proc. Third. Int. Conf. Pharm. Technol.*, III, Paris, 163-170.

Singleton, J.W., Hanauer, S.B., Gitnick, G.L., Peppercorn, M.A., Robinson, M.G., Wruble, L.D., Krawitt, E.L., 1993. Mesalamine capsules for the treatment of active Crohns-Disease - results of a 16-week trial. *Gastroenterology*, 104, 1293-1301.

Singleton, J.W., Summers, R.W., Kern, F., Bechtel, J.M., Best, W.R., Hansen, R.N., Winship, D.H., 1979. Trial of sulfasalazine as adjunctive therapy in Crohn Disease. *Gastroenterology*, 77, 887-897.

Sinha, A., Ball, D., Connor, A.L., Nightingale, J., Wilding, I.R., 2003. Intestinal performance of two mesalamine formulations in patients with active ulcerative colitis as assessed by gamma scintigraphy. *Pract. Gastroenterol.*, 27, 56-69.

Sircar, A.K., Galaska, M.L., Rodrigues, S., Chartoff, R.P., 1999. Glass transition of elastomers using thermal analysis techniques. *Rubber Chem. Technol.*, 72, 513-552.

Snape, W.J., Matarazzo, S.A., Cohen, S., 1980. Abnormal gastrocolonic response in patients with ulcerative colitis. *Gut*, 21, 392-396.

Snyder, L.R., Kirkland, J.J., Glajch, J.L., 1997. Practical HPLC method development. 2nd Ed., John Wiley and Sons, New York.

Souliman, S., Beyssac, E., Cardot, J.M., Denis, S., Alric, M., 2007. Investigation of the biopharmaceutical behavior of theophylline hydrophilic matrix tablets using USP methods and an artificial digestive system. *Drug Dev. Ind. Pharm.*, 33, 475-483.

Sousa, J.J., Sousa, A., Moura, M.J., Podczeck, F., Newton, J.M., 2002. The influence of core materials and film coating on the drug release from coated pellets. *Int. J. Pharm.*, 233, 111-122.

Spiller, G.A., Chernoff, M.C., Hill, R.A., Gates, J.E., Nassar, J.J., Shipley, E.A., 1980. Effect of purified cellulose, pectin, and a low-residue diet on fecal volatile fatty-acids, transit-time, and fecal weight in humans. *Am. J. Clin. Nutr.*, 33, 754-759.

Spiller, R.C., Brown, M.L., Phillips, S.F., 1987. Emptying of the terminal ileum in intact humans - influence of meal residue and ileal motility. *Gastroenterology*, 92, 724-729.

Spitael, J., Kinget, R., 1977a. Factors affecting the dissolution rate of enteric coatings. *Pharm. Ind.*, 39, 502-505.

Spitael, J., Kinget, R., 1977b. Preparation and evaluation of free films - influence of method of preparation and solvent composition upon permeability. *Pharmaceutica Acta Helvetiae*, 52, 47-50.

Spitael, J., Kinget, R., 1979. Solubility and dissolution rate of enteric polymers. *Acta Pharm. Technol.*, Suppl. 7, 163-168.

Stellin, J.H., 1997. Functional anatomy, fluid and electrolyte absorption. In: Feldman, M., Schiller, L. (Eds.), *Gastroenterology and hepatology. The comprehensive visual reference*, Churchill Livingstone, Philadelphia, 1.2-1.4.

Suarez, N., Brocchini, S., Kohn, J., 2001. Study of relaxation mechanisms in structurally related biomaterials by thermally stimulated depolarization currents. *Polymer*, 42, 8671-8680.

Suarez, N., Figueroa, D., Laredo, E., Puma, M., 1982. Thermal depolarization of cubic lead fluoride. *Cryst. Lattice Defects*, 9, 207-210.

Suarez, N., Laredo, E., Bello, A., Kohn, J., 1997. Molecular relaxation mechanisms of tyrosine-derived polycarbonates by thermally stimulated depolarization currents. *J. Appl. Polym. Sci.*, 63, 1457-1466.

Sun, Y.M., Huang, W.F., Chang, C.C., 1999. Spray-coated and solution-cast ethylcellulose pseudolatex membranes. *J. Membr. Sci.*, 157, 159-170.

Svartz, N., 1988. Sulfasalazine .2. Some notes on the discovery and development of salazopyrin. *Am. J. Gastroenterol.*, 83, 497-503.

Szurszewski, J.H., 1969. A migrating electric complex of the canine small intestine. *Am. J. Physiol.*, 217, 1757-1763.

Tanabe, Y., Hirose, J., Okano, K., Wada, Y., 1970. Methyl group relaxations in the glassy phase of polymers. *Polymer J.*, 1, 107-115.

Tarvainen, M., Sutinen, R., Somppi, M., Paronen, P., Poso, A., 2001. Predicting plasticization efficiency from three-dimensional molecular structure of a polymer plasticizer. *Pharm. Res.*, 18, 1760-1766.

Thompson, R.P.H., Bloor, J.R., Ede, R.J., Hawkey, C., Hawthorne, B., Muller, F.A., Palmer, R.M., 2002. Preserved endogenous cortisol levels during treatment of ulcerative colitis with COLAL-PRED (TM), a novel oral system consistently delivering prednisolone metasulphobenzoate to the colon. *Gastroenterology*, 122, A433.

Tortora, G.J., Grabowski, S.R., 1996. Principles of anatomy and physiology. Eighth Ed., Harper Collins Publishers, Menlo Park, California.

Travis, S.P.L., 2006. Review article: induction therapy for patients with active ulcerative colitis. *Aliment. Pharmacol. Ther.*, 24, 10-16.

Travis, S.P.L., Stange, E.F., Lemann, M., Oresland, T., Chowers, Y., Forbes, A., D'Haens, G., Kitis, G., Cortot, A., Prantera, C., Marteau, P., Colombel, J.F., Gionchetti, P., Bouhnik, Y., Turet, E., Kroesen, J., Starlinger, M., Mortensen, N.J., 2006. European evidence based consensus on the diagnosis and management of Crohn's disease: current management. *Gut*, 55.

Tremaine, W.J., Schroeder, K.W., Harrison, J.M., Zinsmeister, A.R., 1994. A randomized, double-blind, placebo-controlled trial of the oral mesalamine (5-ASA) preparation, Asacol, in the treatment of symptomatic Crohn's colitis and ileocolitis. *J. Clin. Gastroenterol.*, 19, 278-282.

Tromm, A., May, B., 2005. Inflammatory bowel diseases: endoscopic diagnostics. First Ed., Falk foundation, Freiburg, Germany.

Tyrer, J.H., Eadie, M.J., Sutherland, J.M., Hooper, W.D., 1970. Outbreak of Anticonvulsant Intoxication in Australian City. *Br. Med. J.*, 4, 271-&.

Van Oss, C.J., Costanzo, P.M., 1992. Adhesion of Anionic Surfactants to Polymer Surfaces and Low-Energy Materials. *J. Adhes. Sci. Technol.*, 6, 477-487.

- Verdonck, E., Schaap, K., Thomas, L.C., 1999. A discussion of the principles and applications of Modulated Temperature DSC (MTDSC). *Int. J. Pharm.*, 192, 3-20.
- Vertzoni, M., Dressman, J., Butler, J., Hempenstall, J., Reppas, C., 2005. Simulation of fasting gastric conditions and its importance for the in vivo dissolution of lipophilic compounds. *Eur. J. Pharm. Biopharm.*, 60, 413-417.
- Vertzoni, M., Fotaki, N., Kostewicz, E., Stippler, E., Leuner, C., Nicolaidis, E., Dressman, J., Reppas, C., 2004. Dissolution media simulating the intraluminal composition of the small intestine: physiological issues and practical aspects. *J. Pharm. Pharmacol.*, 56, 453-462.
- Wadworth, A.N., Fitton, A., 1991. Olsalazine - A Review of its pharmacodynamic and pharmacokinetic properties, and therapeutic potential in inflammatory bowel disease. *Drugs*, 41, 647-664.
- Wan, L.S.C., Prasad, K.P.P., 1989. Uptake of water by excipients in tablets. *Int. J. Pharm.*, 50, 147-153.
- Washington, N., Washington, C., Wilson, C., 2001. The stomach. In: *Physiological pharmaceutics: barriers to drug absorption*, Taylor and Francis, London, 75-108.
- Watkinson, G., 1986. Sulfasalazine - a review of 40 years experience. *Drugs*, 32, 1-11.
- Wiedmann, T.S., Kamel, L., 2002. Examination of the solubilization of drugs by bile salt micelles. *J. Pharm. Sci.*, 91, 1743-1764.
- Wilding, I., 2000. Site-specific drug delivery in the gastrointestinal tract. *Crit. Rev. Ther. Drug Carrier Syst.*, 17, 557-620.
- Wilding, I.R., Davis, S.S., Sparrow, R.A., Smith, K.J., Sinclair, K.A., Smith, A.T., 1993. The evaluation of an enteric-coated naproxen tablet formulation using gamma scintigraphy. *Eur. J. Pharm. Biopharm.*, 39, 144-147.
- Wilding, I.R., Kenyon, C.J., Hooper, G., 2000. Gastrointestinal spread of oral prolonged-release mesalazine microgranules (Pentasa) dosed as either tablets or sachet. *Aliment. Pharmacol. Ther.*, 14, 163-169.
- Wu, C., McGinity, J.W., 2003. Influence of methylparaben as a solid-state plasticizer on the physicochemical properties of Eudragit® RS PO hot-melt extrudates. *Eur. J. Pharm. Biopharm.*, 56, 95-100.

Xiao, C., Wu, J., Yang, L., Yee, A.F., Xie, L., Gidley, D., Ngai, K.L., Rizos, A.K., 1999. Positronium annihilation lifetime and dynamic mechanical studies of gamma-relaxation in BPA-PC and TMBPA-PC plasticized by TOP. *Macromolecules*, 32, 7913-7920.

Yalkowsky, S.H., He, Y..2003. Handbook of aqueous solubility data. CRC Press, Boca Raton.

Zhou, S.Y., Fleisher, D., Pao, L.H., Li, C., Winward, B., Zimmermann, E.M., 1999. Intestinal metabolism and transport of 5-aminosalicylate. *Drug Metab. Dispos.*, 27, 479-485.

PUBLICATIONS RELATED TO THESIS

Fadda, H.M., Basit, A.W., 2005. Dissolution of pH responsive formulations in media resembling intestinal fluids: bicarbonate versus phosphate buffers. *J. Drug Del. Sci. Tech.*, 15, 273-279.

Fadda, H.M., Basit, A.W., 2005. Gastrointestinal tract: obstacles or opportunities in drug targeting. *Pharma*, 1, 53-59.

Fadda, H.M., Hernández, M.C., Margetson, D., McAllister, M., Basit, A.W., Brocchini, S., Suárez, N., The molecular interactions that influence the plasticizer dependent dissolution of acrylic polymer films. Submitted to *J. Pharm. Sci.*